Regulation of Airway Inflammation: Interplay of Cytokine IL-17A/F & Human Host Defence Peptide Cathelicidin LL-37

by

Anthony Altieri

A Thesis submitted to the Faculty of Graduate Studies of The University of Manitoba in partial fulfilment of the requirements of the degree of

Doctor of Philosophy

Department of Immunology

Rady Faculty of Health Sciences

University of Manitoba

Winnipeg, Manitoba

Table of Contents

List of Figures

List of Tables

Abstract

Asthma is a heterogeneous disease. The inhaled allergen-mediated disease phenotype is either Th2-high or Th2-low/Th17-high. The Th2-low/Th17-high phenotype is predominantly associated with neutrophilic inflammation and steroid-unresponsive severe asthma, for which there are no current treatments. Th17-driven neutrophilic airway inflammation is characterized by the concurrent increase of pro-inflammatory cytokine IL-17A/F and immunomodulatory cationic host defense peptide (CHDP) LL-37 in the lungs. However, the effect of LL-37 on IL-17A/F-mediated protein changes and signaling networks in airway inflammation is poorly understood. Therefore, I examined the immunomodulatory activity of LL-37 on IL-17A/F-mediated airway inflammation. I performed proteomic profiling to characterize IL-17A/F-mediated inflammation (in the presence/absence of other pro-inflammatory cytokines, such as TNF-α) in human bronchial epithelial cells (HBEC) and demonstrated that IL-17A/F-mediated inflammation leads to enhancement of secreted proteins, including the CHDP Lipocalin (LCN)-2 and neutrophilic chemokine GROα, which promote neutrophil migration in the context of airway inflammation. These protein targets were used to define the immunomodulatory role of cathelicidin LL-37 in IL-17A/F-driven inflammation. I demonstrated that cathelicidin LL-37 suppressed IL-17A/F-mediated LCN-2 production in HBEC. Further, I demonstrated that LL-37 was negatively correlated with LCN-2 and neutrophil accumulation in the lungs of a mouse model characterized by IL-17-driven neutrophilic airway inflammation. Moreover, I demonstrated that LL-37 suppressed the abundance of transcription factor C/EBPβ mRNA and enhanced the abundance of the RNA-binding protein (RBP) Regnase-1, which are positive and negative regulators of IL-17A/F-mediated LCN-2 production in HBEC, respectively. Taken together, these findings suggest that LL-37 simultaneously alters the transcriptional and post-transcriptional machinery to limit IL-17A/F-mediated neutrophil accumulation in the lung. In subsequent studies I demonstrated that citrullination, a relevant post-translational modification of LL-37 occurring in the lung, results in the selective loss of IκBζ mRNA abundance increases in the presence of IL-17A/F, as well as dampened GROα and CCL20 production in combination with IL-17A/F, compared to native LL-37. These findings suggest that citrullination limits the pro-inflammatory activity of LL-37. Overall, the proteins I identified in this study to be altered by IL-17A/F and/or LL-37 may represent pivotal checkpoints in neutrophilic airway inflammation and can be examined to develop new therapeutic strategies.

Acknowledgements & Dedication -

The completion of my PhD would not have been possible without the support of my colleagues, family, and friends.

I would like to express my sincere gratitude to my advisor, Dr. Neeloffer Mookherjee for their unending guidance, professional mentorship, and commitment to my scientific development throughout the graduate program. Further, I would like to thank the members of my advisory committee, including Dr. Keith Fowke, Dr. Thomas Murooka, and Dr. Jude Uzonna, as well as Dr. John Wilkins and Dr. Andrew Halayko for their scientific insight and mentorship.

I would also like to thank past and present colleagues in the Mookherjee lab, the Manitoba Centre for Proteomics and Systems Biology, and the Department of Immunology. I would like to sincerely thank Dr. Mahadevappa Hemshekhar and Dr. Hadeesha Piyadasa for their contributions to my project, scientific advice, and for teaching me a multitude of experimental procedures. I would also like to thank all colleagues whose work led to the completion of this project, including Dr. Grace Choi, Dr. Vidyanand Anaparti, Dylan Lloyd, Natasha Osawa, Breann Recksiedler, Victor Spicer, Courtney Marshall, Dina Mostafa, Padmanie Ramotar, and Stephanie Borlase.

In addition, I would like to thank Asthma Canada and the Canadian Allergy, Asthma, and Immunology Foundation, the Canadian Respiratory Research Network, Research Manitoba, and the Health Sciences Centre Foundation for research funding and financial support.

Finally, I would like to thank my family and friends for their extraordinary support through my graduate program, including my fiancé Dr. Danielle Lee, as well as my parents Dino and Tracey, and brother Matthew. *This thesis is dedicated to you.*

Chapter 1: Introduction

1.1 Airway immunity & inflammation

1.1.1 Inflammation & Immunity

1.1.1.1 Immune system & Inflammation

In the 1st Century AD, Roman doctor Cornelius Celsus defined the four cardinal signs of inflammation, *rubor et tumor cum calore et dolore* (redness and swelling with heat and pain) while describing therapeutic procedures for chest pain (1, 2). The fifth and final cardinal sign, *functio laesa* (loss of function) was added by Rudolph Virchow in 1858 while establishing the cellular basis of inflammation and subsequently, pathology (1, 2). Continuing investigations into the cellular basis of inflammation has led to the identification of the relationship between the symptoms of inflammation and the immune system (2, 3). Inflammation is currently identified as a biological response which enhances the survival of the host during infection and tissue damage by promoting the local accumulation of immune cells and mediators, generally aimed for the resolution of infection or injury. Enhanced inflammatory responses may be regulated back to baseline or immune homeostasis once infection or injury is resolved. However, dysregulation of the regulatory process resulting in persistent and enhanced inflammation drives pathophysiology in chronic disease.

The immune system is a collection of cells, tissues, and molecules that mediate resistance to disease through the prevention or eradication of infection (4). To protect the host effectively against disease, the immune system executes four major functions: (*1*) immunological recognition, (*2*) immune effector function, (*3*) immunological memory, and (*4*) immune regulation. There are two arms of the immune system, innate and adaptive immunity (detailed below in 1.1.1.2). Immune recognition is primarily driven by innate immunity and ensures that infection is detected and requires a variety of innate immune receptors that are capable of distinguishing self from foreign molecules. Once a foreign molecule is recognized, immune effector functions are initiated with innate immune responses driving adaptive immunity; immune cells produce molecules that act to contain, limit, and destroy infection directly or indirectly. Further, the innate immune response produces molecules which instruct the specific formation of immunological memory, and therefore immediate and stronger immune responses against recurring disease from the same pathogen.

Inflammation is an essential biological response that delivers cellular and molecular mediators to sites of infection and tissue damage to enable survival during infection and injury. These mediators maintain tissue homeostasis under a variety of noxious conditions (2, 4). Successful inflammatory

responses destroy pathogens through the recruitment and activation of immune cells and plasma proteins through blood vessels into the extravascular tissues (4). To achieve this, the local vasculature undergoes a multitude of changes. Increases in vascular diameter and local blood flow occur simultaneously to drive the local accumulation of immune cells at the site of inflammation (5). Endothelial activation occurs, wherein cells which line blood vessels are activated by immunological mediators to express cell-adhesion molecules which bind circulating leukocytes (5). The permeability of blood vessels is enhanced: tightly joined endothelial cells separate, enhancing the local accumulation of immune cells and immunological mediators from the blood to the tissue. The outcome of increased local blood flow, adhesion molecules, and vascular permeability, allows leukocytes to undergo extravasation, where they migrate into pathologically affected tissues to initiate tissue repair or induce anti-infective immunity by effector mechanisms (5). Moreover, increase in the flow of antigens and *antigen presenting cells* (APC) in the lymph to local lymphoid tissues leads to the activation and recruitment of adaptive immune responses at sites of infection. Furthermore, induction of blood clotting in micro-vessels leads to the formation of a physical barrier, preventing systemic spread of infection. Finally, repair of injured tissue is initiated upon elimination of the pathogen (5).

Immune responses and the process of inflammation must be controlled to limit damage to the surrounding tissues. Accordingly, the ability of the immune system to self-regulate and limit inflammation is a critical feature of efficient immune function. Failure of the regulatory processes that control inflammation cause detrimental, persistently enhanced inflammation, a central component of chronic inflammatory conditions including autoimmune disease and allergy.

1.1.1.2 Innate & Adaptive Immunity

The immune system is separated into two arms: innate and adaptive immunity. The primary distinction between the innate and the adaptive immune responses lies in the kinetic of response, mechanisms, and receptors used for immune recognition (6). Innate immune recognition is mediated by germ-line encoded receptors which recognize specific classes of molecules present only during tissue damage or infection (6). As a result, the effector mechanisms used by the innate immune system are induced rapidly with limited repertoire of specificity to the causative noxious element. However, by engaging specific combinations of receptors and accessory molecules, the innate immune response may instruct the formation of different immune responses based on the foreign element detected (4, 6). In contrast, the adaptive immune response uses random, somatically generated, and therefore structurally unique receptors specific to the antigen (6). The unique receptors are a function of immunological memory; Lymphocytes of the adaptive immune response which express useful receptors are selected for clonal

expansion by repeatedly encountering the antigens for which they are specific (6). As a result, the adaptive immune response possesses effector mechanisms which are specialized to the recurring noxious element and more effective in dealing with pathological insults. However, since the binding sites of adaptive antigen receptors arise as a result of random genetic mechanisms, the repertoire contains receptors which bind with innocuous environmental antigens, as well as self-antigens (6). As such, activation of adaptive immune responses in these instances can be harmful to the host and lead to chronic disease, including autoimmune disease and allergy (6). *The role of specific adaptive immune responses will be discussed further in the context of allergic asthma.*

The innate immune response recognizes highly conserved structures present in large groups of microorganisms or present during tissue damage (6). These conserved structures are referred to as *pathogen-associated molecular patterns* (PAMP) or *damage associated molecular patterns* (DAMP) respectively. PAMP are produced by microbial pathogens, are essential to the survival and pathogenicity of the invading microbes, and are shared by entire classes of pathogens (4, 7). Common PAMP include bacterial *lipopolysaccharide* (LPS), peptidoglycan, lipoteichoic acids, mannans, bacterial DNA, double-stranded RNA, and glucans (6). PAMP and DAMP are recognized by *pattern-recognition receptors* (PRR) which evolved to recognize these commonly occurring molecular patterns (6). PRR are not specifically expressed on any particular innate immune cell type or lineage; they are found on both hematopoietic and non-hematopoietic effector cells (6). Varieties of PRR are classified based on the structure of the receptor and/or their functional basis. PRR structural varieties include leucine-rich repeat domains, calcium-dependent lectin domains, and scavenger-receptor protein domains (6). PRR functional classes include secreted, endocytic, and signaling (6, 7). During infection and tissue damage, immune cells become activated and perform effector functions following the recognition of PAMP and/or DAMP (8). For example, *Toll-like receptors* (TLR), a well characterized family of PRR, induce signal-transduction pathways that lead to the activation of transcription factors of the *nuclear factor-κB* (NF-κB) family and therefore play a major role in the induction of immune and inflammatory responses, including the production of immunological mediators such as antimicrobial *cationic host defense peptides* (CHDP), cytokines, and chemokines (6, 9). *TLR-associated NF-κB signaling will be discussed in detail in the context of CHDP cathelicidin LL-37 and pro-inflammatory cytokine IL-17A/F.*

1.1.1.3 Cellular communication: cytokines and chemokines

The human immune response is regulated by a highly complex and intricate network of molecules, including cytokines (5, 10). Cytokines are small (8 to 40,000d), non-structural proteins which are produced and subsequently secreted in response to noxious elements and function as pleiotropic facilitators of communication between cells (4, 11, 12). Cytokines alter biological properties including cell-to-cell signaling, cellular growth, differentiation, proliferation, chemotaxis, immunoglobulin isotype switching, and apoptosis (4, 11, 12). These properties can be altered within the same cell which secretes the cytokines (autocrine action), nearby cells (paracrine action), or on distant cells (endocrine action) (12, 13). However, the net effect of any cytokine is dependent on the timing of cytokine release, cytokine receptor density, tissue responsiveness to each cytokine, and the local milieu in which it acts (14). As a result, the presence of other competing or cooperative molecular elements, including other cytokines, dictate the overall outcome of immune responses. Cytokines produced simultaneously may invoke redundant, antagonistic, or synergistic responses (10, 12). Therefore, the outcome of inflammation is also dependent on the overall composition of cytokines and immunological mediators. *The mechanistic basis of synergistic cytokine signaling will be discussed further in the context of IL-17A/F.*

1.1.1.4 Pro-inflammatory & anti-inflammatory cytokines

Interleukins (IL) are a well characterized class of common cytokines (15). Interleukins are secreted proteins which bind to their specific receptors and alter intracellular communication among leukocytes (15). Although interleukins may be classified according to sequence homogeneity, structure, and common receptor chains they do not fit within one structural category. Therefore, interleukins are typically described in accordance with their biological activities in infection and inflammation (11, 15). As a result, most interleukins are broadly classified as pro-inflammatory and anti-inflammatory depending on the biological response generated (10, 11).

The concept that some cytokines function primarily to induce inflammation while others suppress inflammation is fundamental to cytokine biology (11). Cytokines which promote inflammation are called pro-inflammatory cytokines, whereas cytokines which limit or negatively regulate inflammation are called anti-inflammatory cytokines (11). A dynamic balance exists between pro-inflammatory cytokines and anti-inflammatory cytokines within the mammalian immune system (10).

Pro-inflammatory cytokines are produced and secreted in response to invading pathogens and tissue damage, and consequently enhance inflammation. As a result, these cytokines are typically absent (or produced in very low concentrations) in a healthy, non-diseased state. In general, pro-inflammatory cytokines enhance local inflammation by promoting the proliferation, differentiation, recruitment, and activation of immune cells within the affected tissue (11). Despite their shared mode of action, different pro-inflammatory cytokines trigger the activation of unique biological pathways. Therefore, different pro-inflammatory cytokines enhance inflammation in both overlapping and unique mechanisms (4). *The role of pro-inflammatory cytokines IL-17A/F, TNF-α, and IFN-γ will be discussed further in the context of allergic asthma, as these cytokines were used in this thesis*

One subgroup of structurally related, pro-inflammatory cytokines that play a role in attracting leukocytes to sites of inflammation or infection are called chemokines (12). Chemokines are small (8-10 kDa) cytokines classified based on the presence or absence of one or more interposing amino acids(s) between conserved cysteine residues (known as CXC-, CX3C- and CC-chemokines), or the presence of only one cysteine residue (known as XC-chemokines) (12, 16). Chemokines bind specific seven-transmembrane-spanning *G protein-coupled receptors* (GPCR) and induce the migration of leukocytes and increase immune cell abundance at the site of inflammation, infection, and tissue injury (12, 13, 17).

Resolution of pro-inflammatory responses is required to prevent chronic, detrimental inflammation and damage to host tissues (5, 11). Therefore, cytokines which limit the activity of pro-inflammatory cytokines are called anti-inflammatory cytokines (10, 11). Cytokines, including IL-10, *transforming growth factor* (TGF)-β, and IL-1 *receptor antagonist* (RA) suppress the production of pro-inflammatory cytokines and their effects in immune cells (11). As a result, the equilibrium between pro-inflammatory and anti-inflammatory cytokines is thought to determine the balance between anti-infective immunity and chronic inflammatory disease (10, 11). Immunological mediators that regulate the equilibrium between pro-inflammatory and anti-inflammatory cytokines are critical effectors in the resolution of inflammation and maintenance of immune homeostasis. *CHDP are critical immunological mediators with known roles in resolution of inflammation and maintenance of immune homeostasis (18)*

1.1.1.5 Cationic Host Defense Peptides

CHDP, also known as *antimicrobial peptides* (AMP), are critical immunological mediators that regulate inflammation (19-21). Immunity-related functions of CHDP include the ability to alter signaling pathways initiated in response to inflammatory events and regulation of inflammation based on the microenvironment (22-24). CHDP directly augment the migration of leukocytes to the site of infection (25-33), preferentially trigger apoptosis in damaged and infected cells (34-36), change the composition of the adaptive immune response by altering APC function (37-42), and alter the composition of the cytokine milieu. To alter the balance of cytokines during inflammation, CHDP-mediated biological activity alters TLR-mediated and cytokine-mediated signaling to limit the production of pro-inflammatory cytokines, while enhancing the production of chemokines and anti-inflammatory cytokines (32, 33, 43-46). Therefore, CHDP promote effective immune responses, from initiation of effector mechanisms to resolution of inflammation. *CHDP, in particular the sole human cathelicidin LL-37, will be discussed in greater detail in below in 1.2.*

1.1.2 Airway Inflammation

1.1.2.1 Anatomical interface of immunity in airway inflammation

The lungs simultaneously balance two essential physiological functions: providing all individual cells in the body with oxygen and preventing infection from inhaled pathogens (47). The lung possesses a variety of physical and chemical immune mechanisms to limit infection (47). The interplay of cytokines and CHDP are essential in regulating immune responses in mucosal surfaces that are constantly challenged by the presence of pathogens and external particles, including the conducting airways of the lungs. *The focus of this section is to outline critical immune effector mechanisms which contribute to airway inflammation during infection and pathophysiology of chronic respiratory disease.*

1.1.2.2 Airway epithelium-derived cytokines and CHDP

The primary mechanism by which the lung is separated from the external environment is the epithelia, a mechanical barrier consisting of epithelial cells held together by tight junctions (4, 5). *Airway epithelial cells* (AEC) produce mucins, the components of a viscous fluid called mucus which not only prevents microorganisms from adhering to the respiratory tract, but facilitates their expulsion from the airway by the beating of epithelial cilia (5). In addition to acting as a physical barrier, epithelial cells are non-hematopoietic immune cells which can initiate inflammation. AEC express a variety of PRR, including TLR, *C-type lectin receptors* (CLR), cytoplasmic *retinoic acid-inducible gene* (RIG)-I-like

receptors, and *NOD-like receptors* (NLR), along with their corresponding intracellular signaling proteins, which facilitate recognition of pathogens to initiate subsequent effector innate immune mechanisms (48). During inflammation, AEC produce cytokines, chemokines, and CHDP to induce required immune responses (4, 5). Moreover, AEC express a multitude of cytokine receptors. Innate and adaptive leukocytes produce cytokines that target these receptors and alter the properties of epithelial cells to respond to specific inflammatory events. However, due to their role as dominant immunological effectors during inflammatory events, AEC may propagate inflammation and contribute to detrimental inflammation in chronic respiratory disease. *The focus of this thesis is on the interplay of pro-inflammatory cytokine IL-17A/F and CHDP LL-37 on AEC during airway inflammation.*

1.1.2.3 Airway Phagocytes and Granulocytes

In addition to epithelial cells, the epithelia contain innate immune leukocytes which assist in the defense against pathogens and subsequently inflammation. These leukocytes carry out a multitude of immune functions to protect the host from pathogen-mediated disease.

Upon entering the airway, pathogens may be recognized, ingested, and killed by phagocytes. Circulating phagocytes include neutrophils and monocytes, the precursor to macrophage. These blood cells are recruited to sites of infection where they kill microbes through the production of anti-infective molecules and the ingestion and intracellular degradation of these pathogens, in a process called phagocytosis (4, 5). After recognition and subsequent activation of phagocytes by PRR-mediated signaling, pathogens are surrounded by a phagocytic membrane and internalized in a membrane-enclosed vesicle known as an endocytic vacuole, or phagosome. Upon phagocytosis, neutrophil and macrophage produce anti-infective molecules (delivered by lysosomes) to aid in the destruction of the engulfed pathogen (5). The phagosome fuses with one or more lysosomes and generates a phagolysosome, resulting in release of the anti-infective molecules by the phagolysosome, and destruction of the pathogen (5). In addition to phagocytosis, macrophage and neutrophils are critical producers of cytokines, chemokines, and CHDP during airway inflammation.

Macrophages are critical immune cells which play important roles in anti-infective immunity, clearance of dead tissues, and initiation of tissue repair (4, 5). Monocytes are recruited from the bone marrow during inflammatory reactions into the submucosal tissues of the airway, where they can become long-lasting tissue macrophage (4). Due to their anatomical location, macrophages are among the first hematopoietic immune cells to initiate an immune response after PRR-mediated recognition

of PAMP and/or DAMP (4). Macrophage effector mechanisms, including the production of cytokines and chemokines, are often initiated in combination with phagocytosis and induce the proliferation, differentiation, and recruitment of immune cells at local sites of inflammation. Although macrophage are critical effector cells in anti-infective immunity and tissue damage, macrophage-derived cytokine production has been identified as a causative element in chronic respiratory disease characterized by airway inflammation (49).

In addition to being classified on function, immune cells in the airway can be classified based on morphology. Although they are considered phagocytes, neutrophils also belong to the granulocyte family, along with eosinophils, and basophils (4, 5). Granulocytes are leukocytes with multilobed nuclei and cytoplasmic granules (4, 5). Granulocytes play a major role in airway inflammation through their release of inflammatory mediators into the airways.

Neutrophils, otherwise known as *polymorphonuclear neutrophilic leukocytes* (PMNs), are short-lived, abundant innate immune cells. In response to infection and inflammation, neutrophil production in the bone marrow rapidly increases, rising from 4000 to 10,000 per μL to 20,000 per μL of blood. The large quantity of neutrophils in the blood allows them to be effectively recruited from the circulation into extravascular tissues to contribute to anti-infective immunity and tissue repair (4, 5). Neutrophils are recruited by neutrophil chemoattractants belonging to four different biochemical subfamilies, including chemokines (e.g., GROα and IL-8), chemotactic lipids (e.g., *leukotriene B_4* or LTB4), complement anaphylatoxins, and formyl peptides (50). Due to the rapid nature of their response, neutrophils are a major component of the innate immune response against invading pathogens (51, 52). After entering the tissue, PRR-mediated recognition of PAMP and DAMP lead to the activation of neutrophil effector functions which suppress fungal and bacterial proliferation. These effector mechanisms include phagocytosis, the production of cytokines (e.g., IL-6), CHDP (e.g., LL-37), lipid mediators, *reactive oxygen species* (ROS), *neutrophil elastase* (NE), *myeloperoxidase* (MPO), and net-like complexes of nuclear chromatin called *neutrophil extracellular traps* (NET) (4, 5, 51, 53-57). Despite their effectiveness in preventing infection, neutrophils and neutrophil-derived immunological mediators have been implicated in the pathophysiology of chronic respiratory disease (13, 58). *Neutrophils will be discussed in further detail in the context of T-helper (Th)17-mediated neutrophilic asthma.*

Eosinophils are granulocytes which differentiate and traffic to sites of local inflammation from the bloodstream to facilitate defense against extracellular parasites, including helminths (4, 5, 17, 59). Eosinophils can be differentiated from other members of the granulocyte family (including neutrophils) based on the presence of large specific granules (also known as secondary granules), which contain inflammatory mediators.

Eosinophils express a wide repertoire of surface molecules and receptors allowing their integration into both the innate and adaptive immune system (17). Eosinophil cell surface receptors include chemoattractant, cytokine, growth factor, PRR, and Fc receptors (8, 17). Eosinophils are recruited to local inflammatory sites through activation of *CC-chemokine receptor* 3 (CCR3), a surface receptor which binds all three subtypes of selective eosinophil chemoattractant, Eotaxin (17). After recruitment, eosinophil activation occurs through a variety of mechanisms. Eosinophil activation can occur through cytokine receptors for IL-4, IL-5, IL-13, IL-33 or Fc receptors to *Immunoglobulin* (Ig)A, IgD, IgE, IgG, and IgM (17). In addition to the high-affinity FcεR1 receptor, which binds IgE, FcαRI and FcγRII crosslinking with IgA and/or IgG has been shown to trigger eosinophil activation, degranulation, and release of inflammatory mediators (17). Eosinophil-derived inflammatory mediators include cytokines (e.g., IL-4, IL-5, IL-13, TNF-α, IFN-γ), chemokines (e.g., GROα, IL-8), basic proteins, and enzymes (17, 59, 60). In addition, eosinophils are the primary source of *major basic protein* (MBP), *eosinophil cationic proteins* (ECP), *eosinophil peroxidase* (EPO), and *eosinophil-derived neurotoxin* (EDN), which propagate inflammation through the activation of immune cells (61). For example, MBP can trigger mast cells to release histamine, a potent vasodilator (62, 63). Moreover, eosinophil-derived cytokines, and lipid mediators can induce mucus secretion in AEC (64, 65). Due to the downstream effect of eosinophil-derived mediators, eosinophils have been implicated in immediate hypersensitivity late-phase reactions where they contribute to pathologic processes in allergic airway disease. Furthermore, the prominence of eosinophils in allergic airway disease has positioned them as a key determinant of allergic asthma (13). *Eosinophils will be discussed in further detail in the context of Th2-mediated eosinophilic asthma.*

Mast cells are *bone-marrow derived cells* (BDMC) present in the mucosal epithelium which provide defense against helminths and other pathogens (4, 5). Mast cells are activated by TLR signaling and antibody-dependent mechanisms to produce inflammatory mediators (4, 5). In addition to cytokines, mast cells produce vasoactive amines such as histamine, which function to induce vasodilation and increase capillary permeability. Mast cells also synthesize and secrete lipid mediators

prostaglandins, and cytokines which induce inflammation (4). Mast cell-derived inflammatory mediators have been implicated in chronic respiratory disease (66-69).

1.1.3 Asthma

1.1.3.1 Airway inflammation & Chronic Respiratory Disease

Airway inflammation is a central component of chronic inflammatory disease of the airways, including asthma. In addition to airway inflammation, asthma is characterized by narrowing of the bronchial tubes (bronchoconstriction) and mucus hypersecretion. These processes lead to limited airflow and difficulty breathing (13, 17). Ultimately, chronic airway inflammation can cause permanent structural changes in the airways (airway remodeling), including narrowed and thickened airways. Airway remodeling is irreversible and changes to the structure of the airway may lead to blockages and long-term loss of function (70, 71).

1.1.3.2 Asthma prevalence

Airway diseases, including asthma, are major contributors to morbidity and mortality globally. Asthma affects >300 million people globally and contributes to 1000 deaths each day (70, 71). Asthma affects more than 3.8 million Canadians (70, 71). In Canada, asthma is the third-most common chronic disease (70, 71). Over 300 Canadians are diagnosed with asthma every day and an estimated 250 Canadians die from an asthma attack every year (70, 71).

1.1.3.3 Asthma symptoms

Asthma is characterized by symptoms including shortness of breath, regular coughing, wheezing, chest tightness, increased mucus production, trouble sleeping due to breathing difficulty, and being unable to take part in physical activities without breathing difficulty (13, 17, 72). Symptoms can occur slowly over hours or days, or they can come on as sudden recurring attacks with lasting symptoms that persist for some time before disappearing (70, 71).

1.1.3.4 Asthma treatments

Asthma treatments and/or medications can be broadly grouped into relievers and controllers (70, 71). Relievers, including short-acting bronchodilators, act as rescue medication and provide fast and short-term relief of asthma symptoms, including bronchospasm (tightening of the airways). Controller medication, treat persistent, underlying inflammation in the airways and lead to less symptoms over time. A variety of controller medications exist and are widely prescribed, including long-acting

bronchodilators, anti-leukotrienes, *monoclonal antibody* (mAb)-based biological therapies, and oral and *inhaled corticosteroids (*ICS) (70, 71).

Despite major asthma treatment advances and guideline-directed increases in ICS, a significant number of patients exist who do not respond effectively to current treatment strategies (73). Subsequently it was determined that individuals who did not respond to ICS had distinct differences in underlying airway inflammation from those that did. Asthma is now recognized as a heterogenous disease which can be grouped based on the composition of the inflammatory milieu in the airway (72, 74, 75).

1.1.4 Asthma disease heterogeneity

1.1.4.1 Asthma endotype and phenotype

Asthma is a heterogenous disease characterized by different inflammatory pathways, also referred to as endotypes, which drive the pathophysiology of asthma (17, 72, 74). Despite being governed by disparate inflammatory mediators, these inflammatory pathways consist of unifying components which govern the mechanisms of induction, regulation, and resolution of airway inflammation. These inflammatory pathways are defined by the presence of (*1*) inflammatory inducers; (*2*) the sensors which detect the inducers; (*3*) inflammatory mediators induced by sensors; (*4*) target tissues that are affected by the inflammatory mediators (2). Defining heterogeneous asthma pathways focuses on delineating these mechanistic components with the goal of developing targeted therapeutic intervention (72). Endotype classifications are based on the composition on global characterizations of the inflammatory profile as determined by high information content approaches, including proteomics, transcriptomics, and metabolomics. These global characterizations are organized based on their predicted activation of cellular pathways, primarily the activation of *T-Lymphocyte* (T cell) populations, including (Th)2 high versus Th1/Th17 high pathways (76, 77). Moreover, asthma endotypes may be based on the presence of the resulting cellular profile of inflammation, which can be eosinophilic, neutrophilic, mixed eosinophilic/neutrophilic, or no elevated eosinophils or neutrophils (i.e., paucigranulocytic) (78). T cell-based endotypes are often combined with high content inflammatory profiles to offer a complete picture of inflammatory pathology in asthma. However, there is no consensus on the specific definitions of asthma endotypes (78). In addition to being classified based on endotypes, asthma may also be classified based on phenotype, which does not account for the pathophysiological mediators that contribute to underlying disease (72). Instead, phenotype classification is based on observable clinical characteristics, including disease severity, treatment response, exacerbating factors, age of onset, and comorbid conditions (72, 75). In the context of airway

disease and allergic asthma, efforts to link clinical phenotypes with molecular endotypes are complicated by the synergistic, antagonistic, and redundant nature of cytokines. *The focus here will be on cellular endotypes, the cytokines associated with them, and their suggested phenotypes.*

1.1.4.2 Eosinophilic endotype

Eosinophilic asthma is described as increased sputum (>3%) and/or blood (≥400 cells/mL) eosinophils on >2 occasions and a positive response to treatment strategies that suppress eosinophils (79). Eosinophils may be prompted to release several different mediators with the capacity to cause the exaggerated response to innocuous antigens in the airway, also known as *airway hyperresponsiveness* (AHR), goblet cell proliferation, and mucus hypersecretion (62-65, 80). The eosinophilic endotype highly overlaps with Th2-high allergic asthma. In addition, select sets of biomarker genes can define Th2 endotypes, including *POSTN*, *CLCA1*, and *SERPINB2* for Th2 asthma (81, 82). Accordingly, eosinophilic asthma typically responds to treatment with corticosteroids or novel therapies directed against Th2 cytokines namely IL-4, IL-5, and IL-13 (79).

1.1.4.3 Neutrophilic endotype

Neutrophilic asthma is defined as increased sputum neutrophil counts (≥64%) in the absence of elevated eosinophil counts (<3%), with an increased total cell count (≥9.7 million cells/g) (79). Neutrophilic asthma represents a Th1/Th17-driven disease and has been associated with Th1 cytokines (e.g., IL-1, IFN-γ, TNF-α), Th17-differentiating cytokines (e.g., IL-1, IL-6, IL-23), and Th17-secreted cytokines (e.g., IL-17A, IL-17F, IL-17A/F) (79, 83, 84). Additionally, neutrophilic asthma has been associated with TNF-α-mediated airway remodeling factors including *MMP9*, as well as IL-17-inducible chemokines, including *CXCL1*, *CXCL2*, *CXCL3*, *IL8*, and *CSF3* (79, 82-84). Neutrophil accumulation in the lung is found in severe persistent asthma (85), asthma exacerbations (86-88), sudden onset fatal asthma (89), occupational asthma (90), nocturnal asthma (91), and even childhood asthma (92). Individuals with neutrophilic endotypes typically have poor responses to treatments that suppress eosinophils, including corticosteroids (79, 93).

1.1.4.4 Mixed eosinophilic/neutrophilic endotype

The mixed eosinophilic/neutrophilic endotype is defined by elevated neutrophils and eosinophils either independently or concurrently on more than two independent blood tests that are at least six months apart (79). There is limited data on the phenotype of individuals with a mixed endotype.

1.1.4.5 Paucigranulocytic endotype

The paucigranulocytic endotype is the endotype defined based on exclusion of cell types. Individuals with paucigranulocytic asthma have no increased sputum eosinophil counts (<3%) or neutrophil counts (<64%). In these individuals, anti-inflammatory treatment targeting eosinophils and neutrophils is typically ineffective, and symptoms are primarily driven by AHR (79). Instead, these individuals benefit from smooth muscle-oriented therapy, including bronchial thermoplasty or therapy which targets mast-cells (79).

1.2 CHDP

1.2.1 CHDP biology

CHDP, also known as AMP, are small natural peptides characterized from nearly all life forms, with direct and indirect anti-infective and immunomodulatory capabilities. Some CHDP can directly kill invading pathogens when present at high concentrations at mucosal surfaces, however the antimicrobial function of CHDP is antagonized at physiological concentrations by host anionic factors and divalent cations. CHDP directly alter the properties of immune cells, including migration, antigen presentation, apoptosis, as well as immune signaling (18-24, 94-100). Moreover, CHDP have demonstrated ability to play a role in anti-infective immune response or detrimental chronic inflammation by altering TLR-mediated and cytokine-mediated immune signaling (32, 33, 43, 44, 101-104). Therefore, these peptides demonstrate highly complex immunomodulatory functions which promote or suppress inflammation based on environmental stimuli, response kinetics, cell and tissue type, interaction with different cellular receptors, and the concentration of the peptides (18, 21, 22, 31, 98, 100, 105, 106). The ability to selectively alter pro-inflammatory and anti-inflammatory immune signaling makes CHDP attractive therapeutic candidates for infectious disease, wound healing, and chronic inflammatory disease. A distinct advantage of a CHDP-based therapy would be the ability to control inflammation without compromising the ability to resolve infections.

1.2.1.1 History & discovery

The initial discovery of CHDP is attributed to Kiss and Michl in the speckled frog during the 1960s (107). Further studies in the 1980s identified additional CHDP, including the moth-derived cecropin (108), amphibian-derived magainin (109), and defensins derived from human neutrophils (110). CHDP have subsequently been identified across a wide variety of species, including microorganisms, plants, and invertebrates, to complex amphibians and mammals (19). Currently, the database curating the diversity of antimicrobial peptides has catalogued over 3,000 peptides with immunomodulatory and/or antimicrobial properties (111).

1.2.1.2 Characteristics & structure

CHDP are amphipathic, small peptides (<50 amino acids) with a corresponding a net positive charge of +2 to +9 at physiological pH. These peptides differ significantly in sequence and structure. Essentially, CHDP have been classified into four broad structural conformation categories: (*1*) α-helical linear peptides; (*2*) β-sheets with disulfide bridges; (*3*) cyclic peptides; and (*4*) peptides with extended flexible loop structures (18). In vertebrates, CHDP have two unifying features: they are amphipathic and contain hydrophilic and hydrophobic side chains at opposite sides of the molecules. The dominant families of CHDP in vertebrates are defensins and cathelicidins (18). *The focus hereafter will be on cathelicidins and the sole human cathelicidin LL-37.*

1.2.1.3 Cathelicidin biosynthesis, structure & release/secretion

Cathelicidins are named after the conserved cathelin-like domain in the pro-peptide in this family of CHDP. Cathelicidins are produced as prepropeptides containing an amino-terminal (N-terminal) signal peptide, a cathelin-like domain, and the carboxy-terminal mature peptide. The pro-cathelin-like domain is cleaved off primarily by serine proteases once the peptide is secreted to yield the mature active peptides (18, 112, 113).

As the conserved feature of cathelicidins is cleaved to yield mature active peptides, family members have significant variation in sequence and structure. Most cathelicidins are 23-27 amino acid, α-helical, amphipathic, cationic peptides with a hydrophobic surface allowing interaction and perturbation of membranes with anionic surfaces. The sole human cathelicidin, LL-37 is an α-helical peptide and is one of several cleavage products of hCAP18, the product of cathelicidin gene *CAMP* (95). In addition, α-helical variants of LL-37 exist in other species, including mouse *cathelicidin-related antimicrobial peptide* (CRAMP) (114). In addition to α-helical peptides, there are cathelicidins with β-hairpin peptide structures (12–18 residues) and one intramolecular disulfide bond (bovine bactenecin), β-sheet structures (16–18 residues) with two intramolecular disulfide bonds (Protegrins), and linear cathelicidins (13–39 residues) enriched with specific amino acids (tryptophan-enriched bovine Indolicidin). Despite structural differences, all cathelicidins are immunomodulatory antimicrobials with an important role in the regulation of anti-infective and inflammatory responses (98-100).

1.2.3 LL-37 in infection & inflammation

LL-37-mediated regulation of inflammation is highly complex. LL-37 directly interacts with 16 different proteins in a variety of hematopoietic and non-hematopoietic cell types in the innate and

adaptive immune systems (21). These receptor or protein partner interactions culminate in pleiotropic immune augmentation or resolution, including the induction of innate immune gene transcription, influencing adaptive immune responses, regulation of cell death, direct and indirect leukocyte recruitment, and intervening in inflammatory signaling such as TLR-NF-κB, based on the cell type, kinetics of response, and the microenvironment. As a result, the immunomodulatory activity of LL-37 has emerged as a key biological function.

1.2.3.1 LL-37 intracellular receptors & signal transduction

LL-37 possesses complex signaling activity which targets multiple receptors simultaneously. LL-37 directly interacts with 16 proteins in various cell types, including $P2X_7R$, JNK, SPL_1, ELANE, CREB1, FOS, GAPDH, VDR, JUN, IGF1R, KLK5, PGC, KLK7, PRTN3, CTSG, and FOS (21). In turn, these interacting protein partners or receptors interact with more than 1,000 secondary effector proteins and alter the expression of over 900 genes (21). Recent literature speculates that the wide range of immunity-related functions mediated by LL-37 may depend on its interaction with protein partner(s) which in turn control diverse or opposing downstream responses (32). *The specific receptors, signaling cascades, resulting protein signatures, and biological activities altered in innate immune cells, including AEC, is still being delineated.*

1.2.3.2 LL-37-mediated immunological activity

The ability of LL-37 to induce chemokine release and enhance recruitment of leukocytes has been defined as a primary immunomodulatory mechanism (18). LL-37 directly enhances the recruitment of human monocytes, neutrophils, and T-lymphocytes by activating the seven-transmembrane GPCR, *formyl peptide receptor 1* (FPRL1) (28). In addition to acting as a chemoattractant, and recruiting leukocytes directly, LL-37 enhances indirect recruitment of leukocytes by inducing cytokine and chemokine production in innate immune cells. In human macrophages and *peripheral blood mononuclear cells* (PBMC), LL-37-induced transcription of chemokine genes *CCL4, CCL20, CXCL1* occurred in a GAPDH-dependent manner (44). Further, LL-37-mediated production of chemokines GROα and IL-8 occurs in a Cdc42/Rac1 RhoGTPase-dependent manner engaging GPCRs and results in the enhanced recruitment of monocytes and neutrophils, however LL-37-mediated anti-inflammatory response is independent of this mechanism (32). Furthermore, LL-37 can also mediate induction of cytokine and chemokine genes in non-hematopoietic cells. In human synovial cells, LL-37 induces the transcription of *IL6* and *IL17A (115)*. In keratinocytes, LL-37 induces expression of *IL6* and *IL23A* (116). In AEC, LL-37-mediated secretion of chemokines GROα and IL-8, as well as cytokine IL-6, is associated with NF-κB signaling subunits, p65 and p50 (117). *Although LL-37-*

mediated induction of chemokines and cytokines is well documented in non-hematopoietic cells, the precise impact of enhanced chemokine production on immune cell recruitment during inflammation is not well understood.

LL-37 not only recruits leukocytes, but also influences their function at inflammatory sites. LL-37 can directly recruit neutrophils and influence the function of neutrophils to modify infection outcomes (28, 29, 118). For example, LL-37 enhances release of defensins and ROS in neutrophils (119-121). In addition to being recruited to sites of local inflammation by LL-37, neutrophils store, produce and secrete LL-37 (112). LL-37 is released during neutrophil degranulation and/or NET release and contributes to NET-mediated anti-infective effects (19, 122). Furthermore, LL-37 facilitates NET formation (123), which may lead to a positive feedback loop during inflammation. However, the impact of LL-37 on neutrophils may be time- and/or context- dependent as LL-37 promotes internalization of chemokine receptors CXCR2 on monocytes and neutrophils, consequently dampening chemotaxis (119). *Therefore, the precise relationship between LL-37-mediated functions on neutrophil recruitment and activation is an active area of investigation and not completely understood.*

In addition to directly recruiting T cells (28), LL-37 can modulate APC function to alter adaptive immunity. LL-37 shapes the adaptive response via modulation of DC differentiation and function *in vitro* (37, 38) and *in vivo* (39). LL-37 promotes DC activation (40, 41) and enhances the activation/proliferation of B cells by activating follicular DC (42). Furthermore, LL-37 alters the phenotype of DC by significantly up-regulating endocytic capacity, modifying phagocytic receptor expression and function, up-regulating costimulatory molecule expression, enhancing secretion of Th1-inducing cytokines, and promoting Th1 responses (37). LL-37 can also shape the adaptive immune response by altering the differentiation of Th subsets directly: LL-37 enhances differentiation of IL-17A/F-producing Th17 cells, while limiting differentiation of Th1 cells (124).

LL-37 can influence the mode of cell death and subsequently alter inflammation and infection**.** As different modes of cell death have important roles in maintaining immune homeostasis, LL-37 exhibits the ability to alter cell death properties and amplify or suppress inflammatory responses. As such, LL-37-mediated regulation of neutrophil cell death can induce rapid secondary necrosis of apoptotic neutrophils (125), consequently limiting pro-inflammatory contributions from macrophage (126, 127). Moreover, LL-37 can also target AEC to alter the properties of cell death. LL-37 can enter lung epithelial cells (128) and trigger apoptosis *in vitro* and *in vivo* (34, 35). Further, high

concentrations of LL-37 preferentially induce death in infected epithelial cells represents an additional anti-infective mechanism (35, 36). Therefore, LL-37-mediated regulation of cell death has the potential to change the magnitude and resolution of inflammatory responses, based on peptide concentration and extracellular stimuli.

1.2.3.3 LL-37-mediated immunomodulation

LL-37 and the mouse analog CRAMP shows both pro-inflammatory and anti-inflammatory effects in anti-infective immunity. For example, LL-37 contributes to anti-infective immunity through the resolution of infection by enhancing pro-inflammatory innate immune response to pathogens (36, 118, 123, 129-131). In contrast, LL-37-mediated anti-inflammatory effects have also been demonstrated during inflammatory and/or pathogenic challenges: several studies demonstrate that cathelicidin-deficient mice exhibit enhanced inflammatory responses compared to wildtype mice (121, 132, 133). Additional *in vitro* studies have demonstrated this dichotomy in hematopoietic cells, including monocyte-like cells and PBMC where LL-37 simultaneously upregulates the production of chemokines and anti-inflammatory cytokines, while suppressing pro-inflammatory protein production in the context of endotoxin-mediated signaling (32, 33, 44, 103, 134-136). However, the outcome of LL-37-mediated regulation of immune responses seems to be context dependent and contingent on the inflammatory and cellular environment. For example, studies which detail properties of LL-37 in non-hematopoietic cells focus primarily on LL-37-mediated increases in chemokines and pro-inflammatory cytokines without detailing the impact on anti-inflammatory cytokines (115-117).

As cytokines are dominant regulators of inflammation in chronic inflammatory disease, the ability of LL-37 to alter cytokine-mediated inflammation in hematopoietic and non-hematopoietic immune cells have also been investigated. LL-37 selectively regulates inflammation in the presence of cytokine-mediated inflammation. For example, LL-37 suppresses IL-32-induced pro-inflammatory cytokines TNF-α, IL-6 and IL-1β and enhances anti-inflammatory cytokine IL-1RA through suppression of Fyn (Y420) Src Kinase signaling in human macrophages and PBMC (43). Further, LL-37 can selectively synergize with pro-inflammatory cytokine IL-1β to enhance specific cytokines (e.g., IL-6), chemokines (e.g., MCP-1, MCP-3), and anti-inflammatory cytokines (e.g., IL-10) in human PBMC (104). In non-hematopoietic innate immune cells, LL-37 synergizes with pro-inflammatory cytokines to induce transcription of innate immune genes. For example, combination of LL-37 and IL-17A induce the transcription of *prostaglandin-endoperoxide synthase 2 (PTSG2)* and *TNFα* in a human synovial sarcoma cell line (115). Additionally, LL-37 in combination with IL-1β

synergistically increases IL-8 production in AEC (137). *The anti-inflammatory properties of LL-37 during cytokine-mediated inflammation in non-hematopoietic immune cells requires further investigation.*

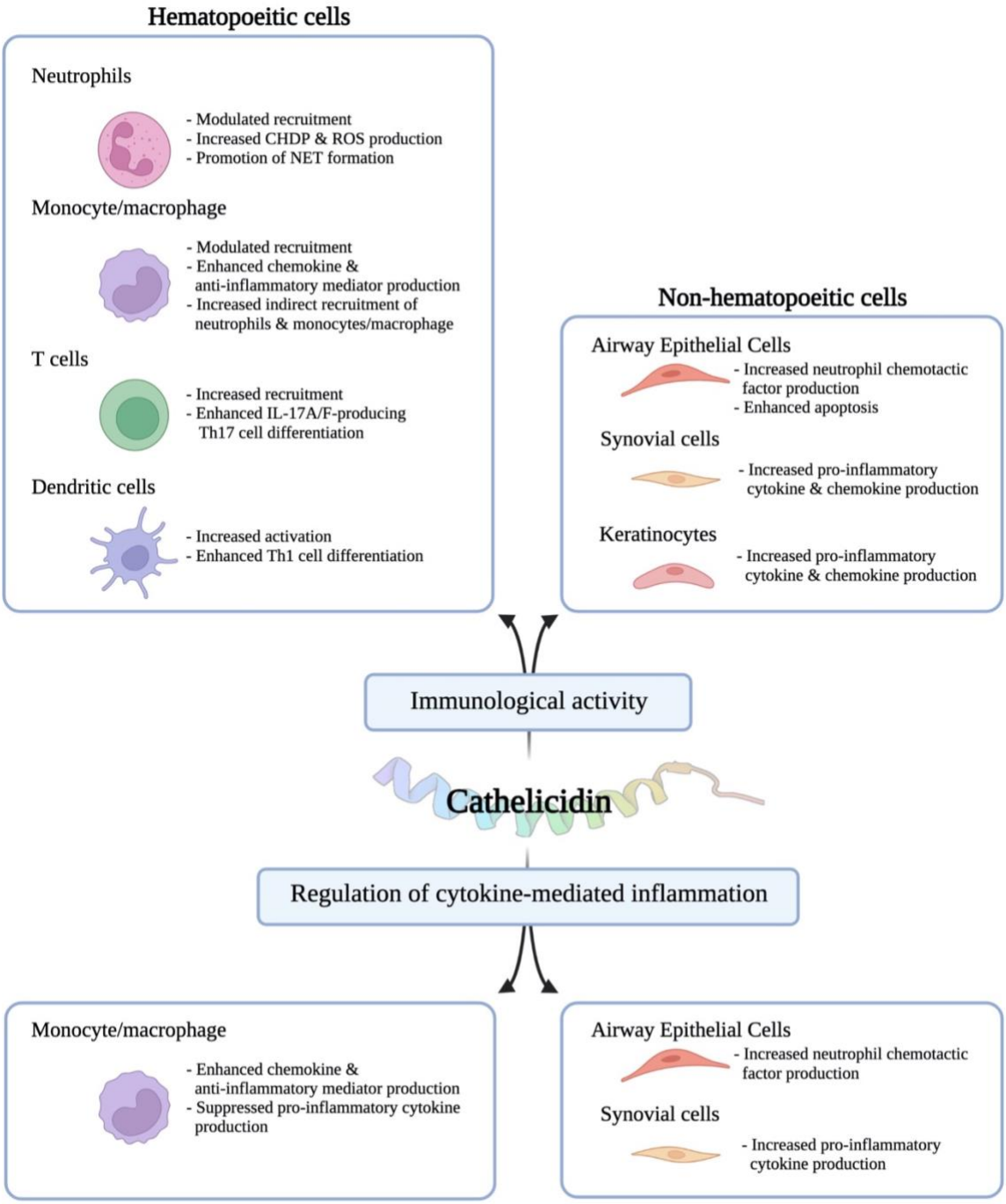

Figure I: Select immunomodulatory activity of cathelicidin. Immunomodulatory activities of cathelicidin include (but are not limited to) direct and indirect modulation of cell recruitment, alteration of cytokine and chemokine production, altered cell activation and/or differentiation, altered cell death, and regulation of cytokine-mediated inflammation. *This figure created using biorender.com.*

1.2.2.4 Citrullinated LL-37

Enzymes in the extracellular environment can alter the biological function of LL-37. Limited studies have shown that LL-37 undergoes specific *post-translational modifications* (PTM) which can modify its biological activities. One such modification is citrullination, the conversion of arginine residues to citrulline by *peptidyl arginine deiminases* (PAD) enzymes which are enhanced in inflammatory conditions. *In vitro* and *in vivo* studies have demonstrated that one to five arginine residues in LL-37 can be converted to citrulline (138-140). *In vitro*, activity of recombinant human PADI2 and PADI4 enzymes resulted in a time- and dose-dependent citrullination of LL-37 (139). It has been shown that citrullination alters biological activities of LL-37, such as decreasing the ability of the peptide to neutralize LPS and consequent pro-inflammatory mediators (139-141), as well as significantly attenuating anti-bacterial (138, 139) and anti-viral properties (142), compared to native LL-37. Additionally, LL-37-mediated suppression of pro-inflammatory mediator production in response to lipoteichoic acid and poly(I:C) is also mitigated by citrullination (140). Moreover, citrullination of LL-37 increases serum levels of IL-6, as well as exacerbates sepsis, morbidity, and mortality in a mouse model of d-galactosamine–sensitized endotoxin shock (140). Finally, citrullinated LL-37 (citLL-37) possesses higher chemotactic ability against mononuclear leukocytes (139). Therefore, citrullination appears to suppress the anti-inflammatory capability of LL-37 during infection. Some studies have suggested that citLL-37 may limit inflammation by converting apoptotic neutrophils into a state of secondary necrosis (125-127, 139). *The impact of citrullination on the biological activities of LL-37 warrants detailed investigation as this PTM is associated with inflammation, and LL-37 can mediate both effector and regulatory activity in inflammatory diseases.*

In summary, the broad capabilities of LL-37 to supress the abundance of pro-inflammatory cytokines while enhancing chemokines and anti-inflammatory cytokines have led to speculation that LL-37 selectively regulates inflammation, promotes balanced immune responses, and therefore plays a critical role in promoting immune homeostasis (19). The ability of LL-37 to promote immune homeostasis, along with its altered abundance in chronic inflammatory diseases has led to investigations into the role of LL-37 in regulating cytokine-mediated inflammation in the context of chronic inflammatory disease.

1.2.4 LL-37 in health & disease

The abundance of LL-37 is altered chronic inflammatory disease, including rheumatoid arthritis (102, 143), psoriasis (144), systemic lupus erythematosus (145), as well as chronic lung diseases characterized by neutrophil accumulation in the lung (139, 146-148). In particular, the relationship

between LL-37 and chronic inflammation is well documented in respiratory disease and *rheumatoid arthritis* (RA).

1.2.4.1 Rheumatoid arthritis

LL-37-derived peptides have been investigated in the context of RA. IG-19, the internal segment of human cathelicidin has been shown to suppress inflammation in a mouse model of *collagen-induced arthritis* (CIA) (101, 102). Specifically, IG-19 reduces cellular infiltration in joints, prevents cartilage degradation, and suppresses pro-inflammatory cytokines in the CIA mouse model. Furthermore, administration of IG-19 significantly decreases the abundance of CHDP in the joints, including mouse cathelicidin CRAMP, S100A8, and S100A9 proteins in CIA mice (102). Clinical studies have shown that LL-37 is increased in the joints in RA, wherein the role of the peptide in disease pathogenesis is not well understood (149).

1.2.4.2 LL-37, airway inflammation, and asthma

LL-37 is increased in individuals with chronic respiratory diseases, including *chronic obstructive pulmonary disease* (COPD) and asthma (139, 146-148). LL-37 abundance in chronic inflammatory lung diseases may be dependent on neutrophil accumulation. In a mouse model of mixed neutrophilic and eosinophilic lung inflammation, cathelicidin was decreased compared to naïve controls (102). However, additional studies have demonstrated that LL-37 abundance positively correlates with the presence of neutrophils and NET (147), a critical component of Th17-mediated neutrophilic asthma (150). Individuals with neutrophilic asthma and COPD had significantly higher levels of LL-37, *extracellular DNA* (eDNA), and NE compared to individuals with non-neutrophilic asthma as well as healthy controls. Furthermore, cathelicidin potentiates Th17 but suppresses Th1 differentiation in the airways, by enhancing *aryl hydrocarbon receptor* (AHR) and *retinoic acid receptor-related orphan receptor-γt* (RORγt) expression in a TGF-β1-dependent manner (124). In addition to native LL-37, citLL-37 has also been detected in the *bronchoalveolar lavage* (BAL) in healthy individuals (138) and is increased in chronic respiratory disease, including COPD (139). *The effect of citLL-37 in the lungs in chronic inflammatory disease has not been characterized.*

1.3 Cytokine-mediated airway inflammation & disease:

1.3.2 Interleukin-17 biology

1.3.2.1 History, discovery, characterization, and evolutionary significance

IL-17 is a highly complex pro-inflammatory cytokine crucial for a variety of processes, including host defense, tissue repair, as well as the pathogenesis of inflammatory disease (151). IL-17 was first discovered as the *Il17a* gene in T cells, as an expressed transcript which shared homology with an open reading frame in *Herpesvirus saimiri (152)*. IL-17A (originally named CTLA8) was first cloned in 1993, with the gene for its receptor cloned 2 years later. As of 2005, Th17 cells were observed as a distinct lineage of *cluster of differentiation* (CD)4+ T cells characterised by expression of IL-17A under the influence of transcription factor RORγt (153-157). Subsequent studies determined that IL-17A (also often denoted as IL-17) is a member of a distinct cytokine family containing five additional members, which include IL-17A, IL-17A/F, IL-17B, IL-17C, IL-17D, IL-17E, and IL-17F. *The focus of this thesis will be on pro-inflammatory cytokine IL-17A/F heterodimer, which is a biologically active member produced by Th17 cells.*

1.3.2.2 IL-17R & IL-17R family members

Human IL-17A is a 155-amino acid secreted glycoprotein which represents a family of homologous proteins (158). IL-17A is most similar in structure and function to IL-17F, which shares 50% sequence homology and consists of 158 amino acids. In addition to IL-17A and IL17F homodimers, these subunits can form a heterodimer called IL-17A/F. IL-17A, IL-17F, and IL-17A/F all facilitate the induction of similar gene expression profiles upon activation of the *IL-17 receptor* (IL-17R), albeit at different magnitudes: IL-17A is the most potent, followed by IL-17A/F, then IL-17F, as measured by downstream gene activation upon IL-17R activation (159, 160).

Other members of the IL-17 family, including IL-17B, IL-17C, IL-17D, and IL-17E (also known as IL-25) are functional and structurally diverse (161). IL-17C and IL-25 are the best characterized cytokines in this poorly understood subset. IL-17C is released by epithelia after stimulation by pro-inflammatory cytokines IL-1β and TNF-α, or through cell damage sensed by PRR, including TLR2 and TLR5 (162). Subsequent release of IL-17C enhances IL-17A and IL-17F release from Th17 cells and drives Th17-mediated inflammation (163). In addition to activating Th17 cells, IL-17C functions in an autocrine manner to enhance the induction of by IL-17A-, IL-17F-, and IL-17A/F-mediated gene targets in non-hematopoietic innate immune cells (163). IL-17E promotes Th2- rather than Th17-mediated inflammation, in part by inhibiting Th17-polarising cytokine release

including IL-23, IL-1β and IL-6 (164). *Subsequent sections will highlight the biological and mechanistic activity of heterodimer IL-17A/F.*

1.3.2.3 Cellular sources of IL-17

IL-17A, IL-17F, and IL-17A/F are produced by a number of different cells. Firstly, IL-17 release defines the distinct CD4+ Th17 cell lineage (154, 155). Differentiation of the Th17-cell lineage requires antigen presentation on *major histocompatibility complex* (MHC) class II accompanied by a specific cytokine milieu, including IL-6, IL-1β, TGF-β, IL-21, and IL-23 (155, 161). In addition to Th17 cells, IL-17 is produced by a functionally diverse group of cells restricted by a range of nonclassical MHC-like molecules (165, 166), including CD8+ (Tc)17 effector cells, γδ-T cells, *Natural Killer T* (NKT) cells (167), *Mucosal-Associated Invariant T* (MAIT) cells (168, 169), and type 3 *innate lymphoid cells* (ILC)-3 (158, 170-172). Furthermore, B cells can also produce IL-17A and IL-17F in a temporally separated manner, wherein IL-17A is released earlier (induced by TGF-β and IL-23) and IL-17F later (induced by IL-23 and IL-6) (173). In addition to adaptive immune cells, a variety of innate immune cells secrete IL-17, including neutrophils (174) and macrophage (153). Ultimately, a multitude of different leukocytes produce IL-17A, IL-17F, and IL-17A/F, but the quantities, kinetics and signals which instruct the release of these cytokines are incredibly diverse and require further investigation.

1.3.3 IL-17 receptor biology & signal transduction pathways

1.3.3.1 IL-17 receptor structure & binding domains

IL-17 signal transduction pathways, downstream gene induction, and protein production are dependent on the binding and activation of specific IL-17R subunits. The expression of these subunits is restricted to specific cell moieties, and therefore alters the impact of IL-17-mediated inflammation. IL-17A, IL-17F, and IL-17A/F signal through the IL-17RA and IL-17RC receptor subunits to mediate downstream inflammatory responses (160, 175). IL-17RA is ubiquitously expressed, but IL-17RC expression is restricted to non-hematopoietic cells and limits IL-17-mediated inflammation to structural cells, including AEC (176, 177). Although IL-17A, IL-17F, and IL-17A/F and signal through IL-17RA and IL-17RC, only IL-17A can signal through IL-17RD (178). The precise significance of IL-17A/IL-17RD interaction is still not fully understood as the expression profile of IL-17RD on immune cells is not well defined (179).

IL-17C and IL-17E (IL-25) activate the IL-17RA subunit, but not the IL-17C subunit, altering the cellular moiety of these cytokines and allowing them to target hematopoietic immune cells (158). IL-17C signaling is dependent on the IL-17RA–IL-17RE receptor complex, whereas IL-17E signaling is dependent on the IL-17RA–IL-17RB receptor complex (180, 181). As such, the impact of disparate receptor expression and activation are still being delineated (178).

1.3.3.3 IL-17-mediated intracellular signaling cascades

Members of the IL-17R family are defined by a conserved region in the cytoplasmic tail known as the *SEF/IL-17R* (SEFIR) (182) which is uniquely bound by *Nuclear factor kB activator 1* (Act1), the only other protein containing a SEFIR domain (183-186). Act1 contains a *tumor-necrosis factor receptor–associated factor* (TRAF)-binding motif that recruits different TRAF to initiate multifunctional signaling pathways, including the (canonical) induction of IL-17 gene transcripts and the (non-canonical) regulation of proteins which control longevity of these transcripts (187).

IL-17-mediated induction of target gene transcripts (canonical signaling) is dependent on Act1-mediated ubiquitylation of TRAF6, which results in the activation of NF-κB as well as *mitogen-activated protein kinase* (MAPK) pathways (p38, ERK and JNK) (161, 176). As such, IL-17 target genes show enrichment for binding sites of transcription factors NF-κB and AP-1 in their proximal promoters (188). Blocking MAPK and NF-κB pathways typically impair the induction of IL-17-induced target genes (189). In addition, IL-17RA has a distinct C-terminal region which contains TRAF-binding sites required for activation of the transcription factor *CCAAT/enhancer-binding protein-β* (C/EBPβ), another essential factor in the induction of IL-17 target genes (190, 191).

In addition to promoting the induction of target genes, IL-17-mediated inflammatory signaling increases the stability of mRNA and therefore the production of effector proteins (176, 180, 188, 190). *Messenger RNA* (mRNA) transcripts encoding inflammatory molecules are often intrinsically unstable, a property driven by sequences in the 3′ *untranslated region* (UTR) that serve as binding platforms for *RNA-binding proteins* (RBP) (192, 193). As a result, RBP can alter the stability of mRNA transcripts and the abundance of proteins translated (193, 194). IL-17 alters the abundance, subcellular localization, and activity of RBP therefore altering the quantity and type of inflammatory mediators produced.

IL-17-mediated inflammation initiates the regulation of post-transcriptional signaling by Act1-dependent activation of TRAF2 and TRAF5, resulting in the activation of RBP (195). RBPs including

Arid5a, HuR, DDX3X and Act1 itself, are activated and increase the expression of IL-17-mediated pro-inflammatory mRNA (184, 195-198). TRAF2 and TRAF5 also sequester the RNA destabiliser SF2 (153, 180), preventing degradation of unstable inflammatory chemokine mRNA transcripts (198, 199). Alternatively, IL-17-activated RBP such as the endonuclease Regnase-1 can promote RNA decay and thereby constrain inflammation (197-199). The net effect of IL-17-mediated activation of post-transcriptional regulation often depends on the complex interplay of these RBP, which compete for 3' UTR occupancy on several pro-inflammatory gene transcripts, often in a time- and location-dependent manner (197, 200, 201). Moreover, the activity of RBPs does not affect all IL-17-induced mRNAs in the same way (151). For example, IL-17 induces the expression of both Arid5a and Regnase-1 in an NF-κB-dependent manner (188, 197, 200-203). However, Arid5a promotes the translation of specific IL-17 target mRNAs, including *NFKBIZ* and *CEBPB* (197), and thereby amplifies IL-17-mediated responses (188, 202). Conversely, Regnase-1 promotes degradation of *NFKBIZ* as well as *Il6*, *Il17ra*, and *Il17rc* (200). In addition, regulation of Regnase-1 is dynamic; Regnase-1 activity may be constrained temporarily, allowing inflammatory protein production. This activity is later followed by a return to function, and therefore immune homeostasis (151, 158, 176, 197, 200, 201). *The precise interplay between positive and negative regulators of mRNA binding proteins in the context of IL-17-mediated inflammation is not fully delineated.*

1.3.3.4 IL-17-mediated synergistic signaling pathways

Ultimately, IL-17-mediated regulation of RBP may have a complex role in driving inflammation. In addition to inducing inflammation alone, IL-17 synergistically enhances protein production in the presence of other inflammatory mediators (115, 151, 204-208). As IL-17-mediated inflammation is dependent on the activation of a diverse group of RBP (188, 196, 198, 200, 203, 204, 209-211), the ability of IL-17 to signal synergistically with a diverse group of inflammatory mediators is thought to be dependent on activation of specific RBP, and results in the increased half-life of shared target genes (151). For example, IL-17A augments TNF-α-induced expression of *IL6* and *CXCL8* in *airway smooth muscle* (ASM) cells (212, 213). However, the precise mechanisms which contribute to IL-17-mediated synergy with other pro-inflammatory cytokines in inflammation are still not completely understood.

1.3.4 IL-17-mediated regulation of inflammation

The ability of IL-17 to induce inflammation alone, and in combination with other pro-inflammatory cytokines, makes it an integral component of anti-infective immunity to pathogens (214). IL-17 plays a role in immune responses which control bacterial and fungal infections by promoting epithelial

barrier integrity, CHDP production, and the recruitment of leukocytes to sites of inflammation (215, 216). However, the ability of IL-17 to initiate and propagate inflammation have implicated IL-17 in a variety of chronic inflammatory diseases, including psoriasis, multiple sclerosis, and asthma.

1.3.4.1 Epithelial barrier protection

IL-17-mediated biological activity is essential for maintaining barrier protection. In addition to regulating the proliferation and differentiation of epithelial cells (217, 218), IL-17-mediated biological activity regulates the abundance of proteins which control permeability of mucosal surfaces, called tight junctions (219). In the intestinal epithelium, IL-17A produced by γδ-T cells regulate the cellular localization of the tight junction protein occludin in an Act-1 dependent manner to limit excessive gut permeability during epithelial injury (220). Conversely, in human corneal epithelial cells, IL-17 induces a structural and functional disruption of the epithelial barrier by decreasing *Zonula occludin* (ZO)-2 protein expression (221). Although these mechanisms may be tissue specific, IL-17-mediated alterations to tight junction proteins have been suggested as a mechanism promoting homeostasis during infection and chronic inflammation (161).

1.3.4.2 CHDP / AMP

IL-17 drives anti-infective immunity at epithelial surfaces by inducing the release of CHDP / AMP, including *Lipocalin* (LCN)-2 and β-defensin (161). IL-17 induces the production of LCN-2 (200, 202) which is required for pulmonary host defense against Klebsiella infection (215) and protective against *E. coli* based pneumonia (222). In addition, IL-17A and IL-17F were shown to be required for CRAMP, *mouse β-defensin* (mBD)-3 and mBD-14 expression in response to a mouse model of *S. aureus* colonization *in vivo* (223). In addition to being directly antimicrobial, these peptides are also immunomodulatory molecules (CHDP) which recruit leukocytes to sites of inflammation. For example, human β-defensin-2 (hBD)-2 recruits CCR6+ cells to the sites of inflammation (27), whereas LCN-2 promotes the recruitment and activation of neutrophils at sites of inflammation (200, 202, 223, 224).

1.3.4.3 Indirect cellular recruitment

In addition to contributing to anti-infective immunity through the induction of CHDP/AMP genes, IL-17 drives the production of neutrophil-recruiting chemokines, including *CXCL1*, *CXCL5*, *CXCL8*, and *CCL2* in non-hematopoietic innate immune cells (158, 225-227). Furthermore, IL-17 induces *granulocyte–macrophage colony-stimulating factor* (GM-CSF), thereby driving neutrophil production

in the bone marrow (228). In addition to recruiting neutrophils, IL-17 induces the production of CCL20, which recruits IL-17A-producing TH17 CCR6+ cells (229). Ultimately, the ability of IL-17 to recruit additional IL-17 producing leukocytes, including neutrophils and Th17 cells during inflammatory events may contribute to detrimental positive feedback loops in chronic inflammatory disease.

1.3.5 IL-17-mediated pathophysiology

1.3.5.1 Associations of IL-17 with chronic inflammatory disease

Although transient and regulated IL-17 biological activity elicits physiological responses for host defense and tissue repair, chronic IL-17 activity orchestrates pathophysiological responses in chronic inflammatory diseases, including psoriasis, multiple sclerosis, and asthma (151, 158).

Psoriasis is a common, chronic inflammatory skin disease characterised by painful plaques on the skin (230). Data from pre-clinical mouse models (231, 232), genetic studies (233), clinical data (162, 234), and therapeutic trials (235, 236) suggest that Th17-mediated inflammation is the dominant pathological process in psoriasis. In mice, therapeutic blockade of Th17-polarizing cytokine IL-23 limits pathogenesis and disease progression (231). Similarly, mice lacking IL-17RA are resistant to imiquimod-induced psoriasis (232). In genetic studies, risk alleles upstream and downstream of IL-17 expression are associated with psoriasis (233). Moreover, IL-17A, IL-17F, and IL-17C are elevated in active psoriatic lesions in humans (162, 234). Biologics targeting the IL-17 pathway are highly effective in psoriasis, wherein IL-17A blockade by secukinumab and ixekizumab or IL-17RA blockade by brodalumab (235) alleviate clinical symptoms of the disease.

Multiple sclerosis (MS) is a chronic inflammatory disease of the *central nervous system* (CNS) characterized by damage to demyelinated axons, leading to loss of myelin sheath which provides insulates electrical impulses along nerves (237). Continual damage caused by inflammatory processes in the CNS lead to transient or permanent neurological damage and therefore dementia (238). The pathogenesis of MS is primarily investigated in preclinical studies using a model of an analogous disease in mice, *Experimental Autoimmune Encephalitis* (EAE) (239, 240). In EAE, activation of innate immune cells by PAMP and/or DAMP leads to the production of cytokines which promote the differentiation of Th1 and Th17 cell populations, including IL-1, IL-6, IL-12, IL-18, and IL-23 (241, 242). Myelin-specific Th1 and Th17 cells then produce inflammatory cytokines which induce glial cells to produce Th17 target genes, including inflammatory mediators, chemokines, matrix metalloproteinases, and free radicals (241). Ultimately, this inflammatory cascade leads to myelin

damage and neurological deficits (237). IL-17 has also been identified as a causative cytokine due to its increased abundance in MS plaques collected at autopsy (243), as well as serum samples of patients experiencing relapses and/or remission (244-246). Early-stage clinical trials are underway to investigate the impact of IL-17A-neutralizing antibodies in MS (247).

1.3.5.2 IL-17, airway inflammation, chronic respiratory disease, and asthma

Data from pre-clinical mouse models (248-250), *in vitro* studies (87, 251-254), genetic analyses (255-257), and clinical data (258-261) have implicated IL-17 as a critical cytokine in the pathogenesis of neutrophilic and/or treatment unresponsive asthma.

Clinical data demonstrates that the presence of IL-17A in asthmatics positively correlates with disease severity, IL-8 abundance, and neutrophilic inflammation in the lungs (258-263). In addition to promoting neutrophilic inflammation in the lung, IL-17A may also contribute to decreased lung function, as shown by weak negative correlation between IL-17A and *forced expiratory volume in 1 second* (FEV1) in human BAL (263). Furthermore, IL-17A enhances smooth muscle cell contractility with methacholine, suggesting that IL-17A may drive AHR (264). Moreover, IL-17A may promote allergic inflammation by stimulating the production CCL28 from human bronchial epithelial cells, thereby increasing the recruitment of IgE-containing B cells (265).

The biological activity of IL-17A, IL-17F, and the heterodimer IL-17A/F is increased in asthma (266-271). For example, a previous study demonstrated that mucosa airway biopsies of patients with neutrophilic asthma have increased expression of both IL-17A and IL-17F (268). While IL-17F-producing Th17 cells are increased in the lung submucosa of both eosinophilic and neutrophilic asthmatics, IL-17A-producing Th17 cells are only increased in eosinophilic asthmatic subjects (270). These studies suggest that the heterodimer IL-17A/F is more likely to be enhanced in severe asthma, compared to IL-17A alone.

In addition, there is further direct evidence that IL-17F is a key molecular determinant in the development of asthma; mutations in IL-17F genes increase the probability of developing asthma and increased abundance of IL-17F *in vivo* enhances neutrophil recruitment to the lung and amplifies pulmonary inflammation (272).

IL-17 receptors are widely expressed in lung tissues of asthmatic individuals. In children with severe treatment-refractory asthma IL-17RA-positive cells are enriched in the submucosa and

epithelium (273). Furthermore, stimulation of these individuals' bronchial epithelial cells with IL-17A enhances mRNA expression of *IL17RA* and *IL17RC* (273). Human lung endothelial cells also express *IL17RA* and *IL17RC* and release the neutrophil chemoattractant *CXCL1* in response to both IL-17A and IL-17F (274). Moreover, human eosinophils express both *IL17RA* and *IL17RC*, and release neutrophil chemokines in response to IL-17 stimulation (275). Although many lung cells have IL-17RA and IL-17RC receptors, the differential expression and precise contributions to airway disease have not been fully examined (161).

Exacerbations are a major cause of morbidity and mortality in asthmatics (276). In asthmatics, exacerbations may be induced by viruses and environmental exposures. Viral-induced exacerbations are commonly characterised by neutrophilic inflammation (277, 278) suggesting the activation of IL-17-producing cells. Moreover, diesel fume exposure and cigarette smoke are associated with increase in IL-17A abundance and neutrophilic inflammation in the lungs in asthma (279, 280). IL-17F-producing bronchial cells also contribute to exacerbations via the promotion of airway neutrophil accumulation in the lung (77, 281).

Corticosteroids are effective in reducing symptoms and exacerbations in asthma and have multiple anti-inflammatory effects. However, Th17-mediated neutrophilic asthma is less responsive to corticosteroids (282-285). Pre-clinical mouse models of *ovalbumin* (OVA)-induced Th2-mediated inflammation and AHR are sensitive to dexamethasone (285, 286), whereas dexamethasone has been shown to promote and maintain Th17-mediated inflammation (286). In bronchial epithelial cells, IL-17A reduces the sensitivity of neutrophil chemokine IL-8 to suppression by budesonide by activating PI3K signal transduction pathway and reducing *histone deacetylase* (HDAC)2 activity (287).

IL-17 has also been implicated as a causative factor in other chronic respiratory diseases, including COPD (266, 270, 288), which is characterized by chronic bronchitis, emphysema, and impaired gas exchange in the lung (289). Furthermore, IL-17A is associated with severe, steroid-unresponsive COPD (266, 290, 291). For example, transcriptomic analysis of COPD patient-derived AEC cell brushings found upregulation of IL-17 target genes, including *CXCL3*, *CSF3*, *SAA1* and *CCL20* in approximately one-third of patients with COPD, associated with increased airway obstruction and decreased responses to corticosteroids (266). Moreover, high concentrations of IL-17A induce IL-17RA- and IL-17RC- dependent induction of pro-angiogenic factors from mast cells in severe COPD, potentially contributing to vascular remodeling in the airway (291). Treatments for IL-

17-associated COPD are still being developed, although IL-17 blockade has been shown to reduce pathologies triggered by environmental challenges in pre-clinical settings (289).

1.4 Thesis Overview

1.4.1 Study Rationale

CHDP are naturally occurring immunomodulatory molecules that play a critical role in immunity. CHDP alter signaling events induced by infection and inflammation (18, 21), maintain immune homeostasis (18), and regulate inflammation mediated by pathogens (36, 118, 129), as well as pro-inflammatory cytokines (43, 101). The sole human cathelicidin, LL-37, mediates its immunomodulatory activity through complex interactions with accessory proteins and alteration of many signalling pathways. LL-37 directly interacts with 16 proteins and receptors, affecting the activity of more than 1,000 secondary effector proteins, including signaling nodes and transcription factors, culminating in the altered expression over 900 genes (21, 33, 44, 103). LL-37 levels in the lungs are altered during chronic respiratory disease (102, 139, 146-148), however the impact of LL-37 on inflammatory signaling in respiratory disorders characterized by airway inflammation, such as severe asthma, is not understood.

Asthma affects 3.8 million Canadians and has an annual healthcare expenditure of $2.1 billion (CAD) per year (70, 71, 292). Asthma is a heterogenous disorder characterized by airway inflammation, wherein different pathophysiological pathways contribute to different manifestations of disease (72, 74, 75). Common treatments include ICS, however around 10% of patients do not respond to these treatments and have chronic disease (73). Severe, steroid-unresponsive disease characterized by neutrophil predominant lung inflammation is primarily mediated by Th1/Th17-skewed immune responses, as opposed to Th2-driven inflammation found in eosinophilic asthmatics (76, 77, 79, 85, 93, 150).

Neutrophil-predominant lung inflammation is characterized by the complex interplay of neutrophils that secrete LL-37 and IL-17-producing Th17 lymphocytes (147, 150). IL-17A/F is a critical mediator in airway inflammation, which primarily targets structural cells, including bronchial epithelial cells (176, 180, 197, 200). The IL-17A/F-LL-37-axis in airway inflammation may be a function of neutrophil accumulation in the lung, as NETs produced by neutrophils are enriched with complexes of extracellular DNA and LL-37 (147). Moreover, formation of NET can further enhance Th17-induced responses (IL-17 production) and increase LL-37 in the airways (150). Furthermore, LL-37 has been shown to specifically enhance IL-17A/F-producing Th17 cells during airway inflammation (124). However, the effect of LL-37 on IL-17A/F-mediated protein changes and signaling networks in airway inflammation is poorly understood. *Therefore, in this thesis, I examine the immunomodulatory activity of LL-37 on IL-17A/F-mediated airway inflammation.*

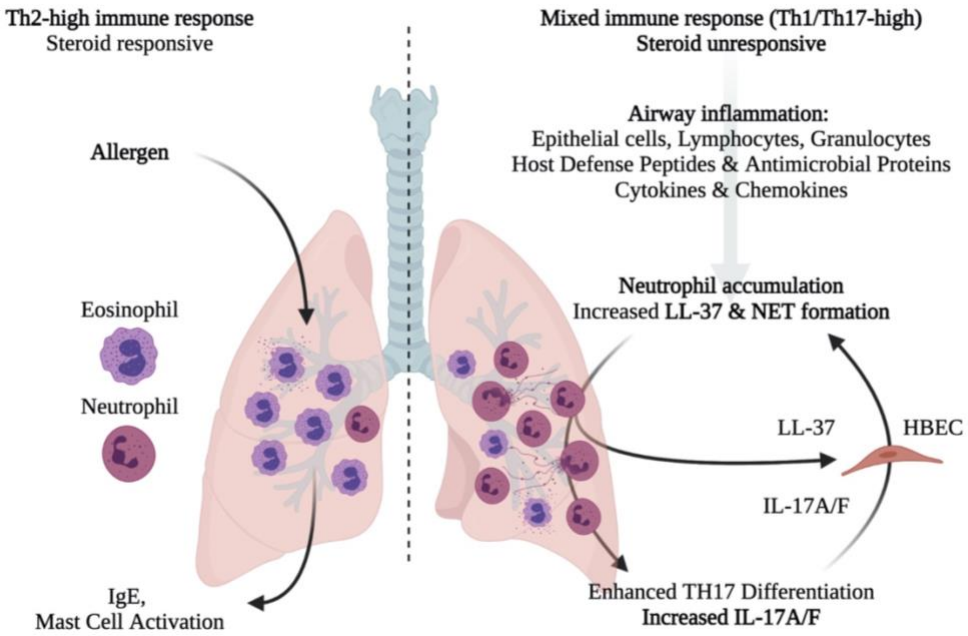

Figure II: Interplay of LL-37 and IL-17A/F in Th1/Th17-high airway inflammation, indicative of severe asthma. Th2-high inflammation (steroid responsive disease) is characterized by eosinophil accumulation in the lung. Th1/Th17-high airway inflammation (steroid unresponsive disease) is characterized by the interplay of neutrophils which secrete LL-37 and IL-17A/F-producing Th17 cells. *This figure created using biorender.com.*

1.4.2 General Hypothesis

I hypothesized that LL-37 will selectively alter IL-17A/F-mediated inflammation to limit neutrophil recruitment in the lung; LL-37 will suppress the production of select IL-17A/F-mediated pro-inflammatory mediators *in vitro* in bronchial epithelial cells and *in vivo* in a mouse model of neutrophilic airway inflammation.

1.4.3 Specific Aims

This thesis aimed to (*1*) characterize IL-17A/F-mediated inflammation (in the presence/and absence of other pro-inflammatory cytokines) in bronchial epithelial cells, (*2*) define regulation of IL-17A/F-mediated inflammatory signaling by LL-37 in bronchial epithelial cells and (*3*) validate these processes in a physiologically relevant mouse model of neutrophilic airway inflammation.

Chapter 2: Materials & Methods

2.1 Reagents:

2.1.1 Peptides

Sequences of the human Cathelicidin LL-37, Citrullinated LL-37 (citLL-37), and scrambled control peptide sLL-37 are shown in Table I, below. Peptides LL-37 and sLL-37 were manufactured by CPC Scientific (Sunnyvale, CA, USA). citLL-37 was obtained from Innovagen AB (Lund, Sweden). All peptides were reconstituted in endotoxin-free E-Toxate^{TM} water to obtain desired concentrations, aliquoted, and stored at -20^{o}C in glass vials until use. Peptides were used within 3 months of reconstitution. Peptides were thawed at room temperature, sonicated for 30 seconds, then vortexed for 15 seconds before use. In cell culture experiments, peptides were diluted to desired concentrations in airway epithelial cells basal medium containing 6 mM L-glutamine without growth factors to final concentrations as indicated.

Table I. Peptide Sequences.

Peptide	Sequence
LL-37	LLGDFFRKSKEKIGKEFKRIVQRIKDFLRNLVPRTES
citLL-37	LLGDFF(Cit)KSKEKIGKEFK(Cit)IVQ(Cit)IKDFL(Cit)NLVP(Cit)TES
sLL-37	RSLEGTDRFPFVRLKNSRKLEFKDIKGIKREQFVKIL

2.1.2 Cytokines, Chemical Inhibitors & Antibodies

Recombinant human cytokines IL-17A/F (carrier free; Cat # 5194-IL-025/CF), TNF-α (Cat # 210-TA) and IFN-γ (Cat # 285-IF) were all obtained from R&D Systems (Oakville, ON, CA).

Pharmacological inhibitors, phosphoinositide 3-kinase (PI3K) inhibitor LY294002 (Cat # S1177), protein kinase-C (PKC) inhibitor GO6976 (Cat # S7119), MAPK/ERK kinase (MEK) inhibitor PD98059 (Cat # S1105), SRC inhibitor 1 (Cat # S6567), and SRC inhibitor Dasatinib (Cat # S1021) were obtained from SelleckChem (Burlington, ON, CA). The inhibitors were used at a concentration range according to the manufacturer's instructions. Selected inhibitors were reconstituted in DMSO (then diluted in airway epithelial cells basal medium containing 6 mM L-glutamine without growth factors to a final dilution of <1:2000 (v/v). Cells were pre-treated with selected inhibitors one hour prior to cytokine stimulation.

Antibodies specific to human LCN-2 (Cat # ab41105), Elafin (Cat # ab184972), Cathepsin S (Cat # ab134157), Cathepsin V (Cat # ab24508), MCPIP1/Regnase-1 (Cat # ab97910), were obtained from Abcam (Toronto, ON, Canada). Antibodies specific to human NF-κB p65 (Cat # 8242S), phospho-IKKα/β D14E12 (Cat # 2697S), Ikβ-ζ (Cat # 9244S), C/EBPβ (Cat # 3082S), phospho-SRC (Cat # 2101S), phospho-AKT(T308) (Cat # 13038S), and phospho-AKT(S473) (Cat # 4060S) were obtained from Cell Signaling Technology. The antibody specific to human Arid5a (#HPA023879) was obtained from Sigma (Toronto, ON, Canada). Anti-human actin antibody (Cat # MAB1501R) was obtained from Millipore (Burlington, MA, USA). Antibodies specific to anti-mouse LCN-2 (Cat # ab70287), IL-17 (Cat # MAB421-100) and TNF-α (Cat #ab1793) were all obtained from Abcam (Toronto, ON, Canada). HRP-linked purified anti-rabbit IgG- (Cat # 707S) and anti-mouse IgG- (Cat # 7076S) secondary antibodies were all obtained from Cell Signaling Technology (distributed by New England Biolabs, ON, Canada). HRP-linked purified anti-goat IgG- (Cat # ab97110) was obtained from Abcam (Toronto, ON, Canada).

2.2 Human Bronchial Epithelial Cell Cultures:

2.2.1 HBEC-3KT cell line

Human bronchial epithelial cell (HBEC)-3KT cell line was obtained from American Type Culture Collection (ATCC® CRL-4051™). HBEC-3KT were cultured in airway epithelial cell basal medium (ATCC® PCS-300-030™) and supplemented with bronchial epithelial cell growth kit (ATCC® PCS-300-040™) containing 6 mM L-Glutamine, 4% w/v Extract-P, HLL supplement (containing 500 μg /mL HSA; 0.6 μg /mL Lecithin; 0.6 μM Linoleic Acid), and Airway Epithelial Cell Supplement (containing 1.0 μM Epinephrine; 5 μg/mL Transferrin; 10 nM T3; 5 μg/mL Hydrocortisone; 5 ng/mL rh-EGF; 5 μg/mL rh-Insulin), according to the manufacturer's instructions. For passaging purposes, HBEC-3KT were maintained at ~80% confluency, trypsinized with 1:3 dilution of 0.5% trypsin-EDTA (Invitrogen™, Life Technologies Inc, Burlington, ON, Canada) in PBS (Gibco), neutralized with 2% FBS (Gibco) in PBS before culturing HBEC-3KT in new T75 flasks or cell culture dishes. HBEC-3KT at ~80% confluency was used for cell stimulation experiments. Culture medium was changed to AEC basal medium containing 6 mM L-glutamine without growth factors, 24 h prior to stimulation with various cytokines and/or peptides as indicated.

2.2.2 Primary Bronchial Epithelial Cells

Human *primary bronchial epithelial cells* (PBEC) were isolated from resected tumor-free lung tissues obtained from four anonymized donors (n=4) undergoing lung resection surgery for lung cancer at the

Leiden University Medical Centre (LUMC; The Netherlands), as previously described (45, 293). These cells were obtained in collaboration from Dr. Pieter Hiemstra's research group at LUMC. The use of available lung tissue for research occurred within the framework of patient care detailed in the "Human Tissue and Medical Research: Code of conduct for responsible use" (2011) (www.federa.org), which describes opt-out procedures for coded anonymous use of these tissues. PBEC were expanded in T75 flasks pre-coated with coating media (containing 30 μg/mL PureCol (Advanced Biomatrix, California, USA), 10 μg/mL fibronectin (Sigma), 10 μg/mL bovine serum albumin (BSA; Sigma) in PBS (Gibco)), and maintained in supplemented keratinocyte serum-free medium (KSFM; Gibco) containing 0.2 ng/mL epidermal growth factor (EGF; Life Technologies), 25 μg/mL bovine pituitary extract (BPE; Gibco), 1 μM isoproterenol (Sigma), and 1:100 dilution of antibiotics Penicillin and Streptomycin (Lonza), until ~80% confluent. PBEC were trypsinized with 0.3 mg/mL trypsin (Gibco) containing 0.1 mg/mL EDTA (Gibco), 1 mg/mL glucose (Gibco) and 1:100 dilution of Penicillin and Streptomycin, in PBS. PBEC were seeded at a density of 5000/cm^2 in TC plates pre-coated with coating media (as described above). PBEC were cultured with a 1:1 mixture of supplemented Dulbecco's modified Eagle's medium (DMEM; Gibco) with a 1:40 dilution of HEPES (Invitrogen), and basal bronchial epithelial cell medium (ScienCell) containing bronchial epithelial cell growth supplement (ScienCell), a 1:100 dilution of Penicillin/Streptomycin and 1 nM of a light stable analog of retinoic acid, EC-23 (Tocris, UK). PBEC were cultured to a maximum of ~80% confluency with the culture medium replaced every 48 h. Culture medium was replaced 24 h prior to stimulation with various cytokines with medium without EGF, BPE, BSA and hydrocortisone (starvation media).

2.3 Mouse models of acute airway inflammation:

2.3.1 Mouse model of House Dust Mite (HDM)-challenged airway inflammation

HDM-challenge protocol used in this study was previously described by us (45, 294, 295), approved by the University of Manitoba Animal Research Ethics Board, and compliant with ARRIVE guidelines for *in vivo* animal research (296). Female BALB/c mice (6 to 7 weeks) were obtained from the Genetic Modeling of Disease Centre (University of Manitoba), randomly sorted, and housed with maximum 5 mice per cage in the central animal care facility at the University of Manitoba. After a one-week acclimatization period, mice were challenged with *intranasal* (i.n.) administration of ~25 μg (35 μL of 7 μg/mL saline) of HDM protein extract (Greer Laboratories, Lenoir, NC, USA), daily for five consecutive days per week for two weeks. The HDM used in this study was of low endotoxin content (<300 EU/mg protein weight). Administration of i.n. HDM were performed in the morning between 9 am and 12 pm. Mice were visually monitored daily for grooming and behavioural abnormalities. Mice

were anesthetized using 90 mg/kg *intraperitoneal* (i.p.) sodium pentobarbital and BAL and lung tissue samples were collected 24 h after the last HDM-challenge studies (45, 294).

2.3.2 Mouse model of HDM- & LPS-challenged neutrophil-skewed airway inflammation

The mouse model of HDM- & LPS-challenge used in this study was previously demonstrated to induce a profile of IL-17-dependent neutrophilic lung inflammation (150). The challenge protocol used in this study was approved by the University of Manitoba Animal Research Ethics Board (protocol #18-038) and experiments compliant with ARRIVE guidelines for *in vivo* animal research (296). Male and Female BALB/c mice (6 to 7 weeks) were obtained from Charles River Laboratories, randomly sorted within sexes, and housed with maximum 5 mice per cage, in the central animal care facility at the University of Manitoba. Following a one-week acclimatization period, mice were administered (i.n.) with 25 μg (35 μL of 7 μg/mL saline) of HDM protein extract (Greer Laboratories, Lenoir, NC, USA) with or without 1 μg LPS (35 μL of 0.03 μg/mL saline), once daily for 3 days (days 0 to 2). Control groups included mice administered with saline (35 μL), or 1 μg LPS (35 μL of 0.03 μg/mL saline). Subsequently, mice were rested for 4 days. Beginning on day 7, 25 μg of HDM (as described above) was administered i.n. for 8 days (days 7 to 14), once daily, to groups previously challenged with either HDM or combination of HDM and LPS. Mice (i.n.) challenged with saline or LPS were administered treated with saline control. HDM used in this study was of low endotoxin content (<300 EU/mg protein weight). Mice were visually monitored daily for grooming and activity. Mouse weight was measured on days 0 to 3 and on alternating days starting on day 7. Mice were anesthetized using sodium pentobarbital and samples were collected 24 h after the last HDM-challenge on day 15.

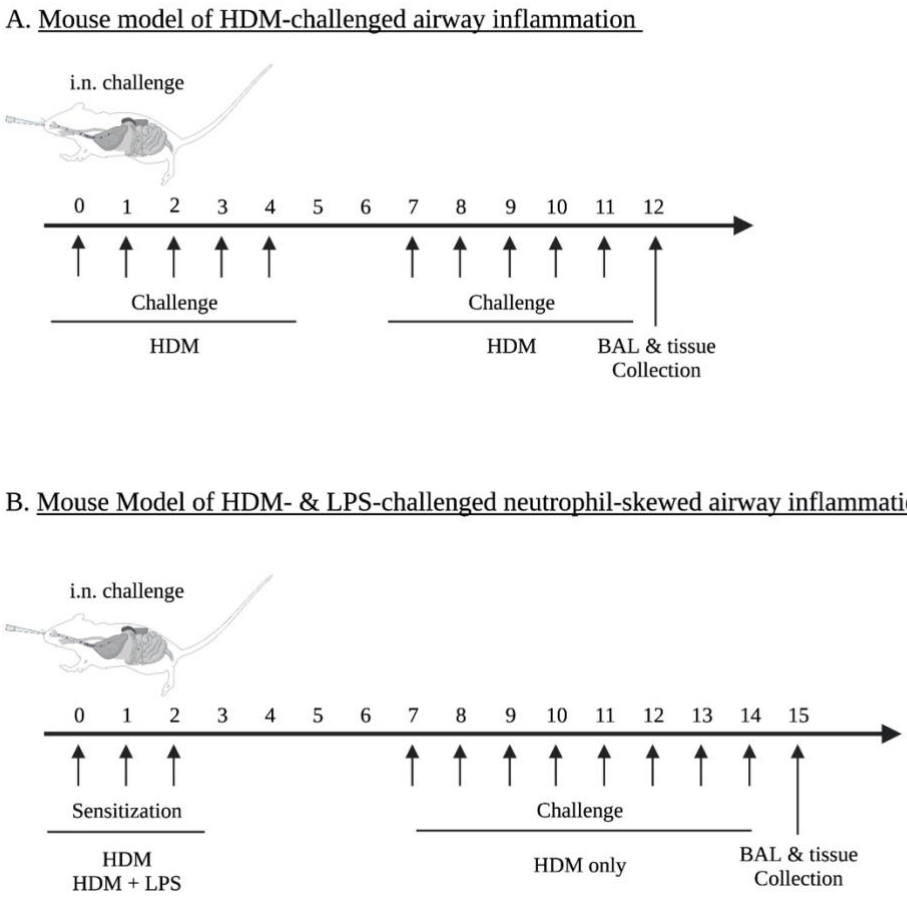

Figure III: Mouse Models of Airway Inflammation.
BALB/c mice, 6-7 weeks of age **(A)** HDM-challenged airway inflammation model; mice were challenged with intranasal (i.n.) administration of ~25 µg (35 µL of 7 µg/mL saline) of HDM for five consecutive days per week for two weeks. **(B)** HDM- & LPS-challenged neutrophil-skewed airway inflammation model; mice were administered (i.n.) with 25 µg (35 µL of 7 µg/mL saline) of HDM protein extract with or without 1 µg LPS (35 µL of 0.03 µg/mL saline), once daily for 3 days (days 0 to 2). Beginning on day 7, 25 µg of HDM (as described above) was administered i.n. for 8 days (days 7 to 14), once daily, to groups previously challenged with either HDM or combination of HDM and LPS. *This figure created using biorender.com.*

2.3.3 Cytokine detection in bronchoalveolar lavage fluid (BAL) and lung tissue

BAL and lung tissue were monitored for the abundance of CHDP, cytokines, and chemokines. BAL samples were centrifuged (150xg for 10 minutes at 4ºC) to obtain cell-free supernatant. Lung tissue specimen from the right lung middle lobe was collected in *Tissue Protein Extraction Reagent* (T-Per) (Pierce; ThermoFisher Scientific, Rockford, IL, USA) containing Protease Inhibitor Cocktail (Sigma Aldrich, Oakville, ON, Canada). Lung tissue was homogenized on ice using the Cole-Parmer LabGEN 125 Homogenizer (Canada Inc, Montreal, QC, Canada). Homogenates were centrifuged (10,000xg at 4ºC) to obtain tissue lysates. Protein abundance in the tissue lysates was quantified with *bicinchoninic acid* (BCA) Protein Assay (Pierce). BAL and lung tissue lysates were aliquoted and stored at -20°C until use.

The abundance of a panel of 29 mouse cytokines and chemokines in the mouse model of HDM-challenged airway inflammation, including IL-17A, IL-17A/F, IL-17F, TNF-α, and KC was measured in BAL and lung tissue lysates using the V-plex Mouse Cytokine 29-Plex Kit and the multiplex *Meso Scale Discovery* (MSD) platform (Meso Scale Discovery, Rockville, MD, USA), as per the manufacturer's instructions. Data was analyzed using the Discovery Workbench 4.0 software (Meso Scale Discovery). Abundance of CRAMP (Cat # EKC36669) was measured by ELISA (Biomatik, Kitchener, Ontario, Canada), and that of LCN-2 (Cat # MLCN20) and IL-17A/F (Cat # M17AF0) were measured by individual Quantikine ELISA assays (R&D Systems, Minneapolis, MN, USA). BAL (50 µL) was used to assess the abundance of LCN-2 and IL-17A/F. BAL (100 µL) was used to determine the abundance of CRAMP. Lung tissue samples were normalized to 50 µg of total protein for cytokine evaluation.

2.3.4 BAL cell differential assessment

Mice were anesthetized using sodium pentobarbital followed by tracheostomy in which a cannula was inserted into the trachea and lung was washed twice, each time with 1 ml (total 2 ml) of cold saline to obtain BAL samples. BAL obtained was centrifuged at (150xg at 10 minutes at *room temperature* (RT)) and cell differentials were assessed using a modified Wright-Giemsa staining (Hema 3® Stat Pack, Fisher Scientific, Hampton, NH, USA) using a Carl Zeiss Axio Lab A1 (Carl Zeiss, Oberkochen, Germany) microscope for imaging. Cell differentials were counted blinded by two different individuals in 8-10 image frames at 20X magnification per slide.

2.4 High content proteomic approaches:

2.4.1 Slow Off-rate Modified Aptamer (SOMAmer)-based proteomics

HBEC-3KT were stimulated with IL-17A/F (50 ng/mL), TNF-α (20 ng/mL), IFN-γ (30 ng/mL) or combinations thereof for 24 h. Total cell lysates were prepared in lysis buffer containing M-PER™ (ThermoFisher Scientific, Burlington, ON, Canada) and HALT protease and phosphatase inhibitor cocktail (ThermoFisher Scientific). Protein concentration was determined by microBCA protein assay kit (Thermo Fisher Scientific, Massachusetts, USA). 14 µg total protein per sample obtained from five independent experiments were probed independently using the Slow off-rate Modified Aptamer (SOMAmer®)-based proteomic array (SomaLogics®-licensed platform at the Manitoba Center of Proteomics and Systems Biology, Canada). The SOMAmer® V.2 technology uses high affinity binding aptamer-based probes called SOMAmers™ (SomaLogic Inc., Boulder CO, USA), with each aptamer (single strand oligonucleotide that bind to protein) probe binding to a specific human protein. SOMAmer® V.2 protein arrays were used for profiling the abundance of 1322 protein targets in each sample. Arrays were processed and analyzed according to the manufacturer's recommended protocol (SOMALogic, Inc) and as detailed in previous studies (297-301). Protein abundance was quantified using the Agilent hybridization array scanner in relative fluorescence unit (RFU), as previously described (297-301). The RFU readout values were log2-transformed and used for pairwise differential analysis as indicated in individual figure legends. Heatmap with hierarchical clustering was generated using the Multi-Experiment Viewer Version 10.2 and GraphPad PRISM 9 was used for visual representation of changes in protein expression profile.

2.4.2 Analysis of protein abundance profiles

Proteins that were significantly altered by the combination IL-17A/F and TNF-α, compared to either cytokine alone (obtained from the proteomics data described above), were used for further analyses using Ingenuity Pathway Analysis (IPA) bioinformatics software (Qiagen), to predict associated chemical inhibitors. Predicted chemical inhibitors selected for *in vitro* validation were those that were predicted by IPA-based informatics analysis to selectively mitigate the production of multiple proteins induced by the combination of IL-17A/F + TNF-α, as compared to either cytokine alone. In addition, prediction of over-represented biological pathways (statistically significant pathway enrichment) was determined by selecting proteins that were significantly enhanced by the combination of IL-17A/F and TNF-α compared to each cytokine alone, by using an in-house analytical tool which was developed to compute enrichment specific to the SOMAmer®-based collection of >1300 proteins in an unbiased

manner. An enrichment score was used for this analysis which represented the probability that the submitted collection of proteins would occur within a given biological process due to randomness.

2.5 Immunological and other biological assays:

2.5.1 Cytotoxicity assay

Lactate Dehydrogenase (LDH) release assay was performed to determine cellular cytotoxicity by monitoring the release of the enzyme LDH in fresh TC supernatants collected after each stimulation. This was performed using a colorimetric LDH detection assay kit from Roche Diagnostic (Laval, QC, Canada), according to the manufacturer's instructions. Briefly, 2% triton X100 (Sigma) was added to a well containing HEC-3KT cells and incubated at 37ºC for 30 minutes for cell lysis and used as a 100% positive control in the LDH assay. 50 µL of cell-free TC supernatant was incubated with LDH substrate mix, containing catalyst diaphorase/NAD^+ and tetrazolium salt INT, for at least 30 minutes at RT. The release of LDH, a cytoplasmic enzyme released due to disruptions in the plasma membrane, was measured at 490 nm and cytotoxicity was calculated relative to the triton-treated positive control at 100%.

2.5.2 Quantitative Real-Time Polymerase Chain Reaction (qRT-PCR)

HBEC-3KT cells were stimulated with cytokines as indicated and total RNA isolated using the Qiagen RNAeasy Plus Mini Kit according to the manufacturer's instructions at 6 h. Total RNA was eluted in RNAse-free water (Ambion) and the concentration and purity of the eluted RNA were determined using a NanoDrop 2000 Spectrophotometer (ThermoFisher Scientific). mRNA expression was analyzed using SuperScript III Platinum Two-Step qRT-PCR Kit with SYBR Green (Invitrogen), according to the manufacturer's instructions using the ABI Prism 7000 sequence detection system (Applied Biosystems, CA, USA), as previously described by us (32). Briefly, total RNA (100 ng) was reverse transcribed in a 20 µl reaction volume for 10 min at 25°C, followed by 50 min at 42°C, after which the reaction was stopped by incubating the reaction solution at 85°C for 5 min. cDNA was aliquoted and stored at -20°C until used for qRT-PCR amplification. For qRT-PCR amplification, the reaction mix containing 2.5 µl of 1/10 diluted cDNA template, 0.5 µl of 10 µM primer mix, 6.25 µl of Platinum SyBr Green qPCR-Super-Mix UDG with Rox reference. RNase-free water was used to bring the total volume to 12.5 µl. Primers used for qRT-PCR are detailed below in Table II. Quantitect Primer Assays were used for qRT-pCR detection of ARID5A (#QT00049672), ZCH312A (#QT00229838), NFKBIZ (#QT00049672), CEBPB (#QT00237580) and 18S (#QT00199367) were obtained from Qiagen. PCR specificity was measured by melting curve analysis. Fold changes were

calculated using the comparative ΔΔCt method (302), after normalization with 18S RNA as the housekeeping gene (selected as it was unchanged in response to pro-inflammatory cytokines).

Table II: Primers used for quantitative real-time PCR

Gene	Forward Primer (5'-3')	Reverse Primer (5'-3')
LCN2	CTCCACCTCAGACCTGATCC	ACATACCACTTCCCCTGGAAT
IL-8	AGACAGCAGAGCACACAAGC	AGGAAGGCTGCCAAGAGAG
CXCL1 (GROα)	TCCTGCATCCCCCATAGTTA	CTTCAGGAACAGCCACCAGT
PI3 (Elafin)	TTATCCCTTGTAAATACCACAGACC	GCCATACCAATCTTTATGCAGTC
MMP-13	CCAGTCTCCGAGGAGAAACA	AAAAACAGCTCCGCATCAAC
18S RNA	GTAACCCGTTGAACCCCATT	CCATCCAATCGGTAGTAGCG

2.5.3 Western blots

Cells were washed with cold PBS, scraped from 60 mm TC plates using a 25 cm cell scrapper (VWR) and collected in *phosphate-buffered saline* (PBS) containing protease inhibitor cocktail (Cell Signaling Technology, Massachusetts, USA). To determine the intracellular abundance of AMP, including LCN-2, Elafin, Cathepsin S, and Cathepsin V, cells were centrifuged at 250xg for 5 min at RT. The cell pellets were lysed in PBS containing Protease Inhibitor Cocktail (PIC) (New England Biolabs, ON, Canada) and 0.5% NP40 (Sigma, Missouri, USA). Cell pellets underwent one 24 h freeze thaw cycle followed by centrifuging (10 000xg at 10 minutes) to obtain cell-free lysates. To determine the abundance of MCPIP1/Regnase-1, NF-κB p65, phospho-IKKα/β, and Ikβ-ζ, cell pellets were lysed in cold PBS containing 1X Cell Lysis Buffer (Cell Signaling Technology, catalogue #9803) containing PIC (New England Biolabs), incubated on ice for 5 minutes, sonicated for 15 seconds, and centrifuged at (14,000xg at 10 minutes) to obtain cell-free lysates. Total protein concentrations in the various cell lysates were determined using a microBCA protein assay kit (Thermo Fisher Scientific, Massachusetts, USA). 10 to 25 μg protein was resolved on 4-12% NuPage™ 10% Bis-Tris Gels (Invitrogen) followed by transfer to nitrocellulose membranes (Millipore, Massachusetts, USA). Membranes were blocked with Tris-buffered saline (TBST) (20 mM Tris–HCl, pH 7.5, 150 mM NaCl, 0.1% Tween-20) containing 5% milk powder. Membranes were probed for antibodies (as indicated above) in TBST containing 2.5% milk powder, subsequently developed using ECL Prime detection system (Thermo Fisher Scientific, Massachusetts, USA) according to the manufacturer's instructions.

2.5.4 Enzyme-linked immunosorbent assay (ELISA)

TC supernatants were collected from HBEC-3KT cells stimulated with peptide and cytokine combinations as indicated. TC supernatants were centrifuged (250xg for 5 minutes) to obtain cell-free samples and the aliquots were stored at -20ºC until use. Abundance of CHDP LCN-2 (Cat # 1757) and Elafin (Cat # 1747), chemokines GROα (Cat # DY275), IL-8 (Cat # DY208), and CCL20 (Cat # DY360), as well as airway remodeling factors MMP13 (Cat # DY511) and MMP9 (Cat # DY911), were measured in the TC supernatants by ELISA using specific antibody pairs (R&D Systems), as per the manufacturer's instructions. Production of chemokine MCP-1 was monitored using an ELISA kit obtained from eBioscience/ThermoFisher Scientific (Mississauga, ON, CA), as per the manufacturer's instructions. Briefly, capture antibodies were diluted in 10 mL PBS. Clear, high binding 96-well flat-bottom plates (Costar™; Cat # 9018) were coated with capture antibodies (100 µL/ well) and incubated overnight at RT or 4ºC as per the manufacturer's instructions for the specific antibody used. Plates were further blocked with 3% (w/v) Bovine Serum Albumin (BSA) in 1X PBS (200 µL/ well) for 1 h at RT. Sample and standards were added to the plate (100 µL/ well) and incubated for 2 h. Standards were added according to the manufacturer's instructions. Sample dilutions for each analyte measured are described in individual figure legends. Detection antibodies were diluted in 1% (w/v) BSA in 1X PBS as per the manufacturer's instructions and incubated for 2 h. Avidin-HRP (eBioscience; Cat # 18-41-0051) in 1% BSA in PBS was added to the plate (100 µL/ well) and incubated for 20 minutes. Following all incubation stages, plates were washed x3 with washing buffer containing 0.05% Tween 20 in 1X PBS. 3,3' 5,5' Tetramethylbenzidine (TMB; Sigma; Cat # T0440) was added to the plate (100 µL/ well) for 10 – 30 minutes for development of the colorimetric reaction. 2N Sulfuric Acid (H_2SO_4) was used to stop the colorimetric reaction. ELISA plates were read at 450 nM (colorimetric detection) and 540 nM (for background).

2.5.5 Neutrophil isolation & migration assay

Venous blood was collected from healthy volunteers with written informed consent, in EDTA vacutainer tubes, according to a protocol approved by the University of Manitoba Research Ethics Board (protocol #H11105). Human neutrophils were isolated using EasySep™ Direct Human Neutrophil Isolation Kit (STEMCELL technologies Canada Inc., Vancouver, BC, Canada; Cat #19666) according to the manufacturer's protocol. Briefly, ~25 ml of blood was gently mixed with the isolation cocktail as well as 50 µl of RapidSpheres™ provided in the kit. After a 5-minute incubation period at RT, D-PBS (containing 1 mM EDTA and free of Ca2+ and Mg2+) was added to bring the total volume to 50 mL. This solution was mixed gently, and neutrophils were isolated through magnetic

negative selection for 10 min. The clear cell suspension was once again subjected to magnetic separation using RapidSpheres™ according to the manufacturer's instructions, to obtain enriched human neutrophils.

TC supernatants were collected from HBEC-3KT cells stimulated with cytokines and chemical inhibitors, as indicated, for 24 h. TC supernatants were stored at -20C until use. TC supernatants (600 µL) were added to the bottom chamber of a Transwell plate. The plates containing TC supernatant were incubated at 37ºC in a humidified chamber with 5% of CO_2 for 30 minutes. Neutrophils isolated from human blood (6×10^5 cells/well, 200 µL) were added to the upper chamber of the inserts of 5.0 µM polycarbonate membrane Transwell permeable supports (Costar, Corning, NY, USA) and incubated for 2 h. The number of neutrophils that migrated to the across the transwell membrane and into the bottom chamber was counted using a Scepter™ 2.0 Handheld Automated Cell Counter (Millipore Ltd, ON, Canada). Human recombinant neutrophil chemokine IL-8 (30 ng/mL) in airway epithelial cells basal medium containing 6 mM L-glutamine was used in the bottom chamber as a positive control for neutrophil migration (32).

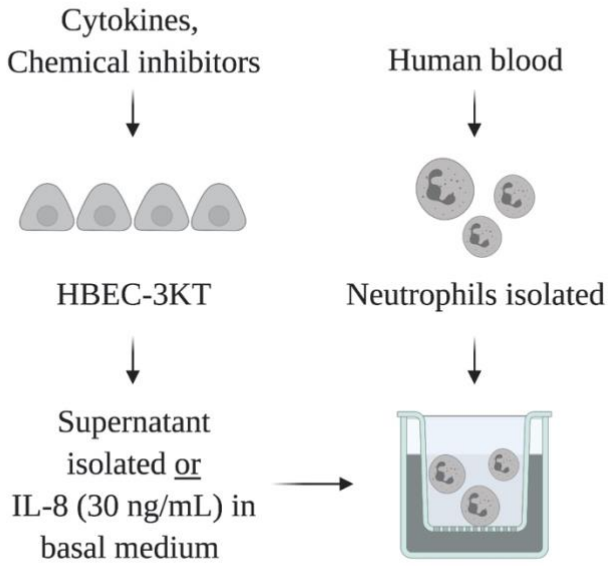

Figure IV: Neutrophil isolation & migration assay. Representative schematic illustrating the principle of the indirect neutrophil migration assay. Human neutrophils were isolated using EasySep™ Direct Human Neutrophil Isolation Kit. TC supernatants were collected from HBEC-3KT cells stimulated with cytokines or chemical inhibitors, as indicated. TC supernatants were added to the bottom chamber of a Transwell plate. The plates containing TC supernatant were incubated at 37ºC in a humidified chamber with 5% of CO_2 for 30 minutes. Neutrophils isolated from human blood (6×10^5 cells/well, 200 µL) were added to the upper chamber of the inserts of 5.0 µM polycarbonate membrane Transwell permeable supports and incubated for 2 h. The number of neutrophils that migrated to the across the transwell membrane and into the bottom chamber was counted using a Scepter™ 2.0 Handheld Automated Cell Counter. *This figure created using biorender.com.*

2.6 Statistical analyses

Specific statistical analyses used are detailed in each figure legend. Briefly, Mann-Whitney U test was used to compare chemokine abundance, including GROα, IL-8, and MCP-1, in response to stimulation with different individual cytokines. *One-way analysis of variance* (ANOVA) was used to compare different RFU values between a panel of 39 different CHDP/AMP in response to cytokines IL-17A/F, TNF-α, and IFN-γ. Mann-Whitney U test was used to compare intracellular abundance of LCN-2, Elafin, Cathepsin S, and Cathepsin V, in response to different cytokines. Pairwise differential analysis was conducted on normalized log2 protein expression values and Welch's t-test was used to determine protein abundance changes that were significantly different from unstimulated HBEC-3KT in response to cytokines IL-17A/F, TNF-α, and IFN-γ. One-way ANOVA with Fisher's least significance difference (LSD) test was used to determine secreted protein changes of airway remodeling factors, including MMP9 and MMP13, response to TNF-α. Two-way ANOVA with Fisher's LSD test was used to determine the impact of chemical inhibitors for Src-Kinase on secreted protein changes of MMP9 and MMP13, response to TNF-α. Two-way ANOVA with Fisher's LSD test was used to determine secreted protein abundance changes between 6 and 48 h of chemokines GROα, IL-8, and MCP-1 in response to cytokines IL-17A/F, TNF-α, and IFN-γ and combinations thereof. Pairwise differential analysis was conducted on normalized log2 protein expression values and Welch's t-test was used to determine protein abundance changes in response to combinations of IL-17A/F + TNF-α that were significantly different from either cytokine alone. Fisher's LSD test was used to determine statistical significance between the abundance of mRNA, intracellular protein, and secreted protein in response to IL-17A/F, TNF-α, and IFN-γ and combinations thereof. One-way ANOVA with Bonferroni's post-hoc test for multiple comparisons was used to determine differences in neutrophil migration is response to IL-17A/F, TNF-α, and IFN-γ and combinations thereof. Two-way ANOVA with Dunnett's test for multiple comparisons was used to determine the impact of chemical inhibitors for PI3K, PKC, and MEK on secreted protein changes in in response to IL-17A/F, TNF-α, and IFN-γ and combinations thereof. Two-way ANOVA with Bonferroni's post-hoc test for multiple comparisons was used to determine differences in protein production in the lungs of a mouse model of HDM-induced airway inflammation. Two-way ANOVA with Dunnett's post-hoc test for multiple comparisons was used to determine differences in peptide-induced cellular cytotoxicity and peptide-mediated chemokine production. One-way ANOVA with Fisher's LSD test was used to determine statistically significant differences in peptide-mediated immunomodulation of cytokine induced responses, including secreted CHDP/AMP and chemokine abundance, as well as the abundance of intracellular signaling proteins including NF-κB- and Arid5a-associated signaling proteins.

Chapter 3: Cytokines IL-17A/F, TNF-α & IFN-γ elicit disparate responses in human bronchial epithelial cells

This section contains some text and figures from a paper published as an original article in *Vaccines* 2018, 6(3), 51. **Anthony Altieri**, Hadeesha Piyadasa, Breann Recksiedler, Victor Spicer, and Neeloffer Mookherjee.

A.A. performed most of the experiments and analyses, contributed to the development of scientific concepts and wrote the text. H.P. validated select protein targets and contributed to scientific concepts. B.R. assisted in the validation of select protein targets. V.S. was involved in curation of the proteomic dataset. N.M. conceived and directly supervised the study, contributed to the development of scientific concepts, and edited the text.

3.1 Abstract

Background: CHDP are immunomodulatory molecules required to resolve infections in the lungs. Despite reports which demonstrate that CHDP exhibit broad immune functions and regulate inflammation, the cytokines which control the production of CHDP in the lung are not defined.

Objective: To profile the ability of pro-inflammatory cytokines IL-17A/F, TNF-α, and IFN-γ to alter the abundance 39 different CHDP in HBEC using high-content aptamer-based proteomic profiling.

Methods: HBEC-3KT were stimulated with pro-inflammatory cytokines IL-17A/F, TNF-α, and IFN-γ for 24 h. The resulting changes in CHDP abundance profiles were determined via targeted aptamer-based proteomic profiling. Independent validation was performed for selected proteins, i.e., proteins that were altered > 2-fold changes ($p<0.01$) in the proteomic array by Western blots. These confirmatory experiments were used to determine the accuracy of the proteomic array and independently demonstrate changes in selected CHDP abundance in HBEC.

Results: IL-17A/F, TNF-α, and IFN-γ altered the abundance of 13 different CHDP. For example, the abundance of *Cathepsin S* (CTSS) was uniquely enhanced by IFN-γ, whereas LCN-2 abundance was uniquely enhanced by IL-17A/F. The abundance of Elafin was increased by IL-17A/F and TNF-α, but was decreased by IFN-γ. All three cytokines decreased the abundance of *Cathepsin V* (CTSV).

Conclusion: These results demonstrate that pro-inflammatory cytokines alter the abundance of CHDP disparately. Moreover, these results suggest that the composition of the inflammatory milieu may influence CHDP abundance and therefore alter the process required for infection control and regulation of inflammation in the lungs.

3.2 Rationale & Introduction

CHDP are critical immunological mediators that regulate inflammation (19-21). In addition to promoting the resolution of inflammation by directly destroying invading pathogens, CHDP also alter signaling pathways initiated in response to inflammatory events (22-24). CHDP are amphipathic, small peptides (<50 amino acids) with a corresponding a net positive charge of +2 to +9 at physiological pH. However, CHDP differ significantly in sequence and structure. Therefore, CHDP have been classified into four broad structural conformation categories, including α-helical linear peptides, β-sheets with disulfide bridges, cyclic peptides, and peptides with extended flexible loop structures (18). Conversely, antimicrobial proteins contain multiple polypeptide subunits and exhibit catalytic activity (303). Hereafter, both diverse families of molecules, including CHDP and antimicrobial proteins will be referred to as *antimicrobial peptides and proteins* (APP) in this chapter. APP are found in a wide variety of complex lifeforms, including insects, plants, and complex animals (21, 23, 304). Over 3,000 APP have been identified to date (111). APP are produced by a wide variety of hematopoietic and non-hematopoietic immune cells, including monocyte/macrophage, neutrophils, and epithelial cells at mucosal surfaces (305, 306). Despite evidence that APP production is altered during inflammatory events (307), and that APP modulate inflammation (19, 33), the ability of pro-inflammatory cytokines to regulate APP production has not been defined.

APP are critical for controlling inflammation in the lung (308). Previous reports have demonstrated that APP exhibit immunomodulatory functions in the lungs, including enhancing phagocytosis and altering innate immune signal transduction pathways initiated by pathogens (308). It has also been demonstrated that the expression of specific APP increases during pneumonia (307). Moreover, previous studies have demonstrated that the expression of specific APP in the lung changes in response to inflammatory stimuli, including infection, allergens, air pollution, and in chronic inflammatory disease (309-314). These changes often originate in the lung epithelia, where they are produced by bronchial epithelial cells (308, 310, 315). Therefore, HBEC are ideal to examine how pro-inflammatory cytokines alter the abundance of APP. Here, we examined the production of APP in

HBEC in response to pro-inflammatory cytokines IL-17A/F, TNF-α, and IFN-γ using a targeted, aptamer-based proteomics approach.

IL-17A/F, TNF-α, and IFN-γ are critical pro-inflammatory cytokines that are elevated in airway inflammation (316-320). IL-17A/F drives the production of chemokines, including GROα and IL-8 in non-hematopoietic innate immune cells, which recruit neutrophils to sites of inflammation (158, 225-227). Furthermore, IL-17 induces GM-CSF production, thereby driving neutrophil production in the bone marrow (228). TNF-α also promotes neutrophil mobilization and recruitment to enhance lung inflammation (205, 213, 321). In contrast, IFN-γ is capable of activating macrophage, dendritic cells, eosinophils, and basophils (322). Despite advancements in understanding the complex role of IL-17A/F, TNF-α, and IFN-γ in airway inflammation, the impact of these cytokines on APP production in the lung is not well defined. Therefore, I performed targeted proteomic profiling to characterize the protein abundance profiles of 39 APP in HBEC in response to IL-17A/F, TNF-α, and IFN-γ. I demonstrate that the production of 13 different APP is altered in response to pro-inflammatory cytokines IL-17A/F, TNF-α, and IFN-γ in HBEC. Overall, protein abundance profiles in HBEC stimulated with IL-17A/F or TNF-α were similar, whereas HBEC stimulated with IFN-γ had a distinct protein abundance profile. The results in this study highlight the disparate alteration of APP expression by IL-17A/F, TNF-α, and IFN-γ in bronchial epithelial cells. These results suggest that changes in specific APP abundance due to the composition of inflammation in the airway may affect the ability to resolve pulmonary infection and inflammation.

3.3 Results

3.3.1 Chemokine production in response to IL-17A/F, TNF-α, and IFN-γ

To select an appropriate timepoint for proteomic profiling of APP, I evaluated chemokine production as a read out for downstream response to cytokines IL-17A/F, TNF-α, and IFN-γ in HBEC-3KT (ATCC CRL-4051). HBEC-3KT were stimulated with IL-17A/F (50 ng/mL), TNF-α (20 ng/mL), or IFN-γ (30 ng/mL) for 24 h. The cytokine concentrations were selected based on previous studies (45, 323). Previous studies have demonstrated that IL-17A/F and TNF-α can stimulate neutrophil chemokines, whereas IFN-γ typically stimulates chemokines that attract monocytes (45, 323). Therefore, we evaluated the production of neutrophil-associated chemokines IL-8 and GROα, and *monocyte chemoattractant protein-1* (MCP-1), in the TC supernatants at by ELISA. IL-17A/F significantly induced the production of GROα, and TNF-α induced the production of both IL-8 and GROα in HBEC-3KT after 24 h (Figure 1.1A). In contrast, IFN-γ significantly induced the production of MCP-1, but not IL-8 or GROα, in HBEC-3KT cells after 24 h (Figure 1.1A). There were no changes in cellular cytotoxicity in response to any of the three cytokines at the selected concentrations (Figure 1.1B). Based on these results a 24 h time point was selected for the targeted proteomic screen in HBEC-3KT.

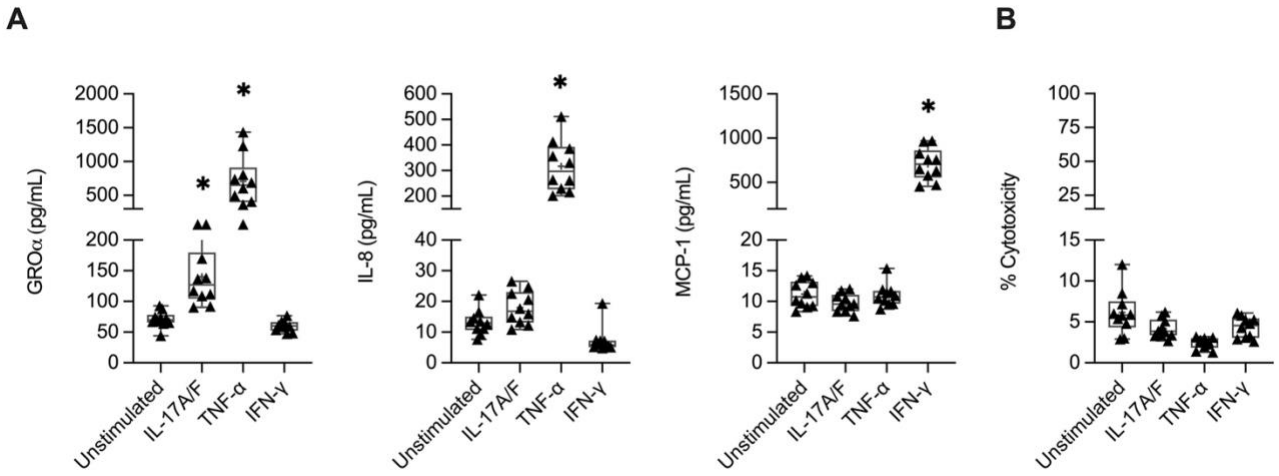

Figure. 1.1: Chemokine production in response to IL-17A/F, TNF-α, and IFN-γ. HBEC-3KT were stimulated with either IL-17A/F (50 ng/mL), TNF-α (20 ng/mL), or IFN-γ (30 ng/mL). Tissue culture supernatants were monitored for **(A)** chemokines GROα, IL-8, and MCP-1 by ELISA, and **(B)** cellular cytotoxicity by LDH assay, 24 h post-stimulation. The dashed lines represent baseline value from unstimulated cells. Results are shown as boxplots, wherein bars show median and IQR, and whiskers show minimum and maximum values. Each data point represents an independent experimental replicate (N=10). Mann-Whitney U test was used to determine statistical significance (*$p < 0.01$).

3.3.2 APP abundance profile in response to IL-17A/F, TNF-α, or IFN-γ

The abundance of 39 different APP was examined in HBEC-3KT cell lysates following stimulation with either IL-17A/F (50 ng/mL), TNF-α (20 ng/mL), or IFN-γ (30 ng/mL) for 24 h, using an aptamer-based proteomic profiling array. Differential analysis was performed on log2 protein abundance values using ANOVA ($p < 0.01$) to identify APP that were differentially abundant in response to IL-17A/F, TNF-α, or IFN-γ, compared to unstimulated cells (Figure 1.2). The abundance of 13 different APP was significantly ($p < 0.01$) altered in response to cytokine stimulation compared to unstimulated cells (Figure 1.2). HBEC-3KT stimulated with IL-17A/F and TNF-α showed similar APP abundance profiles, whereas IFN-γ increased a distinct abundance profile of APP (Figure 1.2).

The 13 APP that were differentially altered by cytokine stimulation were sorted based on abundance values, which demonstrated that the abundance of five specific APP, CTSS, CTSV, Elafin, LCN-2, and *Tenascin* (TNC), were altered by more than 2-fold ($p < 0.01$) in response to IL-17A/F, TNF-α, or IFN-γ compared to unstimulated cells (Figure 1.3). All three cytokines decreased CTSV protein abundance compared to unstimulated cells (Figure 1.3). IL-17A/F uniquely increased the abundance of LCN-2 ~4-fold, whereas TNF-α uniquely enhanced the abundance of TNC ~3-fold compared to unstimulated cells. IL-17A/F and TNF-α similarly increased the abundance of Elafin by 2-fold, whereas IFN-γ decreased Elafin abundance by ~4-fold compared to unstimulated cells. Moreover, IFN-γ, increased the abundance of CTSS ~20-fold compared to unstimulated cells (Figure 1.3). These results indicated that inflammatory cytokines IL-17A/F- and TNF-α-mediated alteration of APP abundance profiles is disparate compared to the APP profile altered by IFN-γ in HBEC-3KT. Specifically, the IL-17A/F- and TNF-α-mediated protein abundance profiles are similar, whereas the IFN-γ-mediated APP abundance profile is distinct.

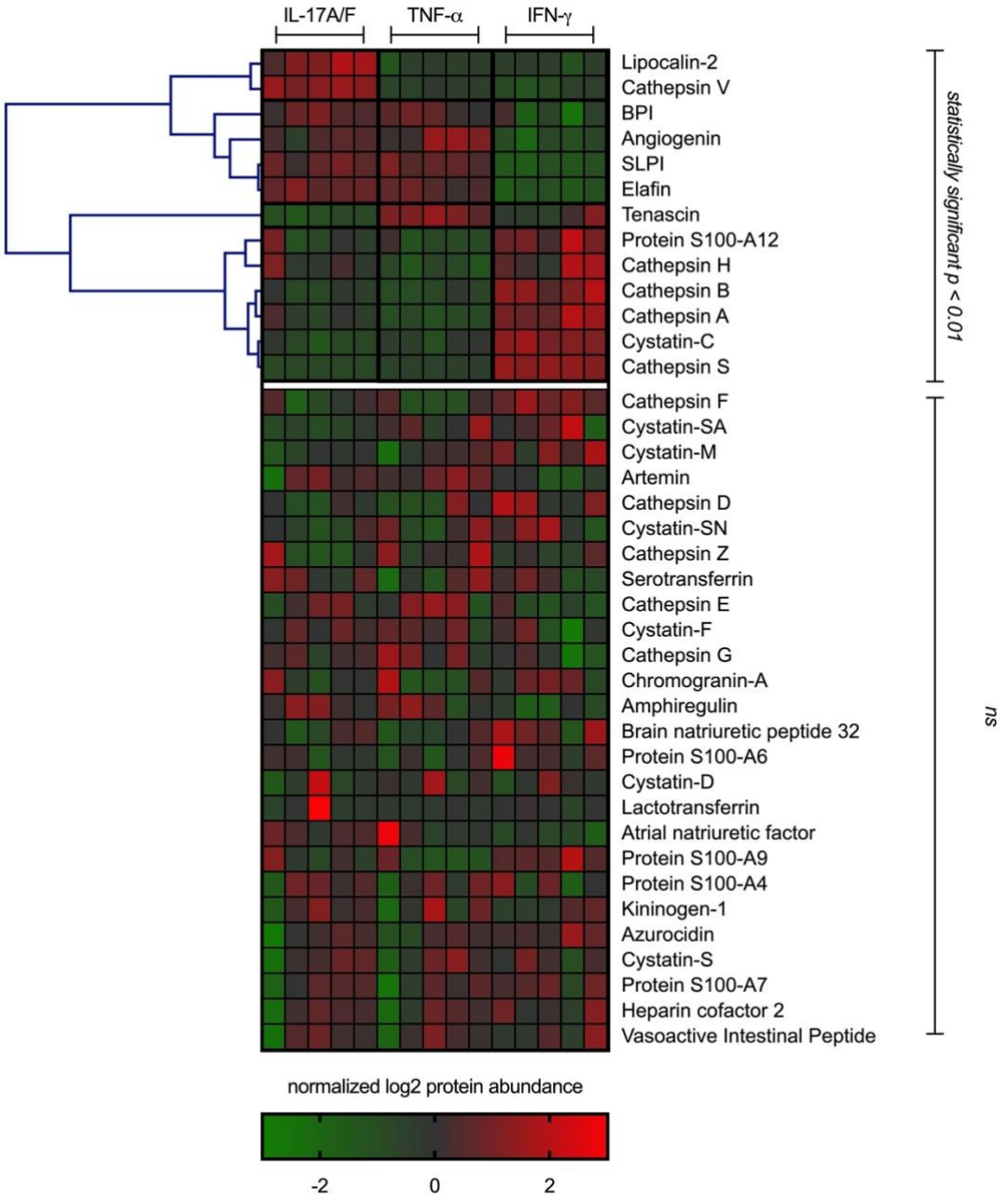

Figure 1.2: APP abundance profile in response to IL-17A/F, TNF-α, or IFN-γ. HBEC-3KT cells were stimulated with either IL-17A/F (50 ng/mL), TNF-α (20 ng/mL), or IFN-γ (30 ng/mL) for 24 h. Equivalent amount of protein (14 µg per sample) from each total cell lysate was processed using aptamer-based proteomic profiling. The RFU readout in the heat map was normalized to yield a consistent dynamic range for visualization. One-way ANOVA was used to compare RFU values between the different conditions in the proteomic array, and $p < 0.01$ was considered statistically significant. Heat map was generated using Multi-Experiment Viewer Version 10.2

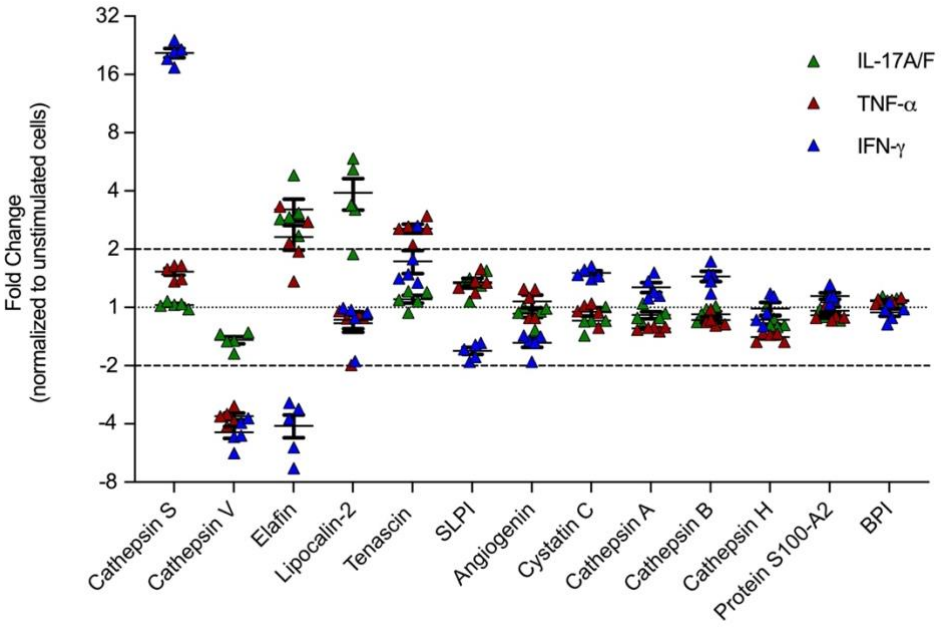

Figure 1.3: Relative abundance of APP significantly altered by IL-17A/F, TNF-α, or IFN-γ. HBEC-3KT were stimulated with either IL-17A/F (50 ng/mL), TNF-α (20 ng/mL), or IFN-γ (30 ng/mL) for 24 h. Equivalent amount of protein (14 μg) from each total cell lysate was processed using aptamer-based proteomic profiling. RFU readout values were log2 transformed for differential analysis. Pair-wise differential analysis was performed to select proteins that were statistically significant using one-way ANOVA and $p < 0.01$ was considered statistically significant. APPs with abundance values ≥ 2-fold relative to unstimulated cells ($p < 0.01$) were selected for further independent confirmatory studies. Each dot represents the expression value from an independent cell lysate, the plots show mean ± standard error.

3.3.3 Independent validation of specific APP production in HBEC-3KT

APP altered ≥ 2-fold ($p < 0.01$) compared to unstimulated cells ($p < 0.01$) specifically CTSS, CTSV, Elafin, and LCN-2 (Figure 1.4) were selected for further independent confirmatory experiments. TNC could not be examined by Western blots or any other immunoassay approach due to challenges associated with the antibody reagent. The abundance of these selected protein targets was determined by Western blot in cell lysates of HBEC-3KT 24 h after stimulation with IL-17A/F (50 ng/mL), TNF-α (20 ng/mL), or IFN-γ (30 ng/mL), in independent experiments. Western blots confirmed that the protein abundance of the selected APP were aligned with that observed in the proteomic aptamer-based protein array analyses. All three cytokines resulted in a decrease of the abundance of CTSV (Figure 1.4). LCN-2 abundance was uniquely enhanced ~10-fold in response to IL-17A/F alone (Figure 1.4). IL-17A/F and TNF-α increased the abundance of Elafin by ≥ 5-fold (Figure 1.4), whereas IFN-γ decreased Elafin protein abundance in HBEC-3KT. IFN-γ uniquely increased the abundance CTSS compared to unstimulated cells (Figure 1.4).

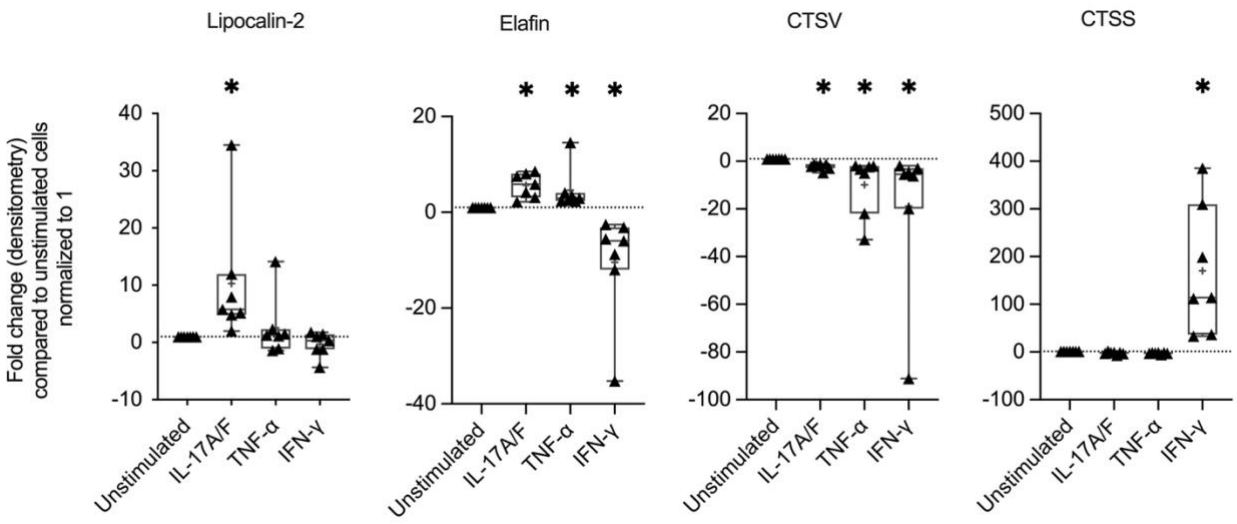

Figure 1.4: Production of APP altered by cytokines IL-17A/F, TNF-α or IFN-γ. HBEC-3KT were stimulated with either IL-17A/F (50 ng/mL), TNF-α (20 ng/mL), or IFN-γ (30 ng/mL) for 24 h. Total cell lysates (10 µg total protein per sample) were probed in Western blot to assess the abundance of LCN-2, Elafin, CTSS, and CTSV, and quantified by densitometry. Abundance of β-actin was used for normalization of protein load across samples. Y-axis represents relative band intensity compared to unstimulated cells normalized to 1. The dashed lines represent baseline value from unstimulated cells. Results are shown as boxplots, wherein bars show median and IQR, and whiskers show minimum and maximum values. Each data point represents an independent experimental replicate (N=7). Mann-Whitney U test was used for statistical analysis (*$p < 0.01$). Cathepsin V (CTSV); Cathepsin S (CTSS).

3.4 Discussion

These results demonstrate that pro-inflammatory cytokines IL-17A/F, TNF-α, and IFN-γ result in disparate alteration of APP abundance in HBEC. These cytokines often play an important role in promoting inflammatory processes in the lungs during chronic respiratory disease, including asthma and COPD (45, 316-319, 324, 325). One mechanism by which these cytokines enhance airway inflammation is by activating bronchial epithelial cells of the airway epithelium, thereby increasing the production of chemokines and therefore leukocyte migration to the lung (269, 326, 327). Consistent with these previous reports, I demonstrate that IL-17A/F and TNF-α enhance the production of neutrophil-associated chemotactic factors (e.g., GROα, IL-8), whereas IFN-γ enhances the production of the monocyte recruiting chemokines (e.g., MCP-1). Some previous studies have suggested that enhanced airway inflammation is a risk factor for increased infections due to the altered expression of specific APP (309). The abundance of several APP is altered in chronic inflammatory diseases, such as COPD and asthma and contribute to pathogenesis (102, 147, 310). Indeed, mediators of airway inflammation such as air pollution and allergens have been associated with altered production of specific APP in the lungs and in bronchial epithelial cells (102, 294, 313). However, despite reports demonstrating a strong association between inflammatory mediators and APP expression, the effect of inflammatory cytokines on APP production in the lung remains unclear.

In this study, I showed that inflammatory cytokines IL-17A/F, TNF-α, and IFN-γ mediate distinct APP abundance signatures in HBEC-3KT. I demonstrated that cytokines IL-17A/F and TNF-α induce a similar APP abundance profile. For example, results from the proteomic array show that IL-17A/F and TNF-α enhance the abundance of similar APP including Elafin, the Elafin-related APP *Secretory-antileukoproteinase* (SLPI), *Bacterial Permeability Increasing Protein* (BPI), and *Angiogenin* (ANG). My findings suggest that IL-17A/F and TNF-α activate similar pathways to alter APP production in HBEC and therefore the bronchial epithelium. Previous studies have demonstrated that IL-17A and TNF-α functionally cooperate to amplify responses via the transcriptional factor C/EBPβ (207, 328). Interestingly, C/EBPβ has been suggested to be involved in the regulation of expression of specific antimicrobial peptides (329, 330). Therefore, the regulation of APP that are similarly altered by cytokines IL-17A/F and TNF-α may be controlled by common transcription factors such as C/EBPβ. In addition, the proteomics screen also shows TNF-α uniquely enhances the abundance of certain APP such as TNC. This is consistent with previous studies that have demonstrated enhancement of TNC levels by TNF-α in bronchial epithelial cells (331). TNC is known to be enhanced in asthma and is indicative of airway remodeling and fibrosis (331, 332). Moreover, I showed

that stimulation with IFN-γ induces an APP profile distinct from both IL-17A/F or TNF-α. A previous study has shown that IL-17A/F and IFN-γ differentially regulate downstream responses in synovial fibroblasts (333). Therefore, I can speculate that IFN-γ-mediated regulation of the APP expression profile in HBEC could be different from that induced by IL-17A/F or TNF-α. Overall, the results in this study provide the impetus to further investigate regulatory mechanisms that are similar and distinct in controlling the expression of APPs that are altered by specific inflammatory cytokines.

Independent confirmatory experiments examining the abundance of APP selected from the proteomics screen demonstrates that IL-17A/F significantly enhances the abundance of LCN-2 and Elafin in HBEC-3KT. The ability of IL-17A/F to enhance LCN-2 was unique, as the other cytokines did not enhance LCN-2 significantly. In addition, both IL-17A/F and TNF-α enhanced Elafin production. In contrast, IFN-γ did not enhance the abundance of LCN-2 and significantly decreases the production of Elafin. LCN-2 is upregulated in epithelial tissues during inflammation and has two critical functions: it is directly antimicrobial at high concentrations and is a neutrophil chemotactic factor (202, 334). The functions of LCN-2 is aligned with previously known functions of IL-17A/F in inflammation; the indirect recruitment of neutrophils through the induction of neutrophil-chemotactic factors GROα and IL-8 at the epithelial surface of the lungs (335). As such, these results suggest that LCN-2 contributes to IL-17A/F-mediated airway inflammation via the recruitment of neutrophils to the lung. Furthermore, LCN-2 may thus also promote the pathophysiology of chronic respiratory disease, as previous reports have indicated that LCN-2 contributes to neutrophilic inflammation leading to epithelial damage (334). In addition to these findings, our lab has demonstrated that inhaled allergens and diesel exhaust (environmental exposures known to enhance airway inflammation and increase susceptibility to infections) enhance the abundance of lipocalins in the human bronchoalveolar lavage fluid (312). In contrast to LCN-2, Elafin is an APP that exhibits anti-inflammatory properties (336). Elafin inhibits serine proteases, including NE to prevent damage to the airway epithelium during lung inflammation (337). The opposing roles of APP in the context of airway inflammation demonstrate the complexity of defining the immunomodulatory functions of APP.

In this study I demonstrate that IFN-γ significantly enhances CTSS but decreases CTSV abundance in HBEC-3KT. Cathepsins are cysteine proteases which contribute to tissue remodeling. Previous studies have demonstrated that IFN-γ regulates CTSS expression in airway epithelial cells as well as in the lung parenchyma in an *Interferon Regulatory Factor* (IRF)-1 dependent manner (338). Additionally, CTSS-mediated activity results in the apoptosis of epithelial cells (339) and the digestion

of elastic tissue (340). Taken together, this suggests that CTSS may play a role in tissue remodeling during inflammation in the airways. In contrast to its effect of CTSS, IFN-γ significantly decreases the abundance of CTSV. CTSV has potent elastase activity and plays a role in airway remodeling (341). Overall, this study demonstrates that IFN-γ regulates the abundance of cathepsins in HBEC-3KT, but the comparative activity of cathepsins and therefore impact of CTSS and CTSV on airway remodeling is not well understood.

3.5 Summary

Previous studies have demonstrated that IL-17A target genes include CHDP (e.g., LCN-2) in non-hematopoietic innate immune cells (188, 202). However, the global impact of IL-17A/F-mediated inflammation on CHDP production was not precisely defined in bronchial epithelial cells. Therefore, I characterized IL-17A/F-mediated inflammation in bronchial epithelial cells to determine the impact on CHDP production.

Proteomic profiling and subsequent independent validation by Western blots demonstrated that IL-17A/F-mediated inflammation significantly enhanced the production of neutrophil-associated CHDP LCN-2 and Elafin in HBEC-3KT at 24 h. In addition to is antimicrobial function, LCN-2 enhances neutrophil recruitment and activation (202, 224, 334), suggesting that IL-17A/F-mediated inflammation recruit neutrophils to the lungs through the induction of neutrophil-associated chemokines and CHDP. In addition, I determined the impact of TNF-α- and IFN-γ-mediated inflammation on CHDP production in HBEC-3KT at 24 h. Here, I demonstrated the disparate nature in which cytokines alter the abundance during CHDP in airway inflammation. Within the 39 CHDP targets in the proteomic array, 13 were altered by the presence of these cytokines. Here, IL-17A/F- or TNF-α-mediated inflammation had similar expression profiles (as compared to IFN-γ-mediated inflammation) in HBEC-3KT at 24 h. IL-17A/F and TNF-α-enhanced the production of neutrophil-associated CHDP, including LCN-2 (202, 334) and Elafin (337). This data indicates that different cytokines shape disparate immunological responses in the lung, including infection control and regulation of inflammation by augmenting the production of CHDP. However, the precise impact of these CHDP on the immune response are not well understood.

Overall, this study demonstrates that pro-inflammatory cytokines which enhance airway inflammation disparately alter the abundance of APP in bronchial epithelial cells. The protein profile altered by IL-17A/F or TNF-α, is distinctly different from that mediated by IFN-γ in bronchial

epithelial cells. These results thus suggest that the composition of the inflammatory milieu influences the abundance of specific APP, which may in turn impact the ability to resolve infection and inflammation in the lung. Further, these findings demonstrate that a pro-inflammatory cytokine can mediate enhancement of APP with opposing functional effects (e.g., IL-17A/F enhances both LCN-2 and Elafin production). The findings in this study highlight the complexity of delineating the immunomodulatory function of APP in the context of lung inflammation.

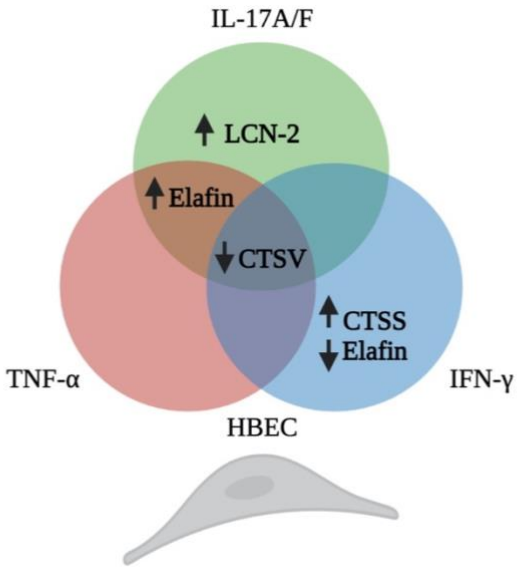

Figure 1.5: Disparate regulation of APP by cytokines IL-17A/F, TNF-α, or IFN-γ in HBEC. Pro-inflammatory cytokines IL-17A/F (green), TNF-α (red), and IFN-γ (blue) alter the production of APP in HBEC. IL-17A/F enhances the production of APP LCN-2 and Elafin. TNF-α enhances the production of Elafin. IFN-γ enhances the production of CTSS and suppresses the production of Elafin. All three cytokines suppress CTSV production. *This figure created using biorender.com.*

Chapter 4: Combination of IL-17A/F and TNF-α uniquely alters the bronchial epithelial cell proteome, and synergistically enhances proteins associated with neutrophil migration

This section contains some text and figures from a manuscript submitted as an original article in the *Journal of Inflammation* (2022). **Anthony Altieri**, Hadeesha Piyadasa, Mahadevappa Hemshekhar, Natasha Osawa, Breann Recksiedler, Victor Spicer, Pieter S Hiemstra, Andrew J Halayko, and Neeloffer Mookherjee.

A.A. and N.M. conceived and designed the study. A.A. performed majority of the experiments, analyzed the data, and wrote the manuscript. H.P. assisted with PBEC experiments and performed the experiments with the animal model of airway inflammation. M.H. assisted with transcriptional analyses, neutrophil migration assays, and provided intellectual input for the study. N.O. and B.R. performed the pharmacological inhibition studies under supervision of A.A. V.S. performed computational analyses. P.H. provided the human PBEC, provided intellectual input into optimization of the protocols with PBEC, and edited the manuscript. A.H. provided intellectual input with animal model studies and edited the manuscript. N.M. obtained funding and supervised the study.

4.1 Abstract

Background: IL-17A/F and TNF-α are elevated in the lungs in chronic respiratory disease, including severe asthma. Previous studies have demonstrated that IL-17A/F and TNF-α cooperate to exacerbate airway inflammation, however proteins altered by their interaction are not elucidated. The impact on the bronchial proteome has not been defined.

Objective: To determine proteins that are altered by the concurrent biological activity of IL-17A/F and TNF-α in human bronchial epithelial cells.

Methods: I used a high-content aptamer-based proteomic array to identify proteins that are uniquely and/or synergistically enhanced by concurrent stimulation with IL-17A/F and TNF-α in HBEC-3KT and PBEC isolated from patients undergoing lung resection. Abundance of selected protein targets were also confirmed in a physiologically representative mouse model of allergen-challenged airway inflammation characterized by eosinophil and neutrophil accumulation in the lung.

Results: The abundance of 70 proteins were significantly altered by the combination of IL-17A/F and TNF-α, compared to either cytokine alone, of which 38 proteins was significantly enhanced by the cytomix. Seven out of these 38 proteins were enhanced ≥ 2-fold, of which 4 proteins were those that promote neutrophil migration. These 4 proteins were CHDP LCN-2 and Elafin, and chemokines IL-8 and GROα. The synergistic increase of these four proteins was further confirmed in independent experiments by western blots and ELISA. I further functionally confirmed that factors secreted by HBEC stimulated with the combination of IL-17A/F and TNF-α uniquely enhances neutrophil migration. In mechanistic studies, I showed that PI3K and PKC pathways selectively control IL-17A/F+TNF-α-mediated synergistic production of LCN-2 and Elafin, but not chemokines. Using an allergen HDM-challenged mouse model of airway inflammation, I also demonstrated enhancement of IL-17A/F, TNF-α, LCN-2 and the neutrophil chemokine KC in the lungs, corroborating the *in vitro* findings *in vivo.*

Conclusion: This study identifies proteins and signaling mediated by concurrent IL-17A/F and TNF-α exposure in the lungs. The protein targets identified in this study may be useful for the development of interventional strategies to target biological processes enhanced by the concurrent presence of IL-17A/F and TNF-α, relevant to chronic respiratory disease.

4.2 Rationale & Introduction

IL-17 is a critical mediator of airway inflammation, associated with the development and increased severity in chronic respiratory disease (93, 150, 267). IL-17 levels are significantly higher in patients with severe asthma, in the disease phenotype that cannot be effectively controlled with available treatments (266-268, 271, 324, 342-344). A challenge in the development of new treatments is the lack of a comprehensive understanding of the range of molecular changes orchestrated by the interplay of IL-17 with other cytokines that are enhanced in the lungs during chronic inflammatory respiratory disease.

The IL-17 family of cytokines includes six different members. The highly homologous IL-17A and IL-17F, and its heterodimer IL-17A/F, are predominantly associated with airway inflammation in humans (172, 288). IL-17A, IL-17F, and IL-17A/F are produced by multiple cell types found at mucosal surfaces of the lung, including $CD4^+$ T-Helper (TH)17 cells, CD8+ Tc17 effector cells, γδ-T cells, NK T cells, and ILC3 (158, 171, 172). IL-17A, IL-17F, and IL-17A/F have been demonstrated to induce qualitatively similar gene activation; however, these are quantitatively different (159). These

cytokines bind to the dimeric IL-17RA and IL-17RC receptor complex to mediate downstream inflammatory responses (160, 175). IL-17RA is ubiquitously expressed, but IL-17RC is primarily restricted to non-hematopoietic cells (176, 177). During airway inflammation the activation of the IL-17RA/RC receptor complex in structural cells, such as airway epithelial cells, results in the production of known IL-17 downstream targets which includes pro-inflammatory cytokines, chemokines, airway remodeling factors, and CHDP with antimicrobial functions (15, 158, 176, 297). Although many of these downstream targets have been identified, these are primarily characterized for IL-17A, but not for the heterodimer IL-17A/F.

The biological activity of IL-17A, IL-17F, and the heterodimer IL-17A/F is increased in asthma (266-271). A previous study demonstrated that mucosa airway biopsies of patients with severe asthma have increased expression of both IL-17A and IL-17F (268). While IL-17F-producing Th17 cells are increased in the lung submucosa of both mild-moderate and severe asthmatics, IL-17A-producing Th17 cells are only increased in mild-moderate asthmatic subjects (270). These studies suggest that the heterodimer IL-17A/F is more likely to be enhanced in severe asthma, compared to IL-17A alone. In severe asthma, although the heterodimer IL-17A/F is known to interplay with other cytokines enhanced in the lungs such as TNF-α (317, 318), the downstream targets, signaling intermediates, and functional outcomes of this interaction remain largely unknown. Thus, the aim of this study was to define global protein changes and signaling intermediates mediated by the heterodimer IL-17A/F, and how these responses change in the presence of TNF-α, in bronchial epithelial cells.

I have previously demonstrated that IL-17A/F and TNF-α alone alters specific APP and various chemokines in HBEC (297). Therefore, in this study I comprehensively characterized the human bronchial epithelial cellular proteome altered by IL-17A/F, in the presence and absence of TNF-α. I further independently confirmed the abundance of selected proteins, performed functional validation, and examined mechanistic signaling pathways, involved in the combinatorial effect of IL-17A/F and TNF-α in HBEC. Moreover, I confirmed the induction of selected proteins uniquely induced by the combination of IL-17A/F and TNF-α in a mouse model of airway inflammation. Overall, the findings in this study provide a comprehensive assessment of downstream protein targets and signaling intermediates enhanced in response to the combinatorial effect of IL-17A/F and TNF-α, and indicates its relevance in the augmentation of neutrophilic airway inflammation.

4.3 Results

4.3.1 IL-17A/F and TNF-α combination uniquely alters the bronchial epithelial cell proteome

HBEC-3KT (ATCC CRL-4051) were stimulated with IL-17A/F (50 ng/mL), in the presence and absence TNF-α (20 ng/ml) or IFN-γ (30 ng/ml), for 6, 12, 24 and 48 h. As I have demonstrated that IFN-γ mediated protein changes are distinctly different from either IL-17A/F or TNF-α (chapter 3), in these experiments IFN-γ was used as a paired control. Cytokine concentrations were selected based on previous studies (45, 267, 271, 297) and results in chapter 3. Chemokines GROα, IL-8, and MCP-1 production was examined in TC supernatants by ELISA (Figure 2.1). Kinetics of chemokine response showed that all three chemokines were significantly enhanced after 24 h stimulation (Figure 2.1), albeit differently by the different stimuli, and thus the 24 h time point was selected for the proteomics study.

Cell lysates (14 µg total protein per sample) were obtained from five independent experiments of HBEC-3KT cells stimulated with IL-17A/F (50 ng/mL), in the presence and absence TNF-α (20 ng/mL) or IFN-γ (30 ng/mL), for 24 h. Each lysate was independently probed using the high-content aptamer-based proteomic array (n=5 for each group). Pairwise differential analysis conducted on normalized log2 protein abundance values showed that IL-17A/F + TNF-α cytomix significantly altered ($p<0.05$) the abundance of 70 proteins, compared to either cytokine alone (Supplementary Table II). Hierarchical clustering of the 70 uniquely abundant proteins showed a distinct protein profile following stimulation of HBEC-3KT with the combination of IL-17A/F and TNF-α, compared to either cytokine alone (Figure 2.2A), whereas IL-17A/F did not significantly alter IFN-γ-mediated protein production in HBEC-3KT (data not shown). Of these 70 proteins, IL-17A/F + TNF-α cytomix increased the abundance of 38 proteins and decreased the abundance of 32 proteins, compared to either cytokine alone (Supplementary Table II). The 38 proteins that were significantly enhanced by the combination of IL-17A/F + TNF-α were primarily associated with three functional categories: CHDP, neutrophil chemotactic factors, and airway remodeling factors. Seven of the 38 proteins were significantly increased by ≥ 2-fold, compared to either cytokine alone (Figure 2.2B). Of these seven proteins, five belonged to the above mentioned three functional categories: CHDP (LCN-2 and Elafin), neutrophil chemokines (IL-8 and GROα), and airway remodeling factor *matrix metalloproteinase* (MMP)13. Therefore, I selected these five proteins for further independent validation and mechanistic studies. Four out of the five selected proteins (LCN-2, Elafin, GROα and IL-8) are also known to enhance neutrophil migration at mucosal surfaces (215, 224, 315, 345), albeit LCN-2 and Elafin have been predominantly described in the context of antimicrobial functions (215, 222, 346). Based on these results, and my previous study (chapter 3) demonstrating that the protein expression profile mediated

by IFN-γ is distinctly different from either IL-17A/F or TNF-α (297), I used IFN-γ as a paired negative control in subsequent *in vitro* validation experiments.

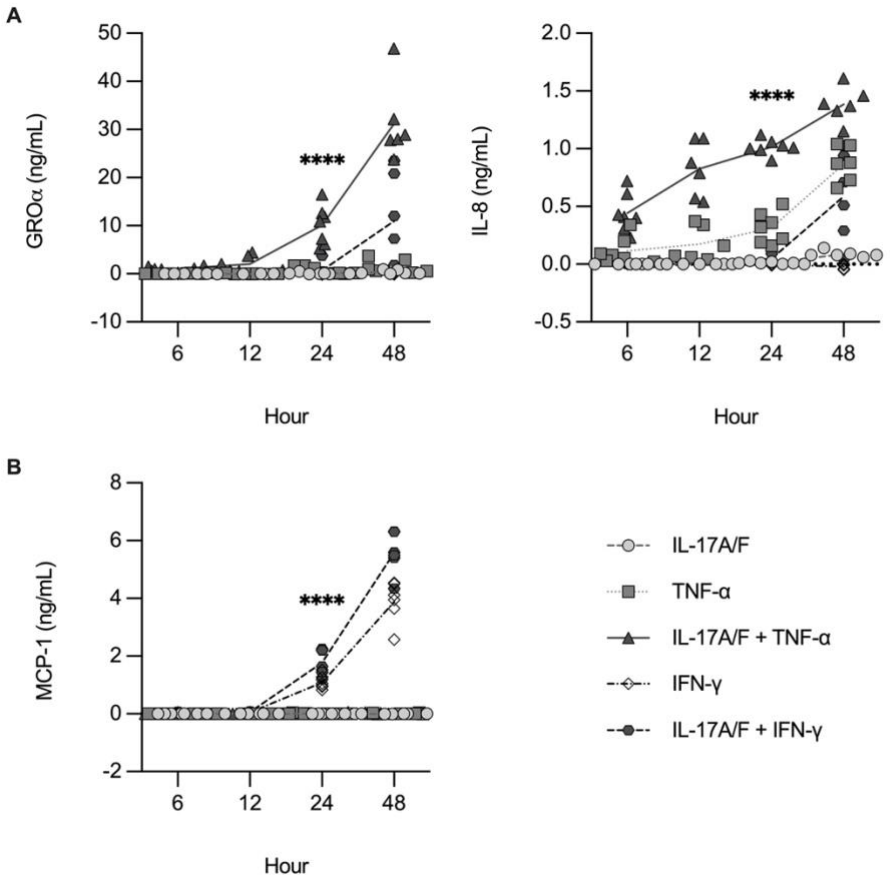

Figure 2.1: Kinetic profile of protein production in human bronchial epithelial cells. HBEC-3KT cells were stimulated with either IL-17A/F (50 ng/mL), TNF-α (20 ng/mL), IFN-γ (30 ng/mL), or cytokine combinations as indicated, for 6, 12, 24, and 48 h. TC supernatants were examined by ELISA for secreted protein abundance of **(A)** IL-17A/F and/or TNF-α-associated neutrophil chemokines GROα and IL-8, and **(B)** IFN-γ-associated monocyte chemokine MCP-1. Increases in protein abundance are shown after subtraction of background values in paired unstimulated cell samples in each replicate. Each data point represents an independent experimental replicate (N≥6), and lines represent the average. Fisher's LSD test for two-way ANOVA was used to determine statistical significance of IL-17A/F-mediated enhancement of acute pro-inflammatory cytokines TNF-α and IFN-γ (*****p<0.0001*).

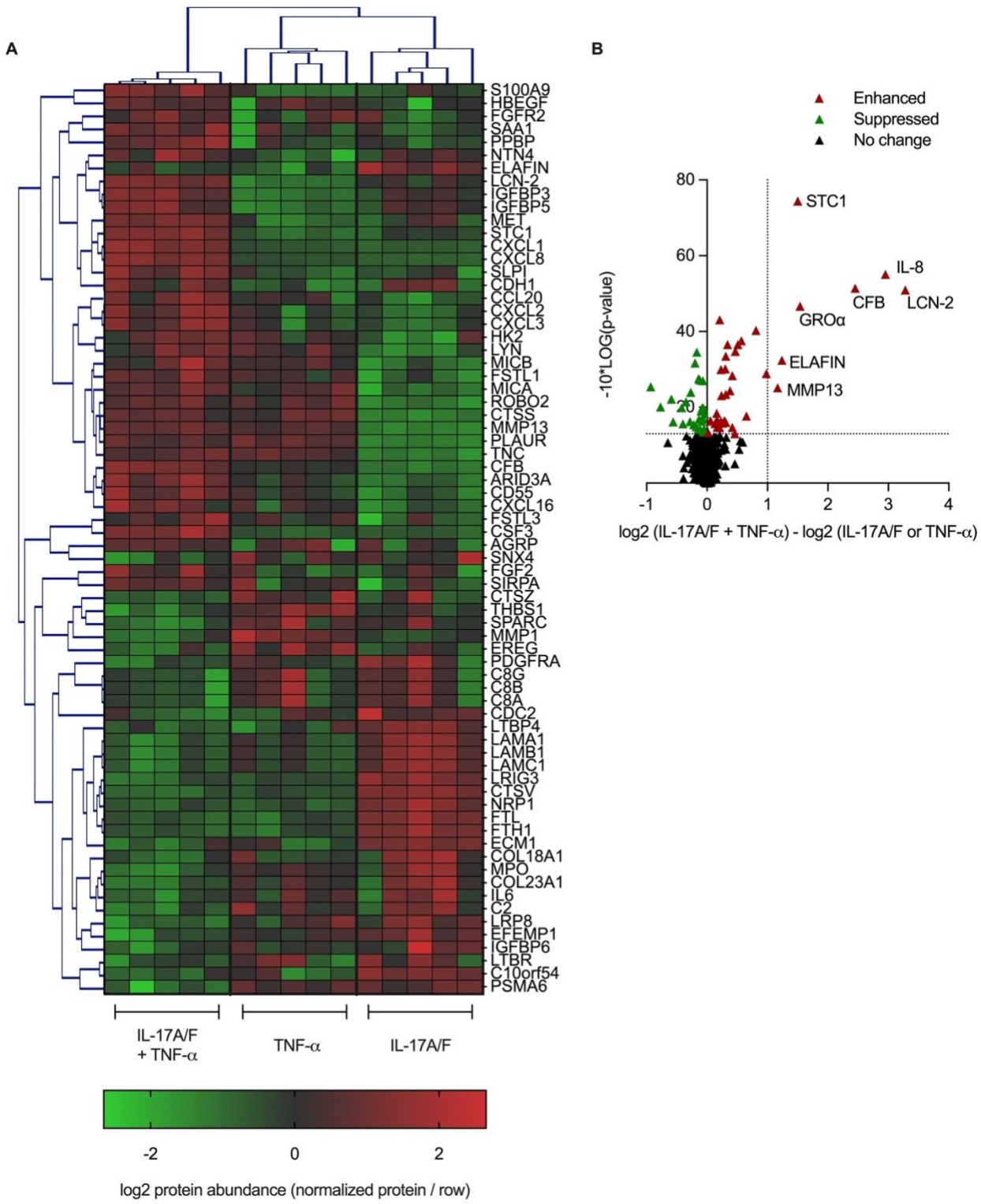
A
S100A9
HBEGF
FGFR2
SAA1
PPBP
NTN4
ELAFIN
LCN-2
IGFBP3
IGFBP5
MET
STC1
CXCL1
CXCL8
SLPI
CDH1
CCL20
CXCL2
CXCL3
HK2
LYN
MICB
FSTL1
MICA
ROBO2
CTSS
MMP13
PLAUR
TNC
CFB
ARID3A
CD55
CXCL16
FSTL3
CSF3
AGRP
SNX4
FGF2
SIRPA
CTSZ
THBS1
SPARC
MMP1
EREG
PDGFRA
C8G
C8B
C8A
CDC2
LTBP4
LAMA1
LAMB1
LAMC1
LRIG3
CTSV
NRP1
FTL
FTH1
ECM1
COL18A1
MPO
COL23A1
IL6
C2
LRP8
EFEMP1
IGFBP6
LTBR
C10orf54
PSMA6
IL-17A/F + TNF-α
TNF-α
IL-17A/F
-2
0
2
log2 protein abundance (normalized protein / row)
B
Enhanced
Suppressed
No change
80
60
40
20
-10*LOG(p-value)
STC1
IL-8
CFB
LCN-2
GROα
ELAFIN
MMP13
-1
0
1
2
3
4
log2 (IL-17A/F + TNF-α) - log2 (IL-17A/F or TNF-α)

Figure 2.2: Characterization of the human bronchial epithelial cell proteome. HBEC-3KT were stimulated with IL-17A/F (50 ng/mL) in the presence and absence of TNF-α (20 ng/mL) for 24 hours. Cell lysates (14 µg total protein per sample) obtained from five independent experiments were probed using the high-content aptamer-based proteomic array. Pairwise differential analysis was conducted on normalized log2 protein expression values, and Welch's t-test with a cut-off of $p<0.05$ was used to select proteins that were significantly enhanced in response to the combination of IL-17A/F + TNF-α, compared to either cytokine alone. Log2 protein abundance values were normalized per row in the heat map to yield a consistent dynamic range for visualization. **(A)** Heat map generated using Multi-Experiment Viewer Version 10.2 to visualize protein expression profile, where each column represents an independent experiment (N=5 per condition). **(B)** Volcano plot demonstrating differentially abundant proteins in response to the combination of IL-17A/F and TNF-α, compared to either cytokine alone.

4.3.2 IL-17A/F and TNF-α combination synergistically enhances transcription of LCN-2 and neutrophil chemokines

HBEC-3KT cells were stimulated with IL-17A/F (50 ng/mL), TNF-α (20 ng/mL), IFN-γ (30 ng/mL), and cytomix as indicated, for 6 h. mRNA expression of genes encoding for the proteins selected from the proteomics data were examined by qRT-PCR. mRNA expression of *NGAL2* (encoding for LCN-2), but not *PI3* (gene for Elafin), was enhanced in a supra-additive manner (synergistically) by the combination of IL-17A/F + TNF-α (by >19-fold) compared to unstimulated cells or each cytokine alone (Figure 2.3A). Expression of *CXCL1* and *CXCL8* (encoding GROα and IL-8 respectively) were also enhanced in a supra-additive manner by the cytomix IL-17A/F + TNF-α (>650-fold and >400-fold respectively) compared to unstimulated cells or each cytokine alone (Figure 2.3B). TNF-α alone significantly enhanced the expression of *MMP13* by ~100-fold compared to unstimulated cells, and this was further significantly enhanced by IL-17A/F (Figure 2.3C). Transcription of none of the selected proteins was enhanced in response to either IFN-γ or its combination with IL-17A/F. These results demonstrated that transcription of three out of the five selected proteins (LCN-2, GROα and IL-8) was synergistically enhanced by the combinatorial action of IL-17A/F and TNF-α in HBEC-3KT.

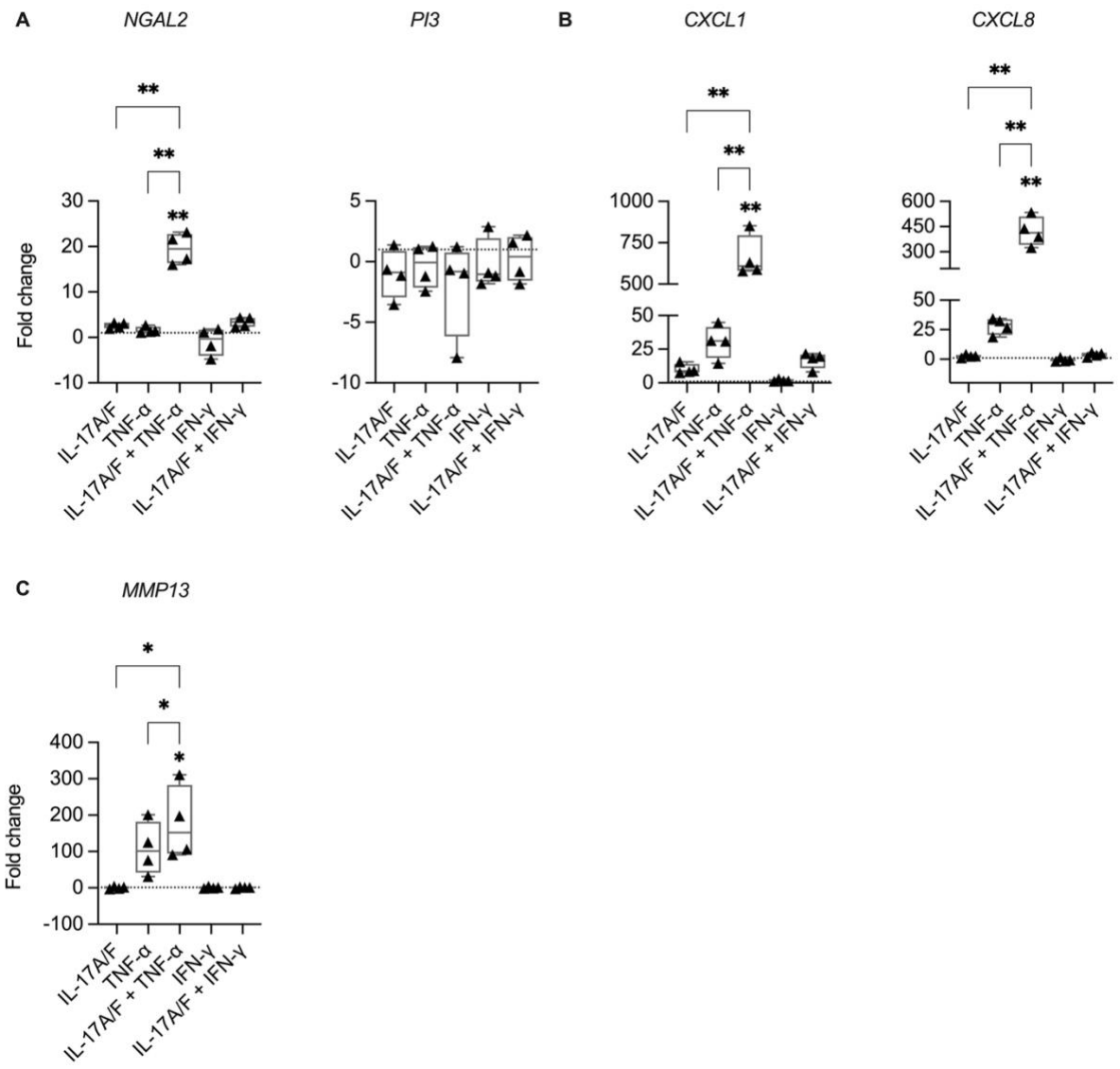

Figure 2.3: Independent validation of transcriptional responses of selected protein targets. HBEC-3KT were stimulated with either IL-17A/F (50 ng/mL), TNF-α (20 ng/mL), IFN-γ (30 ng/mL), or cytokine combinations as indicated, for 6 h. mRNA was isolated and transcriptional responses evaluated by quantitative real-time PCR for **(A)** CHDP LCN-2 (*NGAL2*) and Elafin (*PI3*), **(B)** neutrophil chemokines GROα (*CXCL1*) and IL-8 (*CXCL8*), and **(C)** *MMP13*. Fold changes (y-axis) for each gene was normalized to 18S RNA, and compared to unstimulated cells normalized to 1, using the comparative ΔΔCt method. Results are shown as boxplots, wherein bars show median and IQR, and whiskers show minimum and maximum values. Each data point represents an independent experimental replicate (n=4). Fisher's LSD test for one-way ANOVA was used to determine statistical significance (*$p<0.05$, **$p<0.01$). The dashed line represents normalized baseline value of 1 for unstimulated cells.

4.3.3 IL-17A/F and TNF-α combination synergistically enhances protein abundance of neutrophil chemokines, LCN-2 and Elafin

I independently examined protein production of the five proteins (LCN-2, Elafin, GROα, IL-8, and MMP13) selected from the proteomics dataset, in HBEC-3KT, and in human PBEC isolated from patients undergoing lung resection.

Independent Western blot analyses showed that protein abundance of both CHDP, LCN-2 and Elafin, were synergistically enhanced by the cytomix IL-17A/F + TNF-α in a supra-additive manner, compared to either cytokine alone in HBEC-3KT cell lysates (Figure 2.4). Thus, these results were consistent with the findings from the proteomics data set.

As secreted proteins primarily mediate cellular communication and pathophysiological changes, I also examined the abundance of the five selected proteins by ELISA in TC supernatants obtained from HBEC-3KT cells stimulated with cytokines or cytomix as indicated, after 24 h. Abundance of LCN-2, Elafin, GROα, and IL-8 were all significantly enhanced by the combination of IL-17A/F and TNF-α in a supra-additive manner, compared to either cytokine alone, in TC supernatants obtained from HBEC-3KT cells (Figures 2.5A and 2.5B). In contrast, protein abundance of MMP13 was significantly increased by TNF-α alone and modestly enhanced by the cytomix IL-17A/F + TNF-α in TC supernatants (Figure 2.5C).

To confirm observed effects of protein production in primary cells, I further monitored the abundance of the five selected proteins by ELISA in TC supernatants obtained from human PBEC stimulated with cytokines or cytomix as indicated, after 24 h. Log2 protein abundance values obtained from TC supernatants of PBEC and HBEC-3KT, and from the cellular proteome dataset, was normalized per row in a heat map to obtain comparable dynamic range for visualization and for comparative analyses. The protein abundance profile in response to combination of IL-17A/F and TNF-α compared to either cytokine alone, in HBEC-3KT cellular proteome (Figure 2.6A) was similar to that observed in the TC supernatants from HBEC-3KT (Figure 2.6B) and PBEC (Figure 2.6C), except for IL-8 production. Taken together, these results overall demonstrate that the protein production of LCN-2, Elafin, IL-8 and GROα are synergistically enhanced by the combinatorial effect of IL-17A/F and TNF-α, and that this increased protein abundance is also found in the extracellular milieu.

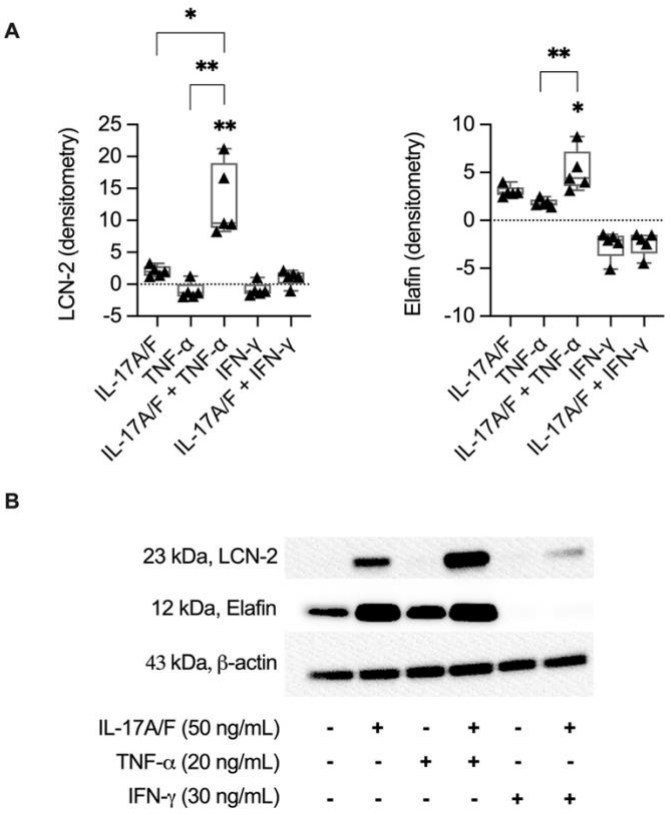

Figure 2.4: Lipocalin-2 and Elafin protein production is synergistically enhanced in human bronchial epithelial cell lysate. HBEC-3KT were stimulated with either IL-17A/F (50 ng/mL), TNF-α (20 ng/mL), IFN-γ (30 ng/mL), or cytomix as indicated, for 24 h. Equivalent loading of cytosolic cell lysates (10 µg per sample) were monitored for the protein abundance of LCN-2 and Elafin by Western blot. Changes in protein abundance are shown as the ratio of abundance in cytokine-treated cells compared to unstimulated cells. The dashed lines represent baseline value from unstimulated cells. Results are shown as boxplots, wherein bars show median and IQR, and whiskers show minimum and maximum values. Each data point represents an independent experimental replicate (N=5). Fisher's LSD test for one-way ANOVA was used to determine statistical significance (*$p<0.05$, **$p<0.01$).

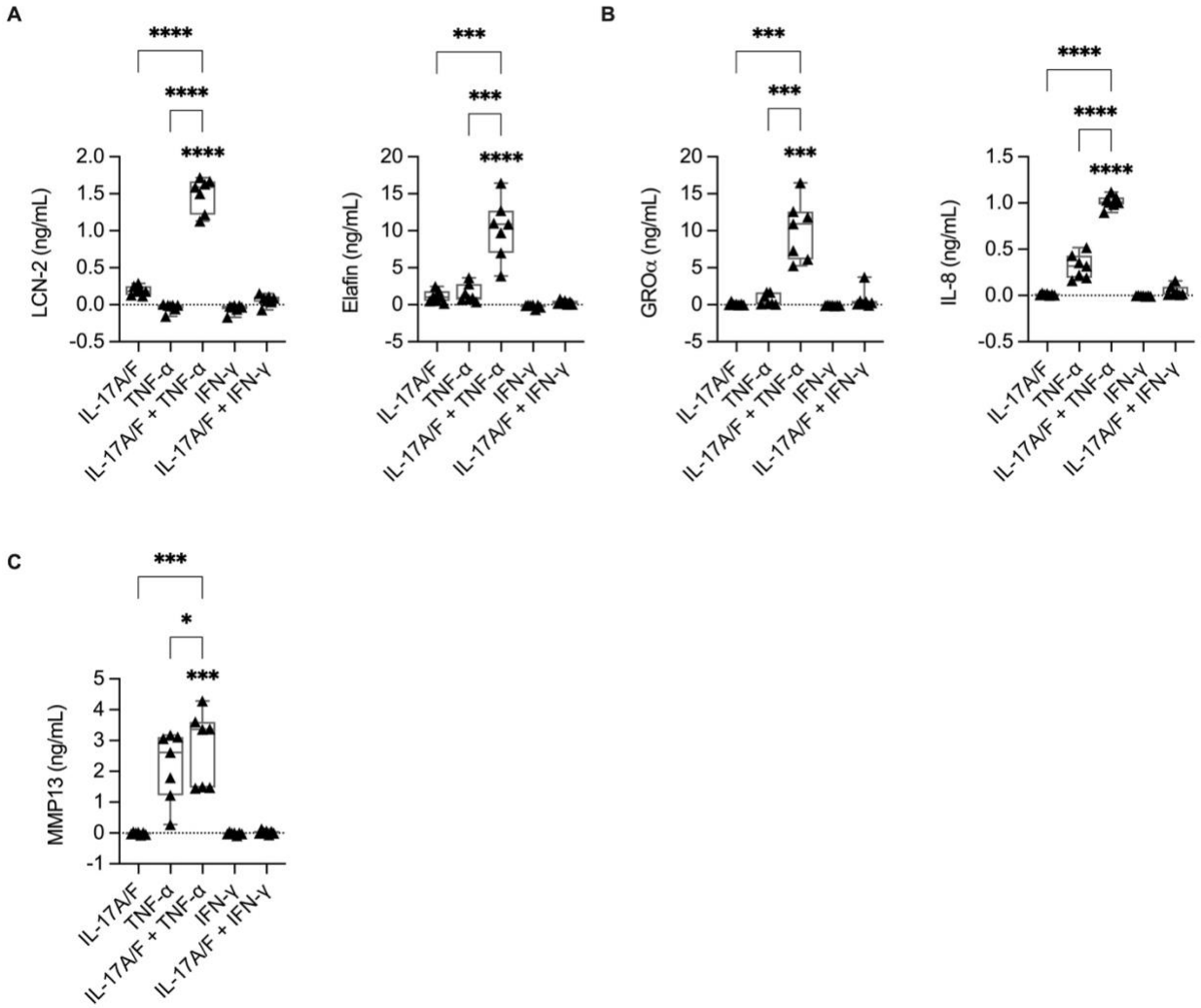

Figure 2.5: Independent examination of selected protein abundance in tissue culture supernatants, in human bronchial epithelial cells. HBEC-3KT were stimulated with either IL-17A/F (50 ng/mL), TNF-α (20 ng/mL), IFN-γ (30 ng/mL), or cytokine combinations as indicated, for 24 h. TC supernatants were examined by ELISA for the protein abundance of **(A)** CHDP LCN-2 and Elafin, **(B)** neutrophil chemokines GROα and IL-8, and **(C)** MMP-13. Increases in protein abundance are reported after subtraction of background values in paired unstimulated cell samples per replicate. The dashed lines represent average baseline value in unstimulated cells. Results are shown as boxplots, wherein bars show median and IQR, and whiskers show minimum and maximum value. Each data point represents an independent experimental replicate (N=7). Fisher's LSD test for one-way ANOVA was used to determine statistical significance (*$p<0.05$, ***$p<0.001$, ****$p<0.0001$).

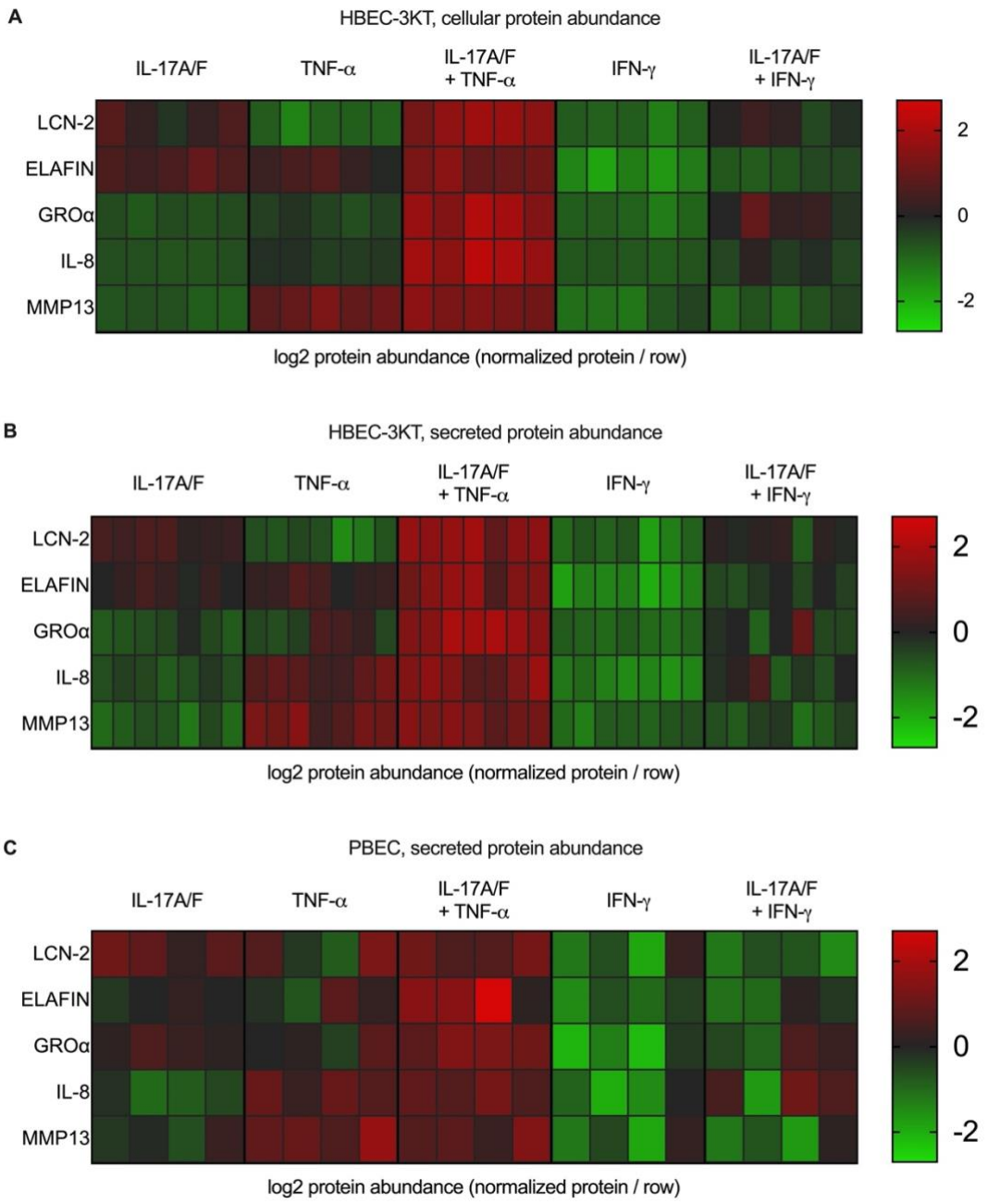

Figure 2.6: Comparative analyses of protein abundance profile in human bronchial epithelial cells and primary cells isolated from lungs. HBEC-3KT (N=5) were stimulated with IL-17A/F (50 ng/mL), TNF-α (20 ng/ml), IFN-γ (30 ng/mL), or cytokine combinations, as indicated for 24 h. **(A)** Cell lysates were probed for select protein targets by aptamer-based proteomic array. **(B)** HBEC-3KT (N=7) and **(C)** human PBEC (N=4 independent donors) TC supernatant was monitored for protein abundance of LCN-2, Elafin, GROα, IL-8, and MMP13, by ELISA after 24 h. Increases in protein abundance was calculated after subtraction of background values in paired unstimulated cells for each biological replicate. Log2 protein abundance values were normalized per row in the heat map to yield a consistent dynamic range for visualization and comparative analyses.

4.3.4: The combination of IL-17A/F and TNF-α uniquely enhances neutrophil migration

Chemokines IL-8 and GROα, as well as CHDP LCN-2 and Elafin, are known to contribute to neutrophil accumulation at sites of inflammation (215, 224, 315, 345). Chemoattractant functions of these proteins are primarily mediated when secreted in the extracellular milieu. My results have demonstrated that the combination of IL-17A/F and TNF-α synergistically enhance the abundance of these proteins in TC supernatants secreted from human bronchial epithelial cells (both HBEC and PBEC), compared to either cytokine alone. Thus, these results suggest that the combination of IL-17A/F and TNF-α may synergistically enhance neutrophil migration. In addition, bioinformatics assessment of the cellular proteome that was enhanced by IL-17A/F + TNF-α compared to either cytokine alone, using an in-house software tool specific to the aptamer-based proteomic array, identified biological processes which drive neutrophil accumulation in the lungs, such as neutrophil chemokine receptor binding, positive regulation of neutrophil chemotaxis, and chemokine-mediated signaling pathways, as overrepresented biological pathways (Figure 2.7). Therefore, I further performed functional assays to assess the effect of TC supernatants obtained from HBEC stimulated with the combination of IL-17A/F and TNF-α on neutrophil migration.

HBEC-3KT cells were stimulated with IL-17A/F (50 ng/mL) in the presence and absence of TNF-α (20 ng/mL) for 24 h. Subsequently TC supernatants were used in the bottom chamber of Transwell plates to examine trans-well migration of neutrophils isolated from human blood (Figure 2.8A). Recombinant chemokine IL-8 (30 ng/mL) was used as a positive control in the bottom chamber of Transwell plates. TC supernatant obtained from cells stimulated with the combination of IL-17A/F and TNF-α significantly enhanced neutrophil migration, compared to that obtained from unstimulated cells (Figure 2.8B). TC supernatants obtained from cells stimulated with either IL-17A/F or TNF-α alone did not significantly enhance neutrophil migration (Figure 2.8B). These results demonstrated that factors secreted in the TC supernatants obtained from bronchial epithelial cells stimulated with the combination of IL-17A/F and TNF-α uniquely enhanced neutrophil migration.

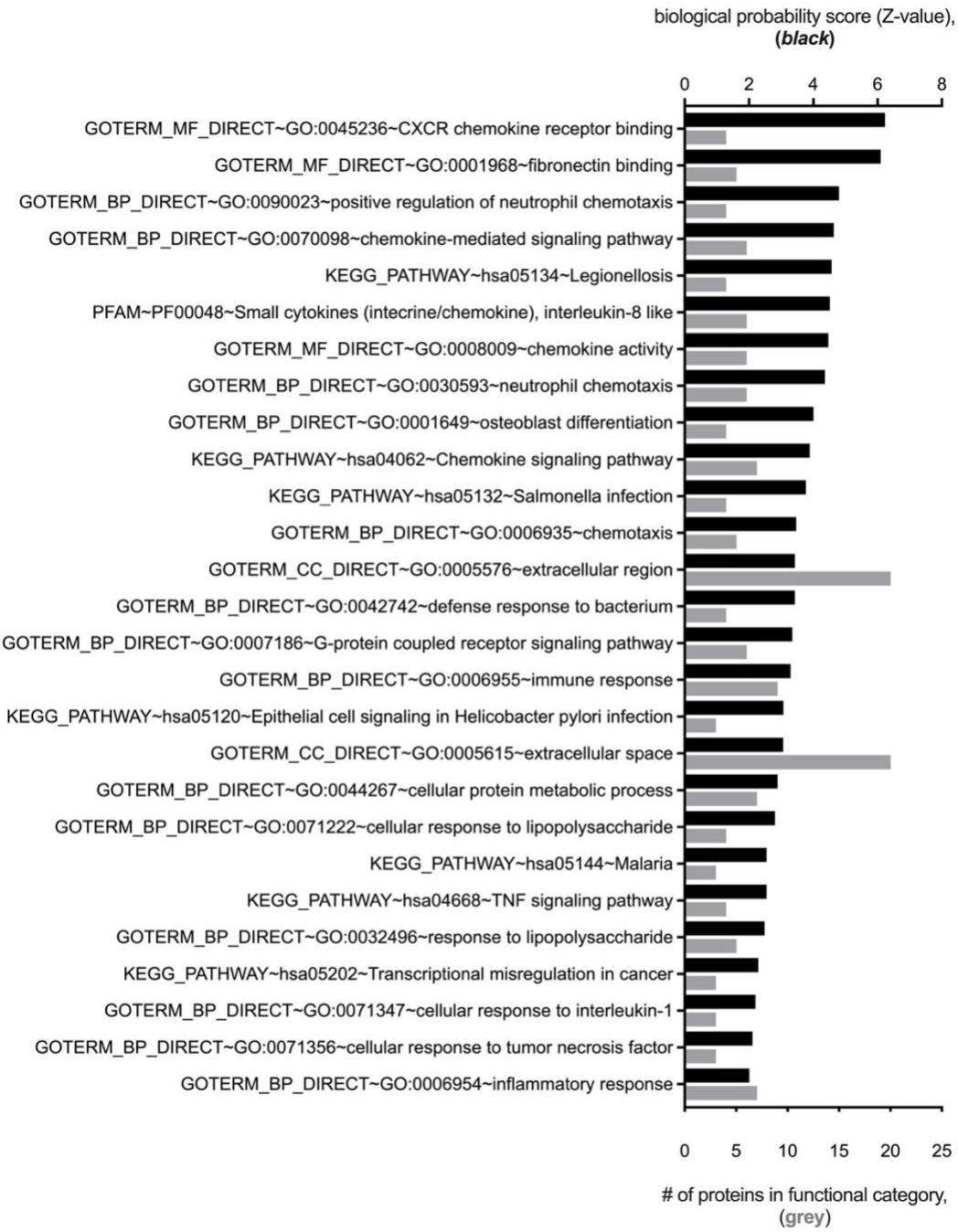

Figure 2.7: Pathway enrichment analysis. HBEC-3KT cells were stimulated with IL-17A/F (50 ng/mL) in the presence/absence of TNF-α (20 ng/mL) for 24 hours. Cell lysates (14 µg total protein per sample) obtained from five experimental replicates were probed independently using the high-content aptamer-based proteomic array. Pairwise differential analysis was conducted on normalized log2 protein expression values, and Welch's t-test with a cut-off of $p<0.05$ was used to select proteins that were significantly enhanced in response to the combination of IL-17A/F + TNF-α, compared to either cytokine alone. Statistically significant pathway enrichment was also determined by selecting positively up-regulated (>0.2 log2 protein abundance) proteins (n=30) using an in-house analytical tool developed to compute enrichment specific to the aptamer-specific collection of >1300 proteins. The enrichment score represents the probability that the submitted collection of proteins would occur within a given biological process due to randomness.

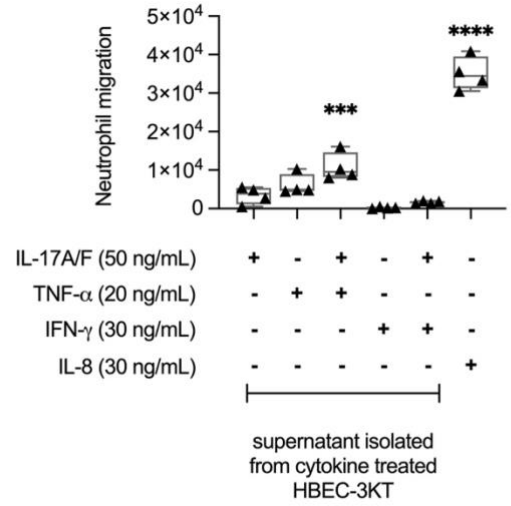

Figure 2.8: Functional validation of neutrophil migration enhanced by the combination of IL-17A/F and TNF-α. HBEC-3KT were stimulated with IL-17A/F (50 ng/mL), TNF-α (20 ng/mL), IFN-γ (30 ng/mL), or cytomix combinations, as indicated. Tissue culture supernatants were collected after 24 h and used in trans-well cell migration assays, to monitor the migration of neutrophils isolated from human blood. Cell culture medium spiked with human recombinant IL-8 (30 ng/mL) was used as a positive control. Results are shown as boxplots with the median line and IQR, and whiskers show minimum and maximum values. Each data point represents an independent experimental replicate with HBEC supernatant (N=4), using neutrophil isolated from one donor. Each dot represents the average number of neutrophils that traversed the membrane within two hours in each experiment. One-way ANOVA with Bonferroni's post-hoc test for multiple comparisons was used for statistical significance compared to unstimulated cells as control *(***p<0.001, ****p < 0.0001).*

4.3.5 LCN2 and Elafin production mediated by the combination of IL-17A/F and TNF-α involves PKC and PI3K signaling pathways

Protein expression profiles obtained from the proteomics dataset were analyzed using the IPA bioinformatics platform (Qiagen) to identify inhibitors of overrepresented signaling pathways. Comparative analyses of log2 expression values of the proteins that were differentially expressed in response to IL-17A/F + TNF-α (Supplementary Table II), identified PI3K inhibitor LY294002, PKC inhibitor GO6976, and MEK inhibitor PD98059, as upstream chemical inhibitors for proteins that were significantly altered by IL-17A/F + TNF-α compared to either cytokine alone. Based on these *in silico* results, HBEC-3KT cells were pre-treated with LY294002, GO6976, and PD98059 at various concentrations (4 to 16 μM) for one hour prior to stimulation with IL-17A/F, TNF-α, or IL-17A/F + TNF-α cytomix as indicated. TC supernatants collected 24 h after stimulation were used to examine the protein abundance of LCN-2, Elafin, GROα, and IL-8, as these proteins were demonstrated to be synergistically enhanced by the combination of IL-17A/F and TNF-α (Figure 2.5). PI3K inhibitor LY294002 significantly suppressed IL-17A/F + TNF-α-mediated production of LCN-2 and Elafin at all concentrations tested, in a dose-dependent manner (Figure 2.9A). PKC inhibitor GO6976 also decreased the production of LCN-2 and Elafin, albeit at the higher concentrations (Figure 2.9B). MEK inhibitor PD98059 suppressed Elafin production in a dose dependent manner but did not affect LCN-2 production (Figure 2.9C).

In contrast, none of the inhibitors suppressed IL-17A/F + TNF-α-mediated enhancement of neutrophil chemokines GROα and IL-8 (Figure 2.10). These results demonstrate that PI3K and PKC pathways selectively control the synergistic effect of IL-17A/F + TNF-α-mediated production of CHDP LCN-2 and Elafin, but not the production of IL-8 and GROα, in HBEC. These results suggest that disparate mechanisms are involved in the synergistic enhancement of CHDP and chemokines, mediated by the combination of IL-17A/F and TNF-α.

To determine the impact of select pharmacological inhibitors on neutrophil migration, HBEC-3KT cells were pre-treated with 16 μM LY294002 or GO6976 for 1 h at 37ºC, prior to stimulation with IL-17A/F + TNF-α cytomix as indicated. TC supernatants were collected 24 h after stimulation and ELISA was used to confirm that 16 μM LY294002 or GO6976 significantly suppressed IL-17A/F + TNF-α-mediated enhancement of LCN-2 and Elafin (Figure 2.11). Next, I functionally validated the effect of the combination of IL-17A/F and TNF-α on neutrophil migration in the presence/absence of select pharmacological inhibitors. TC supernatants were then used in the bottom chamber of Transwell

plates to examine trans-well migration of neutrophils isolated from human blood. Recombinant chemokine IL-8 (30 ng/mL) was used as a positive control, whereas media was used as a vehicle control. TC supernatant obtained from cells stimulated with the combination of IL-17A/F and TNF-α tended enhanced neutrophil migration ($p = 0.07$), compared to that obtained from unstimulated cells, but suppression of LCN-2 and Elafin by pharmacological inhibition did not alter neutrophil migration (Figure 2.11). These results indicate that the bronchial proteome induced in response to the combination of IL-17A/F + TNF-α has multiple redundant, secreted proteins which can enhance neutrophil recruitment. These results highlight that unique proteome enhanced in response to the combination of IL-17A/F + TNF-α drives neutrophil migration, as compared to any protein alone.

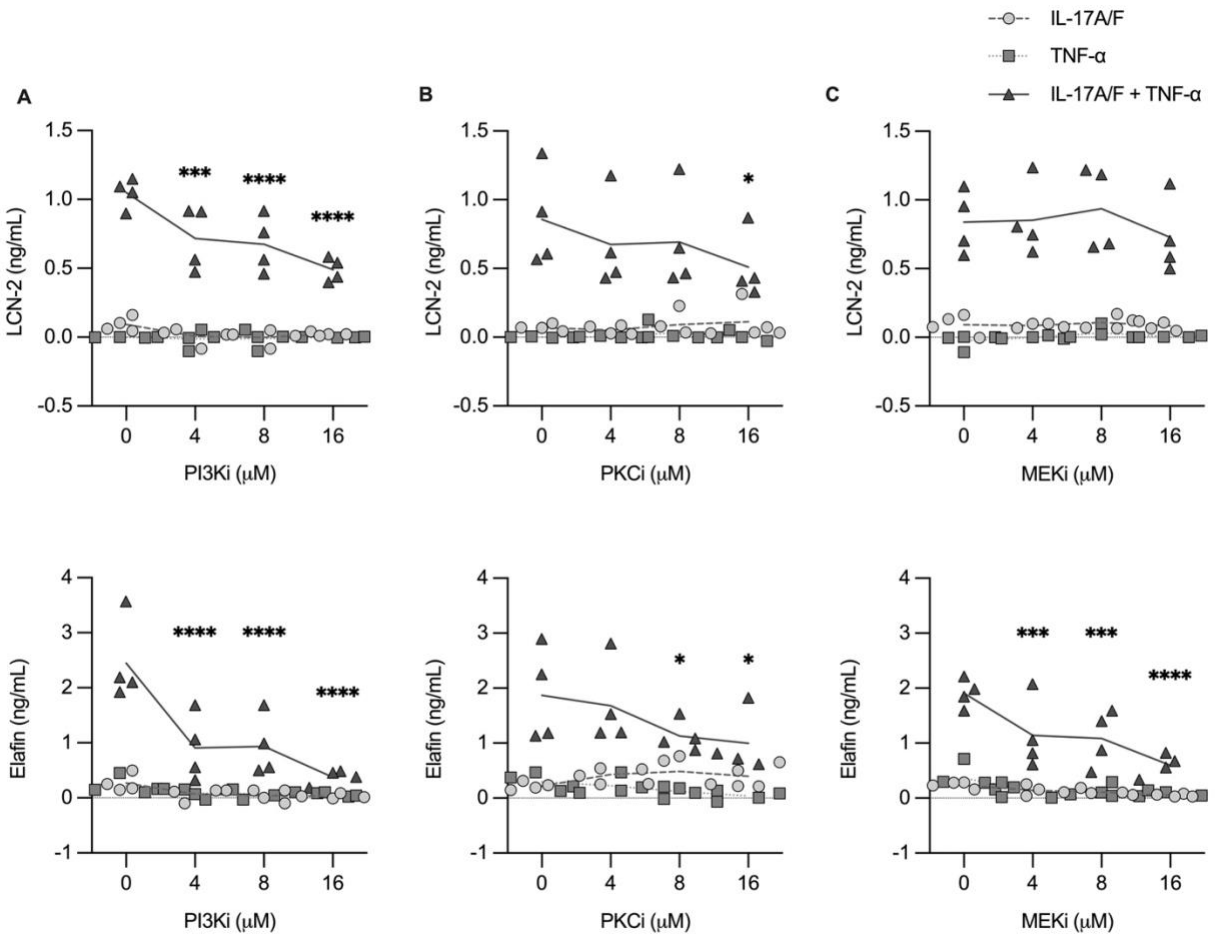

Figure 2.9: Assessment of pharmacological inhibitors on IL-17A/F + TNF-α mediated LCN-2 and Elafin production. HBEC-3KT cells were pre-treated with pharmacological inhibitors **(A)** LY294002 (PI3Ki), **(B)** GO6976 (PKCi), and **(C)** PD98059 (MEKi), for 1 h prior to stimulation with IL-17A/F (50 ng/mL), TNF-α (20 ng/mL), or the combination of IL-17A/F and TNF-α. TC supernatants were collected after 24 h and examined for LCN-2 and Elafin abundance by ELISA. Protein abundance shown is after subtraction of background abundance in paired unstimulated cells in each independent replicate. Each data point represents an independent experimental replicate (N=4), and the line represents the average. Two-way ANOVA with Dunnett's test for multiple comparisons was used to determine statistical significance *(*p<0.05, **p<0.01, ***p<0.001, ****p<0.0001).*

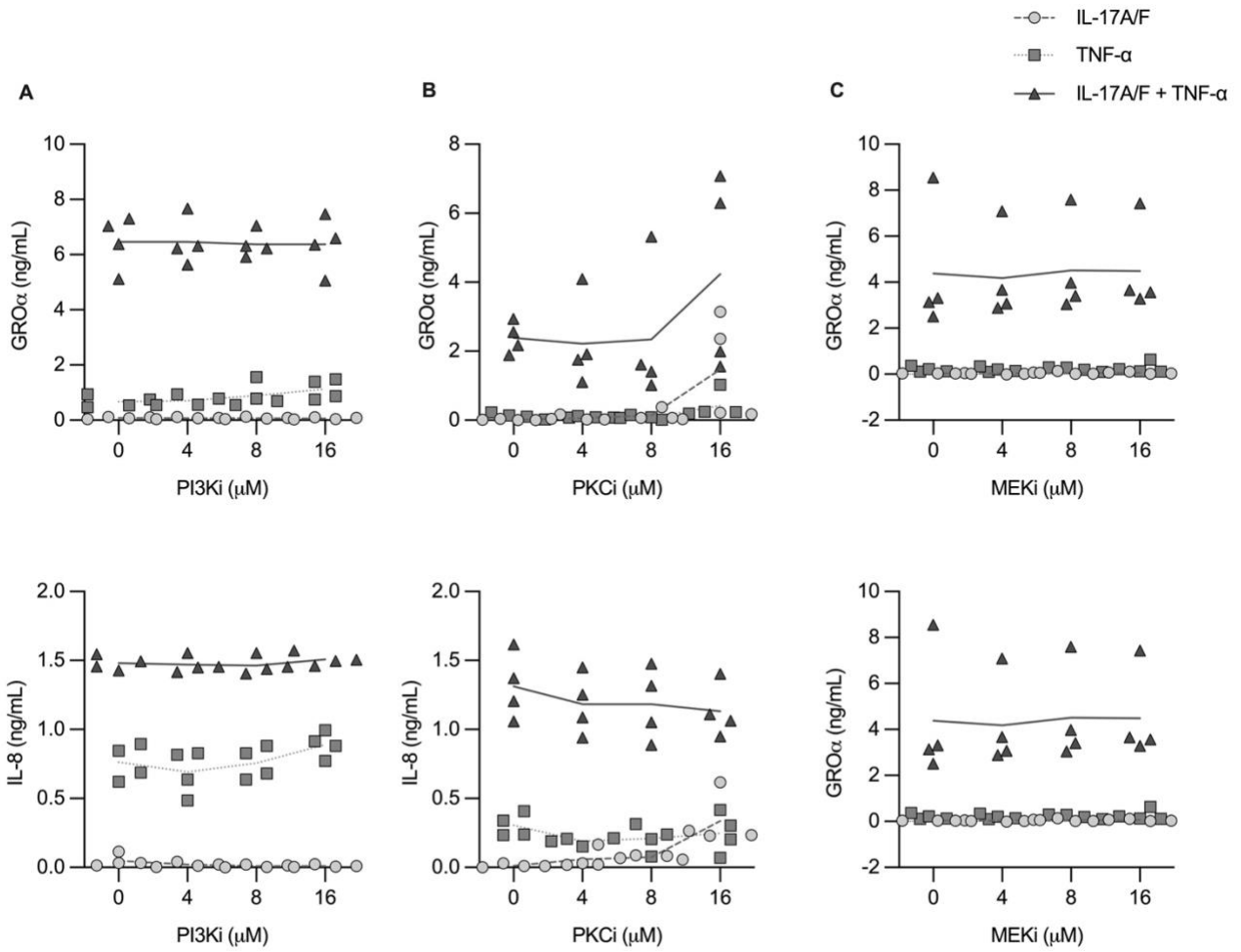

Figure 2.10: Assessment of pharmacological inhibitors on IL-17A/F + TNF-α mediated GROα and IL-8 production. HBEC-3KT cells were pre-treated with pharmacological inhibitors **(A)** LY294002 (PI3Ki), **(B)** GO6976 (PKCi), and **(C)** PD98059 (MEKi), for 1 h prior to stimulation with IL-17A/F (50 ng/mL), TNF-α (20 ng/mL) or the combination of IL-17A/F and TNF-α. TC supernatants were collected after 24 h and examined for GROα and IL-8 abundance by ELISA. Protein abundance shown is after subtraction of background abundance in paired unstimulated cells from each independent replicate. Each data point represents results from an independent experimental replicate (N=4) and the line represents the average. Two-way ANOVA with Dunnett's test for multiple comparisons was used to determine statistical significance.

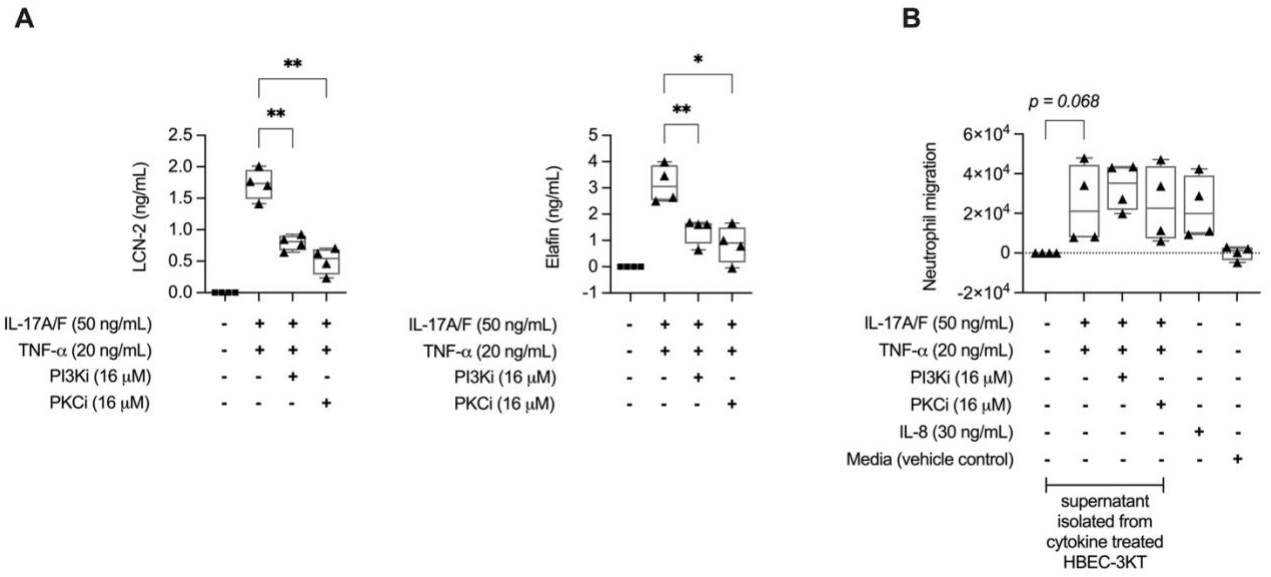

Figure 2.11: Assessment of pharmacological inhibitors on IL-17A/F + TNF-α mediated neutrophil migration. HBEC-3KT were stimulated with combination of IL-17A/F (50 ng/mL) and TNF-α (20 ng/mL) in the presence/absence of pharmacological inhibitors LY294002 (PI3Ki; 16 uM) and GO6976 (PKCi; 16 uM) as indicated. (A) Tissue culture supernatants were collected after 24 h and monitored for the abundance of LCN-2 and Elafin by ELISA. Protein abundance shown is after subtraction of background abundance in paired unstimulated cells from each independent replicate. Each data point represents results an independent experimental replicate (N=4). (B) Tissue culture supernatants were collected after 24 h and used in trans-well cell migration assays, to monitor the migration of neutrophils isolated from human blood. Cell culture medium spiked with human recombinant IL-8 (30 ng/mL) was used as a positive control, whereas media was used as a vehicle control. Each dot represents the average number of neutrophils that traversed the membrane within two hours in each experiment. Increases in neutrophil migration was calculated after subtraction of background values in paired unstimulated cells for each biological replicate. Results are shown as boxplots, wherein bars show median and IQR, and whiskers show minimum and maximum value. Each data point represents results an independent experimental replicate (N=4). One-way ANOVA with Bonferroni's post-hoc test for multiple comparisons was used for statistical significance compared to unstimulated cells as control (*$p<0.05$, **$p<0.01$).

4.3.6: In vivo validation of selected protein targets in a murine model of airway inflammation

Previous reports have shown that repeated intranasal challenge with HDM for two weeks results in airway inflammation with increased neutrophil accumulation in the lungs of BALB/c mice (45, 294). To corroborate our *in vitro* findings in a physiologically representative model of airway inflammation, we measured the abundance of IL-17A, IL-17F, heterodimer IL-17A/F, and TNF-α in the BAL and lung tissue lysates obtained from mice challenged with HDM for two weeks. IL-17A and IL-17A/F, but not IL-17F, were significantly higher in BAL from HDM-challenged mice, compared to allergen-naïve mice (Figure 2.12A). The concentration of TNF-α was also significantly higher in the BAL from HDM-challenged mice (Figure 2.12A).

As both IL-17A/F and TNF-α were increased in the BAL of HDM-challenged mice, next I examined the abundance of the proteins that was identified to be increased by the combination of these two cytokines in the *in vitro* studies described above. Therefore, I examined the abundance of CHDP LCN-2, Elafin, and the murine neutrophil chemokine KC (mouse homolog of human GROα) in BAL and lung tissue lysates. Abundance of LCN-2 and KC was significantly increased in BAL, but not in the lung tissue lysates, in HDM-challenged mice compared to allergen-naïve mice (Figures 2.12B & 212C). These results demonstrated a concurrent increase of IL-17A/F and TNF-α in BAL of allergen-challenged mice, along with the neutrophil chemoattractant KC and CHDP LCN-2 and Elafin (also known to be neutrophil chemoattractants). These results corroborated the *in vitro* findings in bronchial epithelial cells (Figures 2.4 & 2.5) confirming the proteins targets synergistically enhanced by IL-17A/F and TNF-α in an *in vivo* model.

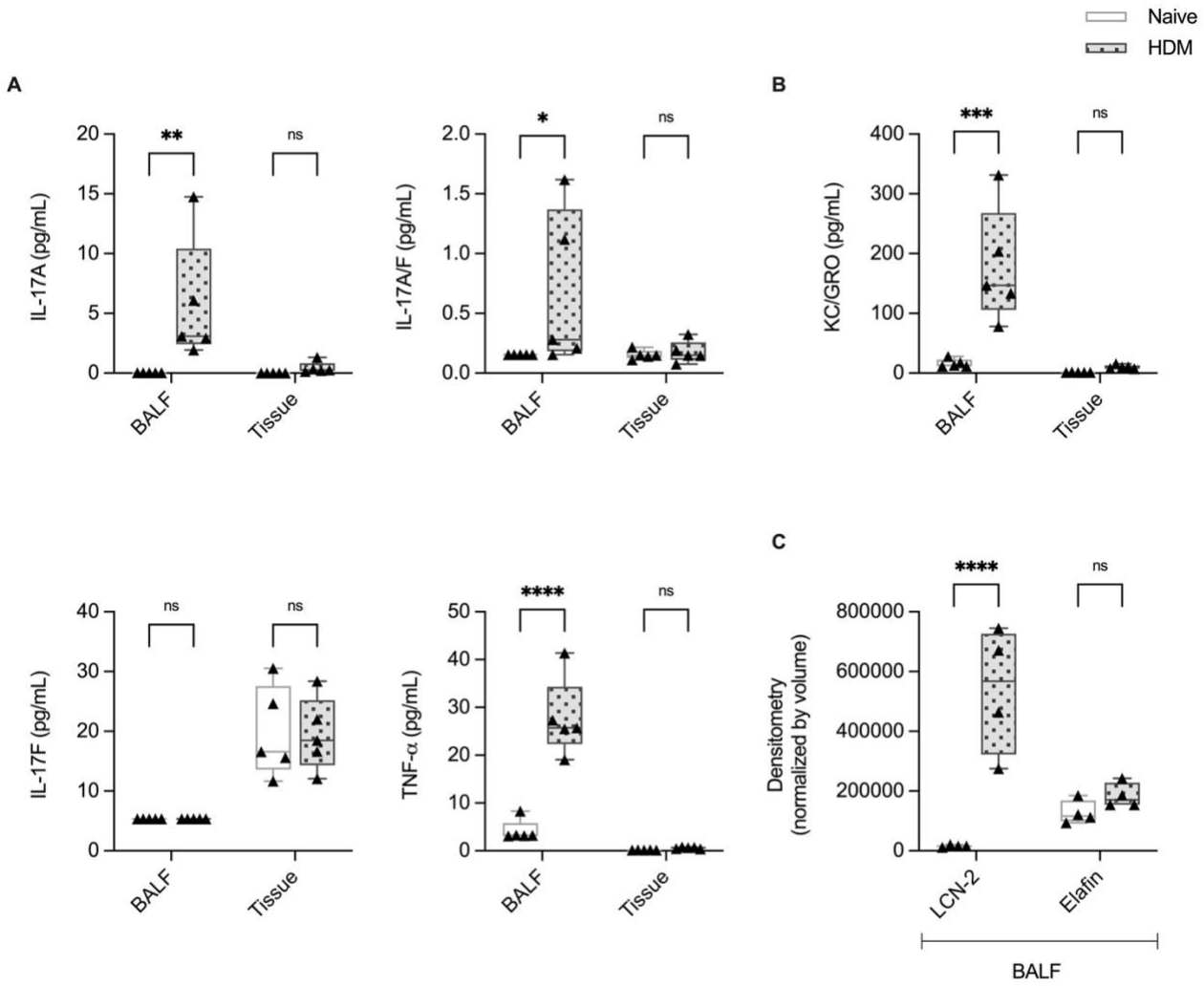

Figure 2.12: Assessment of protein production in the lungs of a mouse model of house dust mite-induced airway inflammation. Female BALB/c mice challenged with i.n. administration of ~25 µg (35 µL of 7 µg/mL saline) of HDM for five consecutive days per week for two weeks. BAL and lung tissue lysates obtained from allergen-naïve (N=5) and HDM-challenged (N=5) mice were monitored for the abundance of **(A)** cytokines IL-17A, IL-17A/F, IL-17F, and TNF-α, and **(B)** KC by multiplex MSD platform. Undetectable values of cytokine were assigned a value of 1/4 the minimum detectable limit. **(C)** BAL of HDM-challenged (N=4) and allergen-naïve (N=4) mice were monitored for the abundance of LCN-2 and Elafin by Western blot. Results are shown as boxplots, wherein bars show median and IQR, and whiskers show minimum and maximum points. Each data point represents an individual mouse. Statistical analysis was performed using two-way ANOVA with Bonferroni's post-hoc test for multiple comparisons. Statistical significance denotes differences compared to control *(*p < 0.05, **p < 0.01, ***p < 0.001).*

4.4 DISCUSSION

In this study, I showed that the combinatorial effect of IL-17A/F and TNF-α uniquely alters the proteome of HBEC, and primarily enhances proteins in three functional categories, neutrophilic chemokines, CHDP with antimicrobial and immunomodulatory functions, and airway remodeling factors. In independent validation studies, I demonstrated that the combination of IL-17A/F and TNF-α synergistically enhances the production of LCN-2, Elafin, GROα, and IL-8, in TC supernatants from HBEC (cell line and primary cells). Interestingly, the two CHDP (LCN-2 and Elafin) identified to be synergistically enhanced by the combination of IL-17A/F and TNF-α also promote neutrophil migration (215, 224, 315). These findings were functionally corroborated by my results demonstrating that secreted factors from HBEC-3KT stimulated with the combination of IL-17A/F and TNF-α uniquely promote neutrophil migration, while those from cells stimulated with either cytokine alone do not. In further mechanistic studies, I showed that PI3K and PKC pathways are involved in the synergistic enhancement of CHDP LCN-2 and Elafin, but not neutrophilic chemokines. My results indicate that disparate pathways control the synergistic enhancement of CHDP compared to the induction of chemokines, in response to concurrent activation by IL-17A/F and TNF-α in HBEC-3KT. I also demonstrated *in vivo* that IL-17A/F and TNF-α, as well as the proteins identified from the *in vitro* studies e.g., LCN-2, and the mouse homolog of GROα (KC), are significantly increased in the BAL of allergen-challenged mice, using a murine model of allergen-challenged airway inflammation known to increase neutrophil accumulation in the lungs (45, 294). These results are corroborated by previous studies demonstrating individual CHDP and chemokine induction in response to IL-17A (215, 347). The findings in this study identify proteins that are uniquely altered in response to concurrent activation with the heterodimer IL-17A/F and TNF-α in the lung, and conclusively demonstrate that the synergistic effect of these two cytokines leads to the enhancement of secreted proteins that promote neutrophil migration in the context of airway inflammation.

This is the first study to detail proteins that are uniquely or synergistically altered by the combined effect of IL-17A/F and TNF-α in HBEC, using a proteomics approach. Although previous studies have demonstrated synergy between IL-17 and TNF-α in promoting inflammatory responses in different cell types such as endothelial cells, hepatocytes, synovial fibroblasts, and AEC, these previous studies were primarily focused on IL-17A (176, 204-206, 348). Relative quantitation of protein candidates identified to be uniquely or synergistically enhanced by the combination of IL-17A/F and TNF-α within the bronchial epithelial proteome in this study, suggests that the IL-17A/F-centric protein biosignature is further enhanced by TNF-α during concurrent activation by these two cytokines. This

is corroborated by a recent study demonstrating that pro-inflammatory responses mediated by IL-17A and IL-17F are potentiated by TNF-α in synoviocytes (349). A previous study has demonstrated that IL-17A enhances the expression *CXCL3*, *CSF3*, *SAA1*, and *CCL20* in primary AEC (266), and these molecular candidates were also found to be enhanced by the combination of IL-17A/F and TNF-α in our proteomics dataset. It is thus likely that the combination of IL-17A and TNF-α may result in a similar protein biosignature that is defined here for the heterodimer IL-17A/F. Nonetheless, these studies indicate that acute pro-inflammatory cytokines such as TNF-α, produced in the presence of pathogenic and/or environmental factors e.g., air pollution, allergens, and fungi, exacerbate IL17A/F-mediated responses to promote airway inflammation (312, 313, 342).

The pathophysiology of chronic respiratory diseases characterized by airway inflammation is known to be driven by the cooperative interaction between various pro-inflammatory mediators (158). TNF-α along with the IL-17 family of cytokines, including IL-17A/F, is enhanced in severe asthma (15, 93, 150, 266-268, 270, 317, 318, 324, 342, 343). Research in the phenotypic heterogeneity of asthma has shown that the immunophenotype of severe asthma is complex, which includes both Th2-high and Th2-low/Th1+Th17-high disease (93, 150). Typically, severe steroid-unresponsive asthma characterized by neutrophilia exhibits a Th2-low/Th17-high airway inflammation, with elevated levels of IL-17A, IL-17A/F, and TNF-α at mucosal surfaces of the airway (93, 150, 320, 350, 351). Neutrophil accumulation in the lung also results in NET formation in the airways (147, 150), which can increase Th17 differentiation and subsequently IL-17 production (150). In addition, neutrophils are also capable of recruiting Th17 cells via CCL20 and CCL2 (352). Therefore, neutrophilic accumulation in the airways may prolong IL-17A/F-mediated airway inflammation through a positive feedback loop, resulting in sustained inflammation and subsequent tissue damage. The only IL-17 family member produced by AEC is IL-17C, which is released by epithelia following activation with various stimuli, including pro-inflammatory cytokines such as TNF-α (162). IL-17C enhances the transcription of downstream targets which includes S100A9, GROα, IL-8, CSF3, and CCL20 via the activation of IL-17RA and IL-17RE receptors (163). Although, I did not show the involvement of autocrine IL-17C signaling in the combinatorial effect of IL-17A/F and TNF-α, some of the IL-17C targets such as GROα and IL-8 were shown to be synergistically enhanced by the combination of IL-17A/F and TNF-α in this study. Therefore, it is possible that concurrent activation with IL17A/F and TNF-α may enhance IL-17C abundance in bronchial epithelial cells, perhaps at an earlier time point than that examined in this study and amplify the autocrine activity of IL-17C. Interestingly, clinical trials with either anti-TNF-α strategies or blocking the IL-17RA receptor did not adequately control

severe asthma (353-355). In this context, the list of proteins and pathways defined in this study may be valuable to design new interventions to specifically target the combinatorial effect of IL-17A/F and TNF-α for the control of severe asthma.

Molecular mechanisms that underlie the cooperative effect of IL-17A/F and TNF-α are not understood. IL-17A, IL-17F, and IL-17A/F signal via the heterodimeric receptor IL-17RA/RC, with varying affinities (153). These IL-17 members induce modest levels of downstream signaling and inflammatory responses, instead synergistically enhance signaling pathways through cooperative effect with acute pro-inflammatory cytokines such as TNF-α (356). Previous studies have demonstrated that synergistic effects of IL-17A and TNF-α are mediated through the activation of pathways such as NF-κB, MAPK, protein kinase B and PI3K pathways (204, 357, 358). Aligned with this, I demonstrated that the synergistic effect of IL-17A/F and TNF-α involves the PI3K and PKC pathways in HBEC-3KT. However, my results also suggest that there may be disparate signaling mechanisms that control different downstream responses mediated by the combinatorial action of IL-17A/F and TNF-α. This is indicated by my results demonstrating that cytomix IL-17A/F + TNF-α-mediated synergistic enhancement of CHDP LCN-2 and Elafin is dependent on PKC and PI3K signaling pathways, but this is not the case for enhancement of chemokines IL-8 and GROα. Mechanisms previously suggested for the synergistic effects of IL-17A and TNF-α include IL-17A-mediated increase in the expression of TNF-α receptor II in hepatocytes and synoviocytes (204, 359), and post-transcriptional mRNA stabilization of TNF-α-induced chemokines by IL-17A (198, 209, 360). As TNF-α-family receptors were not demonstrated to be uniquely enhanced by the combination of IL-17A/F and TNF-α in our proteomics dataset, our results suggest that the combinatorial effects of IL-17A/F and TNF-α may not be driven by TNF-α-receptor. Previous studies have also shown that production of the murine neutrophilic chemokine KC is initiated transcriptionally through activation of the NF-κB pathway by TNF-α, while IL-17A drives chemokine mRNA stabilization through an Act-1 dependent mechanism (198, 360). However, the chemokines defined in this study, GROα and IL-8, were enhanced in a supra-additive manner both at the transcriptional level and protein production. Thus, my results suggest that the mechanisms associated with the synergistic enhancement of neutrophilic chemokines by IL-17A/F and TNF-α may not be solely dependent on post-transcriptional regulation. However, my findings also indicate that the synergistic increase of Elafin protein production may be regulated post-transcriptionally, as mRNA expression of Elafin was not enhanced by IL-17A/F and TNF-α in HBEC-3KT. These studies highlight the complex, overlapping and unique,

signaling mechanisms involved in the regulation of downstream responses mediated by the concurrent activation of IL-17 family of cytokines and TNF-α in the lungs, which needs to be fully elucidated.

4.5 Summary

The outcome of inflammation is dependent on the overall composition of cytokines (14), wherein the multitude of cytokines present in the inflammatory milieu may invoke redundant, antagonistic, or synergistic effects which dictate immune responses (10, 12). Therefore, to determine if IL-17A/F-mediated inflammation was relevant in a complex environment representative of neutrophilic airway inflammation, I defined global protein changes in response to IL-17A/F in the presence/absence of other pro-inflammatory mediators involved neutrophilic airway inflammation, including TNF-α and IFN-γ in bronchial epithelial cells and in a mouse model of mixed eosinophilic/neutrophilic airway inflammation.

In this study, I showed that the combinatorial effect of IL-17A/F and TNF-α uniquely enhanced the production of 38 proteins, compared to either cytokine alone, in HBEC-3KT at 24 h. These 38 proteins primarily belonged to three functional categories, including CHDP with antimicrobial and immunomodulatory functions, neutrophil-associated chemokines, and airway remodeling factors. Four of seven dominant protein targets (increased > 2-fold) were those that promote neutrophil migration. These included the CHDP LCN-2 and Elafin, as well as the neutrophil-associated chemokines GROα and IL-8. Expression and abundance changes for these proteins were confirmed in independent validation studies in HBEC-3KT and PBEC isolated from patients undergoing lung resection. Further, these changes were functionally corroborated by my results which demonstrated that proteins secreted from HBEC-3KT stimulated with combinations of IL-17A/F and TNF-α for 24 h uniquely enhance neutrophil migration compared to those stimulated with either cytokine alone. In mechanistic studies, I demonstrated that activation of PI3K and PKC regulated the production of neutrophil-associated CHDP (e.g., LCN-2 and Elafin), but not neutrophil-associated chemokines (e.g., GROα and IL-8). I demonstrated *in vivo* that IL-17A, IL-17A/F, TNF-α, as well as select protein targets including LCN-2 and KC (mouse analog of GROα) were concurrently increased in the BAL of allergen-challenged mice, using a mouse model of airway inflammation characterized by airway inflammation in the lungs.

Taken together, this study conclusively demonstrates that IL-17A/F-mediated inflammation leads to enhancement of secreted proteins which promote neutrophil migration in the context of airway

inflammation. The findings in this study provide insight into the fundamental understanding of downstream protein targets and pathways in response to the combinatorial activity of TNF-α along with the IL-17-family heterodimer IL-17A/F, in the context of airway inflammation. The protein targets identified in this study will be useful for the development of interventional strategies to target biological processes enhanced by the presence of IL-17A/F and TNF-α, relevant to chronic respiratory diseases such as steroid-unresponsive severe asthma.

In addition, this study along with the study detailed in chapter 3, characterized complex IL-17A/F-mediated inflammation (in the presence/absence of other cytokines) in bronchial epithelial cells and demonstrated the role of this cytokine in enhancing neutrophil migration to sites of inflammation via the induction of neutrophil-associated CHDP. Therefore, these studies provided novel CHDP targets (e.g., LCN-2, Elafin) and immunological processes (e.g., neutrophil accumulation in the lung) in which to investigate the role of cathelicidin LL-37 in regulating IL-17A/F-mediated inflammation in the lung. Furthermore, these results, when taken together with previous studies, facilitated the selection of a physiologically representative mouse model of IL-17-dependent neutrophil accumulation in the lung. As a result, IL-17A/F-mediated protein targets (e.g., LCN-2) and a mouse model of neutrophilic airway inflammation were selected to define regulation of IL-17A/F-mediated inflammatory signaling by LL-37 *in vitro* and *in vivo*.

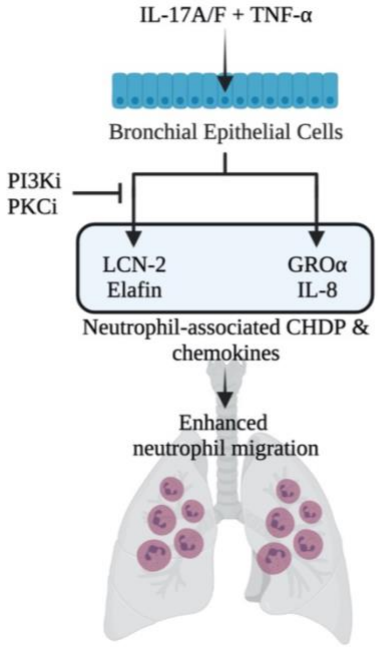

Figure 2.13: Combination of IL-17A/F + TNF-α uniquely alters the bronchial epithelial cell proteome to enhance proteins which enhance neutrophil migration. IL-17A/F + TNF-α indirectly enhance neutrophil migration to the lung by increasing production neutrophil-associated CHDP (e.g., LCN-2) and chemokines (e.g., GROα and IL-8) in HBEC. *This figure created using biorender.com.*

Chapter 5: Cathelicidin LL-37 Modulates IL-17A/F-Mediated Transcription Factors and RNA Binding to Proteins to Suppress Lipocalin-2 Production and Limit Neutrophil Accumulation

This section contains some text and figures from a manuscript to be submitted as an original article in the *Journal of Mucosal Immunology* (2022). **Anthony Altieri**, Dylan Lloyd, Mahadevappa Hemshekhar, and Neeloffer Mookherjee.

A.A. and N.M. conceived and designed the study. A.A. performed majority of the experiments, analyzed the data, and wrote the manuscript. D.L. performed the Western blots. M.H. assisted with animal model studies and provided intellectual input for the study. N.M. obtained funding and supervised the study.

5.1 Abstract

Background: Asthma is a heterogeneous disease reflecting different pathophysiology. Inhaled allergen-mediated disease can be Th2-driven or Th2-low/Th17-driven. The Th2-low/Th17-driven disease shows predominantly neutrophilic inflammation and is associated with non-responsiveness to ICS. There are currently no effective therapies for the control of steroid-unresponsive, severe asthma. This disease is characterized by the increased abundance of IL-17A/F in the lungs. Neutrophilic inflammation also results in increased abundance of the sole human cathelicidin peptide, LL-37, in the lungs. However, molecular changes in response to the interplay of IL-17A/F and LL-37 in the lungs have not been defined.

Objective: I aimed to identify molecular targets of IL-17A/F altered by LL-37 during airway inflammation. These targets may represent pivotal checkpoints in airway inflammation that can be used to develop new therapeutic strategies.

Methods: HBEC-3KT were stimulated with IL-17A/F (50 ng/mL). Cell lysates (N=5) were probed using high-content aptamer-based proteomic profiling. Differential analysis was performed on normalized log2 protein expression values, along with Welch's t-test ($p<0.05$) to identify differentially abundant proteins. The identified IL-17A/F-mediated molecular signature was independently confirmed *in vitro* using HBEC-3KT cell line, and *ex vivo* using PBEC isolated from three individuals undergoing lung resection, in the presence and absence of LL-37 (0.25 μM). These findings were

validated *in vivo* using a physiologically representative model of neutrophilic airway inflammation in male and female mice.

Results: Proteomic profiling and independent confirmatory studies demonstrated that IL-17A/F enhanced the production of 20 proteins in HBEC-3KT. Proteins that were increased by >2-fold included neutrophil-associated CHDP LCN-2 and Elafin. The neutrophil chemokine GROα was also significantly enhanced by IL-17A/F. LL-37 selectively altered IL-17A/F-mediated increase of these proteins in bronchial epithelial cells. LL-37 suppressed the abundance of IL-17A/F-mediated LCN-2, and in contrast enhanced the abundance of GROα. LL-37 did not alter IL-17A/F-mediated Elafin production. Select findings were validated *in vivo* using a physiologically representative mouse model of neutrophilic airway inflammation, using a recall challenge of allergen with low concentration of endotoxin during the allergen sensitization phase. This mouse model is characterized by IL-17-mediated neutrophil accumulation and NETosis in the lung. In this model, I demonstrated that CRAMP (mouse analog of LL-37), IL-17A/F, LCN-2, and NE (a neutrophil activation marker) are concurrently enhanced. LCN-2 positively correlated with NE abundance, whereas CRAMP negatively correlated with LCN-2 abundance and neutrophil accumulation in the lungs. In mechanistic studies I showed that LL-37-mediated regulation of IL-17A/F-signature of inflammatory mediators is associated with decreased abundance of transcription factor C/EBPβ and increased abundance of *RNA binding protein* (RBP) Regnase-1, which promote and suppress IL-17-mediated LCN-2 production respectively.

Conclusion: Results of this study indicate that physiological concentrations of LL-37 selectively alter IL-17A/F-mediated inflammation in bronchial epithelial cells. Taken together, my data suggests that cathelicidin peptides suppresses IL-17A/F-mediated LCN-2 production and limits neutrophil accumulation in the lung. The proteins identified in this study (e.g., C/EBPβ, Regnase-1) to be altered by IL-17A/F and/or LL-37 may represent pivotal checkpoints in neutrophilic airway inflammation and can be used to develop new therapeutic strategies.

5.2 Rationale & Introduction

CHDP, also known as AMP, are small endogenous peptides with direct and indirect anti-infective and immunomodulatory capabilities (19-21). The CHDP human cathelicidin LL-37 and mouse analog CRAMP regulate inflammation in a highly complex manner, as illustrated by their ability to selectively alter inflammation by modulating cell recruitment and activation (28, 32, 44, 117, 119-121, 123, 132, 133). Moreover, in addition to regulating inflammation initiated by pathogenic stimuli (32, 33, 44,

103, 134-136), previous studies have demonstrated that cathelicidins are critical regulators of cytokine-mediated inflammation. For example, LL-37 suppresses the production of pro-inflammatory mediators, while simultaneously enhancing the production of chemokines and anti-inflammatory molecules (43, 115, 137). Furthermore, LL-37 levels are elevated in chronic inflammatory diseases of the lung (138, 147), but the role of LL-37 is not well understood. Therefore, mechanistic studies demonstrating the ability of LL-37 to selectively alter cytokine-mediated inflammation have led to investigations into its role in cytokine-driven chronic inflammatory disease.

Asthma is a heterogenous disease characterized by airway inflammation that is either Th2-driven or Th2-low/Th17-driven. Th2-low/Th17-driven disease is characterized by elevated IL-17A/F levels, neutrophil accumulation in the lung, as well as non-responsiveness to treatment (158, 225-227, 268, 270). IL-17A/F increases neutrophil accumulation in the lung by enhancing the production of neutrophil-associated chemokines in non-hematopoietic cells, including bronchial epithelial cells (160, 175-177). In addition, LL-37 levels are increased in Th2-low/Th17-driven asthma characterized by neutrophil accumulation (147). One previous study demonstrated that individuals with neutrophilic asthma had increased NET formation, significantly higher levels of LL-37, and increased NE levels, compared to individuals with non-neutrophilic asthma and healthy controls (147). Moreover, one recent study has demonstrated that CRAMP potentiates IL-17A/F-producing Th17 cells in the lung by enhancing AHR and RORγt transcription factor expression in a TGF-β1-dependent manner (124). Despite this, the role of LL-37 in asthma characterized by IL-17-driven neutrophil accumulation is not well understood. Therefore, I investigated the impact of LL-37 on IL-17A/F-mediated airway inflammation in HBEC, and in a physiologically representative mouse model of neutrophilic airway inflammation which was previously shown to be characterized by IL-17-dependent neutrophil accumulation in the lung (150). As LL-37 is known to play a role in facilitating immune homeostasis (18, 105), I hypothesized that LL-37 limits neutrophil accumulation in the lung by selectively regulating IL-17A/F-mediated inflammation in bronchial epithelial cells.

In this study I performed proteomic profiling to determine the dominant protein targets enhanced in response to IL-17A/F-mediated inflammation in HBEC-3KT. These protein targets were used to characterize the effect of physiologically representative concentrations of cathelicidin LL-37 on IL-17A/F-mediated inflammation using the HBEC-3KT cell line and in PBEC isolated from individuals undergoing lung resection. In addition, I used a physiologically relevant mouse model of neutrophilic airway inflammation to determine the relationship between neutrophil accumulation as

well as activation, CRAMP (mouse cathelicidin), and selected protein targets from the proteomic array results.

Here, I demonstrated that the sole human cathelicidin LL-37 selectively suppresses IL-17A/F-mediated LCN-2 abundance in bronchial epithelial cells. LCN-2 is a secreted peptide with antimicrobial functions and plays a role in innate immunity by promoting neutrophil chemotaxis and activation (224, 361). Further, I validated these findings *in vivo* using a mouse model of neutrophilic airway inflammation (150). I demonstrated that CRAMP (mouse analog of LL-37), IL-17A/F, LCN-2, and neutrophil activation marker NE were concurrently elevated in the lungs in the mouse model neutrophilic airway inflammation. In addition, I demonstrate that CRAMP is negatively correlated with LCN-2 abundance, as well as neutrophil accumulation in the lung. Moreover, by interrogating novel IL-17-mediated signaling intermediates, I demonstrated that LL-37 suppresses IL-17A/F-mediated C/EBPβ production, a transcription factor required for LCN-2 production, in HBEC-3KT. In addition, I demonstrated LL-37 enhances IL-17A/F-mediated endoribonuclease Regnase-1 production, a feedback inhibitor of IL-17 signal transduction, in human PBEC. Based on my findings, I propose a novel mechanism wherein cathelicidin LL-37 selectively alters cytokine-mediated inflammation and promotes immune homeostasis by simultaneously altering transcription factors and the post-transcriptional machinery which controls mRNA abundance, and therefore the inflammatory milieu. As a result, the proteins identified in this study may represent pivotal checkpoints in neutrophilic airway inflammation and can be examined to develop new therapeutic strategies.

5.3 Results:

5.3.1 IL-17A/F alters the bronchial epithelial cell proteome and significantly increases the abundance of neutrophil chemotactic proteins

To determine the dominant proteins produced in response to IL-17A/F-mediated lung inflammation, I performed aptamer-based proteomic profiling of HBEC-3KT (ATCC® CRL-4051™) at 24 h. Pairwise differential analysis conducted on normalized log2 protein abundance values demonstrated that IL-17A/F significantly alters the abundance of 25 proteins in HBEC-3KT after 24 h; increasing the abundance of 20 and suppressing the abundance of 5 proteins (Figure 3.1A). The proteins with the greatest increase in abundance (>2-fold) in response to IL-17A/F-mediated inflammation were neutrophil-associated CHDP LCN-2, which promotes neutrophil activation in addition to recruitment (224), and Elafin, which prevents damage to the airway epithelium during lung inflammation by degrading serine proteases such as NE (337, 362). GROα was selected for further investigation due to

its role as a neutrophil-recruiting chemokine (363) and as a positive control for selective enhancement by LL-37 (117). Moreover, as secreted proteins primarily mediate cellular communication, I confirmed the abundance of these three selected proteins in HBEC-3KT TC supernatant by ELISA after 24 h post-stimulation (Figure 3.1B). This data suggests that IL-17A/F-mediated inflammation indirectly enhances neutrophil accumulation in the lung by increasing the abundance and secretion of neutrophil-associated chemotactic factor production in bronchial epithelial cells.

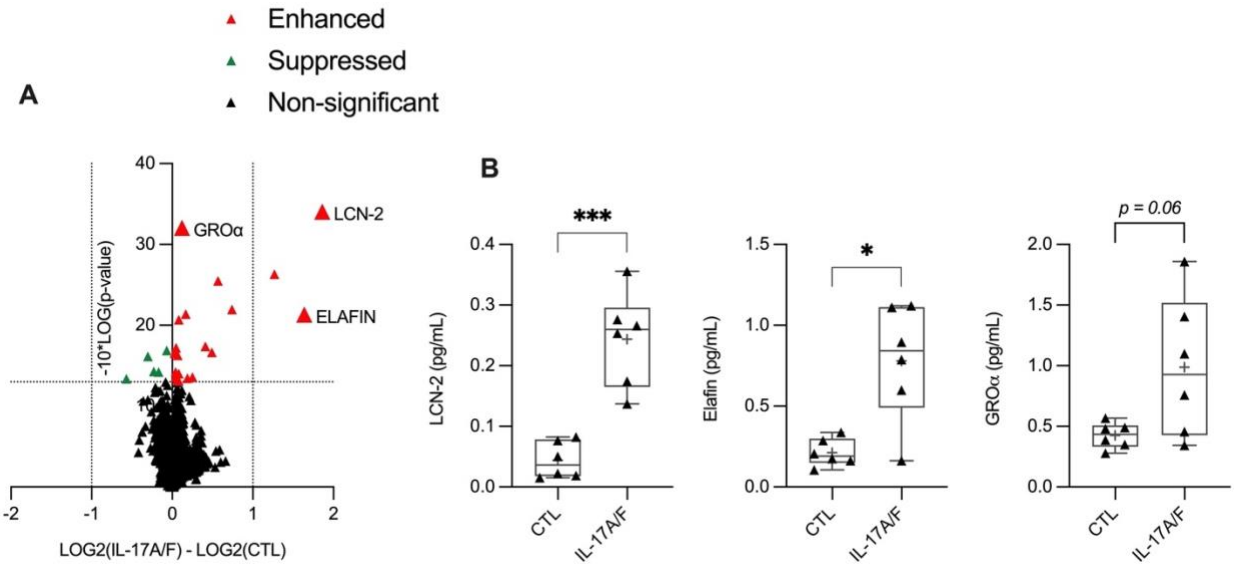

Figure 3.1: IL-17A/F-mediated bronchial proteome. HBEC-3KT were stimulated IL-17A/F (50 ng/mL) and compared to unstimulated controls after 24 h. **(A)** Cell lysates (14 µg total protein per sample) obtained from five independent experiments were independently probed using the high-content aptamer-based proteomic array (N=5). Pairwise differential analysis was conducted on normalized log2 protein expression values, and Welch's t-test with a cutoff of $p<0.05$ was used to select protein abundance changes that were significantly altered in response to the combination of IL-17A/F. **(B)** TC supernatant was collected from cells 24 h post-stimulation, and the abundance of LCN-2, Elafin, and GROα was examined by ELISA. Y-axis represents ng/mL. Each dot represents an independent experiment, and bars show the median and min-max range. Repeated measures one-way ANOVA with Fisher's least significant difference test was used for statistical analysis (*$p\leq0.05$, ***$p\leq0.005$).

5.3.2 LL-37 and citrullinated LL-37 suppress IL-17A/F-mediated LCN-2 production in bronchial epithelial cells

Previous studies have demonstrated that LL-37 indirectly promotes neutrophil recruitment (32) and selectively suppresses cytokine-mediated inflammation (43). Therefore, I hypothesized that cathelicidin LL-37 would selectively alter IL-17A/F-mediated production of neutrophil-associated proteins in bronchial epithelial cells. As the concentration of LL-37 in individuals with neutrophilic airway inflammation ranges from 0.25 μM to 1 μM (147), I performed dose titrations to select a concentration within this range that enhanced chemokine production, but not cellular cytotoxicity. HBEC-3KT cells were stimulated with LL-37 and a scrambled control peptide sLL-37 for 24 h, and the abundance of chemokines GROα and IL-8 was measured in TC supernatants by ELISA. 0.25 μM and 0.5 μM concentrations of LL-37 induced a statistically significant increase in GROα and IL-8 (Figure 3.2A). In addition, cellular cytotoxicity was examined by monitoring the release of LDH, which demonstrated that 0.25 μM and 0.5 μM concentrations did not cause a significant increase in cellular cytotoxicity (Figure 3.2B) in HBEC-3KT 24 h post-stimulation. In addition, I examined whether citrullination of LL-37, a post-translational modification of LL-37 which occurs in the lungs during airway inflammation (138-142), changes the ability LL-37 to enhance the production of GROα and IL-8. HBEC-3KT were stimulated with 0.25 μM LL-37, citLL-37, or sLL-37 and the abundance of chemokines GROα and IL-8 was measured in TC supernatants by ELISA 24 h post-stimulation. 0.25 μM LL-37 significantly increased the abundance of GROα ~26% compared to unstimulated HBEC-3KT, whereas citLL-37 did not (Figure 3.2C). In addition, both LL-37 and citLL-37 significantly increased the abundance of IL-8 by ~323% and ~182% respectively (Figure 3.2C). However, citrullination of LL-37 dampened the enhancement of IL-8 compared to LL-37 by ~33% (*p=0.07*). These results suggest that citrullination of LL-37 reduces pro-inflammatory activity compared to native LL-37. Based on these results, 0.25 μM of LL-37 and related peptides were used in subsequent experiments to determine the impact of LL-37 to on IL-17A/F-mediated protein production on bronchial epithelial cells.

Therefore, HBEC-3KT were stimulated with 0.25 μM of LL-37, citLL-37, or sLL-37, in the presence and absence of IL-17A/F (50 ng/mL). The abundance of selected IL-17A/F-mediated protein targets identified from the results of the proteomic array, including LCN-2, Elafin, and GROα were measured in TC supernatant by ELISA, 24 h post-stimulation. LL-37 and citLL-37 suppressed IL-17A/F-mediated LCN-2 production ~53% and ~50% respectively in HBEC-3KT (Figure 3.3A) but did not alter Elafin production (Figure 3.3B). In contrast, combinations of IL-17A/F and LL-37 or citLL-

37 significantly enhanced GROα production by ~313% and ~210% respectively at 24 h in HBEC-3KT. However, citrullination of LL-37 limited GROα production in combination with IL-17A/F (Figure 3.3C). These results demonstrated that LL-37 selectively alters IL-17A/F-mediated CHDP production and neutrophil chemotactic factors. Moreover, citrullination of LL-37 does not suppress all LL-37 immunomodulatory functions.

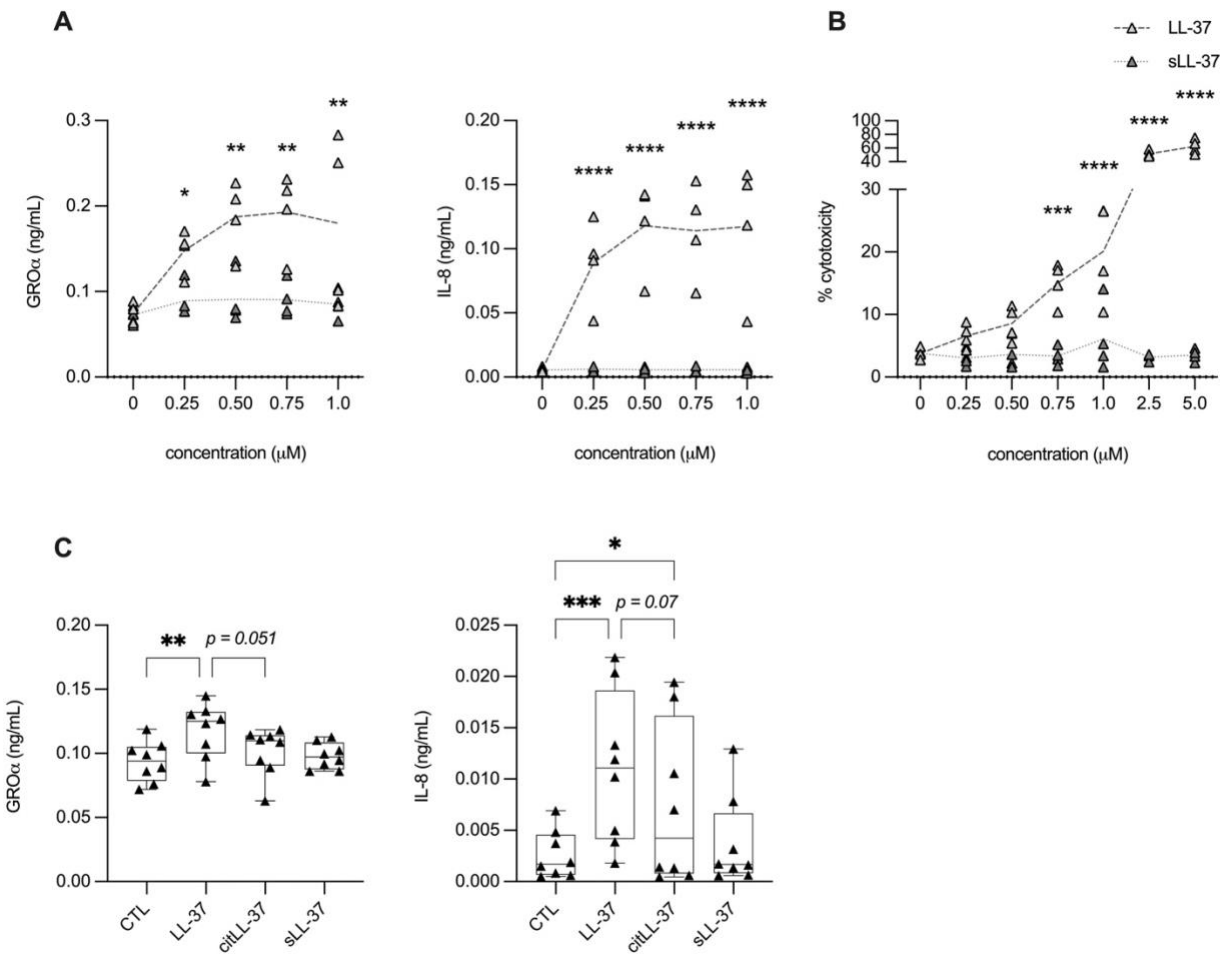

Figure 3.2: Physiological concentration of LL-37 enhances GROα and IL-8 secretion without enhancing cellular cytotoxicity. TC supernatant collected from HBEC-3KT stimulated with various concentrations of LL-37 and scrambled control peptide sLL-37 were examined for the abundance of neutrophil-associated chemokines **(A)** GROα and IL-8 by ELISA and for **(B)** LDH release as a marker for cellular cytotoxicity, 24 h post-stimulation. Each dot represents an independent experiment compared to paired unstimulated HBEC-3KT, and dashed lines show the average. **(C)** HBEC-3KT were stimulated with 0.25 μM LL-37, citLL-37, and sLL-37 and TC supernatant was examined for the abundance of GROα and IL-8 24 h post-stimulation by ELISA. Each dot represents an independent experiment, and bars show the median and min-max range. Repeated measures one-way ANOVA with Fisher's least significant difference test was used for statistical analysis (**p≤0.05, **p≤0.001, ***p≤0.005, ****p≤0.0001*).

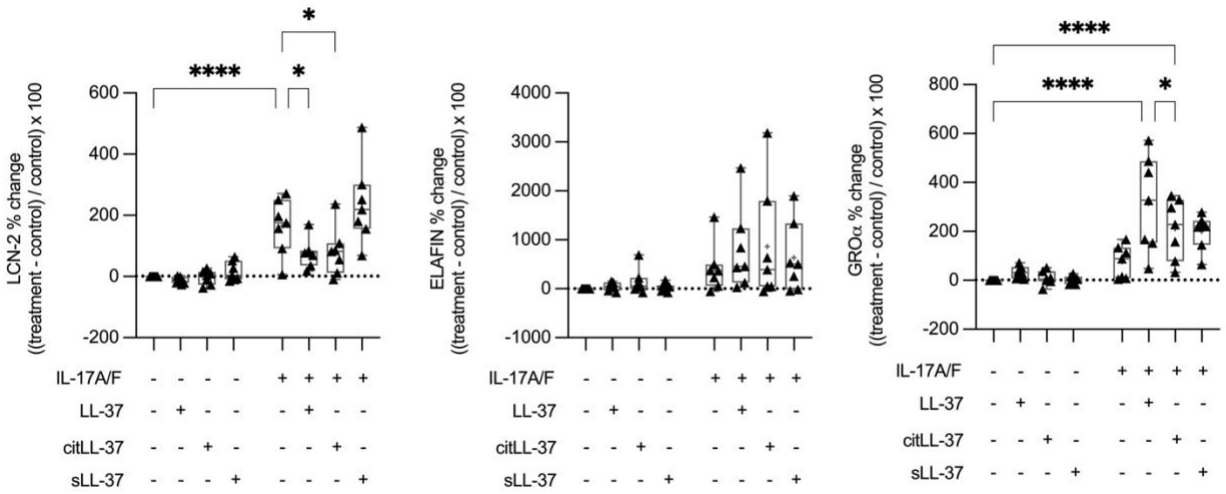

Figure 3.3: LL-37 and citLL-37 selectively alter IL-17A/F-mediated protein production in HBEC-3KT. HBEC-3KT (N=7) were stimulated with LL-37, citLL-37, or sLL-37 (0.25 μM) in the presence and absence of IL-17A/F (50 ng/mL). TC supernatant collected 24 h post-stimulation was examined for abundance of **(A)** LCN-2 Elafin, and GROα by ELISA. Y-axis represents % change compared to paired unstimulated controls within donors. Each dot represents an independent experiment, and bars show the median and min-max range. Repeated measures one-way ANOVA with Fisher's least significant difference test was used for statistical analysis (**p≤0.05, ****p≤0.0001*).

5.3.3 IL-17-mediated neutrophilic mouse model of airway inflammation

To test the relevance of LL-37 in modulating IL-17A/F-mediated inflammation I performed *in vivo* validation of select protein targets in a mouse model of neutrophilic airway inflammation (Figure 3.5A). The model in this study is based on a previous study that demonstrated concomitant *intranasal* (i.n.) administration of HDM and low concentration of LPS during the allergen sensitization phase results in enhanced IL-17-mediated neutrophil accumulation, NET formation, and PADI4-dependent citrullination in the lungs of male mice (150). I expanded on this model and used both male and female mice for this study, as most allergen challenge models use female mice. There were no changes to the survival rate (data not shown) or weight of male or female mice after 15 days (Figure 3.5A & 3.5B). I measured leukocyte accumulation by cell differential analysis in the BAL 24 h after the last HDM challenge. Male and female mice sensitized with co-challenge of HDM and LPS showed a clear neutrophil-skewed airway inflammation compared to other allergen or endotoxin alone sensitized groups of mice (Figure 3.6). There were no differences in total leukocyte accumulation in HDM-challenged mice compared to HDM + LPS sensitized mice (Figure 3.6B). Consistent with the previous study (150), neutrophil accumulation in the BAL was significantly increased in male mice sensitized with HDM + LPS compared to those sensitized with HDM alone, which was not noted in female mice (Figure 3.6C). However, eosinophil accumulation in the BAL decreased in female mice sensitized with HDM + LPS compared to those sensitized with HDM alone (Figure 3.6D), indicating that the ratio of neutrophils to eosinophils would be skewed toward a robust neutrophilic inflammation. In male and female mice, i.n. sensitization with HDM + LPS increased macrophage accumulation in the BAL (Figure 3.6E) while lymphocyte accumulation was unchanged (Figure 3.6F). Moreover, comparative analysis of individual cell populations as compared to overall cell accumulation in the BAL (i.e., cell percentages) demonstrated that eosinophil percentages were significantly lower in female mice sensitized with HDM + LPS (~18%) as compared to female mice sensitized with HDM alone (~32%) (Figure 3.6G). These results were similar in male mice; eosinophil percentages were significantly lower in male mice sensitized with HDM + LPS (~33%) as compared to male mice sensitized with HDM alone (~53%; Figure 3.6H). Moreover, neutrophil percentages were higher ($p = 0.09$) in male mice sensitized with HDM and LPS (~28%) as compared to mice sensitized with HDM alone (~21%). Taken together, these results confirmed that co-challenge of allergen with low concentration of endotoxin during sensitization induces an endotype indicative of neutrophilic inflammation, which is associated with severe asthma, characterized by increased accumulation of neutrophils and/or decreased eosinophils, in the lungs of male and female mice.

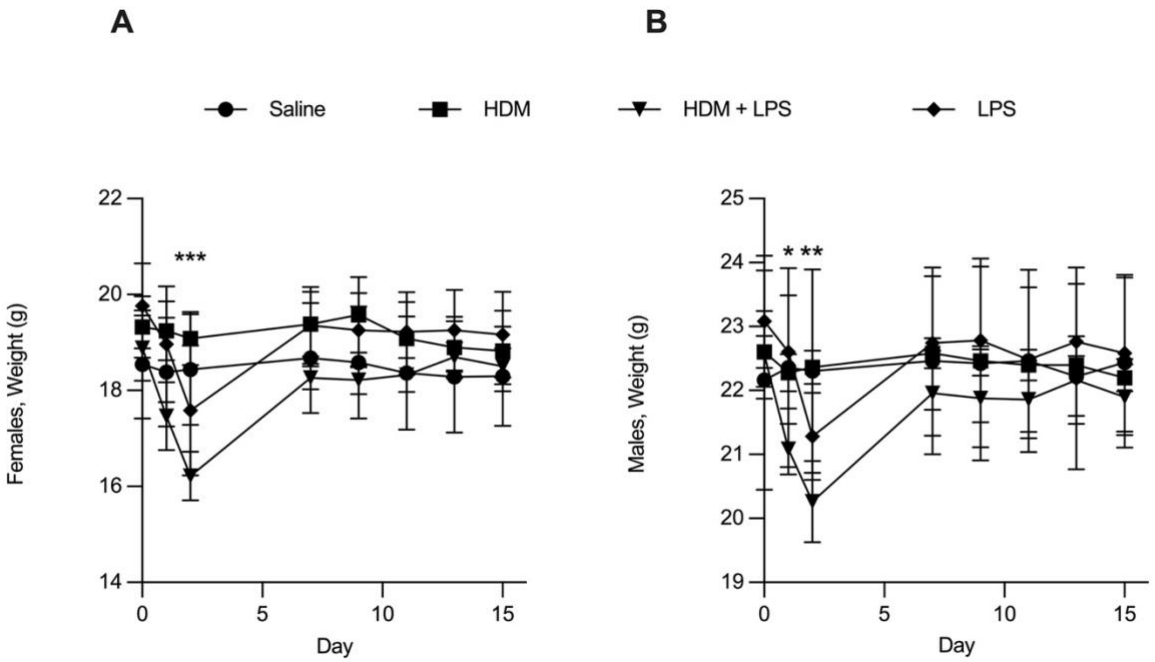

Figure 3.5 HDM + LPS sensitization temporarily decreases body weight after 3 consecutive days of intranasal administration. Female and male BALB/c mice (8-10 weeks; N≥4 per group) were challenged (i.n.) with saline, 25 µg (35 µL of 7 µg/mL saline), HDM protein extract with or without 1 µg LPS (35 µL of 0.03 µg/mL saline), or LPS (35 µL of 0.03 µg/mL saline) once daily for 3 days (days 0 to 2). Beginning on day 7, 25 µg of HDM (as described above) was administered i.n. for 8 days (days 7 to 14), once daily, to groups previously challenged with either HDM or combination of HDM + LPS. Data points represent mean of N=5 mice, and whiskers represent standard error. Statistical analysis was determined by two-way ANOVA with Dunnett's multiple comparisons test and represents statistical comparisons between saline controls and HDM + LPS treated mice (*$**p < 0.01, *p<0.001$*). HDM, house dust mite; LPS, lipopolysaccharide.

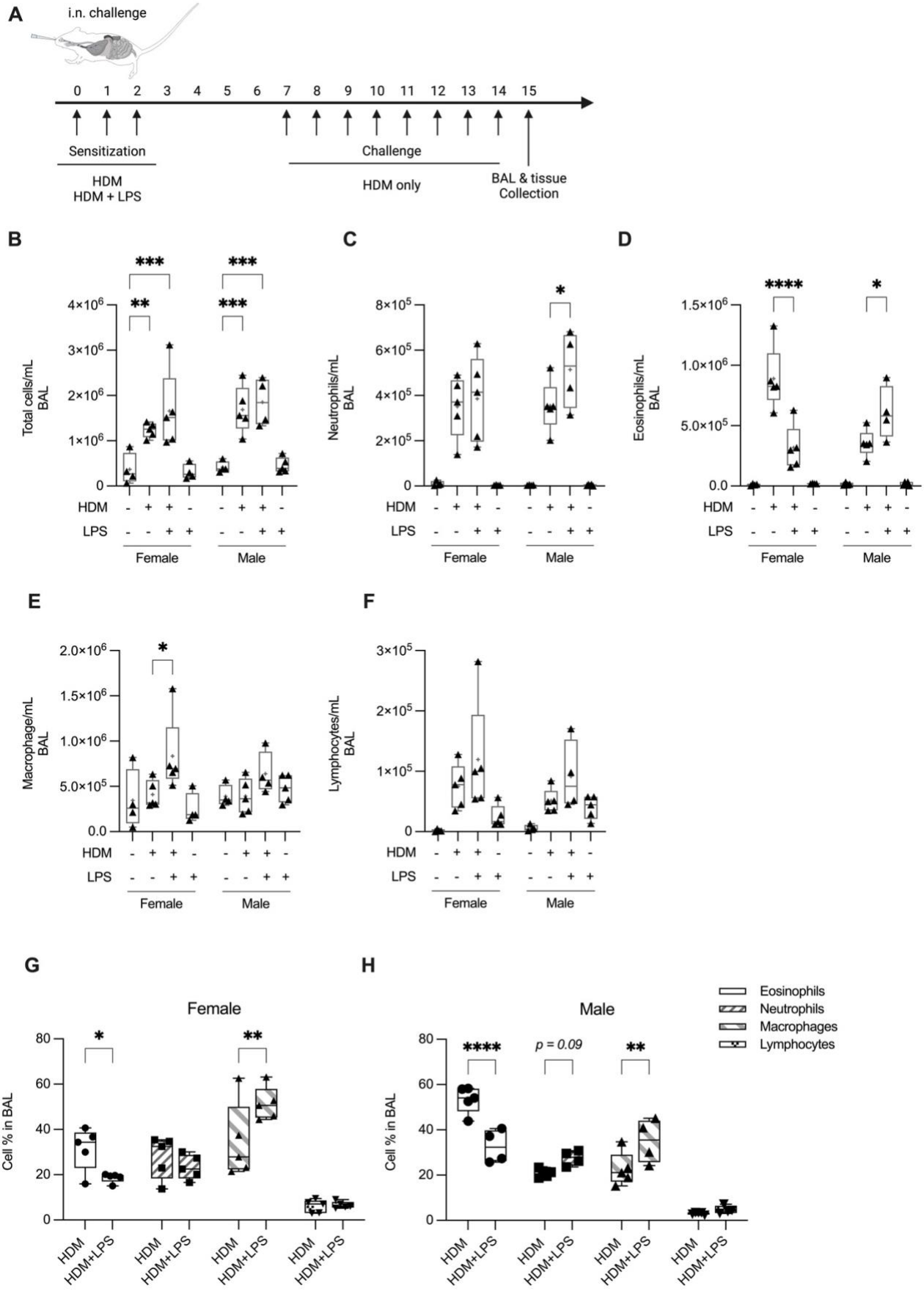
A
i.n. challenge
0 1 2 3 4 5 6 7 8 9 10 11 12 13 14 15
Sensitization
HDM
HDM + LPS
Challenge
HDM only
BAL & tissue
Collection
B
Total cells/mL
BAL
C
Neutrophils/mL
BAL
D
Eosinophils/mL
BAL
E
Macrophage/mL
BAL
F
Lymphocytes/mL
BAL
HDM
LPS
Female
Male
G
Female
H
Male
Cell % in BAL
HDM
HDM+LPS
p = 0.09
Eosinophils
Neutrophils
Macrophages
Lymphocytes

Figure 3.6: Co-challenge of HDM + LPS during sensitization induces disparate immune cell accumulation in the lungs of female and male mice, compared to allergen challenge alone. Female and male BALB/c mice (8-10 weeks; N≥4 per group) were challenged (i.n.) with saline, 25 μg (35 μL of 7 μg/mL saline), HDM protein extract with or without 1 μg LPS (35 μL of 0.03 μg/mL saline), or LPS (35 μL of 0.03 μg/mL saline) once daily for 3 days (days 0 to 2). Beginning on day 7, 25 μg of HDM (as described above) was administered i.n. for 8 days (days 7 to 14), once daily, to groups previously challenged with either HDM or combination of HDM + LPS. **(A)** Schematic of HDM + LPS- challenge. BAL collected 24 h after the last HDM challenge were used for assessment of **(B)** total cells, **(C)** neutrophils, **(D)** eosinophils, **(E)** macrophage, and (**F**) lymphocytes. Cell percentages ((count of individual cell populations / count total cell accumulation) x 100) in the BAL of **(F)** female and **(G)** male mice were assessed. Bars show median and IQR, whiskers show minimum and maximum points, + denotes average. Statistical analysis was determined by one-way analysis of variance with Fisher's LSD test (*$p \leq 0.05$, **$p \leq 0.001$, ***$p \leq 0.005$, ****$p \leq 0.0001$). HDM, house dust mite; LPS, lipopolysaccharide.

5.3.4 CRAMP, IL-17A/F, LCN-2, and NE are concurrently increased in a mouse model of neutrophilic airway inflammation

Patients with neutrophilic asthma have elevated NET formation, LL-37 abundance, and NE levels compared to individuals with non-neutrophilic asthma and healthy controls (147). Despite this, whether CRAMP (mouse analog of LL-37) levels are enhanced during IL-17-driven neutrophil accumulation in the lungs of is not known in murine models. This is an important consideration as murine models of allergen-challenged airway inflammation are used for preclinical studies of asthma. Therefore, I determined the abundance of CRAMP and select protein targets associated with IL-17A/F-mediated inflammation, including IL-17A/F, LCN-2, and NE by ELISA, in the lungs of female and male mice in the neutrophilic airway inflammation model (HDM + LPS sensitization), and compared the findings to all other groups; allergen-naïve, LPS alone, and HDM alone (which typically shows an eosinophilic inflammation profile) (150). CRAMP and IL-17A/F abundance in the BAL of HDM + LPS sensitized mice was significantly increased compared to both HDM sensitized and saline controls. CRAMP abundance in the BAL of mice sensitized with HDM + LPS was significantly increased by ~146% and ~197% in female and male mice, respectively, compared to HDM sensitized mice (Figure 3.7A). Similarly, IL-17A/F abundance in the BAL of mice sensitized with HDM + LPS was significantly increased by ~71% and ~61% in female and male mice, respectively compared to HDM-challenged mice (Figure 3.7B). In mice sensitized with HDM + LPS, NE abundance in the BAL and tissue was significantly increased compared to HDM and saline controls. In female mice, NE abundance in the BAL and tissue was significantly increased ~204% and ~131% respectively, compared to HDM sensitized mice (Figures 3.7C and 3.7D). In male mice, NE abundance in the BAL and tissue was significantly increased ~77% and ~82% respectively, in mice sensitized with HDM + LPS, compared to HDM sensitized mice (Figures 3.7C and 3.7D). The concurrent increase in NE, CRAMP, and IL-17A/F in HDM + LPS sensitized mice compared to both HDM, and saline controls suggest that CRAMP and IL-17A/F are elevated during neutrophilic inflammation in the lung. LCN-2 abundance was increased in the BAL and tissue of female and male mice sensitized with HDM + LPS compared to HDM and controls. In female mice sensitized with HDM + LPS, LCN-2 abundance in the BAL was increased ~8% ($p=0.06$) compared to HDM controls (Figure 3.7E), whereas LCN-2 abundance in the tissue of female HDM + LPS sensitized mice was significantly enhanced ~61% compared to HDM controls (Figure 3.7F). Results were similar in male mice, where LCN-2 abundance in the BAL and tissue was significantly increased ~12% and ~91% respectively, compared to HDM sensitized mice (Figures 3.7E and 3.7F). Taken together, these results suggest that LCN-2 may function as a tissue-derived neutrophil chemotactic factor in neutrophilic inflammation characterized by the concurrent increase of CRAMP and IL-17A/F.

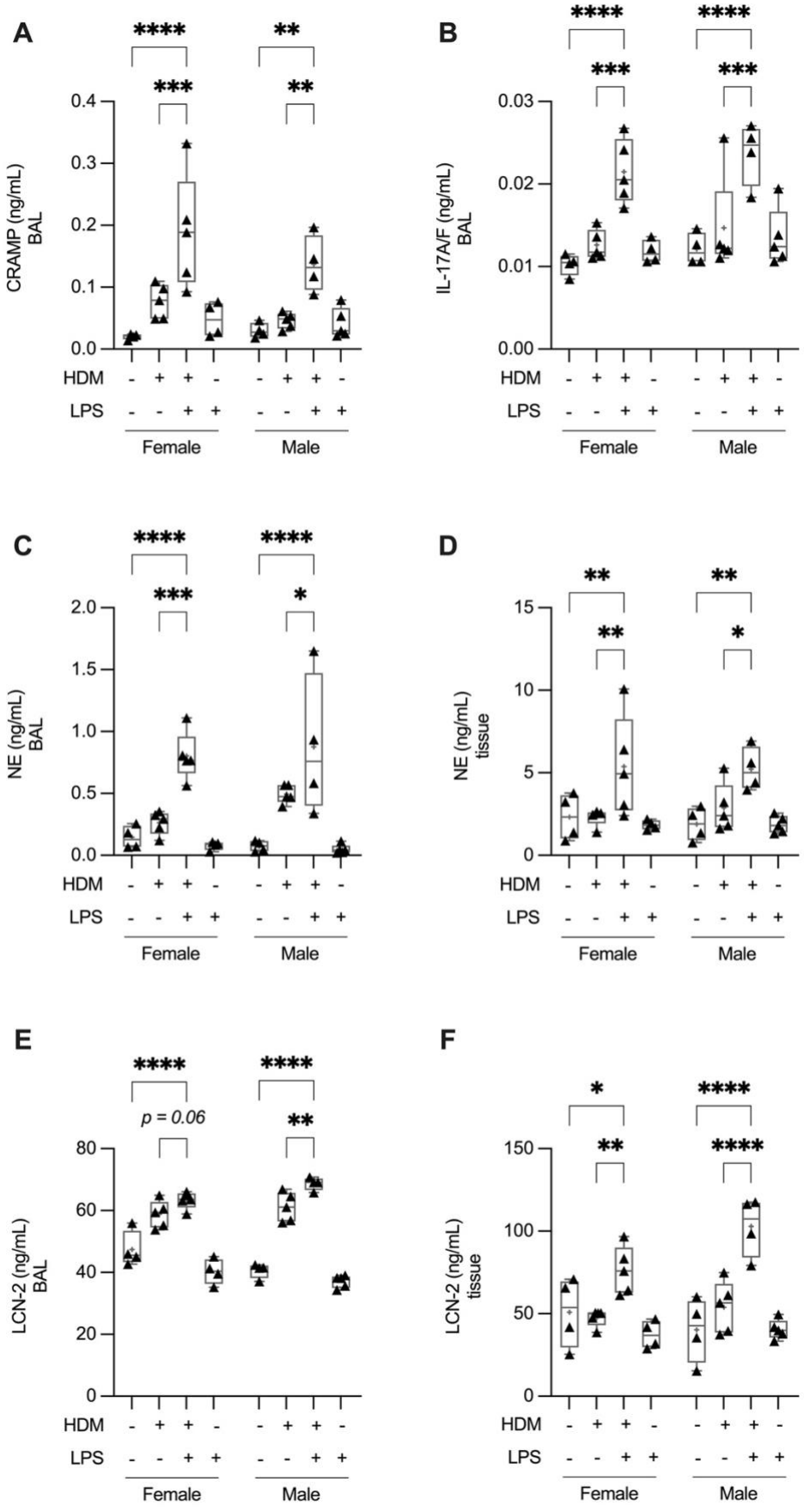
A
CRAMP (ng/mL) BAL
****
**
***
**
0.4
0.3
0.2
0.1
0.0
HDM - + + - - + + -
LPS - - + + - - + +
Female
Male
B
IL-17A/F (ng/mL) BAL
****
****
***
***
0.03
0.02
0.01
0.00
HDM - + + - - + + -
LPS - - + + - - + +
Female
Male
C
NE (ng/mL) BAL
****
****
***
*
2.0
1.5
1.0
0.5
0.0
HDM - + + - - + + -
LPS - - + + - - + +
Female
Male
D
NE (ng/mL) tissue
**
**
**
*
15
10
5
0
HDM - + + - - + + -
LPS - - + + - - + +
Female
Male
E
LCN-2 (ng/mL) BAL
****
****
p = 0.06
**
80
60
40
20
0
HDM - + + - - + + -
LPS - - + + - - + +
Female
Male
F
LCN-2 (ng/mL) tissue
*
****
**
****
150
100
50
0
HDM - + + - - + + -
LPS - - + + - - + +
Female
Male

Figure 3.7: CRAMP, IL-17A/F, LCN-2, and NE are increased in the lung during neutrophilic airway inflammation compared to eosinophilic airway inflammation. Female and male BALB/c mice (8-10 weeks; N≥4 per group) were challenged (i.n.) with saline, 25 μg (35 μL of 7 μg/mL saline), HDM protein extract with or without 1 μg LPS (35 μL of 0.03 μg/mL saline), or LPS (35 μL of 0.03 μg/mL saline) once daily for 3 days (days 0 to 2). Beginning on day 7, 25 μg of HDM (as described above) was administered i.n. for 8 days (days 7 to 14), once daily, to groups previously challenged with either HDM or combination of HDM + LPS. Abundance of **(A)** CRAMP and **(B)** IL-17A/F in the BAL were assessed by ELISA. Abundance of LCN-2 in the **(C)** BAL and **(D)** tissue were assessed by ELISA. Abundance of NE in the **(E)** BAL and **(F)** tissue were assessed by ELISA. Bars show median and IQR, whiskers show minimum and maximum points, + denotes average. Statistical analysis was determined by one-way analysis of variance with Fisher's LSD test (*$p \leq 0.05$, **$p \leq 0.001$, ***$p \leq 0.005$, ****$p \leq 0.0001$). HDM, house dust mite; LPS, lipopolysaccharide.

5.3.5 CRAMP abundance is negatively correlated with LCN-2 and neutrophil accumulation in the lung

To determine the precise relationship between CRAMP, IL-17A/F, LCN-2, neutrophil activity (using NE as a marker), and neutrophil accumulation *in vivo*, I performed correlative assessments in lungs of mice with neutrophilic-skewed airway inflammation (HDM + LPS group), 24 h after the last HDM challenge. LCN-2 and NE abundance were significantly, positively correlated in the lung tissue of female mice (Figure 3.8A), suggesting that LCN-2 drives neutrophil accumulation and activation in the lung. However, CRAMP abundance in the BAL and LCN-2 abundance in the tissue were significantly, negatively correlated in the lungs of female mice (Figure 3.8B), which suggests that CRAMP may limit tissue-derived LCN-2 production to limit neutrophil accumulation and activation in the lung. As CRAMP and LCN-2 were negatively correlated, I determined the relationship between CRAMP and neutrophil accumulation in the lungs of mice challenged with HDM + LPS. In male and female mice, there was a significant negative correlation between CRAMP and neutrophil accumulation that differed by tissue compartment. In female mice, CRAMP abundance in the tissue and neutrophil accumulation in the lung had a significant, negative correlation (Figure 3.8C), whereas in male mice CRAMP abundance in the BAL and neutrophil accumulation were significantly, negatively correlated. Taken together with my previous results, this data suggests that CRAMP limits neutrophil accumulation by decreasing IL-17A/F-mediated LCN-2 production in the lung.

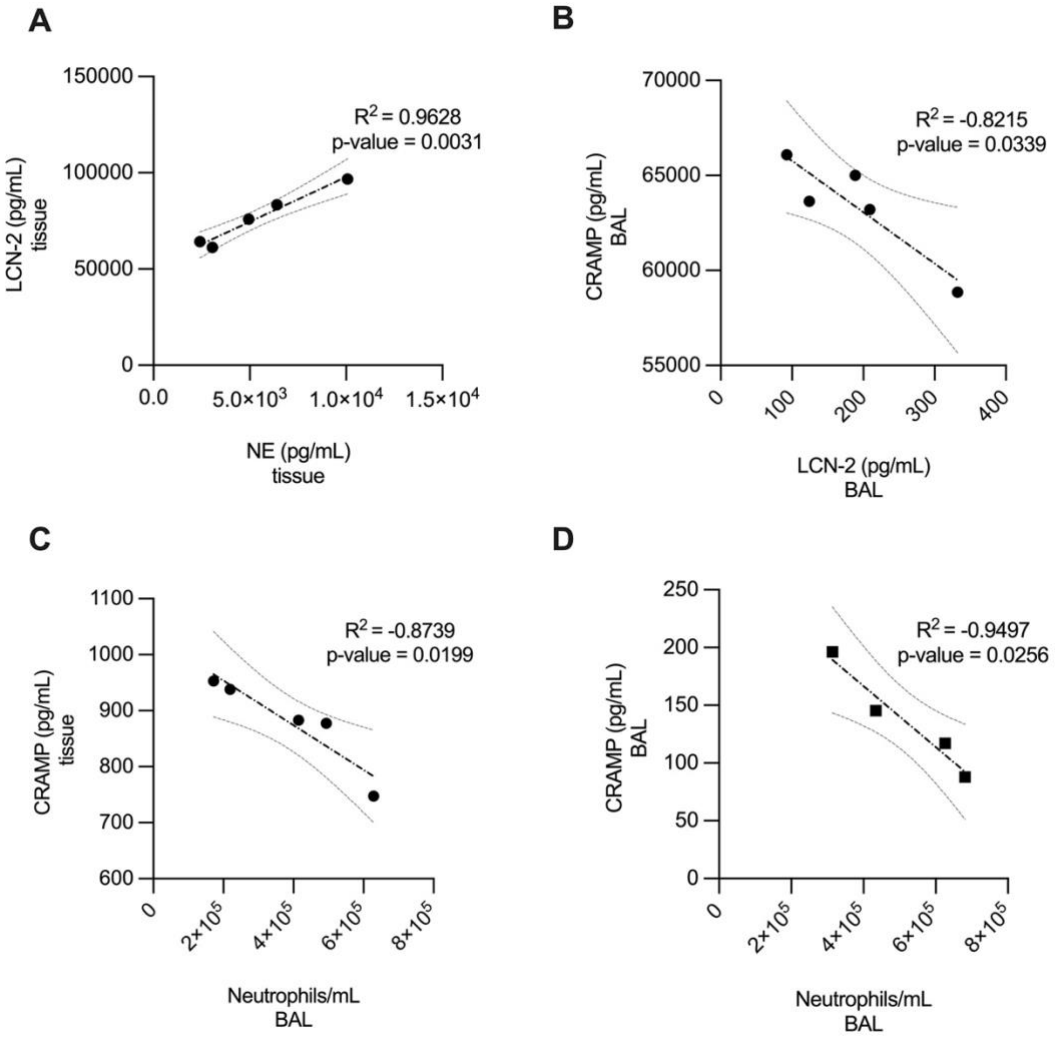

Figure 3.8: CRAMP limits neutrophil accumulation in the lungs of mice with neutrophilic airway inflammation. Female and male BALB/c mice (8-10 weeks; N≥4 per group) were challenged (i.n.) with HDM protein extract with 1 μg LPS (35 μL of 0.03 μg/mL saline) once daily for 3 days (days 0 to 2). Beginning on day 7, 25 μg of HDM (as described above) was administered i.n. for 8 days (days 7 to 14), once daily, to groups previously challenged with combination of HDM + LPS. BAL and lung tissue were collected 24 h after the last HDM challenge. Abundance of CRAMP, LCN-2, and NE was assessed by ELISA. Neutrophil numbers were assessed by cell differential assessment. Pearson's correlation analysis was performed to determine the correlations between the targets as indicated. $p \leq 0.05$ were considered statistically significant.

5.3.6 LL-37 suppresses the abundance of IL-17-mediated CEBPB abundance, a critical transcription factor for LCN-2 production

Previous studies have demonstrated that IL-17A induces NF-κB signal transduction to enhance the transcription of *transcription factors* (TF) which disparately regulate the production LCN-2 and GROα in epithelial cells (197, 202). Here, IL-17A-mediated induction of TF IκBζ and C/EBPβ are required for the transcription of LCN-2, whereas the transcription of GROα is dependent solely of IκBζ (197, 202). In addition, IL-17A activates competing RBP, including Arid5a and endoribonuclease Regnase-1/MCPIP1, which are critical promoters and inhibitors of IL-17-mediated signal transduction, respectively (197, 200). Arid5a positively regulates the translation *NFKBIZ* (gene of IκBζ) and *CEBPB* (gene of C/EBPβ). Arid5a prevents *NFKBIZ*, but not *CEBPB*, degradation by Regnase-1 (197). Further, one previous study performed in epithelial cells demonstrated that Regnase-1 directly degrades *CXCL1* (gene of GROα) mRNA (200). Moreover, a previous study demonstrated that LL-37 alters NF-κB signaling to enhance GROα production in bronchial epithelial cells (117). Therefore, I hypothesized that the mechanisms related to the ability of LL-37 and citLL-37 to suppress IL-17A/F-mediated production of LCN-2 and enhance IL-17A/F-mediated enhancement of GROα are by altering the abundance of *ARID5A* (gene of Arid5a), *ZCH312A* (gene of Regnase-1), *NFKBIZ*, and *CEBPB* in bronchial epithelial cells. As such, HBEC-3KT were stimulated with 0.25 μM of LL-37, citLL-37, or sLL-37, in the presence and absence of IL-17A/F (50 ng/mL). The mRNA abundance of selected IL-17A/F-mediated protein targets, such as *NGAL2*, as well as signaling intermediates, including, *ARID5A*, *ZCH312A*, *NFKBIZ*, and *CEBPB* were measured by qRT-PCR, 3 and 6 h post-stimulation.

At 3 h post-stimulation, there were no significant changes to IL-17A/F-mediated *NGAL2* or *ARID5A* mRNA abundance (Figures 3.9A and 3.9B). However, IL-17A/F significantly enhanced the abundance of *ZCH312A* and *NFKBIZ* by ~2.5- and ~3.5-fold, respectively, compared to unstimulated HBEC-3KT (Figure 3.9B and 3.9C). The combination of LL-37 and IL-17A/F, but not citLL-37 and IL-17A/F significantly enhanced the abundance of *CEBPB* mRNA abundance by ~1.6-fold compared to unstimulated controls (Figure 3.9C). Notably, LL-37 significantly enhanced IL-17A/F-mediated *NFKBIZ* mRNA abundance by ~4.3-fold compared to IL-17A/F stimulated cells, whereas citLL-37 did not (Figure 3.9C). At 6 h post-stimulation, a ~2.2-fold increase in IL-17A/F-mediated *NGAL2* mRNA abundance was suppressed to baseline by both LL-37 and citLL-37 (Figure 3.10A). There were no significant changes to *ARID5A* mRNA abundance (Figure 3.10B). IL-17A/F significantly enhanced *ZCH312A* and *NFKBIZ* mRNA abundance by ~2.8-fold and ~5.1-fold respectively, compared to unstimulated HBEC-3KT (Figures 3.10B and 3.10C). Finally, both LL-37 and citLL-37 significantly

suppressed IL-17A/F-mediated increases in *CEBPB* mRNA abundance from ~1.5-fold to baseline (Figure 3.10C). These results suggest that LL-37 and citLL-37 suppress IL-17A/F-mediated increases in LCN-2 production by decreasing the abundance of *CEBPB* mRNA. In addition, these results suggest that LL-37 enhances GROα production to a greater degree than citLL-37 due to its ability to enhance IL-17A/F-mediated *NFKBIZ* mRNA abundance, which was not enhanced by citLL-37.

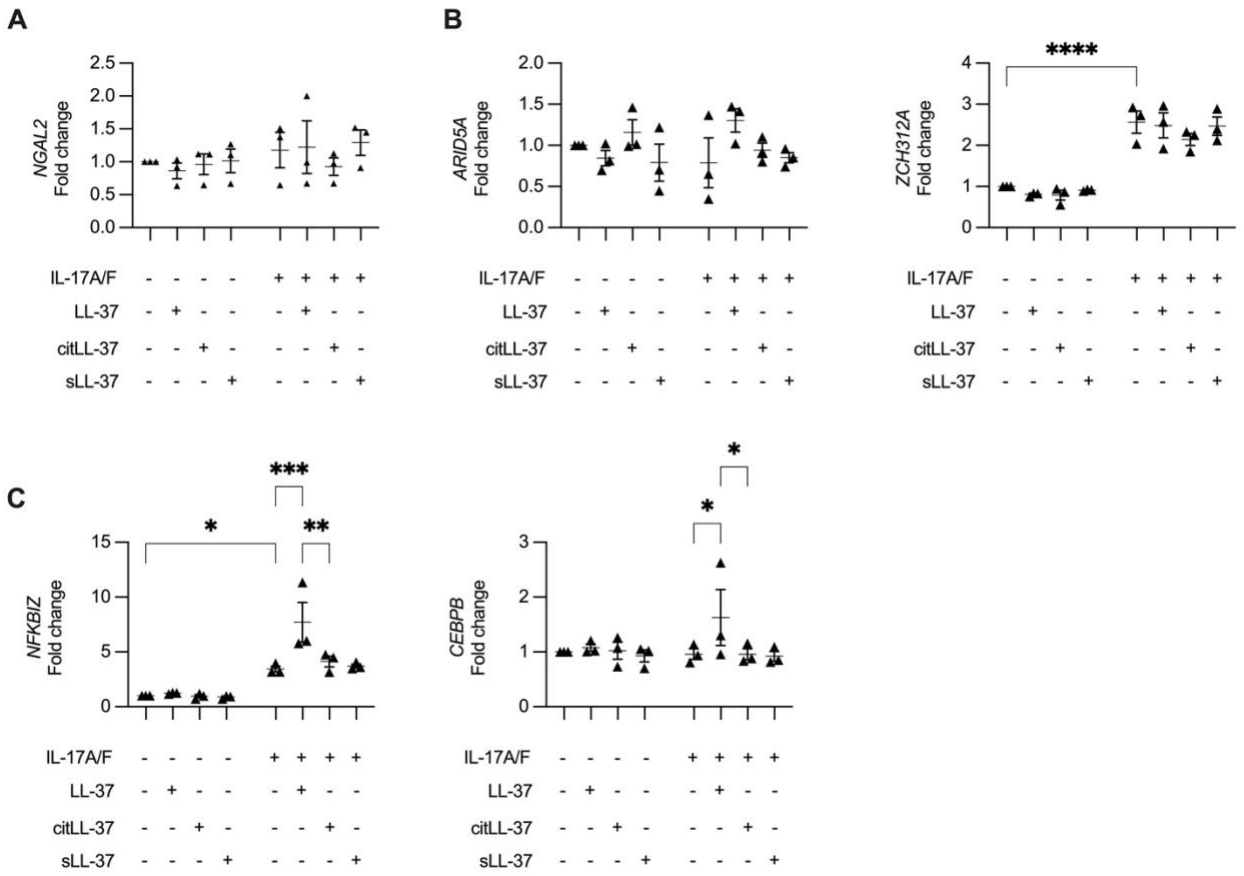

Figure 3.9: LL-37, but not citLL-37, enhances IL-17A/F-mediated increases in *NFKBIZ* and *CEBPB* mRNA abundance. HBEC-3KT (N=3) were stimulated with LL-37, citLL-37, or sLL-37 (0.25 μM) in the presence and absence of IL-17A/F (50 ng/mL). mRNA was isolated 3 h post-stimulation and transcriptional responses evaluated by quantitative real-time PCR for **(A)** CHDP LCN-2 (*NGAL2*) **(B)** RBP Arid5a (*ARID5A*) and Regnase-1 (*ZCH312A*) and **(C)** transcription factors IκBζ (*NFKBIZ*) and C/EBPβ (*CEBPB*). Fold changes (y-axis) for each gene was normalized to 18S RNA, and compared to unstimulated cells normalized to 1, using the comparative ΔΔCt method Each data point represents an independent experimental replicate and bars show the mean and SEM. Fisher's LSD test for one-way ANOVA was used to determine statistical significance (*$p<0.05$, **$p<0.01$, ***$p<0.001$, ****$p<0.0001$).

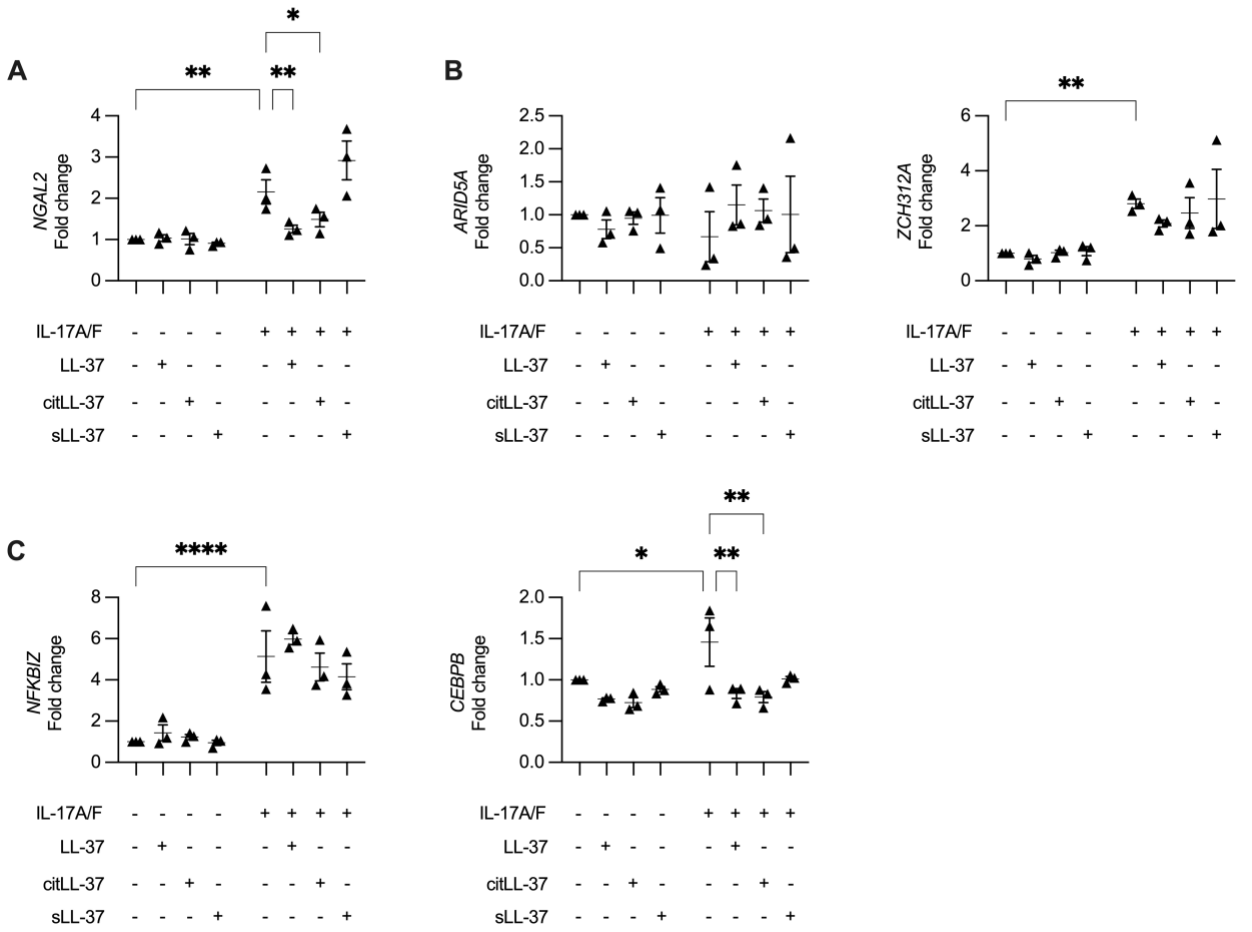

Figure 3.10: LL-37 and citLL-37 suppress IL-17A/F-mediated increases in *NGAL2* and *CEBPB* mRNA abundance. HBEC-3KT (N=3) were stimulated with LL-37, citLL-37, or sLL-37 (0.25 μM) in the presence and absence of IL-17A/F (50 ng/mL). mRNA was isolated 6 h post-stimulation and transcriptional responses evaluated by quantitative real-time PCR for **(A)** CHDP LCN-2 (*NGAL2*) **(B)** RBP Arid5a (*ARID5A*) and Regnase-1 (*ZCH312A*) and **(C)** transcription factors IκBζ (*NFKBIZ*) and C/EBPβ (*CEBPB*). Fold changes (y-axis) for each gene was normalized to 18S RNA, and compared to unstimulated cells normalized to 1, using the comparative ΔΔCt method Each data point represents an independent experimental replicate and bars show the mean and SEM. Fisher's LSD test for one-way ANOVA was used to determine statistical significance (*$p<0.05$, **$p<0.01$, ***$p<0.001$, ****$p<0.0001$).

5.3.7 citLL-37 simultaneously suppresses IL-17A/F-mediated LCN-2 production while enhancing the abundance of IL-17A/F-mediated Regnase-1, a feedback inhibitor of IL-17 signal transduction

In additional confirmational studies, I validated my results from HBEC-3KT in physiologically representative PBEC isolated from patients undergoing lung resection. I stimulated PBEC with 0.25 μM of LL-37, citLL-37, or sLL-37, in the presence and absence of IL-17A/F (50 ng/mL). The abundance of selected IL-17A/F-mediated protein targets identified from the results of the proteomic array, including LCN-2, Elafin, and GROα were measured in TC supernatant by ELISA 24 h post-stimulation. I demonstrated that the protein abundance profiles in response to LL-37, citLL-37, and sLL-37, in the presence and absence of IL-17A/F, were overall similar 24 h post-stimulation in human PBEC compared to that observed in HBEC-3KT cell line. A notable exception in human PBEC was that citLL-37 significantly suppressed IL-17A/F-mediated LCN-2 production by ~95% whereas LL-37 did not (Figure 3.11). Taken together with my previous studies in HBEC-3KT (Figure 3.3), this data suggests that LL-37 limits certain neutrophil chemotactic factors such as CHDP LCN-2 but maintains or enhances chemokines such as Groα. This differential effect of LL-37 on CHDPs compared to chemokines is maintained and/or enhanced by the citrullinated peptide. For example, the ability of LL-37 to suppress IL-17A/F-induced LCN-2 is enhanced by citLL-37, which is notable in human PBEC.

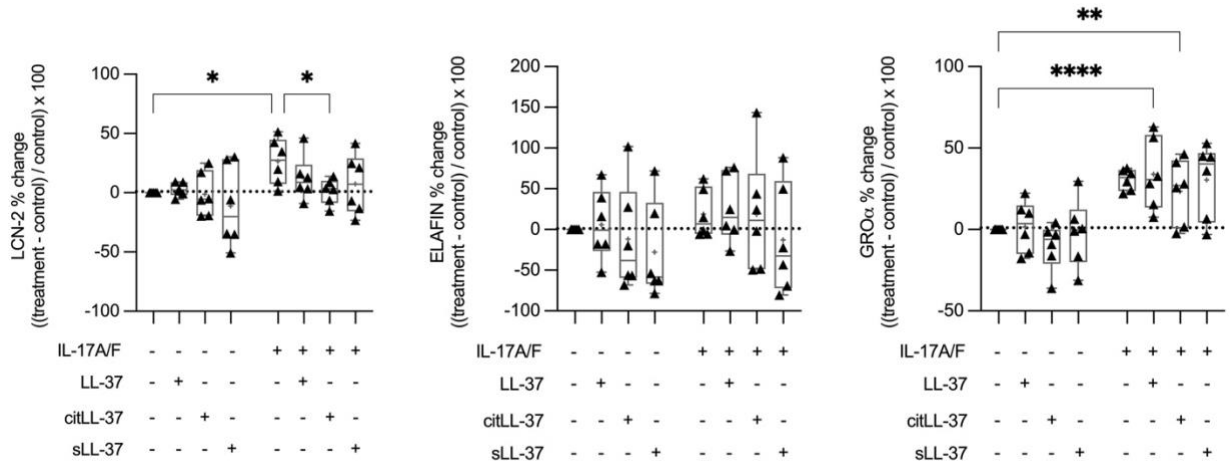

Figure 3.11: LL-37 and citLL-37 selectively alter IL-17A/F-mediated protein production in PBEC. Human PBEC obtained from three independent donors (N=3, n = 2) were stimulated with LL-37, citLL-37, or sLL-37 (0.25 μM) in the presence and absence of IL-17A/F (50 ng/mL). TC supernatant collected 24 h post-stimulation was examined for the abundance of LCN-2, Elafin, and GROα by ELISA. Y-axis represents % change compared to paired unstimulated controls within donors. Each dot represents an independent experiment, and bars show the median and min-max range. Repeated measures one-way analysis of variance with Fisher's least significant difference test was used for statistical analysis (**p≤0.05, **p≤0.001, ****p≤0.0001*).

Moreover, I investigated the ability of LL-37, citL-37, and sLL-37 to alter the abundance of IL-17-mediated transcription factors and RBP in PBEC. I stimulated PBEC with 0.25 μM of LL-37, citLL-37, or sLL-37, in the presence and absence of IL-17A/F (50 ng/mL) and confirmed the ability of LL-37, citLL-37, and sLL-37 to alter the protein abundance of selected protein targets. First, I monitored the abundance of NF-κB p65, as well as phosphorylation of p-IKKα/β (S176/180), which is required for the activation of IKK kinases and subsequent NF-κB activation by Western blots, 30 *minutes* (min) post-stimulation in PBEC. In addition, I investigated the ability of LL-37, citLL-37, and sLL-37 to alter the abundance of select protein targets, including Arid5a, Regnase-1, IκBζ, and C/EBPβ 30 min and 24 h post-stimulation in PBEC. LL-37, but not citLL-37, significantly enhanced phosphorylation of p-IKKα/β (S176/180) by ~63%, and significantly enhanced the abundance of the NF-κB subunit p65 by ~59% compared to unstimulated PBEC after 30 mins (Figure 3.12A). However, LL-37 and citLL-37 significantly enhanced the abundance of Regnase-1 30 mins post-stimulation by ~79% and ~69% respectively, compared to unstimulated PBEC (Figure 3.12B). In addition, IL-17A/F enhanced the abundance of Arid5a by ~112% at 30 mins, compared to unstimulated PBEC (Figure 3.12B). Moreover, IL-17A/F significantly increased the abundance of Arid5a and IκBζ by 65% and ~1212%, respectively compared to unstimulated PBEC 24 h post-stimulation (Figure 3.13). Furthermore, combinations of LL-37 and IL-17A/F significantly enhanced the abundance of Regnase-1 ~394%, compared to IL-17A/F stimulated cells and combinations of citLL-37 and IL-17A/F enhanced the abundance of Regnase-1 ~318% (*p=0.06*) compared to IL-17A/F PBEC (Figure 3.13). Taken together, these results suggest that the biological activity of LL-37 engages both NF-κB activation and Regnase-1, whereas that of citLL-37 enhances Regnase-1 without mediating NF-κB activation, at the time points examined. These results also indicate that suppression of IL-17A/F-mediated LCN-2 production by these peptides by engaging Regnase-1, which is a known feedback inhibitor of IL-17 signaling transduction. Taken together, these studies suggest that citrullination of LL-37 may be a post-translational mechanism to limit the pro-inflammatory arm of LL-37 via the selective loss of NF-κB activation, engaging the feedback inhibitory activity of Regnase-1, to maintain / enhance suppression of IL-17A/F-mediated LCN-2 production in bronchial epithelial cells. In comparison to signal transduction studies performed in HBEC-KT measuring mRNA abundance which suggested that LL-37 and citLL-37 suppress IL-17A/F-mediated LCN-2 production by limiting C/EBPβ production (Figure 3.10), these studies indicate that additional regulatory mechanisms may be activated by LL-37 and citLL-37 in individuals with chronic airway inflammation.

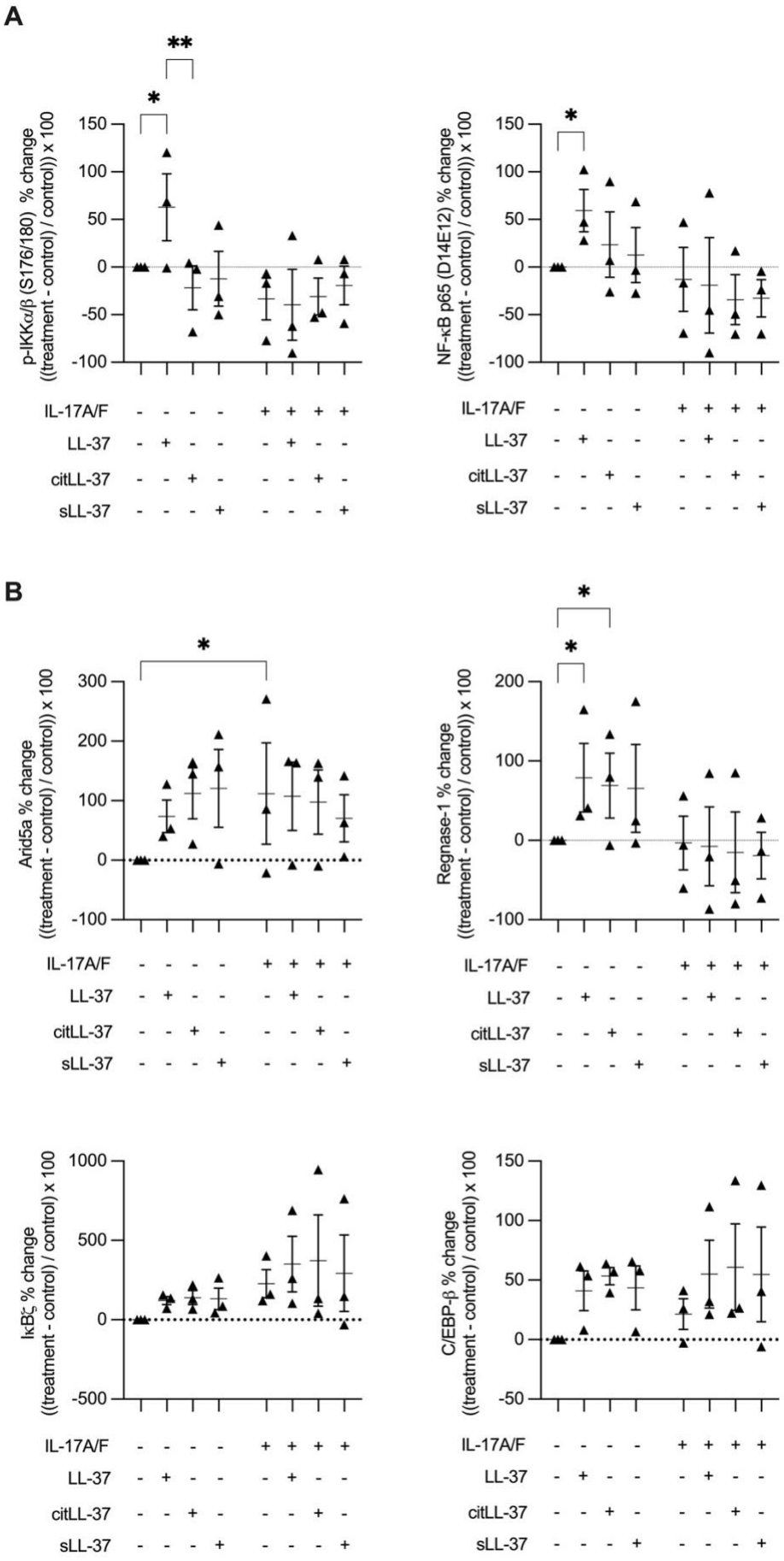
A
p-IKKα/β (S176/180) % change ((treatment - control) / control)) x 100
NF-κB p65 (D14E12) % change ((treatment - control) / control)) x 100
B
Arid5a % change ((treatment - control) / control)) x 100
Regnase-1 % change ((treatment - control) / control)) x 100
IκBζ % change ((treatment - control) / control) x 100
C/EBP-β % change ((treatment - control) / control) x 100
IL-17A/F
LL-37
citLL-37
sLL-37

Figure 3.12: LL-37 and citLL-37 enhance Regnase-1, a feedback inhibitor of IL-17-mediated signal transduction in PBEC. Human PBEC obtained from three independent donors (N=3) were stimulated with IL-17A/F (50 ng/mL) or LL-37, citLL-37, and sLL-37 (0.25 μM). Total cell lysate (25 μg) was collected from cells stimulated with LL-37, citLL-37, and sLL-37 (0.25 μM) to determine the abundance of **(A)** p-IKKα/β (S176/180) and NF-κB p65 30 minutes post-stimulation, as well as (**B**) IL-17 signal transduction proteins including Arid5a, Regnase-1, IκBζ, and C/EBPβ 30 mins post-stimulation by Western blot. Y-axis represents % change compared to paired unstimulated controls within donors. Each dot represents an independent experiment, and bars show the mean and SEM. Repeated measures one-way ANOVA with Fisher's least significant difference test was used for statistical analysis (*$p \leq 0.05$, **$p \leq 0.001$).

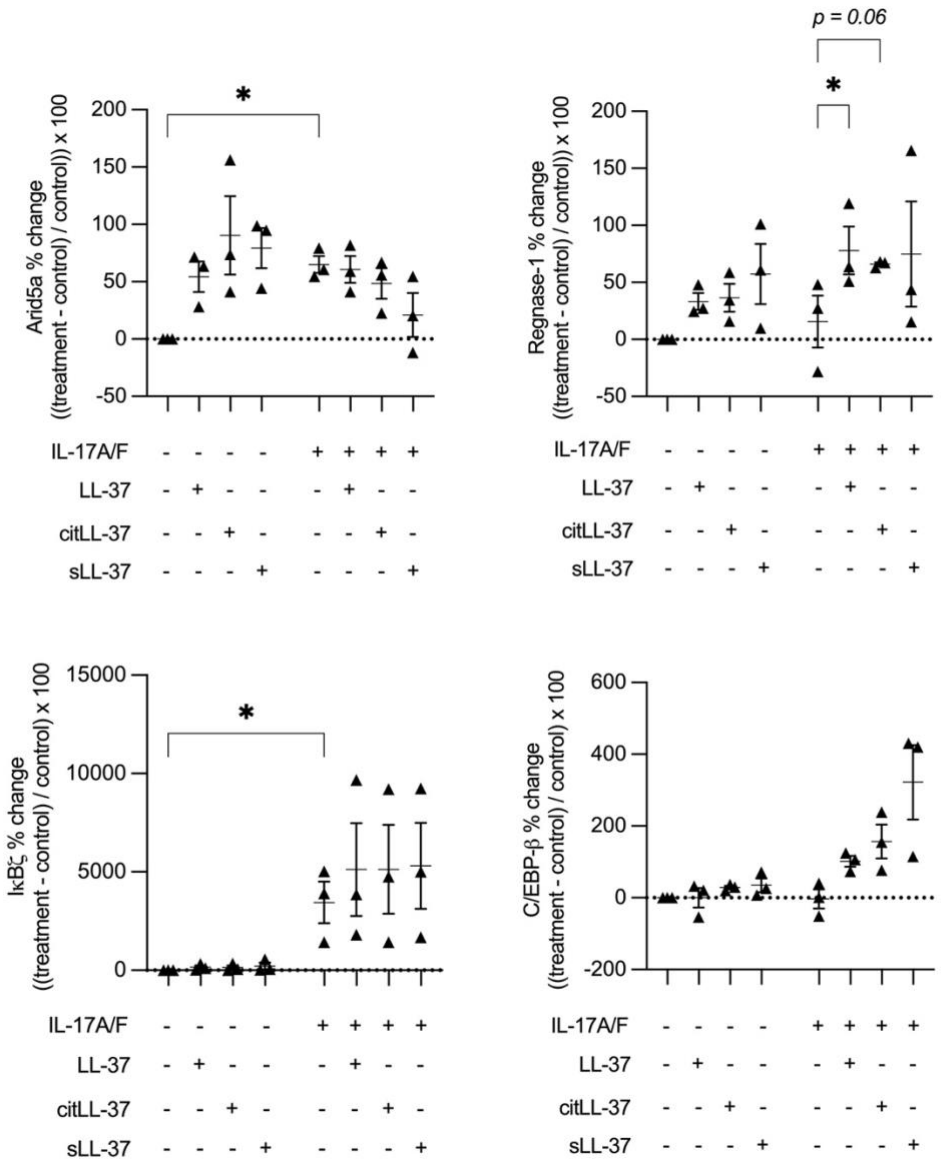

Figure 3.13: LL-37 and citLL-37 enhance Regnase-1 in the presence of IL-17A/F-mediated inflammation in PBEC. Human PBEC obtained from three independent donors (N=3) were stimulated with IL-17A/F (50 ng/mL) or LL-37, citLL-37, and sLL-37 (0.25 μM). Total cell lysate (25 μg) was collected from cells stimulated with LL-37, citLL-37, and sLL-37 (0.25 μM) to determine the abundance of IL-17 signal transduction proteins including Arid5a, Regnase-1, IκBζ, and C/EBPβ 24 h post-stimulation by Western blot. Y-axis represents % change compared to paired unstimulated controls within donors. Each dot represents an independent experiment, and bars show the mean and SEM. Repeated measures one-way ANOVA with Fisher's least significant difference test was used for statistical analysis (*$p \leq 0.05$, **$p \leq 0.001$).

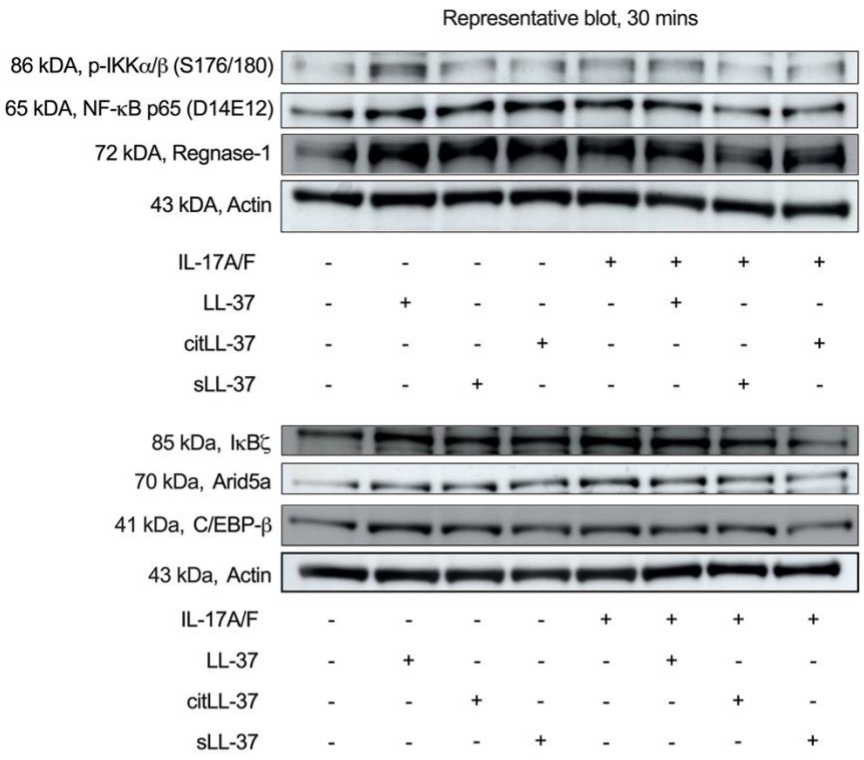
Representative blot, 30 mins
86 kDA, p-IKKα/β (S176/180)
65 kDA, NF-κB p65 (D14E12)
72 kDA, Regnase-1
43 kDA, Actin
IL-17A/F - - - - + + + +
LL-37 - + - - - + - -
citLL-37 - - - + - - - +
sLL-37 - - + - - - + -
85 kDa, IκBζ
70 kDa, Arid5a
41 kDa, C/EBP-β
43 kDa, Actin
IL-17A/F - - - - + + + +
LL-37 - + - - - + - -
citLL-37 - - + - - - + -
sLL-37 - - - + - - - +

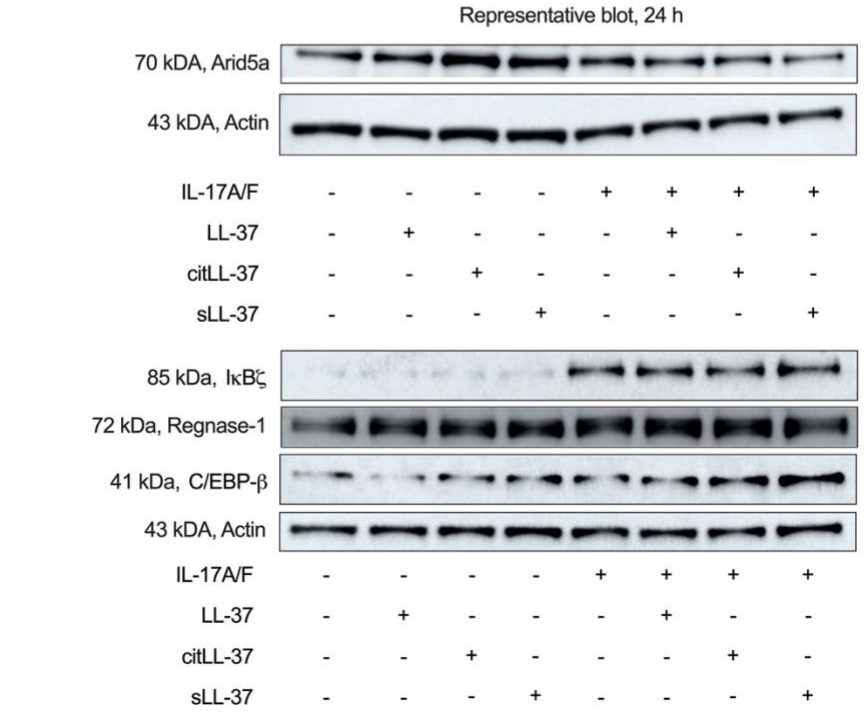
Representative blot, 24 h
70 kDA, Arid5a
43 kDA, Actin
IL-17A/F - - - - + + + +
LL-37 - + - - - + - -
citLL-37 - - + - - - + -
sLL-37 - - - + - - - +
85 kDa, IκBζ
72 kDa, Regnase-1
41 kDa, C/EBP-β
43 kDA, Actin
IL-17A/F - - - - + + + +
LL-37 - + - - - + - -
citLL-37 - - + - - - + -
sLL-37 - - - + - - - +

Figure 3.14: Representative blots for evaluating the impact of LL-37 and citLL-37on IL-17A/F-mediated inflammation in PBEC. Human PBEC obtained from one independent donor (N=1) was stimulated with IL-17A/F (50 ng/mL) or LL-37, citLL-37, and sLL-37 (0.25 μM) and used as a representative blot. Total cell lysate (25 μg) was collected from cells stimulated with LL-37, citLL-37, and sLL-37 (0.25 μM) to determine the abundance of p-IKKα/β (S176/180) and NF-κB p65 30 minutes post-stimulation as well as the abundance of IL-17 signal transduction proteins including Arid5a, Regnase-1, IκBζ, and C/EBPβ 30 mins and 24 h post-stimulation by Western blot. Y-axis represents % change compared to paired unstimulated controls within donors. Each dot represents an independent experiment, and bars show the mean and SEM. Repeated measures one-way ANOVA with Fisher's least significant difference test was used for statistical analysis (*$p \leq 0.05$, **$p \leq 0.001$).

5.3.8 LL-37, but not citLL-37 enhances the production of CCL20 in the presence/absence of IL-17A/F

Previous studies have demonstrated that IL-17A enhances the production of Th17-recruiting chemokine CCL20 in neutrophilic airway inflammation (48) and in epithelial cells (197, 200). In similar fashion to GROα, IL-17A-mediated transcription of CCL20 is solely dependent on IκBζ, but is directly targeted by endonuclease Regnase-1 for mRNA degradation (197, 202). Therefore, as an additional line of investigation, I determined the ability of LL-37 and citLL-37 to alter Th17-recruiting chemokine CCL20 production in the presence/absence of IL-17A/F in bronchial epithelial cells. HBEC-3KT and PBEC isolated from patients undergoing lung resection were stimulated with 0.25 μM LL-37, citLL-37, or sLL-37 in the presence/absence of IL-17A/F (50 ng/mL), and the abundance of CCL20 was measured by ELISA, in TC supernatant 24 h post-stimulation. LL-37 significantly enhanced the production of CCL20 in the presence / absence of IL-17A/F-mediated inflammation by ~121% and ~190%, respectively compared to unstimulated HBEC-3KT (Figure 3.15A). In addition, citrullination of LL-37 abrogated the production of CCL20 in the presence/absence of IL-17A/F in HBEC-3KT (Figure 3.15A). A similar trend was observed in human PBEC, wherein LL-37 significantly enhanced the production of CCL20 in the presence / absence of IL-17A/F-mediated inflammation by ~208% and ~532%, respectively compared to unstimulated PBEC (Figure 3.15B). Further citrullination of LL-37 dampened CCL20 production by ~50% ($p=0.06$) in the absence of IL-17A/F and significantly dampened CCL20 production by ~35% in the presence of IL-17A/F in PBEC (Figure 3.15B). These results provide additional mechanistic that evidence citrullination of LL-37 results in the selective loss of IL-17A/F-mediated IκBζ, activity, without altering the activity of the endoribonuclease Regnase-1. Taken together with previous results, these results suggest that citrullination of LL-37 is a homeostatic feedback mechanism which limits both neutrophil and Th17 accumulation in the lung by limiting chemokine production compared to native LL-37.

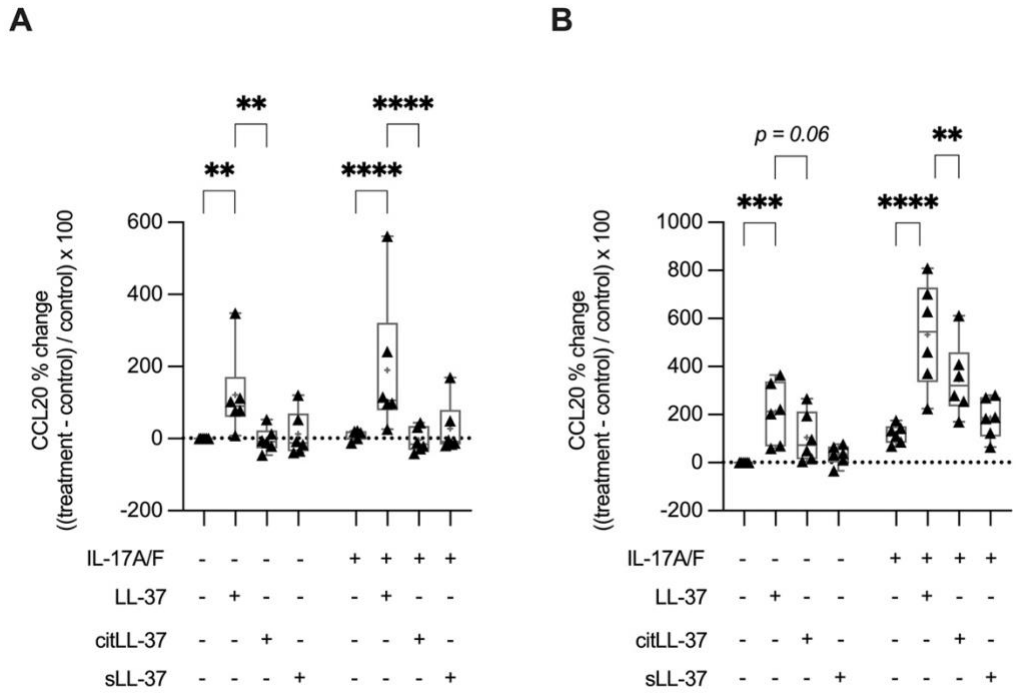

Figure 3.15: LL-37, but not citLL-37, enhances IL-17A/F-mediated CCL20 production in bronchial epithelial cells. (A) HBEC-3KT (N=6) and **(B)** human PBEC (N=3, n=2) were stimulated with LL-37, citLL-37, or sLL-37 (0.25 μM), in the presence/absence of IL-17A/F (50 ng/mL). Tissue culture supernatant collected 24h post-stimulation was examined for abundance of CCL20 by ELISA. Y-axis represents % change compared to paired unstimulated cells for each replicate. Each dot represents an independent experiment, and bars show the median and min-max range. Repeated measures one-way analysis of variance with Fisher's least significant difference test was used for statistical analysis (***p≤0.001, ***p≤0.005, ****p≤0.0001*).

5.4 Discussion

In this study, I identified proteins that are enhanced by IL-17A/F in bronchial epithelial cells, which included two CHDP, LCN-2 and Elafin. In addition to its anti-infective activity (215, 222), LCN-2 enhances neutrophil migration in chronic inflammatory disease (224, 361, 364). For example, a previous study investigating the role of LCN-2 in a mouse model of psoriasis, demonstrated that neutralization of LCN-2 significantly reduced neutrophil accumulation in sites of inflammation (224). In addition, this study demonstrated that administration of recombinant mouse (rm)LCN-2 resulted in a dose dependent increase in neutrophil-derived TNF-α, IL-6, and IL-8 via the extracellular signal-related kinase (Erk)-1/2 and p38-mitogen-activated protein kinase (MAPK) signaling pathways. Another study demonstrated that recombinant human (rh)LCN-2 and rmLCN-2 enhanced neutrophil migration in an Erk-1/2-dependent manner and subsequently demonstrated that monoclonal antibody-based neutralization of LCN-2 reduced neutrophil migration in the early phase of acute inflammation (361). Moreover, in addition to its antimicrobial activity against respiratory pathogens (346), previous studies have demonstrated cytokines IL-1β and TNF-α enhance the transcription of NE inhibitor Elafin in AEC to protect the epithelial barrier from neutrophil-mediated damage (365). This study was corroborated by another which demonstrated that NE increases Elafin transcription in PBEC to limit epithelial damage in the lung (315). My results demonstrating that IL-17A/F enhances neutrophil-associated CHDP, including LCN-2 and Elafin, are corroborated by previous studies demonstrating that IL-17 indirectly recruits neutrophils to the lung by stimulating the production of chemokines in non-hematopoietic immune cells (158, 225-227, 335).

Based on these results, LCN-2 and Elafin were selected to further investigate the impact of physiologically relevant concentrations of cathelicidin LL-37 on IL-17A/F-mediated protein production in the lung. It should be noted that LL-37 is increased in the lungs during neutrophilic inflammation and found enhanced in NET (147). Therefore, how LL-37 changes IL-17A/F-mediated downstream responses warrant investigation. Here, I demonstrate that LL-37 selectively suppresses IL-17A/F-mediated LCN-2 production, without altering Elafin production in human bronchial epithelial cells. These results indicate that LL-37 may be regulating specific mediators that promote neutrophil recruitment in the lungs such as LCN-2, without compromising proteins which protect against airway remodeling such as Elafin. Prolonged, chronic airway inflammation leads to permanent structural changes, called airway remodeling, which include narrow and thickened airways and ultimately, difficulty breathing, a critical feature of asthma pathogenesis (366). Elafin has been previously shown to be protective in the process of airway remodeling (315, 365). Thus, my results

suggest that LL-37 may have a protective effect on airway remodeling, as it does not suppress Elafin production. However, both LCN-2 and Elafin also have potent antimicrobial functions (215, 222, 346). Therefore, the impact of a CHDP such as LL-37 on other CHDPs during bronchial inflammation remains unclear in the context of antimicrobial functions. Nevertheless, my findings show that LL-37 selectively suppress IL-17A/F-mediated LCN-2 without impairing Elafin production, which indicates disparate functions in the context of airway inflammation compared to remodeling, which needs further investigation.

I confirmed some of my findings *in vivo* using a physiologically representative mouse model of airway inflammation with allergen HDM along with low concentration of endotoxin during the sensitization phase which results in IL-17-driven neutrophil accumulation and NET formation in the lung (150). I demonstrated that CRAMP (the mouse analog of LL-37), IL-17A/F, LCN-2, and NE are all concurrently elevated in the lungs with increased neutrophilic accumulation in this mouse model. These proteins were comparatively lower in mice challenged with allergen alone wherein the inflammatory milieu is typically eosinophilic airway inflammation. I demonstrated that LCN-2 positively correlates with NE in the lungs, suggesting that LCN-2 may play a role in facilitating neutrophilic airway inflammation in IL-17A/F-driven airway inflammation. Moreover, I demonstrated that CRAMP negatively correlates with both LCN-2 abundance and neutrophil accumulation. Taken together, the *in vitro* and *in vivo* results suggest that cathelicidins may be limiting neutrophilic inflammation by suppressing the production of LCN-2, which needs further functional investigation. Further, in mechanistic studies, I showed that LL-37 suppresses the abundance of C/EBPβ mRNA, a critical transcription factor required for LCN-2 production in HBEC-3KT (197), whereas LL-37 enhances the RNA-binding protein Regnase-1, which is a critical feedback inhibitor of IL-17-mediated signal transduction and LCN-2 production in PBEC (197, 200). My results suggest that LL-37 selectively alters the inflammatory milieu by modifying both transcription factors and post-transcriptional signaling, a finding that is novel in the context of the immunobiology of cathelicidins

To my knowledge, this is the first study to demonstrate that LL-37 selectively suppresses cytokine-mediated production of pro-inflammatory mediators (e.g., LCN-2) in non-hematopoietic cells, a process that was previously demonstrated in leukocytes. For example, a previous study demonstrated that LL-37 suppresses IL-32-induced pro-inflammatory cytokines TNF-α, IL-6 and IL-1β and enhances anti-inflammatory cytokine IL-1RA through suppression of Fyn (Y420) Src Kinase signaling in human macrophages and PBMC (43), highlighting the anti-inflammatory capacity of LL-

37 in cytokine-mediated inflammation in leukocytes. Conversely, other studies investigating the function of LL-37 in non-hematopoietic innate immune cells demonstrated that combination of LL-37 and IL-17A induces the transcription of TNF-α in a human synovial sarcoma cell line (115), and LL-37 with IL-1β synergistically increases IL-8 production in AEC (137). To the best of my knowledge, my results are the first to demonstrate that LL-37 can selectively suppress pro-inflammatory mediator such as LCN-2 production in non-hematopoietic immune structural cells, such as epithelial cells. In addition, the ability of LL-37 to selectively suppress IL-17A/F-mediated LCN-2 production highlights the role of crosstalk between CHDPs in regulating the inflammatory cascade. Previous studies investigating the regulatory activity of CHDP primarily focused on downstream pro-inflammatory and anti-inflammatory cytokines as readouts for inflammation (32, 33, 43, 44). Here, I demonstrate that cathelicidin disparately alters the production of other CHDP such as LCN-2 and Elafin. To the best of my knowledge, this is the first report that demonstrates the ability of LL-37 to alter the production of other CHDP. The aspect of how the network of various CHDP is altered by the activity of cathelicidins is an important regulatory component that needs to further investigation.

The mechanistic underpinnings of LL-37 on IL-17A/F-mediated regulation in bronchial epithelial cells have not been investigated. Here I demonstrate that LL-37 and citLL-37 suppress IL-17A/F-mediated production of *CEBPB* (gene of C/EBPβ) mRNA. One study has demonstrated that IL-17A-mediated production of LCN-2 is dependent on transcription factors C/EBPβ and IκBζ in epithelial cells (197). However, another study demonstrated that LCN-2 production enhanced by the combination of IL-17A and TNF-α was regulated by IκBζ but not C/EBPβ in AEC (202). Nonetheless, my findings suggest that LL-37 and citLL-37 suppress IL-17A/F-mediated LCN-2 production by suppressing IL-17A/F-mediated *CEBPB* transcription. In addition, post-transcriptional regulation plays a critical role in regulation of inflammation (192, 193). Previous studies have demonstrated IL-17-mediated inflammation is a function of the competitive interplay of RBP which regulate the production of critical transcription factors required for the induction of neutrophil-associated chemokines and CHDP, including LCN-2 (197, 200). Further, these studies have demonstrated that Regnase-1 is a critical feedback inhibitor of IL-17-mediated LCN-2 production (197, 200). Here, I demonstrate that LL-37 and citLL-37 increase IL-17AF/-mediated Regnase-1 abundance in human PBEC. This suggests that LL-37 may selectively regulate IL-17A/F-mediated LCN-2 production by altering the proteins which control post-transcriptional regulation. Although the impact of LL-37 on post-transcriptional regulation is not completely defined here, my findings are supported by previous studies investigating the mechanism of LL-37 in inflammation. For example, a previous study

demonstrated that TNF-α suppression was associated with a direct interaction between LL-37 and GAPDH in monocytes (44), whereas another demonstrated that GAPDH moonlights as an RBP to represses TNF-α production in monocytes by increasing the degradation of *TNFα* mRNA (367). Therefore, in addition to the results in this study, previous findings suggest that one of the mechanisms by which LL-37 selectively alters inflammation is by modifying post-transcriptional regulation. The precise role of LL-37 in selectively regulating inflammation through alterations to the post-transcriptional machinery represents is an exciting line of investigation for future mechanistic studies.

Previous investigations delineating the role of LL-37 in regulating inflammation have demonstrated that citrullination of LL-37 impairs its ability to regulate anti-infective inflammation (138-142). For example, citrullination of LL-37 limits LPS neutralizing activity of the native peptide (139-141) and increases serum pro-inflammatory cytokine IL-6 abundance in a model of sepsis (140). Additionally, reports have demonstrated that PADI2- and PADI4-dependent citrullination of LL-37 is a relevant post-translational modification in the human lung (138, 139), and that PADI4 activation is increased in IL-17-driven neutrophilic airway inflammation (150). Taken together, this suggests that citrullination may alter the ability of LL-37 to regulate cytokine-driven inflammation, a process that has yet to be investigated. In contrast to previous reports, I demonstrate that citrullination does not limit the ability of LL-37 to suppress inflammation. For example, I demonstrated that citrullination of LL-37 dampens the ability of LL-37 to enhance GROα and CCL20 production in the presence of IL-17A/F. Furthermore, I demonstrated that LL-37, but not citLL37, enhanced IL-17A/F-mediated enhancement of IκBζ mRNA abundance. As a previous study has demonstrated that KD of IκBζ abrogated IL-17A-mediated induction of *CXCL1* (gene of GROα) (200), this suggests that the differential activity of LL-37 and citLL-37 on IL-17A/F-mediated GROα and CCL20 production is due to the selective loss of IκBζ mRNA abundance increases by citLL-37. In addition, I demonstrated that citrullinated LL-37 suppresses IL-17A/F-mediated LCN-2 production in human bronchial epithelial cells, wherein LCN-2 levels were suppressed to baseline in human primary cells. Moreover, I demonstrate that citrullination of LL-37 results in the selective loss of pro-inflammatory NF-κB signal transduction, without altering the increase in anti-inflammatory Regnase-1 abundance in human PBEC. Overall, these results suggest that citrullination may selectively limit pro-inflammatory functions of LL-37 without impairing the ability to limit its anti-inflammatory functions. Note that my studies are in the context of cytokine-mediated inflammation, as opposed to pathogen-associated inflammation as reported in the above-mentioned previous studies. Thus, the contradictory findings in my study demonstrating that citrullination does not impair all immunomodulatory functions of LL-37

may be because in the above mentioned previous studies the anti-infective / immunomodulatory properties of citLL-37 was examined in the context of endotoxin and the loss of binding negatively charged endotoxin by citLL-37 (138). To my knowledge, my findings show for the first time that citrullination does not impair all immunomodulatory functions of LL-37, and that it may be a mechanism to facilitate immune homeostasis by selectively limiting the peptide's pro-inflammatory functions. This opens new avenue of research for further examining the impact of citrullination on LL-37-mediated regulatory functions within cytokine-driven inflammatory milieu.

Previous studies have demonstrated that cathelicidin levels are altered during airway inflammation (102, 139, 146-148), however whether these peptides are increased or decreased seems to be dependent on the kinetic and type of airway inflammation. Thus, the role of these peptides in the pathogenesis of airway inflammation, including IL-17-driven neutrophilic airway inflammation (and therefore severe asthma) remains unclear. I demonstrate that CRAMP (a mouse analog of LL-37) levels are increased along with IL-17A/F in a model that is characterized by neutrophilic-skewed airway inflammation. Neutrophils are a dominant source of cathelicidins in chronic lung disease characterized by airway inflammation (368). Concomitant increase in LL-37 with markers of NET formation, including NE and extracellular DNA has been previously demonstrated in humans (147). Mouse model studies have shown that CRAMP is decreased in eosinophilic airway inflammation compared to naïve mice (102). Here, I demonstrate that CRAMP is negatively correlated with LCN-2 abundance and neutrophil accumulation in the murine lung. In human cells, I demonstrate that LL-37 suppresses IL-17A/F mediated production of LCN-2. Taken together, these findings suggest that CRAMP secretion by neutrophils may be a negative-feedback loop to limit IL-17A/F-mediated neutrophil recruitment via LCN-2 to the lung. However, regulation of IL-17A/F-mediated downstream processes by cathelicidins may be time-dependent. Recently, one study has demonstrated that cathelicidin potentiates IL-17A/F-producing Th17 cells in the lung (124), suggesting that cathelicidin may drive neutrophil accumulation in the lung during the initiation phase of inflammation. Therefore, based on my results, I speculate that cathelicidins may play a role in limiting neutrophilic airway inflammation at a later time point by intervening in IL-17-mediated downstream response such as LCN-2. As such, the precise role that cathelicidins such as LL-37 plays in the initiation and resolution of IL-17A/F-mediated neutrophilic inflammation warrants further investigation, as that could lead to the identification of new regulatory mechanisms related to severe asthma.

Severe, late-onset, neutrophilic asthma predominantly affects females compared to males (369, 370). In addition, Th17-mediated airway inflammation is enhanced in females compared to males

(370). Therefore, while not the primary focus of my study, I also performed sex-disaggregated data analysis to account for sex-differences in the mouse model of neutrophilic airway inflammation. Here, I demonstrate that cathelicidin CRAMP abundance is negatively correlated with neutrophil accumulation in the lung in both sexes, yet this correlation differed by tissue compartments. In female mice, CRAMP abundance in the tissue was negatively correlated with neutrophil accumulation in the lungs. Conversely, in male mice CRAMP abundance in the BAL was negatively correlated with neutrophil accumulation in the lung. The significance of these sex-specific differences in CRAMP abundance and subsequent impact on neutrophil accumulation requires future investigation.

5.5 Summary

In this study, I demonstrate that LL-37 selectively alters the IL-17A/F-mediated bronchial proteome to suppress CHDP LCN-2 production without limiting other proteins such as Elafin and Gro-α. In mechanistic studies I show that the ability of LL-37 and citrullinated LL-37 to selectively limit LCN-2 production may be by altering the production of transcription factors, such as C/EBPβ or by engaging post-transcriptional machinery, such as Regnase-1. Moreover, I demonstrate that citrullination of LL-37 may be a homeostatic feedback mechanism which dampens the production of neutrophil- and Th17-recruiting chemokines. In an *in vivo* model I show that although cathelicidin CRAMP, LCN-2, NE and IL-17A/F are concurrently enhanced in the lungs in a model of neutrophilic airway inflammation, the level of CRAMP negatively correlates with LCN-2 and neutrophil accumulation. Thus, cathelicidins may play a role in limiting neutrophilic inflammation, albeit that will depend on the kinetics of inflammatory response. Overall, the findings in this study provide insight into the interplay of LL-37 and IL-17A/F during neutrophilic airway inflammation, and therefore relevant to the immunobiology of severe, uncontrolled asthma. As a result, the protein targets identified by this study may be useful to develop interventional strategies derived from cathelicidin LL-37 (e.g., synthetic IDR peptides) which target the biological processes identified to regulate IL-17-driven neutrophil accumulation in the lung. These will be beneficial in chronic respiratory diseases such as steroid-unresponsive asthma or COPD.

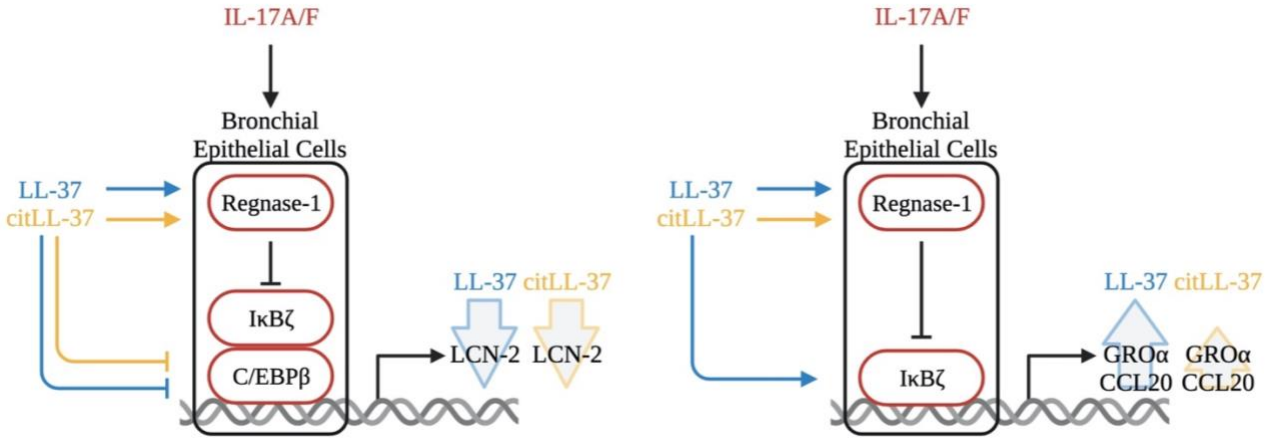

Figure 3.16: LL-37 alters TF and RBP to limit IL-17A/F-mediated LCN-2 production and enhance GROα and CCL20 production in bronchial epithelial cells. IL-17A/F-mediated inflammation disparately enhances production of neutrophil-associated CHDP (e.g., LCN-2) and chemokines (e.g., GROα, CCL20) via differential dependence on the TF C/EBPβ. LL-37 and citLL-37 decreases the abundance of TF (e.g., C/EBPβ) and RBP (e.g., Regnase-1), which positively and negatively regulate LCN-2 production, respectively. Alternatively, LL-37 but not citLL-37, enhances the abundance of IκBζ, resulting in differential production of GROα, CCL20. *This figure created using biorender.com.*

Chapter 6: Cathelicidin LL-37 suppresses TNF-α-mediated production of airway remodeling factors MMP9 & MMP13 in human bronchial epithelial cells

6.1 Abstract

Background: Asthma is a heterogenous disease characterized by chronic inflammation in the lung. Chronic airway inflammation can lead to permanent structural changes (known as airway remodeling) in the lungs. TNF-α is a critical mediator of airway inflammation and is associated with increased severity in chronic respiratory diseases. Similarly, human host defence peptide cathelicidin LL-37 is also enhanced in airway inflammation. LL-37 has been previously shown to increase the production of *tissue inhibitor of metalloproteinase* (TIMP)-1, a negative regulator of matrix metalloproteinases, which is known to play a protective role in airway remodeling and AHR. However, the interplay of TNF-α and LL-37 in the context of airway remodelling has not yet been defined.

Objective: To characterize protein changes in response to TNF-α and LL-37 in bronchial epithelial cells.

Methods: HBEC-3KT were stimulated with TNF-α (20 ng/mL). Cell lysates (N=5) were probed using a high content aptamer-based proteomic array at 24 h. Differential analysis was performed on normalized log2 protein expression values, along with Welch's t-test ($p<0.05$) to identify proteins that were significantly changed in response to TNF-α. Proteins known to be associated with airway remodeling, MMP9 and MMP13, were significantly enhanced by TNF-α and selected for independent studies. These proteins were independently validated by ELISA in HBEC-3KT, and in human PBEC obtained from resected lung tissue (in submerged and physiologically representative, mucociliary-differentiated *air-liquid interface* (ALI) cultures) after 24 h. Related signaling pathways were examined using pharmacological inhibitors targeting SRC, PI3K, and PKC. The ability of physiological concentrations of LL-37 to selectively alter the production of the selected airway remodeling factors MMP9 and MMP13 was further examined in HBEC-3KT and PBEC at 24 h. Western blots were performed to determine alterations to PI3K signal transduction by LL-37 in HBEC-3KT after 30 m.

Results: Proteomic profiling and independent validation studies demonstrated that TNF-α enhanced the abundance of airway remodeling factors MMP9 and MMP13 in HBEC-3KT and human PBEC. Pharmacological inhibition of SRC signaling suppressed TNF-α-mediated production of MMP9 &

MMP13 in HBEC-3KT. Pharmacological inhibition of PI3K suppressed TNF-α-mediated MMP13 production, but not TNF-α-mediated MMP9 production in HBEC-3KT. Physiological concentrations of LL-37 suppressed the abundance of TNF-α-mediated MMP9 and MMP13 production in HBEC-3KT. Mechanistic studies showed that LL-37 enhanced phospho-AKT(T308) in HBEC-3KT after 30 m stimulation.

Conclusion: These results indicate that LL-37 may protect against detrimental airway remodeling by suppressing TNF-α-mediated MMP9 and MMP13 production in human bronchial epithelial cells.

6.2 Introduction

CHDP are small endogenous peptides with direct and indirect anti-infective and immunomodulatory capabilities (19-21). Two best characterized families of CHDP in mammals are defensins and cathelicidins. The sole human cathelicidin is LL-37 has been shown to selectively modulate cytokine-mediated inflammation (19-21). In addition, mounting evidence suggests that LL-37 contributes to wound healing and tissue remodeling (371, 372). For example, one recent study has demonstrated that physiological concentrations of LL-37 enhanced the production of *tissue inhibitor of metalloproteinase* (TIMP)-1, a negative regulator of tissue remodeling factors (i.e., MMP), in gingival fibroblasts (373). However, the impact of LL-37 on inflammatory cytokine-driven processes and its subsequent effect on tissue remodeling factors is not well understood.

Airway inflammation is a central component of chronic inflammatory disease of the airways, including asthma. Chronic airway inflammation can cause airway remodeling, defined by permanent structural changes in the airways (e.g., narrowed, and thickened airways). Airway remodeling is irreversible and changes to the structure of the airway may lead to long-term loss of function (70, 71). The airway inflammation in asthma which leads to airway remodeling is heterogeneous and may be either Th2-driven or Th2-low/Th17-driven. The Th2-low/Th17-driven disease is associated with increased accumulation of neutrophils in the lungs, elevated levels of TNF-α (317, 318, 326, 374), and elevated expression of TNF-α-inducible airway remodeling factor *MMP9* (79, 375). Although neutrophilic asthma is also associated with elevated levels of LL-37 (147), it remains to be defined how LL-37 changes TNF-α-induced airway remodeling factors in bronchial epithelial cells. Therefore, in this study I investigated the effect of LL-37 on TNF-α-mediated MMP production in human bronchial epithelial cells. As a previous study has indicated that LL-37 may decrease total MMP

activity (373), I hypothesized that LL-37 would selectively suppress TNF-α-mediated MMP production in bronchial epithelial cells.

Here, I demonstrate that MMP9 and MMP13 are the dominant airway remodeling factors enhanced in response to TNF-α in HBEC-3KT and human PBEC. Further, I demonstrate that TNF-α-mediated MMP9 and MMP13 production is significantly suppressed by pharmacological inhibitors specific to Src and PKC signaling intermediates, indicating the involvement of these pathways in TNF-α-mediated MMP9 and MMP13 production. In addition, I demonstrate that TNF-α-mediated MMP13 production is significantly suppressed by pharmacological inhibitors specific to PI3K, whereas MMP9 production is not. Moreover, I demonstrate that LL-37 selectively suppresses MMP9 and MMP13 production. I also demonstrate that LL-37 enhances the phosphorylation of PI3K-related signal transduction factor AKT(T308) but not AKT(S473), which is associated with negative regulation of PI3K/AKT signaling (376). These findings suggest that LL-37 suppresses TNF-α-mediated production and secretion of MMP13 in bronchial epithelial cells by modulating the PI3K/AKT signal transduction pathway. Therefore, LL-37 may intervene in the process of airway remodeling in neutrophilic inflammation.

6.3 Results

6.3.1 TNF-α enhances airway remodeling factor MMP9 and MMP13 abundance in bronchial epithelial cells

To identify the proteins that were enhanced in response to TNF-α, I performed proteomic profiling of human bronchial epithelial cells (HBEC-3KT; ATCC® CRL-4051™) stimulated with TNF-α (20 ng/mL) for 24 h. Cell lysates (14 µg total protein per sample) were obtained from five independent experiments of HBEC-3KT cells in the presence/absence of TNF-α (20 ng/mL). Each lysate was independently probed using high content aptamer-based proteomic profiling (N=5 for each group). The concentration of TNF-α and the time point selected were based on previous studies (45, 377). Pairwise differential analysis conducted on normalized log2 protein expression values demonstrated that TNF-α significantly altered the abundance of 124 proteins compared to unstimulated cells (Figure 4.1A); increasing the abundance of 62 proteins and decreasing the abundance of 62 proteins. The protein with the greatest increase in abundance was MMP9 (~10-fold increase), an airway remodeling factor associated with neutrophilic airway inflammation and the development of experimental acute lung injury (79, 378). In addition, the airway remodeling factor MMP13 (~3-fold increase) was also significantly increased. MMP13 is associated with bleomycin-induced pulmonary fibrosis (379). To

confirm TNF-α-mediated increase in these proteins, I performed independent studies to examine MMP production by ELISA. I stimulated HBEC-3KT with TNF-α (20 ng/mL), and in parallel used IFN-γ (30 ng/mL) stimulation as a negative control and monitored TC supernatants by ELISA at 24 h. TNF-α enhanced MMP9 and MMP13 abundance in the supernatant compared to unstimulated controls (~2700% and ~3000% increase respectively) in HBEC-3KT (Figure 4.1B & 4.1C) at 24 h.

In addition, I performed experiments in PBEC isolated from individuals undergoing lung resection, to confirm the findings in primary cells. These experiments were performed in both submerged PBEC cell cultures (2D) and in physiologically representative, mucocilliary-differentiated ALI-PBEC cultures. These cells were stimulated with a range of concentrations of TNF-α and IFN-γ as indicated, and TC were monitored for the abundance of MMP9 and MMP13 by ELISA after 24 h. In submerged PBEC cultures, TNF-α significantly enhanced MMP9 abundance (~1000% increase) and increased MMP13 abundance (~200% increase, $p = 0.062$) TNF-α after 24 h in TC supernatant (Figure 4.2A). In mucocilliary-differentiated PBEC-ALI cultures, TNF-α enhanced MMP9 and MMP13 production (Figure 4.2B), but additional experiments are required to determine if these changes are statistically significant. These results suggest that TNF-α drives airway remodeling by enhancing the abundance of MMP9 and MMP13 in bronchial epithelial cells. Therefore, MMP9 and MMP13 were selected as protein targets to investigate of the impact of the human cathelicidin LL-37 on these proteins and subsequent airway remodelling.

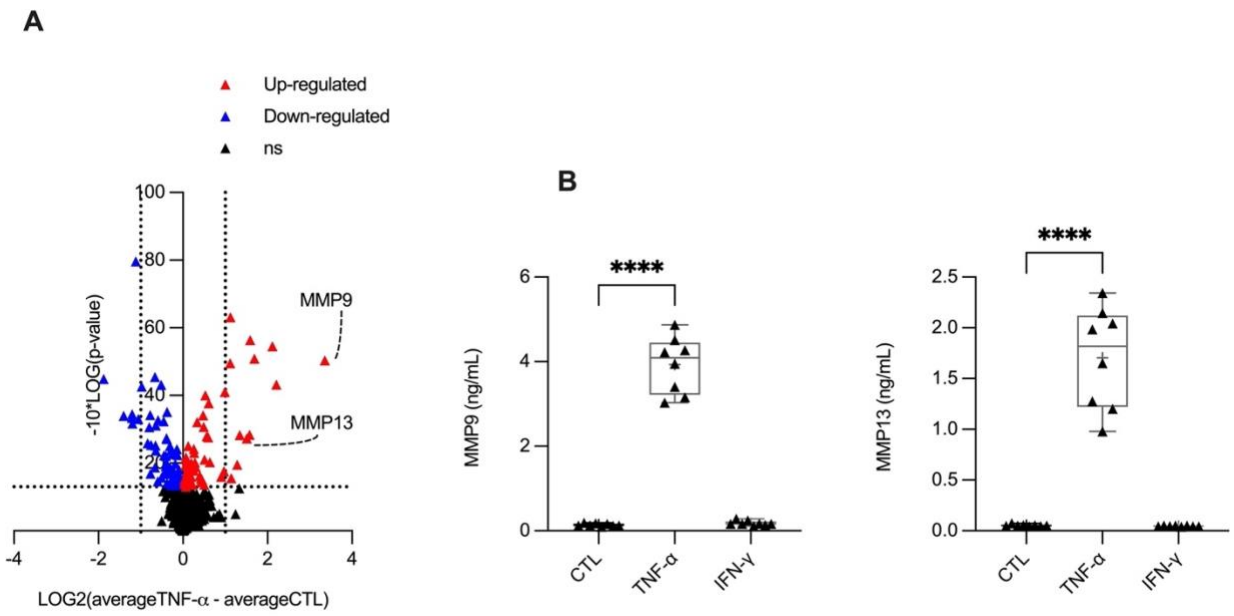

Figure 4.1: TNF-α enhances MMP9 and MMP13 production in HBEC-3KT at 24 h. HBEC-3KT were stimulated with TNF-α (20 ng/mL) and compared to unstimulated (CTL) cells after 24 hours. **(A)** Cell lysates (14 µg total protein per sample) obtained from five independent experiments were probed using the high-content aptamer-based proteomic array. Pairwise differential analysis was conducted on normalized log2 protein expression values, and Welch's t-test with a cutoff of $p<0.05$ was used to select protein abundance changes that were significantly altered in response to the combination of TNF-α. Volcano plot demonstrating differentially abundant proteins in response to TNF-α compared to CTL. **(B)** HBEC-3KT supernatant was collected from cells 24 h post-stimulation to determine the abundance of MMP9 & MMP13. Y-axis represents ng/mL. Each dot represents an independent experiment, and bars show the median and min-max range. One-way ANOVA with Fisher's least significant difference test was used for statistical analysis (****$p<0.0001$).

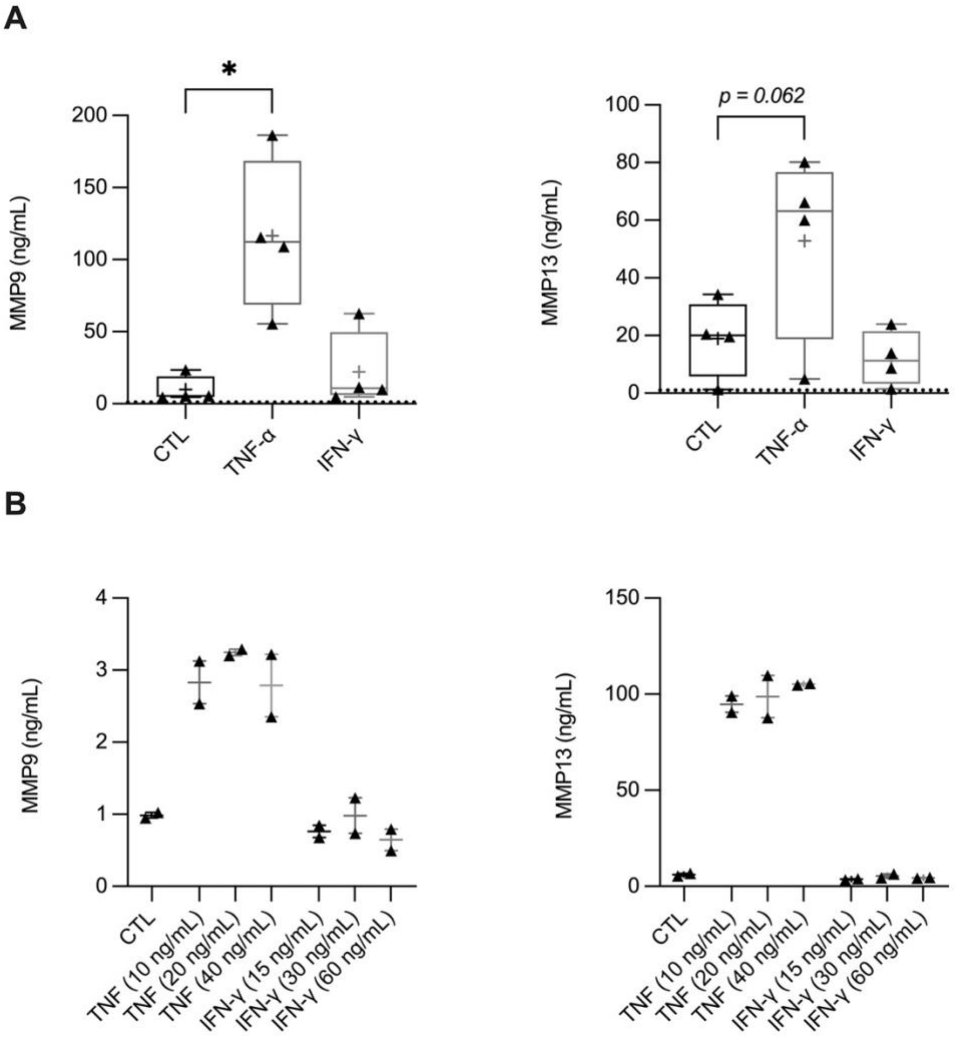

Figure 4.2: TNF-α significantly increases MMP9 & MMP13 abundance in PBEC at 24 h. Human PBEC were stimulated with TNF-α (20 ng/mL) or IFN-γ (30 ng/mL) for 24 hours. **(A)** Tissue culture supernatant from PBEC isolated from 4 separate individuals undergoing lung resection (N=4) was examined for the abundance of airway remodeling factors MMP9 and MMP13 by ELISA. Y-axis represents ng/mL. Each dot represents an independent experiment, and bars show the median and IQR, whereas whiskers show min-max range. Repeated measures one-way ANOVA with Fisher's least significant difference test was used for statistical analysis (*$p \leq 0.05$). **(B)** Supernatants from the basal side of differentiated PBEC air-liquid interface (ALI) cultures (PBEC from N=2 independent donors) was collected after 24 h and examined for the abundance of MMP9 and MMP13 by ELISA. Y-axis represents ng/mL. Each dot represents an independent experiment, and bars show the median and min-max range.

6.3.2 TNF-α-mediated enhancement of MMP9 and MMP13 involves Src-kinase activity

Previous studies have demonstrated that PI3K, PKC, and Src regulate MMP9 production in virally transformed AEC (380). In addition, one study demonstrated that Src is upstream of PI3K signaling in alveolar epithelial cells (381). Therefore, I hypothesized that PI3K, PKC, and Src regulate MMP9 and/or MMP13 production in bronchial epithelial cells. As such, I examined the effect of specific pharmacological inhibitors to determine the impact of these pathways on TNF-α-mediated MMP9 and MMP13 production. HBEC-3KT were pre-treated with pharmacological inhibitors specific to Src (SRCi; SRC1i and Dasatinib), PI3K (PI3Ki; LY294002), and PKC (PKCi; GO6976) at various concentrations as indicated for 1 h prior to treatment with TNF-α (20 ng/mL). SRCi concentrations were selected based on previous studies (380). Abundance of MMP9 and MMP13 were monitored in TC supernatants by ELISA after 24 h. SRCi and Dasatinib at 1μM suppressed the production of TNF-α-mediated MMP9 and MMP13 by ~50%. Further, 5μM concentration of the inhibitors abrogated TNF-α-mediated MMP9 and MMP13 production (Figure 4.3A & 4.3B).

Similarly, PKC inhibitor (GO6976) mitigated MMP13 and MMP9 production in HBEC-3KT after 24 h (Figure 4.4A and 4.4B). In addition, PI3K inhibitor (LY294002) mitigated MMP13 production, but did not alter MMP9 production in HBEC-3KT after 24 h (Figure 4.4A and 4.4B) These results indicate that TNF-α-mediated production of MMP9 and MMP13 are differentially regulated by PI3K signaling in HBEC-3KT.

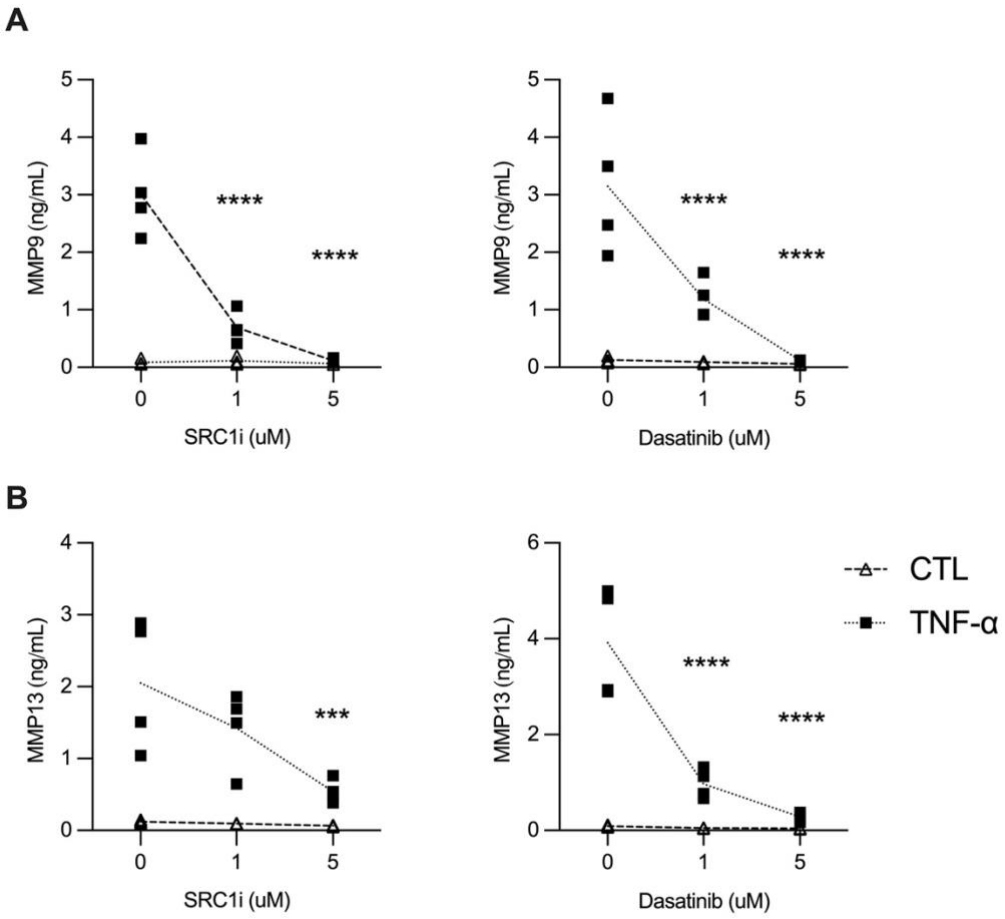

Figure 4.3: Src inhibitors suppress TNF-α-mediated MMP9 and MMP13 production. HBEC-3KT cells were pre-treated with pharmacological inhibitors SRC1 Inhibitor (SRCi) and Dasatinib for 1 h prior to stimulation with TNF-α (20 ng/mL). TC supernatants were collected after 24 h and examined for protein production by ELISA for **(A)** MMP9 and **(B)** MMP13. Y-axis represents ng/mL. Each data point represents one independent replicate (N=4), and the line represents the average values. Two-way ANOVA with Dunnett's test for multiple comparisons was used to determine statistical significance (****p<0.001*, *****p<0.0001*).

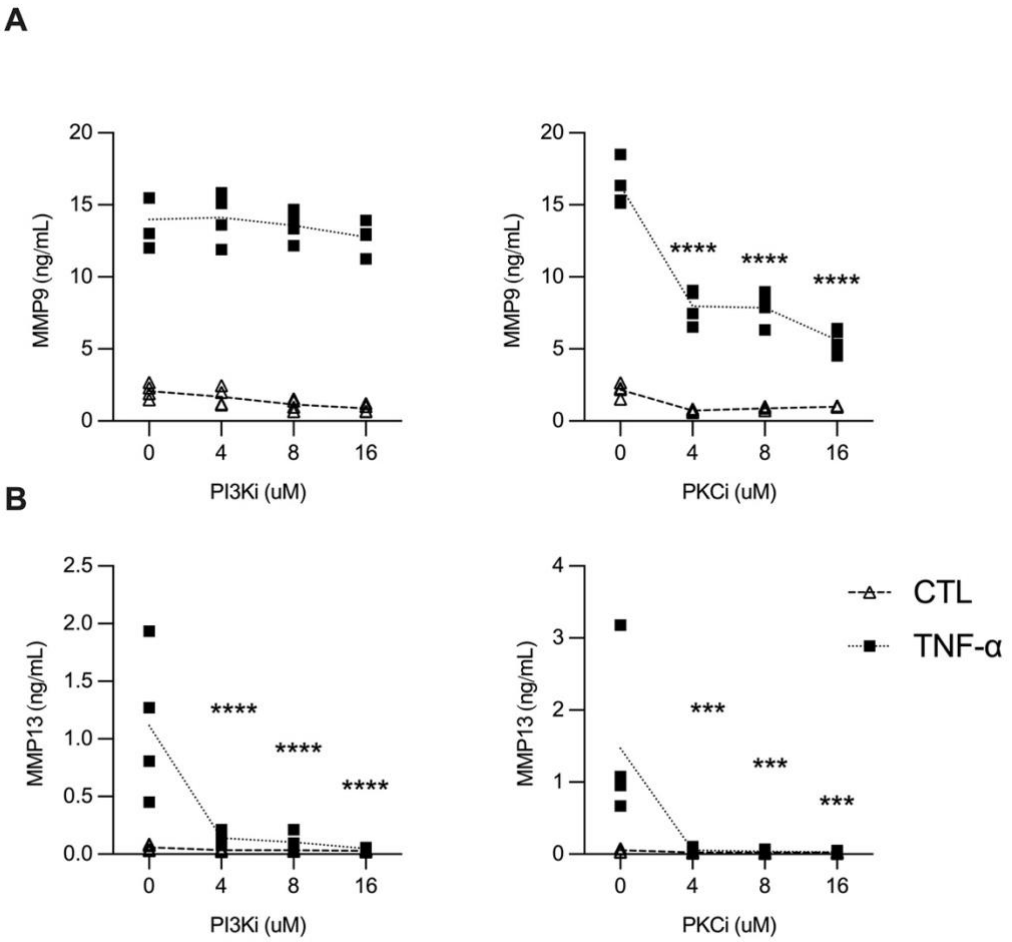

Figure 4.4: PI3Ki and PKCi suppress TNF-α-mediated MMP13 production. HBEC-3KT cells were pre-treated with pharmacological PI3K inhibitor (PI3Ki; LY290042) and PKC inhibitor (PKCi; GO6976) for 1 h prior to stimulation with TNF-α (20 ng/mL). Tissue culture supernatants were collected after 24 h and examined for protein production by ELISA for **(A)** MMP9 and **(B)** MMP13. Y-axis represents ng/mL. Each data point represents one independent replicate (N=4), and the line represents the average. Two-way analysis of variance (ANOVA) with Dunnett's test for multiple comparisons was used to determine statistical significance (****p<0.001, ****p<0.0001*).

6.3.3 LL-37 and citrullinated LL-37 suppress TNF-α-mediated production of MMP9 and MMP13 in bronchial epithelial cells

Next, I measured the impact of LL-37 and the physiologically relevant post-translational modified form of the peptide, citrullinated LL-37 (citLL-37), on TNF-α-mediated MMP9 and MMP13 production in bronchial epithelial cells. *In vitro* and *in vivo* studies have demonstrated that one to all five arginine residues in LL-37 can be converted to citrulline (138-140), which decreases the ability of the peptide to neutralize LPS and consequent pro-inflammatory mediators (139-141), as well as significantly attenuate anti-bacterial (138, 139) and anti-viral properties (142), compared to native LL-37. A scrambled peptide (sLL-37) was used as a paired control. The concentration of LL-37 was selected based of previous experiments, where 0.25 μM LL-37 induced a statistically significant increase in GROα and IL-8 (Figure 3.2A) without a corresponding increase in cellular cytotoxicity (Figure 3.2B) in HBEC-3KT 24 h post-stimulation. HBEC-3KT and human PBEC were stimulated with LL-37, citLL-37, or sLL-37 (0.25 μM of each peptide) in the presence/absence of TNF-α (20 ng/mL). The abundance of MMP9 and MMP13 was measured by ELISA in TC supernatant 24 h post-stimulation. LL-37 and citLL-37 significantly suppressed TNF-α-mediated MMP9 production by ~53% and ~50% respectively in HBEC-3KT (Figure 4.5A). In addition, LL-37 abrogated TNF-α-mediated MMP13 production with a ~91% reduction, whereas citLL-37 suppressed TNF-α-mediated MMP13 by ~54% (*p=0.064*), in HBEC-3KT (Figure 4.5A). The ability of LL-37 and citLL-37 to suppress TNF-α-mediated MMP9 and MMP13 production in bronchial epithelial cells suggests that LL-37 may potentially limit airway remodeling in the lung.

Although TNF-α enhanced MMP9 and MMP13 production in PBEC, LL-37 and citLL-37 did not suppress its production in human PBEC (Figure 4.5B). This discrepancy may be because the PBEC are isolated from patients undergoing lung resection and therefore these individuals may have heightened underlying inflammatory status wherein the process of lung remodeling has already been initiated. Nevertheless, the data from HBEC-3KT suggests that LL-37 suppresses TNF-α-mediated enhancement of MMP9 and MMP13, and that this function is not lost by citrullination of the peptide.

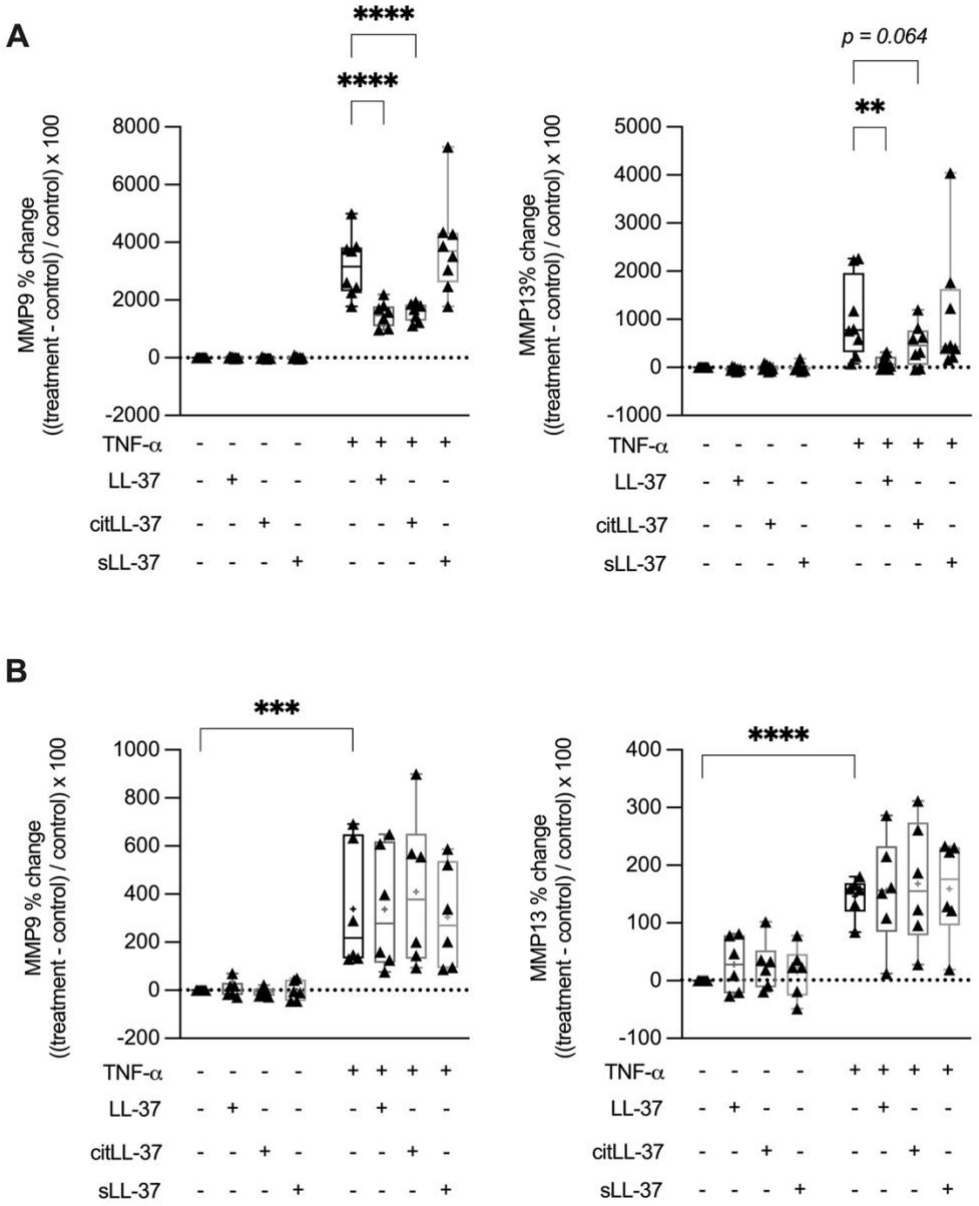

Figure 4.5: LL-37 & citLL-37 suppress TNF-α-mediated MMP9 & MMP13 production in HBEC-3KT, but not PBEC. HBEC were stimulated with LL-37, citLL-37, and sLL-37 (0.25 uM) in the presence/absence of TNF-α (20 ng/mL). Tissue culture supernatant collected after 24 h were used to examine the abundance of MMP9 and MMP13 in **(A)** HBEC-3KT (N=5) and **(B)** human PBEC (N=3, n=2), by ELISA. Supernatant was diluted 1:3 for ELISA. Y-axis represents % change compared to paired unstimulated controls within each independent experimental replicate. Each dot represents an independent experiment, and bars show the median and IQR, whereas whiskers show min-max range. Two-way analysis of variance with Fisher's least significant difference test was used for statistical analysis (***p≤0.001, ***p≤0.005, ****p≤0.0001*).

6.3.4 LL-37 and citLL-37 modulate intracellular AKT signaling.

Previous studies have demonstrated that LL-37 selectively alters inflammation by modifying intracellular PI3K and Src kinase signal transduction pathways. For example, LL-37 enhances PI3K signaling alone (103) and in combination with IL-1β to enhance the production of chemokine MCP-3 in PBMC (104). Moreover, another study demonstrated that LL-37 suppresses IL-32-induced pro-inflammatory cytokines TNF-α, IL-6, and IL-1β through suppression of Fyn (Y420) Src Kinase signaling in human monocyte-like cells and PBMC (43). As I have demonstrated that TNF-α-mediated enhancement of MMP9 and MMP13 involved Src and PI3K pathways (Figures 4.3 & 4.4), I hypothesized that LL-37 suppresses TNF-α-mediated production of MMP9 and MMP13 by altering intracellular signal transduction involving these pathways. AKT signal transduction is regulated by phosphorylation of two critical sites, T308 and S473 (376). Maximal AKT signal transduction requires phosphorylation of T308 and S473 simultaneously, whereas phosphorylation of AKT at site T308, but not S473, results in negative regulation of AKT-signaling (376). Therefore, p-SRC, p-AKT(T308), and p-AKT(s473) were selected as intracellular, mechanistic protein targets to investigate the selective intracellular immunomodulation by LL-37 pertaining to MMP9 and MMP13 production in bronchial epithelial cells. I stimulated HBEC-3KT with 0.25 μM of LL-37, citLL-37, and sLL-37 and monitored phosphorylation intermediates p-SRC, p-AKT(T308), and p-AKT(S473), using phospho site-specific antibodies by Western blot after 30 min stimulation of the cells. There was no significant change on p-SRC by the peptides after 30 min (Figure 4.7A). LL-37 significantly enhanced abundance of p-AKT(T308) by ~32% compared to unstimulated HBEC-3KT. LL-37 did not alter the abundance of p-AKT(S473) after 30 min, suggesting that LL-37 negatively regulates PI3K/AKT signal transduction pathways. Moreover, citLL-37 significantly increased the abundance of p-AKT(T308) by ~50% and p-AKT(S473) by 20% to unstimulated HBEC-3KT, suggesting that the reduced ability of citLL-37 to suppress MMP13 production (Figure 4.5A) is due to dual phosphorylation of AKT(T308, S473). Nonetheless, this data suggests that LL-37 and citLL-37 suppress TNF-α-mediated MMP13 production, by selectively altering PI3K-AKT signal transduction pathways in HBEC-3KT. In addition, this data suggests that LL-37 uses additional regulatory mechanisms to suppress TNF-α-mediated MMP9 production. These additional mechanisms require future investigation.

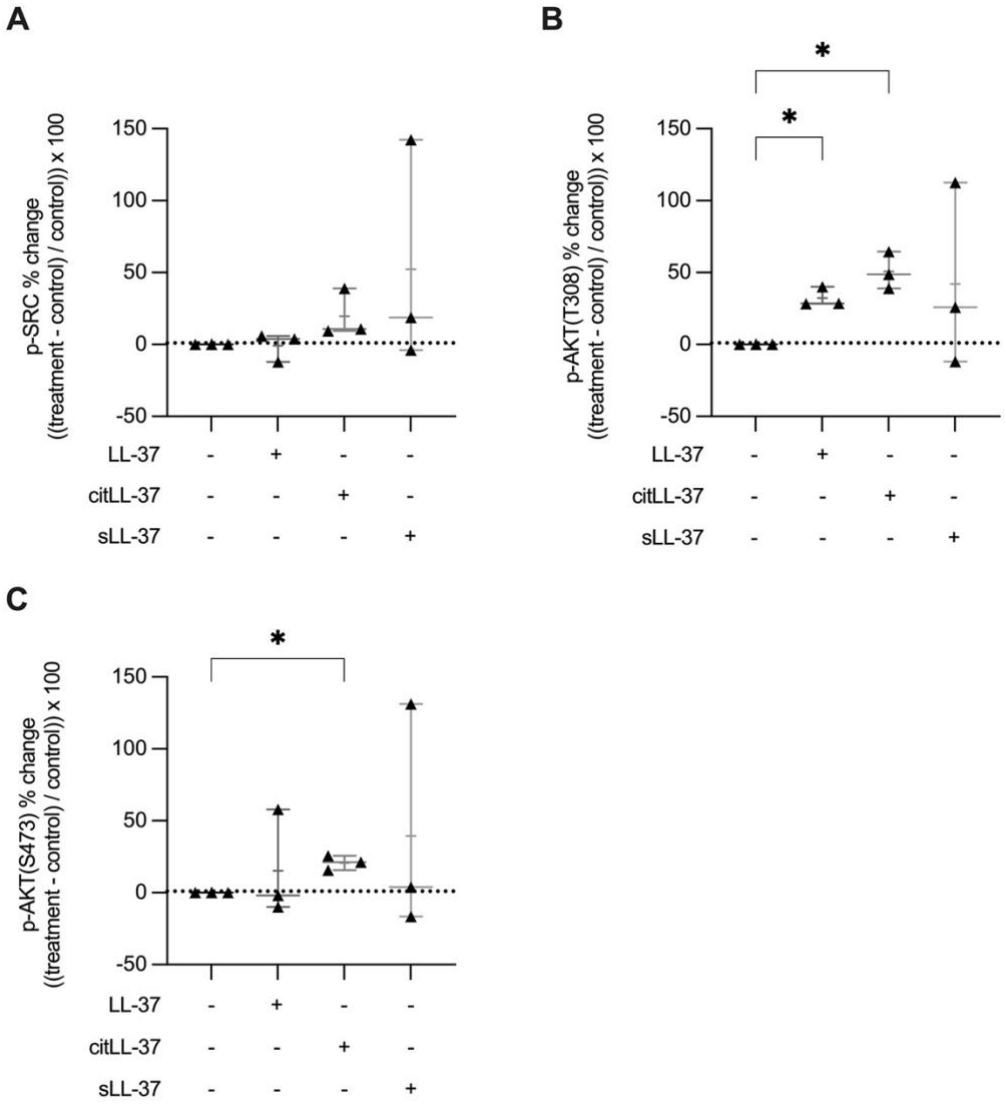

Figure 4.7: LL-37 and citLL-37 alter AKT phosphorylation at sites T308 and S473. HBEC-3KT (N=3) were stimulated with LL-37, citLL-37, and sLL-37 (0.25 μM) in the presence/absence of TNF-α (20 ng/mL). Total cell lysate (25 μg) was collected from cells 30 min post-stimulation to determine the abundance of **(A)** p-SRC, **(B)** p-AKT(T308), and **(C)** p-AKT(S473) by Western blot. Y-axis represents % change compared to paired unstimulated controls within donors. Each dot represents an independent experiment, and bars show the median and min-max range. Repeated measures one-way ANOVA with Fisher's least significant difference test was used for statistical analysis (*$*p \leq 0.05$*).

6.4 Discussion

In this study, I demonstrated that TNF-α enhances the production and secretion of airway remodeling factors MMP9 and MMP13 in HBEC, including both HBEC-3KT and PBEC isolated from patients undergoing lung resection. Neutrophilic asthma is associated with elevated levels of TNF-α (79, 317, 318). Individuals with severe, neutrophilic inflammation typically have poor responses to treatments that suppress eosinophils, including corticosteroids (79, 93). In addition to chronic cytokine-driven inflammation, asthma is characterized by irreversible structural changes to the airways, referred to as airway remodeling (382-384). Previous studies have demonstrated the detrimental effects of TNF-α on airway remodeling, including epithelial barrier integrity (385, 386), epithelial-mesenchymal transition (387), and blood vessel remodeling (388) in the bronchial epithelium. In addition, the altered expression and activity of several MMPs, have been implicated in the pathogenesis of asthma (389, 390). Patients with poor responses to corticosteroids (severe asthmatics), had increased levels of and activity of MMP9 in their sputum compared to patients who responded to corticosteroids and healthy controls (391). Furthermore, reduced sputum MMP9/TIMP-1 ratio in asthmatics is associated with measures of airway remodeling, including increased airway obstruction (392, 393), *computed tomography* (CT)-based measures of increased airway wall area and thickness (393), and increased CT scan lung abnormalities (394). Limited data is available on the levels of MMP13 in severe asthmatics. However, Bayesian network analysis investigating pathobiological parameters in asthmatics identified that MMP13 was positively correlated with markers of neutrophilic airway inflammation, including neutrophil elastase (390), suggesting that MMP13 is associated with the pathogenesis of severe, neutrophilic asthma. In addition, previous studies have demonstrated that MMP9 and MMP13 are associated with the development of experimental acute lung injury (79, 378) and bleomycin-induced pulmonary fibrosis (379), respectively. Taken together, this suggests TNF-α-mediated inflammation drives airway remodeling by enhancing MMP9 and MMP13 production in HBEC of severe, neutrophilic asthmatics.

The sole human cathelicidin, LL-37, is elevated in severe, neutrophilic asthmatics compared to healthy controls (147). In this study, I demonstrated that cathelicidin LL-37 suppresses TNF-α-mediated production of MMP9 and MMP13 to limit the abundance of these airway remodeling factors in bronchial epithelial cells. Previous studies have demonstrated LL-37 (and LL-37 derivative IG-19) selectively alter cytokine-mediated inflammation to suppress the production of pro-inflammatory mediators *in vitro* (43) and *in vivo* (101). LL-37 suppressed IL-32-mediated TNF-α, IL-6, and IL-1β production through suppression of Fyn (Y420) Src Kinase signaling in human macrophages and

PBMC (43). Additionally, one study performed in gingival fibroblasts demonstrated that LL-37 alone tended to decrease the combined enzymatic activity of MMPs in gingival fibroblasts (373). However, this is the first study to detail (*1*) specific, statistically significant changes to MMP production in bronchial epithelial cells by LL-37 and (*2*) demonstrate that LL-37 suppresses TNF-α-mediated airway inflammation and/or remodeling factors. Taken together, these findings suggest that LL-37 limits TNF-α-mediated airway remodeling and protects against detrimental airway structure changes which occur in severe, neutrophilic asthmatics. For example, LL-37 may limit MMP9-driven increases in airway thickness (393), airway obstruction (392, 393), and lung abnormalities (394). However, this requires further investigation, as functional measurements of airway remodeling are beyond the scope of this study. Nonetheless, my finding that LL-37 limits the production TNF-α-mediated remodeling factors MMP9 and MMP13 may be relevant in other chronic inflammatory diseases, including rheumatoid arthritis, which is characterized by MMP-driven tissue remodeling (395), as well as elevated TNF-α (43, 101) and cathelicidin LL-37 (102).

Limited studies have shown that LL-37 undergoes specific PTM which can alter the biological function of LL-37. *In vitro* and *in vivo* studies have demonstrated that one to all five arginine residues in LL-37 can be converted from arginine to citrulline by PADI2 and PADI4 enzymes, which are that are enhanced in inflammatory conditions (138-140). Citrullination decreases the ability of LL-37 to neutralize LPS and limit downstream pro-inflammatory mediators production (139-141), as well as attenuate anti-bacterial (138, 139) and anti-viral properties (142), compared to native LL-37. Citrullination of LL-37 also results in lowered suppression of pro-inflammatory mediator production in response to lipoteichoic acid and poly(I:C) (140). Moreover, citrullination of LL-37 increases serum levels of IL-6 as well as increases sepsis, morbidity, and mortality in a mouse model of d-galactosamine–sensitized endotoxin shock (140). Therefore, citrullination appears to result in the selective loss of the anti-inflammatory capability of LL-37 during infection. The impact of citrullination on the biological activities of LL-37 warrants detailed investigation as this PTM occurs in the human lung (139), and LL-37 can mediate both effector and regulatory activity in inflammatory diseases. In this study, I demonstrate that LL-37 and citLL-37 similarly mitigated TNF-α-mediated MMP9 production in HBEC-3KT. In addition, I demonstrated that LL-37 and citLL-37 suppressed TNF-α-mediated MMP13 production in HBEC-3KT, albeit with a greater reduction by LL-37 when compared to citLL-37. Neither LL-37 or citLL-37 suppressed TNF-α-mediated MMP9 and MMP13 production in PBEC isolated from patients undergoing lung resection, likely due to long standing and/or pre-existing changes to lung remodeling. Nonetheless, these findings demonstrate the disparate

effect that citrullination of LL-37 has on anti-infective as compared to cytokine-driven inflammation. This aligns with previous studies demonstrating that citrullination of LL-37 limits binding of negatively charged infective molecules, including LPS (138), a property which doesn't apply to the interplay of LL-37 and TNF-α in this *in vitro* study. However, additional studies are required to fully delineate the difference between LL-37 and citLL-37 in the context of inflammation and airway remodeling, as this study investigated the differences between LL-37 and citLL-37 on a limited number of airway remodeling factors.

In this study, I also demonstrated that pharmacological inhibitors specific to Src, including SRC1 inhibitor (SRC1i) and Dasatinib, as well as pharmacological inhibitors specific to PKC (GO6976) limited the production of TNF-α-mediated MMP9 and MMP13 production in HBEC. Similarly, I demonstrated that pharmacological inhibitors specific to PI3K (LY294002) limited TNF-α-mediated MMP13 production in HBEC. My results are aligned with previous studies investigating the mechanism of MMP9 production in AEC. One previous study demonstrated that TNF-α-induced MMP9 expression was reduced following pre-treatment with pharmacological inhibitors specific to c-Src (PP1) and PI3K (LY294002) and transfection with siRNA specific to Src and AKT in virally transformed human AEC (380). Moreover, this study demonstrated that pre-treatment with the pharmacological inhibitor specific to PKC (GO6976) used in this study inhibited TNF-α-mediated total phosphorylation of Src and AKT in HBEC (380). Taken together with my results and another study demonstrating that Src is upstream of PI3K signaling in in alveolar epithelial cells (381), this suggests that the interdependence of Src and/or PI3K/AKT signaling is critical in regulating TNF-α-mediated MMP9 and MMP13 production. Furthermore, this suggests that Src and/or PI3K/AKT signal transduction is a critical regulator of airway remodeling, which is aligned with previous studies demonstrating that these signaling pathways contribute to airway remodeling via the proliferation of ASM cells (396, 397) and fibroblasts (398).

LL-37 has been previously demonstrated to intervene Src-, PI3K-, or AKT-associated signaling pathways (43, 104). One study performed demonstrated that LL-37-suppressed Fyn (Y420) Src Kinase signaling in human macrophages and PBMC was associated with the suppression of IL-32-mediated TNF-α, IL-6, and IL-1β production (43). In addition, one previous study has demonstrated that LL-37 synergistically enhanced IL-1β-mediated production of chemokine MCP-3, which was suppressed by inhibition of PI3K (104). Taken together, these studies demonstrate the ability of LL-37 to intervene within Src or PI3K/AKT signaling pathways to selectively modulate cytokine-driven inflammation,

albeit only within hematopoietic immune cells as compared to non-hematopoietic immune cells. Therefore, I investigated the ability of LL-37 and citLL-37 to modulate Src- and PI3K/AKT-signaling and therefore limit TNF-α-mediated MMP9 and MMP13 production in HBEC. Phosphorylation of two AKT phosphorylation sites (T308 and S473) is a critical node within AKT signaling (376). Maximal AKT signal transduction requires phosphorylation of T308 and S473 simultaneously, whereas phosphorylation of AKT at site T308, but not S473, results in negative regulation of AKT-signaling (376). In this study, I demonstrated that LL-37 significantly enhanced the abundance of p-AKT(T308), but not p-AKT(S473) compared to unstimulated HBEC, suggesting that LL-37 negatively regulates AKT signaling to limit TNF-α-mediated MMP13 production in HBEC. In contrast to LL-37, citLL-37 significantly increased the abundance of both phospho-sites AKT(T308 and S473) compared to unstimulated HBEC-3KT. This disparate regulation of phosphorylation may explain the 37% greater reduction of MMP13 production by LL-37 when compared to citLL-37. This study demonstrates the difficulty associated with determining the precise mechanisms by which LL-37 (and citLL-37) alter TNF-α-mediated activation of the Src-PI3K-AKT signaling pathways. Although I determined that (*1*) TNF-α-mediated MMP13 production was suppressed by pharmacological inhibitors specific to PI3K and (*2*) LL-37 negatively regulates AKT-signaling, the precise time points where the selective regulation of T308 and S473 phosphorylation was not determined in dual stimulation conditions. In this instance, additional timepoints or kinetic PI3K/AKT activation assays are required to fully delineate the mechanistic interplay of LL-37 and TNF-α in HBEC. Nonetheless, these findings suggest that LL-37 (and citLL-37) to may limit other detrimental processes in airway remodeling regulated by PI3K/AKT signaling, including airway narrowing by limiting the proliferation of ASM cells (396, 397) and fibroblasts (398). Here, further investigation is required, and *in vivo* strategies, including CRAMP (murine analog of LL-37) KO mice would be beneficial to address the impact LL-37 on airway remodeling in chronic respiratory disease.

6.5 Summary

I previously demonstrated that combinations of IL-17A/F + TNF-α-mediated inflammation enhanced the production of airway remodeling factor MMP13 in HBEC-3KT and PBEC at 24 h, suggesting that MMP13 is a relevant contributor to airway remodeling during neutrophilic asthma. In this study, I investigated the role of cathelicidin LL-37 in regulating TNF-α-mediated airway remodeling factor production in bronchial epithelial cells. Here, I performed proteomic profiling and demonstrated that the dominant airway remodeling factors enhanced by TNF-α-mediated inflammation are MMP9 and MMP13, which have been implicated in the pathogenesis of airway remodeling in the lung (79, 378,

379). Moreover, I demonstrated that pharmacological inhibitors specific to Src and PKC suppressed MMP9 and MMP13 production in HBEC-3KT, and that inhibitors specific to PI3K suppressed TNF-α-mediated production of MMP13. I demonstrated that LL-37 suppressed TNF-α-mediated MMP9 and MMP13 production. Further, I demonstrated that LL-37 significantly enhanced the abundance of p-AKT(T308), but not p-AKT(S473) compared to unstimulated HBEC, demonstrating that LL-37 negatively regulates AKT-signaling. Taken together, these results suggest that LL-37 limits detrimental airway remodeling in the lung by negatively regulating PI3K/AKT signaling to limit TNF-α-mediated MMP13 production in HBEC. In addition, these results suggest that LL-37 uses additional regulatory mechanisms to suppress MMP9 production. This is the first study to demonstrate that LL-37 suppresses MMP production in the presence/absence of cytokine-driven inflammation.

Ultimately, I demonstrated that LL-37 suppresses TNF-α-mediated MMP9 and MMP13 production in bronchial epithelial cells and that suppression of TNF-α-mediated MMP13 is associated with negative regulation of PI3K/AKT signaling. The findings in this study provide insight into the interplay of LL-37 and TNF-α in bronchial inflammation and on subsequent airway remodeling, a process associated with prolonged detrimental inflammation in severe, uncontrolled asthma. Phospho-sites targeted by LL-37, such AKT(T308 and S473) identified by this study may be useful to develop interventional strategies derived from cathelicidin LL-37 (i.e., IDR peptides) to intervene in the biological processes associated with TNF-α-driven airway remodeling in the lung, which is relevant to chronic respiratory diseases including steroid-unresponsive asthma or COPD.

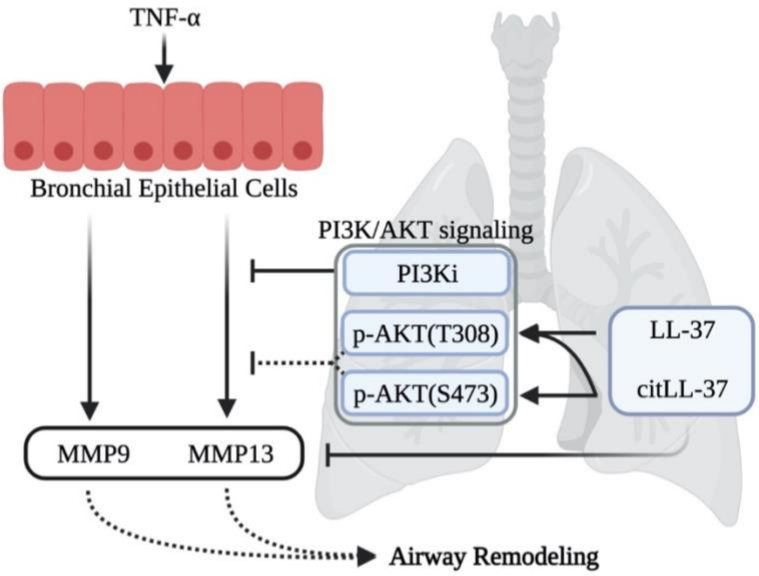

Figure 4.8: LL-37 and citLL-37 limits TNF-α-mediated airway remodeling factor MMP9 and MMP13 production in the lung. TNF-α enhances the production of MMP9 and MMP13 in HBEC. Pharmacological inhibitors specific to PI3K abrogate TNF-α-mediated MMP13, but not MMP9 production. LL-37 and citLL-37 suppress TNF-α-mediated production of airway remodeling factors, MMP9 and MMP13 in HBEC. LL-37 increases the abundance of p-AKT(T308), but not p-AKT(S473) which is associated with negative regulation of PI3K signal transduction. Dashed lines represent predicted impact. *This figure created using biorender.com.*

Chapter 7. Overall Significance

7.1 Significance of LL-37 in IL-17A/F-mediated airway inflammation

The overall aim of this thesis was to determine the interplay between human cathelicidin LL-37 and IL-17A/F during neutrophil predominant lung inflammation indicative of severe, uncontrolled asthma. Neutrophil-predominant lung inflammation is characterized by the complex interplay of neutrophils that secrete LL-37 and IL-17-producing Th17 lymphocytes (147, 150). LL-37 has been shown to specifically enhance the production of IL-17A/F-producing Th17 lymphocytes in the lung (124). Moreover, IL-17A/F is a critical mediator in airway inflammation, which primarily targets structural cells, including bronchial epithelial cells (176, 180, 197, 200). However, the effect of LL-37 on IL-17A/F-mediated protein changes and signaling networks in airway inflammation is poorly understood. Therefore, in this thesis, I examined the immunomodulatory activity of LL-37 on IL-17A/F-mediated airway inflammation. To that end, I (*1*) characterized IL-17A/F-mediated inflammation (in the presence/and absence of other pro-inflammatory cytokines) in bronchial epithelial cells, (*2*) defined regulation of IL-17A/F-mediated inflammatory signaling by LL-37 in bronchial epithelial cells and (*3*) validated these processes in a physiologically relevant mouse model of neutrophilic airway inflammation.

Overall, my thesis has contributed to the scientific literature by defining protein targets and immunological pathways enhanced in response to IL-17A/F-mediated inflammation (in the presence/absence of other acute pro-inflammatory cytokines) *in vitro* and *in vivo*. These molecules, including the neutrophil-associated CHDP LCN-2, may be used as protein targets to interrogate the mechanism of chronic airway inflammation, biomarkers for precise diagnoses, and/or evaluating the potential of novel therapies in diseases characterized by IL-17A/F-mediated inflammation. For example, determining the abundance of a panel of proteins selected from the IL-17A/F + TNF-α-mediated bronchial proteome (e.g., LCN-2 and Elafin) in patient sputum or serum may represent an effective method for determining patient endotypes and providing personalized asthma treatments. Aligned with this, sputum and serum LCN-2 has recently been used as an exploratory endpoint in a clinical trial evaluating the efficacy and safety of riskankizumab, an anti-IL-23 antibody in adults with severe asthma (399). Further, treatment with mAb-based therapies is not typically beneficial for patients with severe, neutrophilic asthma (399) and additional treatment strategies are required due to unmet clinical need. As such, using a dual pharmacology approach to inhibit the combined activity of IL-17A/F and TNF-α to treat severe, neutrophilic asthma may be effective. Dual pharmacology strategies, such as dupilumab, a monoclonal antibody which inhibits both IL-4 and IL-13 signaling

have been exploited to provide effective asthma treatments for patients with eosinophilic asthma (400-402), suggesting this may be a viable strategy in the context of severe, neutrophilic asthma driven by the combined activity of IL-17A/F and TNF-α.

Moreover, my thesis findings elucidate the homeostatic role of cathelicidin LL-37 (and derivative citLL-37) in IL-17A/F-driven, and in TNF-α-driven inflammation, both applicable to severe asthma. Here, I demonstrated that LL-37 (and citLL-37) enhance IL-17A/F-mediated Regnase-1 production, an RBP which negatively regulates IL-17-mediated inflammation (197, 200, 201) in PBEC, suggesting that this enhancement is associated with suppression of IL-17A/F-mediated LCN-2 production. These findings provide insight into the elusive mechanisms by which CHDP regulate inflammation and suggest that this regulation may occur by selective alterations to the intracellular post-transcriptional machinery. However, further studies are required to determine the scope of these alterations and whether RBP function, mRNA decay, and protein translation kinetics are altered by CHDP in cytokine-mediated inflammation. Nonetheless, selectively targeting proteins within the post-transcriptional machinery may be an attractive strategy for therapeutic intervention. Here, molecular candidates capable of modulating the kinetics and/or duration of inflammation may be beneficial in promoting immune homeostasis in chronic inflammatory disease, without compromising the individual's ability to fight infection.

Further, my thesis demonstrates key differences between LL-37 and derivative citLL-37. I demonstrated that citrullination of LL-37 dampens the ability of LL-37 to enhance GROα and CCL20 production in the presence of IL-17A/F in HBEC. I also demonstrated that LL-37, but not citLL37, enhanced IL-17A/F-mediated enhancement of IκBζ mRNA abundance, suggesting that the differential activity of LL-37 and citLL-37 on IL-17A/F-mediated GROα and CCL20 production is due to the selective loss of IκBζ mRNA abundance increases by citLL-37. In addition, I demonstrated that citrullination of LL-37 was required for suppression of IL-17A/F-mediated LCN-2 production and that this suppression was associated with the selective loss of NF-κB signal transduction in PBEC. I demonstrated that citLL-37 suppressed TNF-α-mediated MMP9 and MMP13 production similarly to native LL-37 in HBEC. Therefore, in contrast with previous studies demonstrating that citLL-37 is less effective than LL-37 in suppressing anti-infective inflammation, I demonstrated that citLL-37 has equal or lesser pro-inflammatory properties in the context of cytokine-driven inflammation, representative of chronic inflammatory disease. These findings provide insight into the role of citrullination of LL-37 in cytokine-driven inflammation disease and suggest that citrullination may

suppress the pro-inflammatory properties of LL-37 in chronic inflammatory disease. In addition, these findings suggest that the incorporation of citrulline, rather than arginine into synthesized IDR peptides may suppress their pro-inflammatory activity. However, additional studies are required, as the impact of citrullination on LL-37 was only assessed on a limited number of downstream protein targets in the context of IL-17A/F- and TNF-α-mediated inflammation.

The scope of my thesis findings are broad, as the mechanisms identified in the context of lung inflammation can be expanded to other chronic inflammatory diseases characterized by the interplay of IL-17A/F and cathelicidin LL-37, including psoriasis and MS. Ultimately, the findings in this project can be leveraged to design IDR peptides capable of limiting detrimental prolonged lung inflammation and airway remodeling, without compromising anti-infective immunity in patients with limited therapeutic options such as in treatment-unresponsive severe asthma.

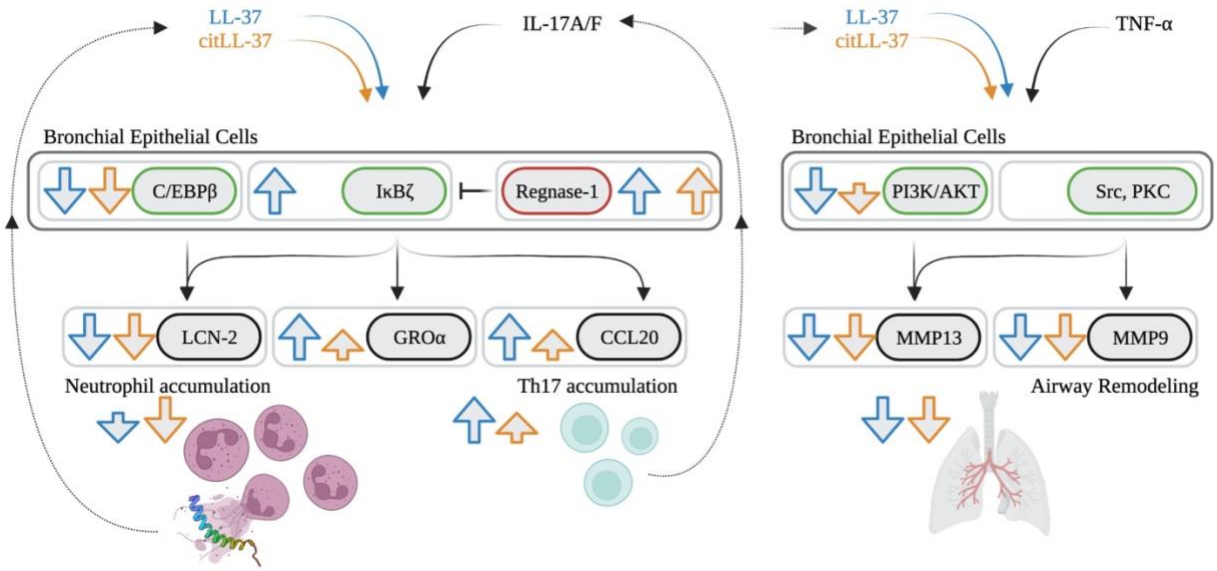

Figure 5.1: LL-37 and citLL-37 limit IL-17A/F-mediated neutrophil accumulation and TNF-α-mediated airway remodeling in neutrophilic asthma. IL-17A/F-mediated inflammation enhances the production of LCN-2 via the transcription factors C/EBPβ and IκBζ, but simultaneously regulates the production of LCN-2 via endoribonuclease Regnase-1. LL-37 and citLL-37 suppress C/EBPβ and enhance Regnase-1 to limit LCN-2 production, and therefore neutrophil accumulation in the lung. Citrullination of LL-37 results in the selective loss of IκBζ,induction, and therefore dampens GRO and CCL20 production, limiting neutrophil and Th17 accumulation in the lung compared to native LL-37. TNF-α-mediated inflammation enhances the production of airway remodeling factors MMP9 and MMP13. LL-37 suppresses TNF-α-mediated MMP13 production through negative regulation of PI3K/AKT signaling but suppresses MMP9 production through an unknown mechanism. Green and red outlines represent positive regulators of signal transduction, respectively. Blue and orange arrows represent activity of LL-37 and citLL-37, respectively. *This figure created using biorender.com.*

Chapter 8: Future Directions and Supplementary Studies

In the course of my PhD program, I have performed several additional experiments that will add to future projects in the Mookherjee lab as detailed in this chapter.

8.1 LL-37 in IFN-γ-mediated airway inflammation:

8.1.1 Rationale

I demonstrated that human cathelicidin LL-37 can selectively alter cytokine driven airway inflammation (chapters 5). My findings also showed that LL-37 has the ability to intervene in airway remodeling (chapter 6). In addition to defining the bronchial proteome in response to IL-17A/F and/or TNF-α, I have defined the bronchial proteome in response to IFN-γ, a dataset that can be used for future studies in the Mookherjee lab. The effect of LL-37 on IFN-γ-mediated changes in the lungs remains relatively unknown, which warrants further investigation. IFN-γ is a dominant cytokine enhanced in steroid-unresponsive airway inflammation (45, 294, 316, 403). Proteins enhanced or suppressed by IFN-γ in human bronchial epithelial cells may represent targets which can be used to determine the impact of (*1*) cathelicidin LL-37 and (*2*) their synthetic derivatives, known as IDR peptides on severe airway inflammation. Although this is beyond the scope of my thesis work, the following protein targets and signaling intermediates may serve as the foundation for future projects.

8.1.2 Preliminary Results

8.1.2.1 IFN-γ-mediated inflammation alters the abundance of 194 different proteins in human bronchial epithelial cells.

To identify proteins altered in response to IFN-γ-mediated lung inflammation, I performed aptamer-based proteomic profiling in HBEC-3KT (ATCC® CRL-4051™) 24 h post-stimulation with IFN-γ (30ng/mL). Pairwise differential analysis was conducted on normalized log2 protein abundance values. I demonstrated that IFN-γ enhances the abundance of 115 proteins and suppresses the abundance of 79 proteins. The proteins with the greatest increases in response to IFN-γ include chemokine CXCL10, CHDP CTSS, and metabolic factor *Apolipoprotein 1* (APOL-1), whereas the proteins with the greatest decreases in response to IFN-γ included the CHDP CTSV and Elafin (Figure 5.1A). To determine the accuracy of the proteomic array in characterizing IFN-γ-mediated inflammation in HBEC-3KT, I performed validated select protein targets in Western blots in HBEC-3KT 24 h post-treatment with IFN-γ. In accordance with the proteomic array, IFN-γ enhanced CXCL10, CTSS, and APOL-1 abundance, but suppressed Elafin and Cathepsin V (Figure 5.1B). These select protein targets may be

used to investigate the impact of the IFN-γ-mediated bronchial proteome on leukocyte recruitment to the lung, and the impact of CHDP such as LL-37 and synthetic IDR peptides on this process.

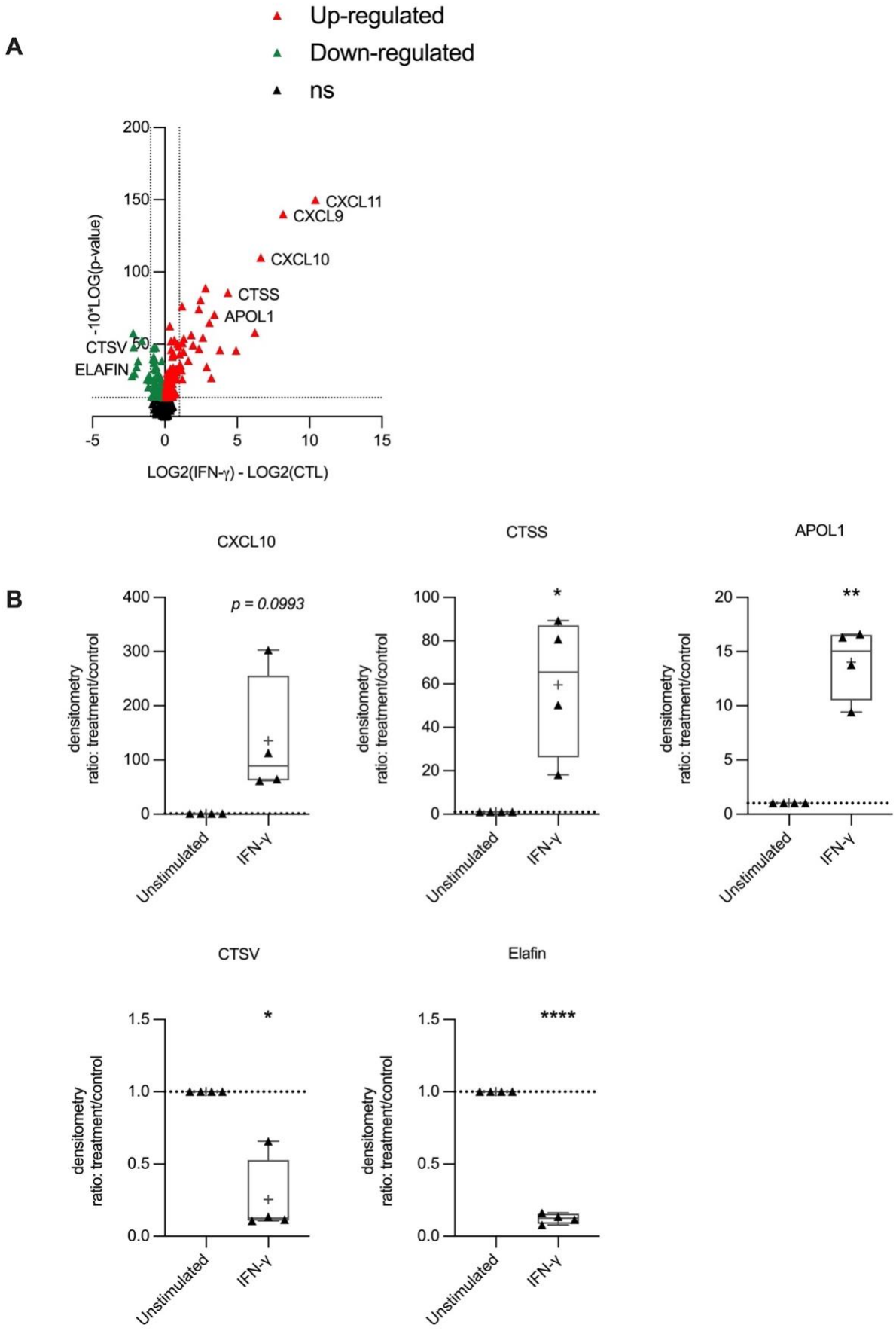
A
Up-regulated
Down-regulated
ns
-10*LOG(p-value)
LOG2(IFN-γ) - LOG2(CTL)
CXCL11
CXCL9
CXCL10
CTSS
APOL1
CTSV
ELAFIN
B
CXCL10
CTSS
APOL1
CTSV
Elafin
densitometry ratio: treatment/control
p = 0.0993
Unstimulated
IFN-γ

Figure 6.1: The IFN-γ-mediated bronchial proteome enhances the abundance of 115 proteins and suppresses the abundance of 79 proteins. HBEC-3KT were stimulated with IFN-γ (30 ng/mL) and compared to unstimulated cells (CTL) after 24 hours. **(A)** Equivalent loading of cytosolic cell lysates (N=5) was monitored for changes in protein profile using a high content aptamer-based proteomic array. Pairwise differential analysis was conducted on normalized log2 protein expression values and Welch's t-test with a cutoff of $p<0.05$ was used to select proteins that were significantly enhanced in response to IFN-γ compared to control. **(B)** Equivalent loading of cytosolic cell lysates (10 μg) was monitored by Western blots for the abundance of protein targets selected from the proteomics dataset. Results shown are the average of (N=4) independent experiments. Y-axis represents the ratio of cell treated with IFN-γ compared to unstimulated cells. Each dot represents an independent experiment, and bars show the median and IQR, whereas whiskers show min-max range. Welch's t-test was used for statistical analysis (*$p\leq0.05$, **$p\leq0.001$, ****$p\leq0.005$).

8.1.2.2 Predicted regulators of IFN-γ-mediated inflammation in HBEC

To predict dominant regulators of IFN-γ-mediated inflammation in bronchial epithelial cells, bioinformatics assessment of log2 protein abundance data from the proteomics array (detailed above) was performed using the program Network Analyst (*networkanalyst.ca*). These results defined lung-specific protein-protein interaction network of proteins that were significantly altered ($p<0.05$) in response to IFN-γ (Figure 5.2A) and predicted upstream regulators for IFN-γ-mediated responses (Figure 5.2B), in HBEC-3KT. The IFN-γ-mediated predicted regulators in HBEC-3KT include (but are not limited to), JAK-STAT associated signaling intermediates (e.g., STAT1, GRB2, CDK1) and LYN kinase (45, 338, 339). These predicted intracellular regulators may serve as intracellular targets to investigate the impact of CHDP and IDR peptides on IFN-γ-mediated airway inflammation.

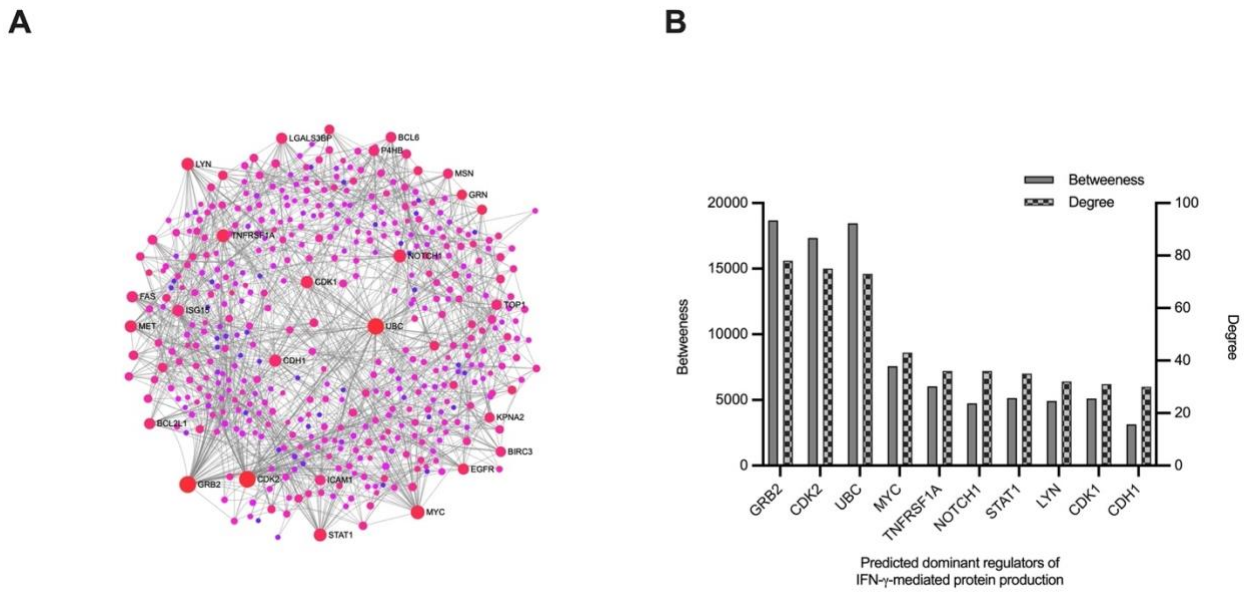

Figure 6.2: Predicted regulators of IFN-γ-mediated protein production. HBEC-3KT were stimulated with IFN-γ (30 ng/mL) and compared to unstimulated cells (CTL) after 24 hours. Equivalent loading of cell lysates was monitored for the abundance of proteins after 24h using a high content aptamer-based proteomic array. Pairwise differential analysis was conducted on normalized log2 protein expression values and Welch's t-test with a cutoff of $p<0.05$ was used to select proteins that were significantly enhanced in response to IFN-γ compared to control. NetworkAnalyst.ca was used to predict the **(A)** lung-specific protein-protein minimum interaction network with one degree of separation (the IFN-γ-mediated interactome) and **(B)** intracellular signaling intermediates for proteins independently validated using Western blots, wherein "betweenness" represents the degree of potential interactions as an overall score for the connectivity of that protein, and "degree" represents the number of interactions that occur with the lung-specific predicted IFN-γ-mediated interaction network.

8.1.2.3 IFN-γ-mediated inflammation alters the phosphorylation of signaling intermediated in the JAK-STAT pathway.

To confirm the involvement of predicted intracellular regulators of IFN-γ-mediated inflammation in HBEC-3KT, independent experiments via kinome array were performed as a second line of investigation. This was done in collaboration with Dr. Jason Kindrachuk (Department of Medical Microbiology, University of Manitoba). HBEC-3KT were stimulated with IFN-γ (30ng/mL) for 15 mins to measure the phosphorylation of 282 unique phospho targets corresponding to 149 proteins. Differential analysis was conducted on normalized log2 protein abundance values with a cut-off of ($p<0.05$) to select proteins that were differentially phosphorylated in response to IFN-γ. The IFN-γ-mediated bronchial phospho-proteome enhanced the phosphorylation of 11 proteins and suppressed the phosphorylation of 15 proteins (Figure 5.4). This independent line of investigation showed results similar to that predicted by the bioinformatics analysis of proteomics dataset in response to IFN-γ. Using the kinome array we confirmed the increased phosphorylation of JAK-STAT associated signaling intermediates, including STAT-1(S708, S727) and the decreased phosphorylation of JAK-STAT associated signaling intermediates CDK2(Y179), and GRB2(Y37). These signaling intermediates and specific phosphorylation sites may serve as protein targets to investigate selective immunomodulation with CHDP and IDR peptides, in the context of airway inflammation.

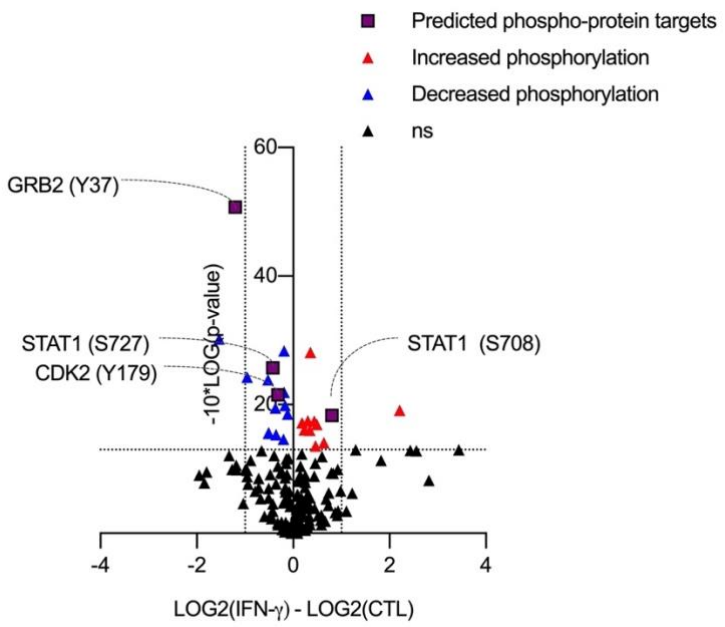

Figure 6.3: IFN-γ-mediated changes in the bronchial phospho-proteome enhances the phosphorylation of 11 proteins and suppresses the phosphorylation of 15 proteins. HBEC-3KT were stimulated with IFN-γ (30 ng/mL) and compared to unstimulated cells (CTL) after 24 hours. Equivalent loading of cell lysates (10 μg) was monitored for the phosphorylation of proteins by a kinome array. Differential analysis was conducted on normalized log2 protein expression values with a cutoff of $p<0.05$ was used to select proteins that were differentially phosphorylated in response to IFN-γ compared to control.

Chapter 9: Appendix

9.1 Supplementary Tables

Supplementary Table I: CHDP significantly altered in response to IL-17A/F, TNF-α, or IFN-γ in HBEC-3KT 24 h post-stimulation.

Protein		Average Log2 Fold Change (compared to unstimulated cells)		
NAME	**SWPROT ID**	**IL-17A/F**	**TNF-α**	**IFN-γ**
ANG	P03950	-0.112	0.088	-0.616
AREG	P15514	0.022	0.01	-0.088
ARTN	Q5T4W7	0.006	0.048	-0.036
AZU1	P20160	-0.11	-0.082	0.052
BPI	P17213	0.124	0.11	-0.09
CHGA	P10645	0.002	-0.006	0.028
CST1	P01037	-0.034	0.004	0.024
CST2	P09228	-0.058	0.024	0.024
CST3	P01034	-0.234	-0.08	0.59
CST4	P01036	-0.066	-0.044	-0.044
CST5	P28325	-0.03	0.022	-0.016
CST6	Q15828	-0.296	-0.268	-0.04
CST7	O76096	-0.01	-0.008	-0.116
CTSA	P10619	-0.136	-0.362	0.334
CTSB	P07858	-0.124	-0.218	0.522
CTSD	P07339	-0.186	-0.182	0.068
CTSE	P14091	0.016	0.04	-0.038
CTSF	Q9UBX1	-0.064	-0.072	0.052
CTSG	P08311	0.018	0.072	-0.082
CTSH	P09668	-0.22	-0.508	-0.038
CTSS	P25774	0.044	0.608	4.36
CTSV	O60911	-0.566	-1.876	-2.16
CTSZ	Q9UBR2	-0.062	-0.02	-0.052
KNG1	P01042	-0.024	-0.034	-0.032

LCN-2	P80188	1.858	-0.31	-0.248
LTF	P02788	0.462	-0.02	0.026
NPPA	P01160	0.046	0.05	-0.048
NPPB	P16860	-0.026	-0.03	0.02
ELAFIN	P19957	1.638	1.144	-2.09
S100A12	P80511	-0.066	-0.136	0.194
S100A4	P26447	0.016	-0.002	-0.008
S100A6	P06703	-0.014	-0.042	0.124
S100A7	P31151	-0.144	-0.234	-0.028
S100A9	P06702	0.098	-0.006	0.206
SERPIND1	P05546	-0.176	-0.202	-0.026
SLPI	P03973	0.408	0.426	-0.75
TF	P02787	-0.098	-0.222	-0.182
TNC	P24821	0.136	1.346	0.746
VIP	P01282	-0.116	-0.098	-0.064

Supplementary Table II: Proteins significantly altered in response to the combination of IL-17A/F and TNF-α, compared to either cytokine alone in HBEC-3KT 24 h post-stimulation.

Protein		AVG LOG2 FC (normalized to unstimulated cells)			Average Log2 Fold Change (IL-17A/F + TNFα vs. IL-17A/F or TNFα)	
NAME	SWPROT ID	IL-17A/F	TNF-α	IL-17A/F + TNF-α	DIFFERENCE	P-SCORE
LCN-2	**P80188**	**1.86**	**-0.31**	**4.05**	**3.28**	**8.06E-06**
IL-8	**P10145**	**0.07**	**0.53**	**3.25**	**2.95**	**3.09E-06**
CFB	P00751	0.15	1.69	3.37	2.45	7.19E-06
GROα	**P09341**	**0.12**	**0.26**	**1.73**	**1.54**	**2.13E-05**
STC1	P52823	1.27	0.90	2.59	1.50	3.61E-08
ELAFIN	**P19957**	**1.64**	**1.14**	**2.63**	**1.24**	**5.73E-04**
MMP13	**P45452**	**-0.19**	**1.51**	**1.82**	**1.17**	**3.04E-03**
IGFBP5	P24593	0.74	-0.11	1.30	0.98	1.29E-03
IGFBP3	P17936	0.57	-0.01	1.09	0.81	9.29E-05
TNC	P24821	0.14	1.35	1.39	0.65	1.70E-02
PPBP	P02775	-0.06	-0.12	0.48	0.57	1.76E-04
ARID3A	Q99856	0.03	0.25	0.65	0.51	2.22E-04
PLAUR	Q03405	0.01	1.13	1.02	0.46	4.96E-02
SLPI	P03973	0.41	0.43	0.88	0.46	3.34E-04
CD55	P08174	0.09	0.32	0.63	0.42	1.46E-03
LYN	P07948	-0.03	0.64	0.72	0.41	3.40E-02
CCL20	P78556	0.16	0.34	0.63	0.38	3.67E-03
S100A9	P06702	0.10	-0.01	0.39	0.34	2.19E-04
FSTL1	Q12841	-0.02	0.30	0.45	0.31	4.55E-03
HK2	P52789	0.19	0.53	0.67	0.31	2.50E-02
CSF3	P09919	0.04	0.05	0.36	0.31	4.48E-04
CXCL3	P19876	0.14	0.19	0.47	0.30	9.66E-04
CXCL2	P19875	0.14	0.19	0.47	0.30	9.66E-04
CTSS	P25774	0.04	0.61	0.62	0.29	2.24E-02

CDH1	P12830	0.07	-0.16	0.21	0.26	2.60E-02
MICA	Q29983	-0.05	0.26	0.34	0.24	4.89E-03
SAA1	P0DJI8	0.17	0.18	0.41	0.23	1.01E-03
ROBO2	Q9HCK4	0.01	0.45	0.46	0.23	2.33E-02
MET	P08581	-0.02	-0.11	0.15	0.21	4.87E-05
FSTL3	O95633	0.01	0.19	0.31	0.21	3.43E-02
HBEGF	Q99075	-0.07	0.06	0.19	0.19	2.49E-02
MICB	Q29980	0.04	0.23	0.30	0.17	3.32E-02
CXCL16	Q9H2A7	0.09	0.19	0.30	0.15	1.42E-02
NTN4	Q9HB63	0.09	-0.06	0.17	0.15	2.19E-02
FGF2	P09038	-0.03	-0.03	0.10	0.13	2.68E-02
FGFR2	P21802	0.00	0.01	0.07	0.06	2.32E-02
SIRPA	P78324	-0.03	0.01	0.03	0.05	2.27E-02
AGRP	O00253	0.02	0.03	0.05	0.02	4.59E-02
PDGFRA	P16234	0.06	0.04	0.01	-0.04	1.47E-02
C8A	P07357	0.01	0.02	-0.03	-0.05	3.67E-02
C8B	P07358	0.01	0.02	-0.03	-0.05	3.67E-02
C8G	P07360	0.01	0.02	-0.03	-0.05	3.67E-02
COL18A1	P39060	-0.07	-0.13	-0.16	-0.06	2.06E-02
LTBR	P36941	-0.01	-0.03	-0.08	-0.06	4.46E-02
CTSZ	Q9UBR2	-0.06	-0.02	-0.10	-0.06	1.04E-02
C2	P06681	-0.06	-0.07	-0.14	-0.07	1.97E-03
PSMA6	P60900	-0.02	-0.02	-0.10	-0.08	1.04E-02
IGFBP6	P24592	-0.08	-0.14	-0.20	-0.09	2.32E-02
IL6	P05231	-0.14	-0.16	-0.25	-0.10	1.24E-02
C10orf54	Q9H7M9	0.00	-0.18	-0.20	-0.11	3.79E-02
COL23A1	Q86Y22	-0.13	-0.18	-0.28	-0.12	1.90E-03
CDC2	P06493	0.00	-0.12	-0.19	-0.13	2.05E-02
MPO	P05164	-0.14	-0.19	-0.30	-0.14	1.75E-03
LTBP4	Q8N2S1	-0.12	-0.38	-0.39	-0.15	3.76E-02
LRP8	Q14114	-0.13	-0.18	-0.32	-0.17	3.50E-04
SNX4	O95219	-0.09	-0.10	-0.28	-0.18	3.24E-02

SPARC	P09486	-0.08	-0.03	-0.25	-0.20	6.71E-04
EREG	O14944	-0.16	0.11	-0.24	-0.22	2.87E-02
LAMA1	P25391	-0.21	-0.52	-0.64	-0.27	4.00E-03
LAMB1	P07942	-0.21	-0.52	-0.64	-0.27	4.00E-03
LAMC1	P11047	-0.21	-0.52	-0.64	-0.27	4.00E-03
ECM1	Q16610	-0.25	-0.65	-0.73	-0.28	2.39E-02
THBS1	P07996	-0.15	0.13	-0.35	-0.34	7.22E-03
NRP1	O14786	-0.30	-1.11	-1.11	-0.40	2.73E-02
EFEMP1	Q12805	-0.17	-0.39	-0.70	-0.42	1.02E-02
FTH1	P02794	-0.27	-1.40	-1.40	-0.56	2.43E-02
FTL	P02792	-0.27	-1.40	-1.40	-0.56	2.43E-02
LRIG3	Q6UXM1	-0.36	-1.20	-1.37	-0.59	6.05E-03
MMP1	P03956	-0.42	0.57	-0.69	-0.77	9.81E-03
CTSV	O60911	-0.57	-1.88	-2.15	-0.93	2.86E-03

Supplementary table III: Proteins significantly altered in response to IL-17A/F in HBEC-3KT 24 h post-stimulation.

NAME	SWPROT ID	AVG LOG2 FC (normalized to unstimulated cells)	p-value
LCN-2	**P80188**	**1.86**	**0.00039384**
ELAFIN	**P19957**	**1.64**	**0.00735901**
STC1	P52823	1.27	0.00233145
IGFBP5	P24593	0.74	0.00638196
IGFBP3	P17936	0.57	0.00283743
IL17A	Q16552	0.49	0.02162217
SLPI	P03973	0.41	0.01828189
FLT3	P36888	0.25	0.04376196
KIR2DL4	Q99706	0.19	0.04528727
SAA1	P0DJI8	0.17	0.00725448
CXCL1	**P09341**	**0.12**	**0.00062497**
EDA2R	Q9HAV5	0.08	0.04865734
CXCL13	O43927	0.08	0.03957933
LEPR	P48357	0.08	0.00857008
TNFSF13B	Q9Y275	0.07	0.02355169
PDGFRA	P16234	0.06	0.04654336
IBSP	P21815	0.05	0.0190153
BMPR1A	P36894	0.04	0.04357518
OMD	Q99983	0.04	0.03799716
UNC5C	O95185	0.03	0.0221567
VEGFA	P15692	-0.07	0.02045688
LGALS3BP	Q08380	-0.17	0.03782374
CST3	P01034	-0.23	0.03730624
NRP1	O14786	-0.3	0.02429623
CTSV	O60911	-0.57	0.04598988

Supplementary table IV: Proteins significantly altered in response to TNF-α in HBEC-3KT 24 h post-stimulation.

NAME	SWPROT ID	AVG LOG2 FC (normalized to unstimulated cells)	p-value
MMP9	**P14780**	**3.354**	**9.23E-06**
IL1R2	P27930	2.208	4.78E-05
OLR1	P78380	2.116	3.52E-06
CFB	P00751	1.69	8.25E-06
PLAU	P00749	1.59	2.30E-06
IL1A	P01583	1.578	1.44E-03
MMP13	**P45452**	**1.508**	**1.86E-03**
TNC	P24821	1.346	1.47E-03
CXCL11	O14625	1.28	1.11E-02
ELAFIN	P19957	1.144	2.82E-02
PLAUR	Q03405	1.126	4.89E-07
IGFBP7	Q16270	1.118	1.12E-05
ICAM1	P05362	0.99	7.88E-05
CCL5	P13501	0.968	1.72E-02
STC1	P52823	0.904	2.51E-02
LYN	P07948	0.64	9.37E-03
CTSS	P25774	0.608	1.70E-04
F3	P13726	0.6	1.72E-03
ISG15	P05161	0.56	1.59E-03
CXCL8	P10145	0.528	9.96E-05
IL6ST	P40189	0.51	7.84E-03
ROR1	Q01973	0.504	4.33E-02
PCSK9	Q8NBP7	0.492	8.57E-04
INHBA	P08476	0.478	3.89E-04
INHBB	P09529	0.478	3.89E-04
ROBO2	Q9HCK4	0.448	3.08E-02
PPIF	P30405	0.436	3.62E-02
SLPI	P03973	0.426	2.86E-02

EIF4A3	P38919	0.398	2.37E-02
IL18R1	Q13478	0.334	6.16E-04
FSTL1	Q12841	0.302	1.29E-02
FUT5	Q11128	0.284	9.46E-03
MMP14	P50281	0.262	5.00E-03
CXCL1	P09341	0.26	3.80E-03
MICA	Q29983	0.26	1.65E-02
ERAP1	Q9NZ08	0.254	1.67E-02
ETHE1	O95571	0.25	1.29E-02
MICB	Q29980	0.232	4.37E-02
TNF	P01375	0.196	1.00E-02
CXCL16	Q9H2A7	0.194	2.53E-02
FSTL3	O95633	0.194	1.29E-02
SET	Q01105	0.176	2.45E-02
FST	P19883	0.154	2.56E-02
ADAMTS1	Q9UHI8	0.14	1.24E-02
LEP	P41159	0.132	3.43E-02
PTPN6	P29350	0.126	3.12E-03
CRELD1	Q96HD1	0.126	1.73E-02
LEP	P41159	0.108	3.65E-02
SERPING1	P05155	0.106	1.69E-02
CCL23	P55773	0.094	1.92E-02
CPB2	Q96IY4	0.092	2.76E-02
FGF17	O60258	0.09	2.01E-02
CLEC11A	Q9Y240	0.088	3.72E-02
VEGFA	P15692	0.086	7.51E-03
LEPR	P48357	0.08	4.28E-02
SERPINA7	P05543	0.074	3.64E-02
NOV	P48745	0.072	6.70E-03
FUT3	P21217	0.072	4.94E-02
GFAP	P14136	0.06	1.15E-02
DDR2	Q16832	0.054	4.07E-02

PDGFRA	P16234	0.038	3.07E-02
PPY	P01298	0.036	3.79E-02
BTK	Q06187	-0.07	2.49E-02
EPHA1	P21709	-0.088	3.92E-02
DIABLO	Q9NR28	-0.1	1.54E-02
MST1R	Q04912	-0.12	2.64E-02
CDC2	P06493	-0.122	4.17E-02
EFNA3	P52797	-0.13	5.79E-03
IGFBP6	P24592	-0.144	3.85E-03
MYC	P01106	-0.162	3.82E-02
EPHA2	P29317	-0.164	4.51E-02
CSF2	P04141	-0.166	4.30E-02
IL20	Q9NYY1	-0.17	2.39E-02
C10orf54	Q9H7M9	-0.182	1.05E-02
ADAM9	Q13443	-0.184	2.81E-02
CDNF	Q49AH0	-0.214	2.61E-02
SORCS2	Q96PQ0	-0.242	1.51E-02
CFH	P08603	-0.254	5.50E-03
CD109	Q6YHK3	-0.276	3.36E-02
POR	P16435	-0.28	4.53E-02
TIMP1	P01033	-0.282	4.21E-03
LIFR	P42702	-0.29	2.05E-02
MFGE8	Q08431	-0.294	1.39E-02
SFRP1	Q8N474	-0.304	3.71E-02
ULBP2	Q9BZM5	-0.308	3.13E-03
CTSA	P10619	-0.362	1.52E-02
LTBP4	Q8N2S1	-0.376	3.05E-04
KPNA2	P52292	-0.38	3.85E-02
IL17RA	Q96F46	-0.384	1.93E-03
TNFRSF10D	Q9UBN6	-0.392	1.82E-03
PTHLH	P12272	-0.392	9.81E-03
PROS1	P07225	-0.402	1.94E-02

TNFRSF1A	P19438	-0.404	6.08E-03
GPC3	P51654	-0.408	1.21E-02
ALCAM	Q13740	-0.426	1.75E-02
LRPAP1	P30533	-0.448	5.88E-03
SEMA5A	Q13591	-0.456	5.82E-04
CDK2	P24941	-0.46	2.10E-02
CCNA2	P20248	-0.46	2.10E-02
CTSH	P09668	-0.508	2.70E-02
LAMA1	P25391	-0.516	4.87E-05
LAMB1	P07942	-0.516	4.87E-05
LAMC1	P11047	-0.516	4.87E-05
EFNA5	P52803	-0.59	5.41E-04
CAT	P04040	-0.598	3.46E-02
ACP5	P13686	-0.644	7.71E-04
THBS2	P35442	-0.646	4.24E-03
ECM1	Q16610	-0.648	2.99E-03
TGFBI	Q15582	-0.66	1.34E-02
IL6R	P08887	-0.66	2.83E-05
IGFBP2	P18065	-0.754	2.88E-03
FGF1	P05230	-0.768	2.04E-02
NOTCH1	P46531	-0.774	3.79E-04
TFF3	Q07654	-0.8	8.65E-04
BCAM	P50895	-0.834	2.60E-03
EFNA2	O43921	-0.978	5.49E-05
CNTN1	Q12860	-1.058	4.95E-04
NRP1	O14786	-1.114	1.10E-08
LRIG3	Q6UXM1	-1.196	6.80E-04
TNFRSF21	O75509	-1.204	3.57E-04
NOTCH3	Q9UM47	-1.21	4.56E-04
FTH1	P02794	-1.402	4.05E-04
FTL	P02792	-1.402	4.05E-04
CTSV	O60911	-1.876	3.29E-05

Supplementary table V: Proteins significantly altered in response to IFN-γ in HBEC-3KT 24 h post-stimulation.

NAME	SWPROT ID	AVG LOG2 FC (normalized to unstimulated cells)	p-value
CXCL11	O14625	0.00E+00	10.4
CXCL9	Q07325	0.00E+00	8.18
CXCL10	**P02778**	**9.88E-12**	**6.63**
C4A	P0C0L4	1.56E-06	6.22
C4B	P0C0L5	1.56E-06	6.22
CCL5	P13501	2.67E-05	4.92
CTSS	**P25774**	**2.67E-09**	**4.36**
CFB	P00751	2.42E-05	3.8
APOL1	**O14791**	**8.75E-08**	**3.42**
STAT1	P42224	2.09E-03	3.21
ICAM1	P05362	3.18E-07	3.07
IL1R2	P27930	3.56E-04	2.89
CD274	Q9NZQ7	1.29E-09	2.81
C1R	P00736	3.50E-06	2.63
CFH	P08603	8.36E-09	2.45
B2M	P61769	2.05E-05	2.35
IL18BP	O95998	3.66E-08	2.34
LIFR	P42702	1.14E-05	1.94
ISG15	P05161	2.29E-06	1.82
ADGRE2	Q9UHX3	1.34E-04	1.62
CCL7	P80098	4.11E-06	1.31
PLAU	P00749	3.18E-05	1.29
LGALS3BP	Q08380	7.96E-06	1.23
TOP1	P11387	2.60E-03	1.2
IL18R1	Q13478	2.26E-08	1.19
IFNG	P01579	6.09E-04	1.16
PLAUR	Q03405	2.87E-04	1.09
LYN	P07948	2.34E-04	1.06

GAS1	P54826	4.75E-05	1.02
PIGR	P01833	1.39E-05	0.95
ERAP1	Q9NZ08	9.17E-06	0.88
CXCL16	Q9H2A7	5.34E-04	0.82
OLR1	P78380	8.26E-04	0.81
MET	P08581	5.17E-04	0.78
IGFBP7	Q16270	2.42E-03	0.78
TNC	P24821	2.53E-02	0.75
SUMO3	P55854	1.47E-03	0.72
IL6ST	P40189	2.64E-03	0.71
SFRP1	Q8N474	5.75E-04	0.68
IL15RA	Q13261	5.06E-06	0.65
UBC	P0CG48	2.96E-02	0.63
CST3	P01034	4.19E-05	0.59
POR	P16435	4.12E-04	0.58
TNFRSF6B	O95407	5.55E-05	0.58
HS6ST1	O60243	4.74E-04	0.58
LGALS8	O00214	4.14E-05	0.57
CCL22	O00626	2.25E-03	0.56
PRKACA	P17612	4.17E-02	0.55
PSME1	Q06323	1.26E-02	0.55
CHST15	Q7LFX5	5.26E-03	0.54
CTSB	P07858	2.76E-03	0.52
SCARF1	Q14162	6.91E-05	0.52
PCSK7	Q16549	5.13E-04	0.51
PLXNB2	O15031	3.50E-02	0.51
CDH1	P12830	4.18E-03	0.48
FGFR1	P11362	1.89E-02	0.47
OAS1	P00973	2.35E-05	0.44
CX3CL1	P78423	1.59E-02	0.44
SECTM1	Q8WVN6	6.06E-06	0.43
GRN	P28799	1.36E-03	0.43

GPT	P24298	4.82E-04	0.39
SERPING1	P05155	5.64E-03	0.38
SCARB2	Q14108	3.34E-02	0.38
LGMN	Q99538	5.99E-04	0.37
BGLAP	P02818	5.99E-04	0.36
MIA	Q16674	5.51E-07	0.34
VEGFC	P49767	4.14E-02	0.34
CTSA	P10619	1.05E-02	0.33
TNFRSF1A	P19438	2.40E-02	0.31
ETHE1	O95571	6.43E-03	0.31
CAMK1	Q14012	3.44E-02	0.27
CTSC	P53634	1.91E-03	0.26
SAA1	P0DJI8	1.91E-02	0.26
C3	P01024	2.28E-02	0.25
MDK	P21741	1.02E-03	0.25
GRB2	P62993	3.26E-02	0.24
COL18A1	P39060	1.40E-02	0.23
MSN	P26038	3.67E-03	0.23
LY86	O95711	3.50E-03	0.22
TLR2	O60603	1.42E-02	0.22
SCGB2A1	O75556	3.87E-02	0.22
FAS	P25445	2.31E-02	0.22
RASA1	P20936	1.91E-02	0.22
SLAMF7	Q9NQ25	1.96E-03	0.22
S100A9	P06702	1.78E-03	0.21
CD27	P26842	1.56E-02	0.2
KIRREL3	Q8IZU9	3.94E-03	0.19
TXNDC12	O95881	1.75E-02	0.19
S100A12	P80511	1.78E-02	0.19
ADM	P35318	2.86E-02	0.18
CYP3A4	P08684	2.11E-02	0.18
BCL2L1	Q07817	3.47E-02	0.18

CDKN1B	P46527	3.82E-03	0.17
AMH	P03971	1.63E-02	0.17
DIABLO	Q9NR28	1.04E-03	0.16
SERPINA5	P05154	3.28E-03	0.16
PTPN2	P17706	4.61E-02	0.16
MAP2K3	P46734	4.62E-02	0.16
IFNB1	P01574	3.44E-03	0.15
BCL2A1	Q16548	4.24E-02	0.15
HPGD	P15428	2.93E-02	0.14
ADSL	P30566	4.26E-02	0.14
HHLA2	Q9UM44	4.23E-03	0.13
NCR2	O95944	2.54E-02	0.13
NOG	Q13253	4.15E-02	0.13
EPHA1	P21709	1.40E-02	0.12
IFNGR2	P38484	3.18E-02	0.12
UBE2G2	P60604	4.21E-02	0.12
CCL8	P80075	1.28E-02	0.11
SOD3	P08294	3.14E-02	0.11
BCL6	P41182	3.51E-02	0.1
MST1R	Q04912	1.62E-02	0.1
NAMPT	P43490	2.50E-02	0.1
IL2RA	P01589	9.39E-03	0.09
SPHK2	Q9NRA0	2.58E-02	0.08
SERPINA7	P05543	2.34E-02	-0.06
NOV	P48745	5.63E-03	-0.07
HP	P00738	4.80E-02	-0.07
BIRC3	Q13489	1.63E-02	-0.07
LTA4H	P09960	6.88E-03	-0.08
HAVCR2	Q8TDQ0	3.63E-02	-0.08
FGF9	P31371	4.51E-02	-0.09
ENTPD3	O75355	4.72E-02	-0.09
CCL11	P51671	1.11E-02	-0.09

CRELD1	Q96HD1	1.74E-02	-0.11
AIP	O00170	3.11E-02	-0.12
MATN3	O15232	3.93E-02	-0.13
RPS6KA5	O75582	2.09E-02	-0.13
MCL1	Q07820	4.28E-02	-0.14
ING1	Q9UK53	3.13E-02	-0.14
CDC2	P06493	2.14E-02	-0.15
P4HB	P07237	2.32E-02	-0.15
C10orf54	Q9H7M9	1.68E-02	-0.17
IL1RAP	Q9NPH3	2.26E-02	-0.18
FST	P19883	2.85E-02	-0.18
MYC	P01106	2.00E-02	-0.19
ULBP3	Q9BZM4	4.08E-02	-0.19
SBDS	Q9Y3A5	2.62E-02	-0.19
CD36	P16671	1.40E-04	-0.21
TFF3	Q07654	8.86E-03	-0.21
PRKAG1	P54619	2.54E-02	-0.22
PRKAA2	P54646	2.54E-02	-0.22
PRKAB2	O43741	2.54E-02	-0.22
LTBP4	Q8N2S1	3.11E-03	-0.23
NOTCH1	P46531	7.35E-03	-0.26
FSTL3	O95633	3.35E-02	-0.27
EFNA5	P52803	2.14E-02	-0.28
ULBP2	Q9BZM5	1.51E-02	-0.28
GPC3	P51654	1.89E-03	-0.3
NTN4	Q9HB63	3.67E-02	-0.31
MMP10	P09238	1.73E-02	-0.32
MFGE8	Q08431	3.23E-02	-0.33
LRP8	Q14114	2.18E-02	-0.34
MATN2	O00339	2.05E-03	-0.35
EREG	O14944	3.22E-02	-0.37
FSTL1	Q12841	7.41E-03	-0.38

GPNMB	Q14956	2.97E-02	-0.4
SPARC	P09486	1.02E-02	-0.42
EIF4G2	P78344	4.02E-02	-0.44
IL6R	P08887	1.06E-03	-0.45
KPNA2	P52292	2.60E-02	-0.5
F3	P13726	9.28E-03	-0.52
CDK2	P24941	1.43E-02	-0.53
CCNA2	P20248	1.43E-02	-0.53
DKK4	Q9UBT3	1.39E-03	-0.56
EFNA2	O43921	3.56E-04	-0.59
EPHB2	P29323	1.59E-02	-0.59
ALCAM	Q13740	6.28E-04	-0.61
IGFBP3	P17936	2.25E-03	-0.62
ANG	P03950	1.61E-05	-0.62
DKK1	O94907	4.15E-03	-0.68
TNFRSF10D	Q9UBN6	1.13E-04	-0.7
LRIG3	Q6UXM1	6.71E-03	-0.72
MICA	Q29983	4.85E-04	-0.73
EFEMP1	Q12805	8.44E-03	-0.74
SLPI	P03973	1.90E-04	-0.75
TNFRSF21	O75509	9.36E-03	-0.77
IGFBP2	P18065	2.70E-03	-0.77
SEMA5A	Q13591	7.08E-05	-0.78
MICB	Q29980	1.83E-05	-0.79
CNTN1	Q12860	2.11E-02	-0.8
ICAM5	Q9UMF0	9.85E-05	-0.83
HAT1	O14929	4.07E-02	-0.93
NOTCH3	Q9UM47	3.09E-03	-0.98
IGFBP5	P24593	2.48E-03	-1.02
L1CAM	P32004	2.84E-03	-1.05
PCSK9	Q8NBP7	1.46E-03	-1.09
IL1RL1	Q01638	8.97E-03	-1.14

FLRT3	Q9NZU0	2.69E-03	-1.24
PTHLH	P12272	5.84E-06	-1.6
STC1	P52823	1.45E-04	-1.86
THBS1	P07996	3.58E-04	-1.96
ELAFIN	**P19957**	**1.05E-03**	**-2.09**
CTSV	**O60911**	**1.54E-05**	**-2.16**
THBS2	P35442	1.71E-06	-2.19
MMP1	P03956	1.53E-03	-2.27

9.2 Abbreviations

Air-liquid interface (ALI)

Airway epithelial cells (AEC)

Airway hyperresponsiveness (AHR)

Airway smooth muscle (ASM)

Analysis of variance (ANOVA)

Angiogenin (ANG)

Antigen presenting cells (APC)

Antimicrobial peptides (AMP)

Antimicrobial peptides and proteins (APP)

Apolipoprotein 1 (APOL-1)

Aryl hydrocarbon receptor (AHR)

Bacterial Permeability Increasing Protein (BPI)

Bicinchoninic acid (BCA)

Bone-marrow derived cells (BDMC)

Bronchoalveolar lavage (BAL)

Cationic host defense peptides (CHDP)

CCAAT/enhancer-binding protein-β (C/EBPβ)

CC-chemokine receptor 3 (CCR3)

Cathelicidin-related antimicrobial peptide (CRAMP)

Cathepsin S (CTSS)

Cathepsin V (CTSV)

Central nervous system (CNS)

Chronic obstructive pulmonary disease (COPD)

Citrullinated LL-37 (citLL-37)

Cluster of differentiation (CD)

Collagen-induced arthritis (CIA)

Computed tomography (CT)

C-type lectin receptors (CLR)

Damage associated molecular patterns (DAMP)

Eosinophil cationic proteins (ECP)

Eosinophil-derived neurotoxin (EDN)

Eosinophil peroxidase (EPO)

Experimental Autoimmune Encephalitis (EAE)

Extracellular DNA (eDNA)

Forced expiratory volume in 1 second (FEV1)

Formyl peptide receptor 1 (FPRL1)

Granulocyte–macrophage colony-stimulating factor (GM-CSF)

G protein-coupled receptors (GPCR)

Histone deacetylase (HDAC)

House dust mite (HDM)

Human bronchial epithelial cell (HBEC)

IL-17 receptor (IL-17R)

Immunoglobulin (Ig)

Ingenuity Pathway Analysis (IPA)

inhaled corticosteroids (ICS)

Innate lymphoid cells (ILC)

Interferon Regulatory Factor (IRF)-1

Interleukins (IL)

Intranasal (i.n.)

Intraperitoneal (i.p.)

Lactate Dehydrogenase (LDH)

leukotriene B_4 (LTB4)

Lipocalin (LCN)

Lipopolysaccharide (LPS)

Major basic protein (MBP)

Major histocompatibility complex (MHC)

Matrix metalloproteinase (MMP)

Meso Scale Discovery (MSD)

Messenger RNA (mRNA)

Mitogen-activated protein kinase (MAPK)

Monoclonal antibody (mAb)

Monocyte chemoattractant protein-1 (MCP-1)

Mucosal-Associated Invariant T (MAIT)

Multiple sclerosis (MS)

Myeloperoxidase (MPO)

Natural Killer T (NKT)

Neutrophil elastase (NE)

Neutrophil extracellular traps (NET)

NOD-like receptors (NLR)

Nuclear factor-κ*B* (NF-κB)

Nuclear factor kB activator 1 (Act1)

Ovalbumin (OVA)

Pathogen-associated molecular patterns (PAMP)

Pattern-recognition receptors (PRR)

Peptidyl arginine deiminases (PADI)

Peripheral blood mononuclear cells (PBMC)

Phosphate-buffered saline (PBS)

Polymorphonuclear neutrophilic leukocytes (PMNs)

Post-translational modifications (PTM)

Primary Bronchial Epithelial Cells (PBEC)

Reactive oxygen species (ROS)

Receptor antagonist (RA)

Retinoic acid-inducible gene (RIG)

Retinoic acid receptor-related orphan receptor-γt (RORγt)

Rheumatoid arthritis (RA)

RNA-binding proteins (RBP)

Scrambled LL-37 (sLL-37)

Secretory-antileukoproteinase (SLPI)

SEF/IL-17R (SEFIR)

Tenascin (TNC)

Tissue inhibitor of metalloproteinase (TIMP)

Tissue Protein Extraction Reagent (T-Per)

T-Lymphocyte (T cell)

Transforming growth factor (TGF)-β

Toll-like receptors (TLR)

Tumor-necrosis factor receptor–associated factor (TRAF)

Untranslated region (UTR)

Zonula occludin (ZO)

9.3 References

1. Majno G. The Healing Hand - Man and wound in the ancient world. Cambridge, MA: Harvard University Press; 1975.
2. Medzhitov R. Inflammation 2010: new adventures of an old flame. Cell. 2010;140(6):771-6.
3. Tauber AI. Metchnikoff and the phagocytosis theory. Nature reviews Molecular cell biology. 2003;4(11):897-901.
4. Abbas A, Lichtman, Andrew H., Pillai, Shiv, Baker, David L, & Baker, Alexandra. . Basic immunology : Functions and disorders of the immune system (Fifth ed.).(2016).
5. Murphy KP, et al. . Janeway's Immunobiology. 7th Edition ed. Madison Avenus, New York, NY: Garland Science, Taylor & Francis Group, LLC; 2008.
6. Medzhitov R, Janeway C, Jr. Innate immunity. The New England journal of medicine. 2000;343(5):338-44.
7. Janeway CA, Jr. The immune system evolved to discriminate infectious nonself from noninfectious self. Immunol Today. 1992;13(1):11-6.
8. Takeuchi O, Akira S. Pattern recognition receptors and inflammation. Cell. 2010;140(6):805-20.
9. Belvin MP, Anderson KV. A conserved signaling pathway: the Drosophila toll-dorsal pathway. Annu Rev Cell Dev Biol. 1996;12:393-416.
10. Opal SM, DePalo VA. Anti-inflammatory cytokines. Chest. 2000;117(4):1162-72.
11. Dinarello CA. Proinflammatory cytokines. Chest. 2000;118(2):503-8.
12. Zhang JM, An J. Cytokines, inflammation, and pain. Int Anesthesiol Clin. 2007;45(2):27-37.
13. Hamid Q, Tulic M. Immunobiology of asthma. Annu Rev Physiol. 2009;71:489-507.
14. Dinarello CA. Interleukin-1, interleukin-1 receptors and interleukin-1 receptor antagonist. Int Rev Immunol. 1998;16(5-6):457-99.
15. Akdis M, Aab A, Altunbulakli C, Azkur K, Costa RA, Crameri R, et al. Interleukins (from IL-1 to IL-38), interferons, transforming growth factor beta, and TNF-alpha: Receptors, functions, and roles in diseases. The Journal of allergy and clinical immunology. 2016;138(4):984-1010.
16. Rossi D, Zlotnik A. The biology of chemokines and their receptors. Annual review of immunology. 2000;18:217-42.
17. McBrien CN, Menzies-Gow A. The Biology of Eosinophils and Their Role in Asthma. Front Med (Lausanne). 2017;4:93.
18. Mookherjee N, Anderson MA, Haagsman HP, Davidson DJ. Antimicrobial host defence peptides: functions and clinical potential. Nature reviews Drug discovery. 2020;19(5):311-32.
19. Mookherjee N, Anderson MA, Haagsman HP, Davidson DJ. Antimicrobial host defence peptides: functions and clinical potential. Nature Reviews Drug Discovery. 2020;19(5):311-32.
20. Mookherjee N, Hancock RE. Cationic host defence peptides: innate immune regulatory peptides as a novel approach for treating infections. Cellular and molecular life sciences : CMLS. 2007;64(7-8):922-33.
21. Hancock RE, Haney EF, Gill EE. The immunology of host defence peptides: beyond antimicrobial activity. Nature reviews Immunology. 2016;16(5):321-34.
22. Hemshekhar M, Anaparti V, Mookherjee N. Functions of Cationic Host Defense Peptides in Immunity. Pharmaceuticals (Basel). 2016;9(3).
23. Hancock RE, Sahl HG. Antimicrobial and host-defense peptides as new anti-infective therapeutic strategies. Nature biotechnology. 2006;24(12):1551-7.
24. Mansour SC, Pena OM, Hancock RE. Host defense peptides: front-line immunomodulators. Trends in immunology. 2014;35(9):443-50.
25. Chertov O, Michiel DF, Xu L, Wang JM, Tani K, Murphy WJ, et al. Identification of defensin-1, defensin-2, and CAP37/azurocidin as T-cell chemoattractant proteins released from interleukin-8-stimulated neutrophils. The Journal of biological chemistry. 1996;271(6):2935-40.
26. Van Wetering S, Mannesse-Lazeroms SP, Van Sterkenburg MA, Daha MR, Dijkman JH, Hiemstra PS. Effect of defensins on interleukin-8 synthesis in airway epithelial cells. Am J Physiol. 1997;272(5 Pt 1):L888-96.
27. Yang D, Chen Q, Chertov O, Oppenheim JJ. Human neutrophil defensins selectively chemoattract naive T and immature dendritic cells. Journal of leukocyte biology. 2000;68(1):9-14.

28. De Y, Chen Q, Schmidt AP, Anderson GM, Wang JM, Wooters J, et al. LL-37, the neutrophil granule- and epithelial cell-derived cathelicidin, utilizes formyl peptide receptor-like 1 (FPRL1) as a receptor to chemoattract human peripheral blood neutrophils, monocytes, and T cells. The Journal of experimental medicine. 2000;192(7):1069-74.
29. Tjabringa GS, Ninaber DK, Drijfhout JW, Rabe KF, Hiemstra PS. Human cathelicidin LL-37 is a chemoattractant for eosinophils and neutrophils that acts via formyl-peptide receptors. Int Arch Allergy Immunol. 2006;140(2):103-12.
30. Scott MG, Davidson DJ, Gold MR, Bowdish D, Hancock RE. The human antimicrobial peptide LL-37 is a multifunctional modulator of innate immune responses. Journal of immunology (Baltimore, Md : 1950). 2002;169(7):3883-91.
31. Choi KY, Mookherjee N. Multiple immune-modulatory functions of cathelicidin host defense peptides. Frontiers in immunology. 2012;3:149.
32. Hemshekhar M, Choi KG, Mookherjee N. Host Defense Peptide LL-37-Mediated Chemoattractant Properties, but Not Anti-Inflammatory Cytokine IL-1RA Production, Is Selectively Controlled by Cdc42 Rho GTPase via G Protein-Coupled Receptors and JNK Mitogen-Activated Protein Kinase. Frontiers in immunology. 2018;9:1871.
33. Mookherjee N, Brown KL, Bowdish DM, Doria S, Falsafi R, Hokamp K, et al. Modulation of the TLR-mediated inflammatory response by the endogenous human host defense peptide LL-37. Journal of immunology (Baltimore, Md : 1950). 2006;176(4):2455-64.
34. Lau YE, Bowdish DM, Cosseau C, Hancock RE, Davidson DJ. Apoptosis of airway epithelial cells: human serum sensitive induction by the cathelicidin LL-37. American journal of respiratory cell and molecular biology. 2006;34(4):399-409.
35. Barlow PG, Beaumont PE, Cosseau C, Mackellar A, Wilkinson TS, Hancock RE, et al. The human cathelicidin LL-37 preferentially promotes apoptosis of infected airway epithelium. American journal of respiratory cell and molecular biology. 2010;43(6):692-702.
36. McHugh BJ, Wang R, Li HN, Beaumont PE, Kells R, Stevens H, et al. Cathelicidin is a "fire alarm", generating protective NLRP3-dependent airway epithelial cell inflammatory responses during infection with Pseudomonas aeruginosa. PLoS Pathog. 2019;15(4):e1007694.
37. Davidson DJ, Currie AJ, Reid GS, Bowdish DM, MacDonald KL, Ma RC, et al. The cationic antimicrobial peptide LL-37 modulates dendritic cell differentiation and dendritic cell-induced T cell polarization. Journal of immunology (Baltimore, Md : 1950). 2004;172(2):1146-56.
38. Bandholtz L, Ekman GJ, Vilhelmsson M, Buentke E, Agerberth B, Scheynius A, et al. Antimicrobial peptide LL-37 internalized by immature human dendritic cells alters their phenotype. Scand J Immunol. 2006;63(6):410-9.
39. Findlay EG, Currie AJ, Zhang A, Ovciarikova J, Young L, Stevens H, et al. Exposure to the antimicrobial peptide LL-37 produces dendritic cells optimized for immunotherapy. Oncoimmunology. 2019;8(8):1608106.
40. Lande R, Gregorio J, Facchinetti V, Chatterjee B, Wang YH, Homey B, et al. Plasmacytoid dendritic cells sense self-DNA coupled with antimicrobial peptide. Nature. 2007;449(7162):564-9.
41. Ganguly D, Chamilos G, Lande R, Gregorio J, Meller S, Facchinetti V, et al. Self-RNA-antimicrobial peptide complexes activate human dendritic cells through TLR7 and TLR8. The Journal of experimental medicine. 2009;206(9):1983-94.
42. Kim SH, Kim YN, Jang YS. Cutting Edge: LL-37-Mediated Formyl Peptide Receptor-2 Signaling in Follicular Dendritic Cells Contributes to B Cell Activation in Peyer's Patch Germinal Centers. Journal of immunology (Baltimore, Md : 1950). 2017;198(2):629-33.
43. Choi KY, Napper S, Mookherjee N. Human cathelicidin LL-37 and its derivative IG-19 regulate interleukin-32-induced inflammation. Immunology. 2014;143(1):68-80.
44. Mookherjee N, Lippert DN, Hamill P, Falsafi R, Nijnik A, Kindrachuk J, et al. Intracellular receptor for human host defense peptide LL-37 in monocytes. Journal of immunology (Baltimore, Md : 1950). 2009;183(4):2688-96.
45. Piyadasa H, Hemshekhar M, Altieri A, Basu S, van der Does AM, Halayko AJ, et al. Immunomodulatory innate defence regulator (IDR) peptide alleviates airway inflammation and hyper-responsiveness. Thorax. 2018.
46. Turner-Brannen E, Choi KY, Lippert DN, Cortens JP, Hancock RE, El-Gabalawy H, et al. Modulation of interleukin-1beta-induced inflammatory responses by a synthetic cationic innate

defence regulator peptide, IDR-1002, in synovial fibroblasts. Arthritis research & therapy. 2011;13(4):R129.
47. Levitzky MG. Pulmonary physiology. 9th ed. New York, NY: McGraw-Hill Education; 2018.
48. Hiemstra PS, McCray PB, Jr., Bals R. The innate immune function of airway epithelial cells in inflammatory lung disease. The European respiratory journal. 2015;45(4):1150-62.
49. Broide DH, Lotz M, Cuomo AJ, Coburn DA, Federman EC, Wasserman SI. Cytokines in symptomatic asthma airways. The Journal of allergy and clinical immunology. 1992;89(5):958-67.
50. Metzemaekers M, Gouwy M, Proost P. Neutrophil chemoattractant receptors in health and disease: double-edged swords. Cell Mol Immunol. 2020;17(5):433-50.
51. Mortaz E, Alipoor SD, Adcock IM, Mumby S, Koenderman L. Update on Neutrophil Function in Severe Inflammation. Frontiers in immunology. 2018;9:2171.
52. Nathan C. Neutrophils and immunity: challenges and opportunities. Nature reviews Immunology. 2006;6(3):173-82.
53. Hayashi F, Means TK, Luster AD. Toll-like receptors stimulate human neutrophil function. Blood. 2003;102(7):2660-9.
54. Selders GS, Fetz AE, Radic MZ, Bowlin GL. An overview of the role of neutrophils in innate immunity, inflammation and host-biomaterial integration. Regen Biomater. 2017;4(1):55-68.
55. Hellebrekers P, Vrisekoop N, Koenderman L. Neutrophil phenotypes in health and disease. Eur J Clin Invest. 2018;48 Suppl 2(Suppl Suppl 2):e12943.
56. Brinkmann V, Reichard U, Goosmann C, Fauler B, Uhlemann Y, Weiss DS, et al. Neutrophil extracellular traps kill bacteria. Science (New York, NY). 2004;303(5663):1532-5.
57. Papayannopoulos V. Neutrophil extracellular traps in immunity and disease. Nature reviews Immunology. 2018;18(2):134-47.
58. Borregaard N, Cowland JB. Granules of the human neutrophilic polymorphonuclear leukocyte. Blood. 1997;89(10):3503-21.
59. Rosenberg HF, Dyer KD, Foster PS. Eosinophils: changing perspectives in health and disease. Nature reviews Immunology. 2013;13(1):9-22.
60. Davoine F, Lacy P. Eosinophil cytokines, chemokines, and growth factors: emerging roles in immunity. Frontiers in immunology. 2014;5:570.
61. Giembycz MA, Lindsay MA. Pharmacology of the eosinophil. Pharmacol Rev. 1999;51(2):213-340.
62. Piliponsky AM, Gleich GJ, Nagler A, Bar I, Levi-Schaffer F. Non-IgE-dependent activation of human lung- and cord blood-derived mast cells is induced by eosinophil major basic protein and modulated by the membrane form of stem cell factor. Blood. 2003;101(5):1898-904.
63. Ben-Zimra M, Bachelet I, Seaf M, Gleich GJ, Levi-Schaffer F. Eosinophil major basic protein activates human cord blood mast cells primed with fibroblast membranes by integrin-β1. Allergy. 2013;68(10):1259-68.
64. Grünig G, Warnock M, Wakil AE, Venkayya R, Brombacher F, Rennick DM, et al. Requirement for IL-13 independently of IL-4 in experimental asthma. Science (New York, NY). 1998;282(5397):2261-3.
65. Hallstrand TS, Henderson WR, Jr. An update on the role of leukotrienes in asthma. Curr Opin Allergy Clin Immunol. 2010;10(1):60-6.
66. Bradding P, Roberts JA, Britten KM, Montefort S, Djukanovic R, Mueller R, et al. Interleukin-4, -5, and -6 and tumor necrosis factor-alpha in normal and asthmatic airways: evidence for the human mast cell as a source of these cytokines. American journal of respiratory cell and molecular biology. 1994;10(5):471-80.
67. Carroll NG, Mutavdzic S, James AL. Increased mast cells and neutrophils in submucosal mucous glands and mucus plugging in patients with asthma. Thorax. 2002;57(8):677-82.
68. Brightling CE, Bradding P, Symon FA, Holgate ST, Wardlaw AJ, Pavord ID. Mast-cell infiltration of airway smooth muscle in asthma. The New England journal of medicine. 2002;346(22):1699-705.
69. Bradding P, Walls AF, Holgate ST. The role of the mast cell in the pathophysiology of asthma. The Journal of allergy and clinical immunology. 2006;117(6):1277-84.
70. Canada A. Asthma Facts and Statistics FAQ. Asthma.ca: Asthma Canada; 2012.
71. Canada ASo. Asthma Facts and Statistics 2013 [2012:[

72. Tyler SR, Bunyavanich S. Leveraging -omics for asthma endotyping. The Journal of allergy and clinical immunology. 2019;144(1):13-23.
73. Thomson NC. Novel approaches to the management of noneosinophilic asthma. Ther Adv Respir Dis. 2016;10(3):211-34.
74. Pavord ID, Beasley R, Agusti A, Anderson GP, Bel E, Brusselle G, et al. After asthma: redefining airways diseases. Lancet (London, England). 2018;391(10118):350-400.
75. Casale TB. Biologics and biomarkers for asthma, urticaria, and nasal polyposis. The Journal of allergy and clinical immunology. 2017;139(5):1411-21.
76. Liu W, Liu S, Verma M, Zafar I, Good JT, Rollins D, et al. Mechanism of T(H)2/T(H)17-predominant and neutrophilic T(H)2/T(H)17-low subtypes of asthma. The Journal of allergy and clinical immunology. 2017;139(5):1548-58.e4.
77. Ricciardolo FLM, Sorbello V, Folino A, Gallo F, Massaglia GM, Favatà G, et al. Identification of IL-17F/frequent exacerbator endotype in asthma. The Journal of allergy and clinical immunology. 2017;140(2):395-406.
78. Tliba O, Panettieri RA, Jr. Paucigranulocytic asthma: Uncoupling of airway obstruction from inflammation. The Journal of allergy and clinical immunology. 2019;143(4):1287-94.
79. Svenningsen S, Nair P. Asthma Endotypes and an Overview of Targeted Therapy for Asthma. Front Med (Lausanne). 2017;4:158.
80. Gundel RH, Letts LG, Gleich GJ. Human eosinophil major basic protein induces airway constriction and airway hyperresponsiveness in primates. The Journal of clinical investigation. 1991;87(4):1470-3.
81. Woodruff PG, Modrek B, Choy DF, Jia G, Abbas AR, Ellwanger A, et al. T-helper type 2-driven inflammation defines major subphenotypes of asthma. American journal of respiratory and critical care medicine. 2009;180(5):388-95.
82. Singhania A, Wallington JC, Smith CG, Horowitz D, Staples KJ, Howarth PH, et al. Multitissue Transcriptomics Delineates the Diversity of Airway T Cell Functions in Asthma. American journal of respiratory cell and molecular biology. 2018;58(2):261-70.
83. Wisniewski JA, Muehling LM, Eccles JD, Capaldo BJ, Agrawal R, Shirley DA, et al. T(H)1 signatures are present in the lower airways of children with severe asthma, regardless of allergic status. The Journal of allergy and clinical immunology. 2018;141(6):2048-60.e13.
84. Choy DF, Hart KM, Borthwick LA, Shikotra A, Nagarkar DR, Siddiqui S, et al. TH2 and TH17 inflammatory pathways are reciprocally regulated in asthma. Sci Transl Med. 2015;7(301):301ra129.
85. Jatakanon A, Uasuf C, Maziak W, Lim S, Chung KF, Barnes PJ. Neutrophilic inflammation in severe persistent asthma. American journal of respiratory and critical care medicine. 1999;160(5 Pt 1):1532-9.
86. Ordoñez CL, Shaughnessy TE, Matthay MA, Fahy JV. Increased neutrophil numbers and IL-8 levels in airway secretions in acute severe asthma: Clinical and biologic significance. American journal of respiratory and critical care medicine. 2000;161(4 Pt 1):1185-90.
87. Fahy JV, Kim KW, Liu J, Boushey HA. Prominent neutrophilic inflammation in sputum from subjects with asthma exacerbation. The Journal of allergy and clinical immunology. 1995;95(4):843-52.
88. Qiu Y, Zhu J, Bandi V, Guntupalli KK, Jeffery PK. Bronchial mucosal inflammation and upregulation of CXC chemoattractants and receptors in severe exacerbations of asthma. Thorax. 2007;62(6):475-82.
89. Sur S, Crotty TB, Kephart GM, Hyma BA, Colby TV, Reed CE, et al. Sudden-onset fatal asthma. A distinct entity with few eosinophils and relatively more neutrophils in the airway submucosa? The American review of respiratory disease. 1993;148(3):713-9.
90. Anees W, Huggins V, Pavord ID, Robertson AS, Burge PS. Occupational asthma due to low molecular weight agents: eosinophilic and non-eosinophilic variants. Thorax. 2002;57(3):231-6.
91. Martin RJ, Cicutto LC, Smith HR, Ballard RD, Szefler SJ. Airways inflammation in nocturnal asthma. The American review of respiratory disease. 1991;143(2):351-7.
92. McDougall CM, Helms PJ. Neutrophil airway inflammation in childhood asthma. Thorax. 2006;61(9):739-41.
93. Ray A, Kolls JK. Neutrophilic Inflammation in Asthma and Association with Disease Severity. Trends in immunology. 2017;38(12):942-54.

94. Hilchie AL, Wuerth K, Hancock RE. Immune modulation by multifaceted cationic host defense (antimicrobial) peptides. Nature chemical biology. 2013;9(12):761-8.
95. Murakami M, Lopez-Garcia B, Braff M, Dorschner RA, Gallo RL. Postsecretory processing generates multiple cathelicidins for enhanced topical antimicrobial defense. Journal of immunology (Baltimore, Md : 1950). 2004;172(5):3070-7.
96. Sochacki KA, Barns KJ, Bucki R, Weisshaar JC. Real-time attack on single Escherichia coli cells by the human antimicrobial peptide LL-37. Proceedings of the National Academy of Sciences of the United States of America. 2011;108(16):E77-81.
97. Schneider VA, Coorens M, Ordonez SR, Tjeerdsma-van Bokhoven JL, Posthuma G, van Dijk A, et al. Imaging the antimicrobial mechanism(s) of cathelicidin-2. Scientific reports. 2016;6:32948.
98. van Harten RM, van Woudenbergh E, van Dijk A, Haagsman HP. Cathelicidins: Immunomodulatory Antimicrobials. Vaccines. 2018;6(3).
99. Mookherjee N, Rehaume LM, Hancock RE. Cathelicidins and functional analogues as antisepsis molecules. Expert Opin Ther Targets. 2007;11(8):993-1004.
100. Zanetti M. Cathelicidins, multifunctional peptides of the innate immunity. Journal of leukocyte biology. 2004;75(1):39-48.
101. Chow LN, Choi KY, Piyadasa H, Bossert M, Uzonna J, Klonisch T, et al. Human cathelicidin LL-37-derived peptide IG-19 confers protection in a murine model of collagen-induced arthritis. Molecular immunology. 2014;57(2):86-92.
102. Hemshekhar M, Piyadasa H, Mostafa D, Chow LNY, Halayko AJ, Mookherjee N. Cathelicidin and Calprotectin Are Disparately Altered in Murine Models of Inflammatory Arthritis and Airway Inflammation. Frontiers in immunology. 2020;11:1932.
103. Mookherjee N, Hamill P, Gardy J, Blimkie D, Falsafi R, Chikatamarla A, et al. Systems biology evaluation of immune responses induced by human host defence peptide LL-37 in mononuclear cells. Molecular bioSystems. 2009;5(5):483-96.
104. Yu J, Mookherjee N, Wee K, Bowdish DM, Pistolic J, Li Y, et al. Host defense peptide LL-37, in synergy with inflammatory mediator IL-1beta, augments immune responses by multiple pathways. Journal of immunology (Baltimore, Md : 1950). 2007;179(11):7684-91.
105. van der Does AM, Hiemstra PS, Mookherjee N. Antimicrobial Host Defence Peptides: Immunomodulatory Functions and Translational Prospects. Adv Exp Med Biol. 2019;1117:149-71.
106. Steinstraesser L, Kraneburg U, Jacobsen F, Al-Benna S. Host defense peptides and their antimicrobial-immunomodulatory duality. Immunobiology. 2011;216(3):322-33.
107. Simmaco M, Kreil G, Barra D. Bombinins, antimicrobial peptides from Bombina species. Biochimica et biophysica acta. 2009;1788(8):1551-5.
108. Steiner H, Hultmark D, Engström A, Bennich H, Boman HG. Sequence and specificity of two antibacterial proteins involved in insect immunity. Nature. 1981;292(5820):246-8.
109. Zasloff M. Magainins, a class of antimicrobial peptides from Xenopus skin: isolation, characterization of two active forms, and partial cDNA sequence of a precursor. Proceedings of the National Academy of Sciences of the United States of America. 1987;84(15):5449-53.
110. Ganz T, Selsted ME, Szklarek D, Harwig SS, Daher K, Bainton DF, et al. Defensins. Natural peptide antibiotics of human neutrophils. The Journal of clinical investigation. 1985;76(4):1427-35.
111. Wang G, Li X, Wang Z. APD3: the antimicrobial peptide database as a tool for research and education. Nucleic acids research. 2016;44(D1):D1087-93.
112. Gudmundsson GH, Agerberth B, Odeberg J, Bergman T, Olsson B, Salcedo R. The human gene FALL39 and processing of the cathelin precursor to the antibacterial peptide LL-37 in granulocytes. Eur J Biochem. 1996;238(2):325-32.
113. van Dijk A, Tersteeg-Zijderveld MH, Tjeerdsma-van Bokhoven JL, Jansman AJ, Veldhuizen EJ, Haagsman HP. Chicken heterophils are recruited to the site of Salmonella infection and release antibacterial mature Cathelicidin-2 upon stimulation with LPS. Molecular immunology. 2009;46(7):1517-26.
114. Gallo RL, Kim KJ, Bernfield M, Kozak CA, Zanetti M, Merluzzi L, et al. Identification of CRAMP, a cathelin-related antimicrobial peptide expressed in the embryonic and adult mouse. The Journal of biological chemistry. 1997;272(20):13088-93.
115. Kuensaen C, Chomdej S, Kongdang P, Sirikaew N, Jaitham R, Thonghoi S, et al. LL-37 alone and in combination with IL17A enhances proinflammatory cytokine expression in parallel with

hyaluronan metabolism in human synovial sarcoma cell line SW982-A step toward understanding the development of inflammatory arthritis. PloS one. 2019;14(7):e0218736.
116. Li N, Yamasaki K, Saito R, Fukushi-Takahashi S, Shimada-Omori R, Asano M, et al. Alarmin function of cathelicidin antimicrobial peptide LL37 through IL-36γ induction in human epidermal keratinocytes. Journal of immunology (Baltimore, Md : 1950). 2014;193(10):5140-8.
117. Pistolic J, Cosseau C, Li Y, Yu JJ, Filewod NC, Gellatly S, et al. Host defence peptide LL-37 induces IL-6 expression in human bronchial epithelial cells by activation of the NF-kappaB signaling pathway. Journal of innate immunity. 2009;1(3):254-67.
118. Beaumont PE, McHugh B, Gwyer Findlay E, Mackellar A, Mackenzie KJ, Gallo RL, et al. Cathelicidin host defence peptide augments clearance of pulmonary Pseudomonas aeruginosa infection by its influence on neutrophil function in vivo. PloS one. 2014;9(6):e99029.
119. Zhang Z, Cherryholmes G, Chang F, Rose DM, Schraufstatter I, Shively JE. Evidence that cathelicidin peptide LL-37 may act as a functional ligand for CXCR2 on human neutrophils. European journal of immunology. 2009;39(11):3181-94.
120. Zheng Y, Niyonsaba F, Ushio H, Nagaoka I, Ikeda S, Okumura K, et al. Cathelicidin LL-37 induces the generation of reactive oxygen species and release of human alpha-defensins from neutrophils. The British journal of dermatology. 2007;157(6):1124-31.
121. Alalwani SM, Sierigk J, Herr C, Pinkenburg O, Gallo R, Vogelmeier C, et al. The antimicrobial peptide LL-37 modulates the inflammatory and host defense response of human neutrophils. European journal of immunology. 2010;40(4):1118-26.
122. Stephan A, Batinica M, Steiger J, Hartmann P, Zaucke F, Bloch W, et al. LL37:DNA complexes provide antimicrobial activity against intracellular bacteria in human macrophages. Immunology. 2016;148(4):420-32.
123. Tripathi S, Verma A, Kim EJ, White MR, Hartshorn KL. LL-37 modulates human neutrophil responses to influenza A virus. Journal of leukocyte biology. 2014;96(5):931-8.
124. Minns D, Smith KJ, Alessandrini V, Hardisty G, Melrose L, Jackson-Jones L, et al. The neutrophil antimicrobial peptide cathelicidin promotes Th17 differentiation. Nat Commun. 2021;12(1):1285.
125. Zhang Z, Cherryholmes G, Shively JE. Neutrophil secondary necrosis is induced by LL-37 derived from cathelicidin. Journal of leukocyte biology. 2008;84(3):780-8.
126. Li HN, Barlow PG, Bylund J, Mackellar A, Björstad A, Conlon J, et al. Secondary necrosis of apoptotic neutrophils induced by the human cathelicidin LL-37 is not proinflammatory to phagocytosing macrophages. Journal of leukocyte biology. 2009;86(4):891-902.
127. Savill J, Dransfield I, Gregory C, Haslett C. A blast from the past: clearance of apoptotic cells regulates immune responses. Nature reviews Immunology. 2002;2(12):965-75.
128. Lau YE, Rozek A, Scott MG, Goosney DL, Davidson DJ, Hancock RE. Interaction and cellular localization of the human host defense peptide LL-37 with lung epithelial cells. Infection and immunity. 2005;73(1):583-91.
129. Cirioni O, Giacometti A, Ghiselli R, Bergnach C, Orlando F, Silvestri C, et al. LL-37 protects rats against lethal sepsis caused by gram-negative bacteria. Antimicrob Agents Chemother. 2006;50(5):1672-9.
130. Hou M, Zhang N, Yang J, Meng X, Yang R, Li J, et al. Antimicrobial peptide LL-37 and IDR-1 ameliorate MRSA pneumonia in vivo. Cell Physiol Biochem. 2013;32(3):614-23.
131. Fukumoto K, Nagaoka I, Yamataka A, Kobayashi H, Yanai T, Kato Y, et al. Effect of antibacterial cathelicidin peptide CAP18/LL-37 on sepsis in neonatal rats. Pediatr Surg Int. 2005;21(1):20-4.
132. Severino P, Ariga SK, Barbeiro HV, de Lima TM, de Paula Silva E, Barbeiro DF, et al. Cathelicidin-deficient mice exhibit increased survival and upregulation of key inflammatory response genes following cecal ligation and puncture. J Mol Med (Berl). 2017;95(9):995-1003.
133. Deng YY, Shamoon M, He Y, Bhatia M, Sun J. Cathelicidin-related antimicrobial peptide modulates the severity of acute pancreatitis in mice. Mol Med Rep. 2016;13(5):3881-5.
134. Kandler K, Shaykhiev R, Kleemann P, Klescz F, Lohoff M, Vogelmeier C, et al. The anti-microbial peptide LL-37 inhibits the activation of dendritic cells by TLR ligands. Int Immunol. 2006;18(12):1729-36.

135. Aidoukovitch A, Anders E, Dahl S, Nebel D, Svensson D, Nilsson BO. The host defense peptide LL-37 is internalized by human periodontal ligament cells and prevents LPS-induced MCP-1 production. J Periodontal Res. 2019;54(6):662-70.
136. Amatngalim GD, Nijnik A, Hiemstra PS, Hancock RE. Cathelicidin peptide LL-37 modulates TREM-1 expression and inflammatory responses to microbial compounds. Inflammation. 2011;34(5):412-25.
137. Filewod NC, Pistolic J, Hancock RE. Low concentrations of LL-37 alter IL-8 production by keratinocytes and bronchial epithelial cells in response to proinflammatory stimuli. FEMS Immunol Med Microbiol. 2009;56(3):233-40.
138. Al-Adwani S, Wallin C, Balhuizen MD, Veldhuizen EJA, Coorens M, Landreh M, et al. Studies on citrullinated LL-37: detection in human airways, antibacterial effects and biophysical properties. Scientific reports. 2020;10(1):2376.
139. Kilsgård O, Andersson P, Malmsten M, Nordin SL, Linge HM, Eliasson M, et al. Peptidylarginine deiminases present in the airways during tobacco smoking and inflammation can citrullinate the host defense peptide LL-37, resulting in altered activities. American journal of respiratory cell and molecular biology. 2012;46(2):240-8.
140. Koziel J, Bryzek D, Sroka A, Maresz K, Glowczyk I, Bielecka E, et al. Citrullination alters immunomodulatory function of LL-37 essential for prevention of endotoxin-induced sepsis. Journal of immunology (Baltimore, Md : 1950). 2014;192(11):5363-72.
141. Wong A, Bryzek D, Dobosz E, Scavenius C, Svoboda P, Rapala-Kozik M, et al. A Novel Biological Role for Peptidyl-Arginine Deiminases: Citrullination of Cathelicidin LL-37 Controls the Immunostimulatory Potential of Cell-Free DNA. Journal of immunology (Baltimore, Md : 1950). 2018;200(7):2327-40.
142. Casanova V, Sousa FH, Shakamuri P, Svoboda P, Buch C, D'Acremont M, et al. Citrullination Alters the Antiviral and Immunomodulatory Activities of the Human Cathelicidin LL-37 During Rhinovirus Infection. Frontiers in immunology. 2020;11:85.
143. Paulsen F, Pufe T, Conradi L, Varoga D, Tsokos M, Papendieck J, et al. Antimicrobial peptides are expressed and produced in healthy and inflamed human synovial membranes. The Journal of pathology. 2002;198(3):369-77.
144. Fuentes-Duculan J, Bonifacio KM, Hawkes JE, Kunjravia N, Cueto I, Li X, et al. Autoantigens ADAMTSL5 and LL37 are significantly upregulated in active Psoriasis and localized with keratinocytes, dendritic cells and other leukocytes. Exp Dermatol. 2017;26(11):1075-82.
145. Sun CL, Zhang FZ, Li P, Bi LQ. LL-37 expression in the skin in systemic lupus erythematosus. Lupus. 2011;20(9):904-11.
146. Sun C, Zhu M, Yang Z, Pan X, Zhang Y, Wang Q, et al. LL-37 secreted by epithelium promotes fibroblast collagen production: a potential mechanism of small airway remodeling in chronic obstructive pulmonary disease. Lab Invest. 2014;94(9):991-1002.
147. Wright TK, Gibson PG, Simpson JL, McDonald VM, Wood LG, Baines KJ. Neutrophil extracellular traps are associated with inflammation in chronic airway disease. Respirology (Carlton, Vic). 2016;21(3):467-75.
148. Yang YM, Guo YF, Zhang HS, Sun TY. Antimicrobial peptide LL-37 circulating levels in chronic obstructive pulmonary disease patients with high risk of frequent exacerbations. Journal of thoracic disease. 2015;7(4):740-5.
149. Kahlenberg JM, Kaplan MJ. Little peptide, big effects: the role of LL-37 in inflammation and autoimmune disease. Journal of immunology (Baltimore, Md : 1950). 2013;191(10):4895-901.
150. Krishnamoorthy N, Douda DN, Bruggemann TR, Ricklefs I, Duvall MG, Abdulnour RE, et al. Neutrophil cytoplasts induce TH17 differentiation and skew inflammation toward neutrophilia in severe asthma. Science immunology. 2018;3(26).
151. Li X, Bechara R, Zhao J, McGeachy MJ, Gaffen SL. IL-17 receptor-based signaling and implications for disease. Nature immunology. 2019;20(12):1594-602.
152. Rouvier E, Luciani MF, Mattéi MG, Denizot F, Golstein P. CTLA-8, cloned from an activated T cell, bearing AU-rich messenger RNA instability sequences, and homologous to a herpesvirus saimiri gene. Journal of immunology (Baltimore, Md : 1950). 1993;150(12):5445-56.
153. Monin L, Gaffen SL. Interleukin 17 Family Cytokines: Signaling Mechanisms, Biological Activities, and Therapeutic Implications. Cold Spring Harb Perspect Biol. 2018;10(4).

154. Harrington LE, Hatton RD, Mangan PR, Turner H, Murphy TL, Murphy KM, et al. Interleukin 17-producing CD4+ effector T cells develop via a lineage distinct from the T helper type 1 and 2 lineages. Nature immunology. 2005;6(11):1123-32.
155. Park H, Li Z, Yang XO, Chang SH, Nurieva R, Wang YH, et al. A distinct lineage of CD4 T cells regulates tissue inflammation by producing interleukin 17. Nature immunology. 2005;6(11):1133-41.
156. Morris SM, Jr., Kepka-Lenhart D, McGill RL, Curthoys NP, Adler S. Specific disruption of renal function and gene transcription by cyclosporin A. The Journal of biological chemistry. 1992;267(19):13768-71.
157. Veldhoen M, Hocking RJ, Atkins CJ, Locksley RM, Stockinger B. TGFbeta in the context of an inflammatory cytokine milieu supports de novo differentiation of IL-17-producing T cells. Immunity. 2006;24(2):179-89.
158. McGeachy MJ, Cua DJ, Gaffen SL. The IL-17 Family of Cytokines in Health and Disease. Immunity. 2019;50(4):892-906.
159. Wright JF, Guo Y, Quazi A, Luxenberg DP, Bennett F, Ross JF, et al. Identification of an interleukin 17F/17A heterodimer in activated human CD4+ T cells. The Journal of biological chemistry. 2007;282(18):13447-55.
160. Wright JF, Bennett F, Li B, Brooks J, Luxenberg DP, Whitters MJ, et al. The human IL-17F/IL-17A heterodimeric cytokine signals through the IL-17RA/IL-17RC receptor complex. Journal of immunology (Baltimore, Md : 1950). 2008;181(4):2799-805.
161. Hynes GM, Hinks TSC. The role of interleukin-17 in asthma: a protective response? ERJ Open Res. 2020;6(2).
162. Johnston A, Fritz Y, Dawes SM, Diaconu D, Al-Attar PM, Guzman AM, et al. Keratinocyte overexpression of IL-17C promotes psoriasiform skin inflammation. Journal of immunology (Baltimore, Md : 1950). 2013;190(5):2252-62.
163. Ramirez-Carrozzi V, Sambandam A, Luis E, Lin Z, Jeet S, Lesch J, et al. IL-17C regulates the innate immune function of epithelial cells in an autocrine manner. Nature immunology. 2011;12(12):1159-66.
164. Kleinschek MA, Owyang AM, Joyce-Shaikh B, Langrish CL, Chen Y, Gorman DM, et al. IL-25 regulates Th17 function in autoimmune inflammation. The Journal of experimental medicine. 2007;204(1):161-70.
165. Godfrey DI, Uldrich AP, McCluskey J, Rossjohn J, Moody DB. The burgeoning family of unconventional T cells. Nature immunology. 2015;16(11):1114-23.
166. Murdoch JR, Lloyd CM. Resolution of allergic airway inflammation and airway hyperreactivity is mediated by IL-17-producing {gamma}{delta}T cells. American journal of respiratory and critical care medicine. 2010;182(4):464-76.
167. Pichavant M, Goya S, Meyer EH, Johnston RA, Kim HY, Matangkasombut P, et al. Ozone exposure in a mouse model induces airway hyperreactivity that requires the presence of natural killer T cells and IL-17. The Journal of experimental medicine. 2008;205(2):385-93.
168. Hinks TS. Mucosal-associated invariant T cells in autoimmunity, immune-mediated diseases and airways disease. Immunology. 2016;148(1):1-12.
169. Cosgrove C, Ussher JE, Rauch A, Gärtner K, Kurioka A, Hühn MH, et al. Early and nonreversible decrease of CD161++ /MAIT cells in HIV infection. Blood. 2013;121(6):951-61.
170. Kim HY, Lee HJ, Chang YJ, Pichavant M, Shore SA, Fitzgerald KA, et al. Interleukin-17-producing innate lymphoid cells and the NLRP3 inflammasome facilitate obesity-associated airway hyperreactivity. Nature medicine. 2014;20(1):54-61.
171. Iwakura Y, Ishigame H, Saijo S, Nakae S. Functional specialization of interleukin-17 family members. Immunity. 2011;34(2):149-62.
172. Goepfert A, Lehmann S, Wirth E, Rondeau JM. The human IL-17A/F heterodimer: a two-faced cytokine with unique receptor recognition properties. Scientific reports. 2017;7(1):8906.
173. Vazquez-Tello A, Halwani R, Li R, Nadigel J, Bar-Or A, Mazer BD, et al. IL-17A and IL-17F expression in B lymphocytes. Int Arch Allergy Immunol. 2012;157(4):406-16.
174. Taylor PR, Roy S, Leal SM, Jr., Sun Y, Howell SJ, Cobb BA, et al. Activation of neutrophils by autocrine IL-17A-IL-17RC interactions during fungal infection is regulated by IL-6, IL-23, RORγt and dectin-2. Nature immunology. 2014;15(2):143-51.

175. Hymowitz SG, Filvaroff EH, Yin JP, Lee J, Cai L, Risser P, et al. IL-17s adopt a cystine knot fold: structure and activity of a novel cytokine, IL-17F, and implications for receptor binding. The EMBO journal. 2001;20(19):5332-41.
176. Amatya N, Garg AV, Gaffen SL. IL-17 Signaling: The Yin and the Yang. Trends in immunology. 2017;38(5):310-22.
177. Gaffen SL, Jain R, Garg AV, Cua DJ. The IL-23-IL-17 immune axis: from mechanisms to therapeutic testing. Nature reviews Immunology. 2014;14(9):585-600.
178. Su Y, Huang J, Zhao X, Lu H, Wang W, Yang XO, et al. Interleukin-17 receptor D constitutes an alternative receptor for interleukin-17A important in psoriasis-like skin inflammation. Science immunology. 2019;4(36).
179. Mellett M, Atzei P, Bergin R, Horgan A, Floss T, Wurst W, et al. Orphan receptor IL-17RD regulates Toll-like receptor signalling via SEFIR/TIR interactions. Nat Commun. 2015;6:6669.
180. Gaffen SL. Structure and signalling in the IL-17 receptor family. Nature reviews Immunology. 2009;9(8):556-67.
181. Brembilla NC, Senra L, Boehncke WH. The IL-17 Family of Cytokines in Psoriasis: IL-17A and Beyond. Frontiers in immunology. 2018;9:1682.
182. Novatchkova M, Leibbrandt A, Werzowa J, Neubüser A, Eisenhaber F. The STIR-domain superfamily in signal transduction, development and immunity. Trends in biochemical sciences. 2003;28(5):226-9.
183. Qian Y, Liu C, Hartupee J, Altuntas CZ, Gulen MF, Jane-Wit D, et al. The adaptor Act1 is required for interleukin 17-dependent signaling associated with autoimmune and inflammatory disease. Nature immunology. 2007;8(3):247-56.
184. Chang SH, Park H, Dong C. Act1 adaptor protein is an immediate and essential signaling component of interleukin-17 receptor. The Journal of biological chemistry. 2006;281(47):35603-7.
185. Sønder SU, Saret S, Tang W, Sturdevant DE, Porcella SF, Siebenlist U. IL-17-induced NF-kappaB activation via CIKS/Act1: physiologic significance and signaling mechanisms. The Journal of biological chemistry. 2011;286(15):12881-90.
186. Liu C, Swaidani S, Qian W, Kang Z, Sun P, Han Y, et al. A CC' loop decoy peptide blocks the interaction between Act1 and IL-17RA to attenuate IL-17- and IL-25-induced inflammation. Science signaling. 2011;4(197):ra72.
187. Swaidani S, Liu C, Zhao J, Bulek K, Li X. TRAF Regulation of IL-17 Cytokine Signaling. Frontiers in immunology. 2019;10:1293.
188. Shen F, Hu Z, Goswami J, Gaffen SL. Identification of common transcriptional regulatory elements in interleukin-17 target genes. The Journal of biological chemistry. 2006;281(34):24138-48.
189. Patel DN, King CA, Bailey SR, Holt JW, Venkatachalam K, Agrawal A, et al. Interleukin-17 stimulates C-reactive protein expression in hepatocytes and smooth muscle cells via p38 MAPK and ERK1/2-dependent NF-kappaB and C/EBPbeta activation. The Journal of biological chemistry. 2007;282(37):27229-38.
190. Maitra A, Shen F, Hanel W, Mossman K, Tocker J, Swart D, et al. Distinct functional motifs within the IL-17 receptor regulate signal transduction and target gene expression. Proceedings of the National Academy of Sciences of the United States of America. 2007;104(18):7506-11.
191. Shen F, Li N, Gade P, Kalvakolanu DV, Weibley T, Doble B, et al. IL-17 receptor signaling inhibits C/EBPbeta by sequential phosphorylation of the regulatory 2 domain. Science signaling. 2009;2(59):ra8.
192. Kafasla P, Skliris A, Kontoyiannis DL. Post-transcriptional coordination of immunological responses by RNA-binding proteins. Nature immunology. 2014;15(6):492-502.
193. Anderson P. Post-transcriptional regulons coordinate the initiation and resolution of inflammation. Nature reviews Immunology. 2010;10(1):24-35.
194. Fan J, Heller NM, Gorospe M, Atasoy U, Stellato C. The role of post-transcriptional regulation in chemokine gene expression in inflammation and allergy. The European respiratory journal. 2005;26(5):933-47.
195. Bulek K, Liu C, Swaidani S, Wang L, Page RC, Gulen MF, et al. The inducible kinase IKKi is required for IL-17-dependent signaling associated with neutrophilia and pulmonary inflammation. Nature immunology. 2011;12(9):844-52.

196. Herjan T, Hong L, Bubenik J, Bulek K, Qian W, Liu C, et al. IL-17-receptor-associated adaptor Act1 directly stabilizes mRNAs to mediate IL-17 inflammatory signaling. Nature immunology. 2018;19(4):354-65.
197. Amatya N, Childs EE, Cruz JA, Aggor FEY, Garg AV, Berman AJ, et al. IL-17 integrates multiple self-reinforcing, feed-forward mechanisms through the RNA binding protein Arid5a. Science signaling. 2018;11(551).
198. Sun D, Novotny M, Bulek K, Liu C, Li X, Hamilton T. Treatment with IL-17 prolongs the half-life of chemokine CXCL1 mRNA via the adaptor TRAF5 and the splicing-regulatory factor SF2 (ASF). Nature immunology. 2011;12(9):853-60.
199. Michlewski G, Sanford JR, Caceres JF. The splicing factor SF2/ASF regulates translation initiation by enhancing phosphorylation of 4E-BP1. Molecular cell. 2008;30(2):179-89.
200. Garg AV, Amatya N, Chen K, Cruz JA, Grover P, Whibley N, et al. MCPIP1 Endoribonuclease Activity Negatively Regulates Interleukin-17-Mediated Signaling and Inflammation. Immunity. 2015;43(3):475-87.
201. Tanaka H, Arima Y, Kamimura D, Tanaka Y, Takahashi N, Uehata T, et al. Phosphorylation-dependent Regnase-1 release from endoplasmic reticulum is critical in IL-17 response. The Journal of experimental medicine. 2019;216(6):1431-49.
202. Karlsen JR, Borregaard N, Cowland JB. Induction of neutrophil gelatinase-associated lipocalin expression by co-stimulation with interleukin-17 and tumor necrosis factor-alpha is controlled by IkappaB-zeta but neither by C/EBP-beta nor C/EBP-delta. The Journal of biological chemistry. 2010;285(19):14088-100.
203. Somma D, Mastrovito P, Grieco M, Lavorgna A, Pignalosa A, Formisano L, et al. CIKS/DDX3X interaction controls the stability of the Zc3h12a mRNA induced by IL-17. Journal of immunology (Baltimore, Md : 1950). 2015;194(7):3286-94.
204. Beringer A, Thiam N, Molle J, Bartosch B, Miossec P. Synergistic effect of interleukin-17 and tumour necrosis factor-α on inflammatory response in hepatocytes through interleukin-6-dependent and independent pathways. Clinical and experimental immunology. 2018;193(2):221-33.
205. Honda K, Wada H, Nakamura M, Nakamoto K, Inui T, Sada M, et al. IL-17A synergistically stimulates TNF-α-induced IL-8 production in human airway epithelial cells: A potential role in amplifying airway inflammation. Exp Lung Res. 2016;42(4):205-16.
206. Hot A, Lenief V, Miossec P. Combination of IL-17 and TNFα induces a pro-inflammatory, pro-coagulant and pro-thrombotic phenotype in human endothelial cells. Ann Rheum Dis. 2012;71(5):768-76.
207. Ruddy MJ, Wong GC, Liu XK, Yamamoto H, Kasayama S, Kirkwood KL, et al. Functional cooperation between interleukin-17 and tumor necrosis factor-alpha is mediated by CCAAT/enhancer-binding protein family members. The Journal of biological chemistry. 2004;279(4):2559-67.
208. Woltman AM, de Haij S, Boonstra JG, Gobin SJ, Daha MR, van Kooten C. Interleukin-17 and CD40-ligand synergistically enhance cytokine and chemokine production by renal epithelial cells. Journal of the American Society of Nephrology : JASN. 2000;11(11):2044-55.
209. Datta S, Novotny M, Pavicic PG, Jr., Zhao C, Herjan T, Hartupee J, et al. IL-17 regulates CXCL1 mRNA stability via an AUUUA/tristetraprolin-independent sequence. Journal of immunology (Baltimore, Md : 1950). 2010;184(3):1484-91.
210. Garg AV, Ahmed M, Vallejo AN, Ma A, Gaffen SL. The deubiquitinase A20 mediates feedback inhibition of interleukin-17 receptor signaling. Science signaling. 2013;6(278):ra44.
211. Sonder SU, Saret S, Tang W, Sturdevant DE, Porcella SF, Siebenlist U. IL-17-induced NF-kappaB activation via CIKS/Act1: physiologic significance and signaling mechanisms. The Journal of biological chemistry. 2011;286(15):12881-90.
212. Henness S, Johnson CK, Ge Q, Armour CL, Hughes JM, Ammit AJ. IL-17A augments TNF-alpha-induced IL-6 expression in airway smooth muscle by enhancing mRNA stability. The Journal of allergy and clinical immunology. 2004;114(4):958-64.
213. Henness S, van Thoor E, Ge Q, Armour CL, Hughes JM, Ammit AJ. IL-17A acts via p38 MAPK to increase stability of TNF-alpha-induced IL-8 mRNA in human ASM. American journal of physiology Lung cellular and molecular physiology. 2006;290(6):L1283-90.

214. Ivanov, II, Atarashi K, Manel N, Brodie EL, Shima T, Karaoz U, et al. Induction of intestinal Th17 cells by segmented filamentous bacteria. Cell. 2009;139(3):485-98.
215. Chan YR, Liu JS, Pociask DA, Zheng M, Mietzner TA, Berger T, et al. Lipocalin 2 is required for pulmonary host defense against Klebsiella infection. Journal of immunology (Baltimore, Md : 1950). 2009;182(8):4947-56.
216. Chen K, Eddens T, Trevejo-Nunez G, Way EE, Elsegeiny W, Ricks DM, et al. IL-17 Receptor Signaling in the Lung Epithelium Is Required for Mucosal Chemokine Gradients and Pulmonary Host Defense against K. pneumoniae. Cell Host Microbe. 2016;20(5):596-605.
217. Wu L, Chen X, Zhao J, Martin B, Zepp JA, Ko JS, et al. A novel IL-17 signaling pathway controlling keratinocyte proliferation and tumorigenesis via the TRAF4-ERK5 axis. The Journal of experimental medicine. 2015;212(10):1571-87.
218. Ha HL, Wang H, Pisitkun P, Kim JC, Tassi I, Tang W, et al. IL-17 drives psoriatic inflammation via distinct, target cell-specific mechanisms. Proceedings of the National Academy of Sciences of the United States of America. 2014;111(33):E3422-31.
219. Zihni C, Mills C, Matter K, Balda MS. Tight junctions: from simple barriers to multifunctional molecular gates. Nature reviews Molecular cell biology. 2016;17(9):564-80.
220. Lee JS, Tato CM, Joyce-Shaikh B, Gulen MF, Cayatte C, Chen Y, et al. Interleukin-23-Independent IL-17 Production Regulates Intestinal Epithelial Permeability. Immunity. 2015;43(4):727-38.
221. Contreras-Ruiz L, Schulze U, García-Posadas L, Arranz-Valsero I, López-García A, Paulsen F, et al. Structural and functional alteration of corneal epithelial barrier under inflammatory conditions. Curr Eye Res. 2012;37(11):971-81.
222. Wu H, Santoni-Rugiu E, Ralfkiaer E, Porse BT, Moser C, Høiby N, et al. Lipocalin 2 is protective against E. coli pneumonia. Respiratory research. 2010;11(1):96.
223. Archer NK, Adappa ND, Palmer JN, Cohen NA, Harro JM, Lee SK, et al. Interleukin-17A (IL-17A) and IL-17F Are Critical for Antimicrobial Peptide Production and Clearance of Staphylococcus aureus Nasal Colonization. Infection and immunity. 2016;84(12):3575-83.
224. Shao S, Cao T, Jin L, Li B, Fang H, Zhang J, et al. Increased Lipocalin-2 Contributes to the Pathogenesis of Psoriasis by Modulating Neutrophil Chemotaxis and Cytokine Secretion. The Journal of investigative dermatology. 2016;136(7):1418-28.
225. Chen K, Pociask DA, McAleer JP, Chan YR, Alcorn JF, Kreindler JL, et al. IL-17RA is required for CCL2 expression, macrophage recruitment, and emphysema in response to cigarette smoke. PloS one. 2011;6(5):e20333.
226. Luo J, An X, Yao Y, Erb C, Ferguson A, Kolls JK, et al. Epigenetic Regulation of IL-17-Induced Chemokines in Lung Epithelial Cells. Mediators of inflammation. 2019;2019:9050965.
227. You Z, Ge D, Liu S, Zhang Q, Borowsky AD, Melamed J. Interleukin-17 Induces Expression of Chemokines and Cytokines in Prostatic Epithelial Cells but Does Not Stimulate Cell Growth In Vitro. Int J Med Biol Front. 2012;18(8):629-44.
228. Brown RL, Sequeira RP, Clarke TB. The microbiota protects against respiratory infection via GM-CSF signaling. Nat Commun. 2017;8(1):1512.
229. Hirota K, Yoshitomi H, Hashimoto M, Maeda S, Teradaira S, Sugimoto N, et al. Preferential recruitment of CCR6-expressing Th17 cells to inflamed joints via CCL20 in rheumatoid arthritis and its animal model. The Journal of experimental medicine. 2007;204(12):2803-12.
230. Griffiths CEM, Armstrong AW, Gudjonsson JE, Barker J. Psoriasis. Lancet (London, England). 2021;397(10281):1301-15.
231. Nakajima K, Kanda T, Takaishi M, Shiga T, Miyoshi K, Nakajima H, et al. Distinct roles of IL-23 and IL-17 in the development of psoriasis-like lesions in a mouse model. Journal of immunology (Baltimore, Md : 1950). 2011;186(7):4481-9.
232. van der Fits L, Mourits S, Voerman JS, Kant M, Boon L, Laman JD, et al. Imiquimod-induced psoriasis-like skin inflammation in mice is mediated via the IL-23/IL-17 axis. Journal of immunology (Baltimore, Md : 1950). 2009;182(9):5836-45.
233. Ray-Jones H, Eyre S, Barton A, Warren RB. One SNP at a Time: Moving beyond GWAS in Psoriasis. The Journal of investigative dermatology. 2016;136(3):567-73.

234. Fitz L, Zhang W, Soderstrom C, Fraser S, Lee J, Quazi A, et al. Association between serum interleukin-17A and clinical response to tofacitinib and etanercept in moderate to severe psoriasis. Clin Exp Dermatol. 2018;43(7):790-7.
235. von Csiky-Sessoms S, Lebwohl M. What's New in Psoriasis. Dermatol Clin. 2019;37(2):129-36.
236. Krueger JG, Fretzin S, Suárez-Fariñas M, Haslett PA, Phipps KM, Cameron GS, et al. IL-17A is essential for cell activation and inflammatory gene circuits in subjects with psoriasis. The Journal of allergy and clinical immunology. 2012;130(1):145-54.e9.
237. Milovanovic J, Arsenijevic A, Stojanovic B, Kanjevac T, Arsenijevic D, Radosavljevic G, et al. Interleukin-17 in Chronic Inflammatory Neurological Diseases. Frontiers in immunology. 2020;11:947.
238. Weinshenker BG. Epidemiology of multiple sclerosis. Neurol Clin. 1996;14(2):291-308.
239. Kuchroo VK, Anderson AC, Waldner H, Munder M, Bettelli E, Nicholson LB. T cell response in experimental autoimmune encephalomyelitis (EAE): role of self and cross-reactive antigens in shaping, tuning, and regulating the autopathogenic T cell repertoire. Annual review of immunology. 2002;20:101-23.
240. Furlan R, Cuomo C, Martino G. Animal models of multiple sclerosis. Methods in molecular biology (Clifton, NJ). 2009;549:157-73.
241. McGinley AM, Edwards SC, Raverdeau M, Mills KHG. Th17 cells, γδ T cells and their interplay in EAE and multiple sclerosis. J Autoimmun. 2018.
242. Mills KH. TLR-dependent T cell activation in autoimmunity. Nature reviews Immunology. 2011;11(12):807-22.
243. Lock C, Hermans G, Pedotti R, Brendolan A, Schadt E, Garren H, et al. Gene-microarray analysis of multiple sclerosis lesions yields new targets validated in autoimmune encephalomyelitis. Nature medicine. 2002;8(5):500-8.
244. Schofield C, Fischer SK, Townsend MJ, Mosesova S, Peng K, Setiadi AF, et al. Characterization of IL-17AA and IL-17FF in rheumatoid arthritis and multiple sclerosis. Bioanalysis. 2016;8(22):2317-27.
245. Brucklacher-Waldert V, Stuerner K, Kolster M, Wolthausen J, Tolosa E. Phenotypical and functional characterization of T helper 17 cells in multiple sclerosis. Brain. 2009;132(Pt 12):3329-41.
246. Durelli L, Conti L, Clerico M, Boselli D, Contessa G, Ripellino P, et al. T-helper 17 cells expand in multiple sclerosis and are inhibited by interferon-beta. Ann Neurol. 2009;65(5):499-509.
247. Havrdová E, Belova A, Goloborodko A, Tisserant A, Wright A, Wallstroem E, et al. Activity of secukinumab, an anti-IL-17A antibody, on brain lesions in RRMS: results from a randomized, proof-of-concept study. J Neurol. 2016;263(7):1287-95.
248. Chesné J, Braza F, Chadeuf G, Mahay G, Cheminant MA, Loy J, et al. Prime role of IL-17A in neutrophilia and airway smooth muscle contraction in a house dust mite-induced allergic asthma model. The Journal of allergy and clinical immunology. 2015;135(6):1643-.e3.
249. Wilson RH, Whitehead GS, Nakano H, Free ME, Kolls JK, Cook DN. Allergic sensitization through the airway primes Th17-dependent neutrophilia and airway hyperresponsiveness. American journal of respiratory and critical care medicine. 2009;180(8):720-30.
250. He R, Oyoshi MK, Jin H, Geha RS. Epicutaneous antigen exposure induces a Th17 response that drives airway inflammation after inhalation challenge. Proceedings of the National Academy of Sciences of the United States of America. 2007;104(40):15817-22.
251. Simpson JL, Scott R, Boyle MJ, Gibson PG. Inflammatory subtypes in asthma: assessment and identification using induced sputum. Respirology (Carlton, Vic). 2006;11(1):54-61.
252. Wenzel SE, Schwartz LB, Langmack EL, Halliday JL, Trudeau JB, Gibbs RL, et al. Evidence that severe asthma can be divided pathologically into two inflammatory subtypes with distinct physiologic and clinical characteristics. American journal of respiratory and critical care medicine. 1999;160(3):1001-8.
253. Laan M, Cui ZH, Hoshino H, Lötvall J, Sjöstrand M, Gruenert DC, et al. Neutrophil recruitment by human IL-17 via C-X-C chemokine release in the airways. Journal of immunology (Baltimore, Md : 1950). 1999;162(4):2347-52.
254. Fujisawa T, Chang MM, Velichko S, Thai P, Hung LY, Huang F, et al. NF-κB mediates IL-1β- and IL-17A-induced MUC5B expression in airway epithelial cells. American journal of respiratory cell and molecular biology. 2011;45(2):246-52.

255. Du J, Han JC, Zhang YJ, Qi GB, Li HB, Zhang YJ, et al. Single-Nucleotide Polymorphisms of IL-17 Gene Are Associated with Asthma Susceptibility in an Asian Population. Med Sci Monit. 2016;22:780-7.
256. Silva MJ, de Santana MBR, Tosta BR, Espinheira RP, Alcantara-Neves NM, Barreto ML, et al. Variants in the IL17 pathway genes are associated with atopic asthma and atopy makers in a South American population. Allergy Asthma Clin Immunol. 2019;15:28.
257. Kawaguchi M, Takahashi D, Hizawa N, Suzuki S, Matsukura S, Kokubu F, et al. IL-17F sequence variant (His161Arg) is associated with protection against asthma and antagonizes wild-type IL-17F activity. The Journal of allergy and clinical immunology. 2006;117(4):795-801.
258. Molet S, Hamid Q, Davoine F, Nutku E, Taha R, Pagé N, et al. IL-17 is increased in asthmatic airways and induces human bronchial fibroblasts to produce cytokines. The Journal of allergy and clinical immunology. 2001;108(3):430-8.
259. Barczyk A, Pierzchala W, Sozañska E. Interleukin-17 in sputum correlates with airway hyperresponsiveness to methacholine. Respiratory medicine. 2003;97(6):726-33.
260. Sun YC, Zhou QT, Yao WZ. Sputum interleukin-17 is increased and associated with airway neutrophilia in patients with severe asthma. Chin Med J (Engl). 2005;118(11):953-6.
261. Bullens DM, Truyen E, Coteur L, Dilissen E, Hellings PW, Dupont LJ, et al. IL-17 mRNA in sputum of asthmatic patients: linking T cell driven inflammation and granulocytic influx? Respiratory research. 2006;7(1):135.
262. Cosmi L, Maggi L, Santarlasci V, Capone M, Cardilicchia E, Frosali F, et al. Identification of a novel subset of human circulating memory CD4(+) T cells that produce both IL-17A and IL-4. The Journal of allergy and clinical immunology. 2010;125(1):222-30.e1-4.
263. Irvin C, Zafar I, Good J, Rollins D, Christianson C, Gorska MM, et al. Increased frequency of dual-positive TH2/TH17 cells in bronchoalveolar lavage fluid characterizes a population of patients with severe asthma. The Journal of allergy and clinical immunology. 2014;134(5):1175-86.e7.
264. Kudo M, Melton AC, Chen C, Engler MB, Huang KE, Ren X, et al. IL-17A produced by αβ T cells drives airway hyper-responsiveness in mice and enhances mouse and human airway smooth muscle contraction. Nature medicine. 2012;18(4):547-54.
265. Scanlon KM, Hawksworth RJ, Lane SJ, Mahon BP. IL-17A induces CCL28, supporting the chemotaxis of IgE-secreting B cells. Int Arch Allergy Immunol. 2011;156(1):51-61.
266. Christenson SA, van den Berge M, Faiz A, Inkamp K, Bhakta N, Bonser LR, et al. An airway epithelial IL-17A response signature identifies a steroid-unresponsive COPD patient subgroup. The Journal of clinical investigation. 2019;129(1):169-81.
267. Vazquez-Tello A, Semlali A, Chakir J, Martin JG, Leung DY, Eidelman DH, et al. Induction of glucocorticoid receptor-beta expression in epithelial cells of asthmatic airways by T-helper type 17 cytokines. Clinical and experimental allergy : journal of the British Society for Allergy and Clinical Immunology. 2010;40(9):1312-22.
268. Al-Ramli W, Préfontaine D, Chouiali F, Martin JG, Olivenstein R, Lemière C, et al. T(H)17-associated cytokines (IL-17A and IL-17F) in severe asthma. The Journal of allergy and clinical immunology. 2009;123(5):1185-7.
269. Laan M, Lotvall J, Chung KF, Linden A. IL-17-induced cytokine release in human bronchial epithelial cells in vitro: role of mitogen-activated protein (MAP) kinases. British journal of pharmacology. 2001;133(1):200-6.
270. Doe C, Bafadhel M, Siddiqui S, Desai D, Mistry V, Rugman P, et al. Expression of the T helper 17-associated cytokines IL-17A and IL-17F in asthma and COPD. Chest. 2010;138(5):1140-7.
271. Vazquez-Tello A, Halwani R, Hamid Q, Al-Muhsen S. Glucocorticoid receptor-beta up-regulation and steroid resistance induction by IL-17 and IL-23 cytokine stimulation in peripheral mononuclear cells. J Clin Immunol. 2013;33(2):466-78.
272. Hizawa N, Kawaguchi M, Huang SK, Nishimura M. Role of interleukin-17F in chronic inflammatory and allergic lung disease. Clinical and experimental allergy : journal of the British Society for Allergy and Clinical Immunology. 2006;36(9):1109-14.
273. Andersson CK, Adams A, Nagakumar P, Bossley C, Gupta A, De Vries D, et al. Intraepithelial neutrophils in pediatric severe asthma are associated with better lung function. The Journal of allergy and clinical immunology. 2017;139(6):1819-29.e11.

274. Fujie H, Niu K, Ohba M, Tomioka Y, Kitazawa H, Nagashima K, et al. A distinct regulatory role of Th17 cytokines IL-17A and IL-17F in chemokine secretion from lung microvascular endothelial cells. Inflammation. 2012;35(3):1119-31.
275. Cheung PF, Wong CK, Lam CW. Molecular mechanisms of cytokine and chemokine release from eosinophils activated by IL-17A, IL-17F, and IL-23: implication for Th17 lymphocytes-mediated allergic inflammation. Journal of immunology (Baltimore, Md : 1950). 2008;180(8):5625-35.
276. Anderson GP. Endotyping asthma: new insights into key pathogenic mechanisms in a complex, heterogeneous disease. Lancet (London, England). 2008;372(9643):1107-19.
277. Johnston SL, Pattemore PK, Sanderson G, Smith S, Lampe F, Josephs L, et al. Community study of role of viral infections in exacerbations of asthma in 9-11 year old children. BMJ (Clinical research ed). 1995;310(6989):1225-9.
278. Wimalasundera SS, Katz DR, Chain BM. Characterization of the T cell response to human rhinovirus in children: implications for understanding the immunopathology of the common cold. J Infect Dis. 1997;176(3):755-9.
279. Brandt EB, Kovacic MB, Lee GB, Gibson AM, Acciani TH, Le Cras TD, et al. Diesel exhaust particle induction of IL-17A contributes to severe asthma. The Journal of allergy and clinical immunology. 2013;132(5):1194-204.e2.
280. Siew LQC, Wu SY, Ying S, Corrigan CJ. Cigarette smoking increases bronchial mucosal IL-17A expression in asthmatics, which acts in concert with environmental aeroallergens to engender neutrophilic inflammation. Clinical and experimental allergy : journal of the British Society for Allergy and Clinical Immunology. 2017;47(6):740-50.
281. Lezmi G, Abou Taam R, Dietrich C, Chatenoud L, de Blic J, Leite-de-Moraes M. Circulating IL-17-producing mucosal-associated invariant T cells (MAIT) are associated with symptoms in children with asthma. Clin Immunol. 2018;188:7-11.
282. Nanzer AM, Chambers ES, Ryanna K, Richards DF, Black C, Timms PM, et al. Enhanced production of IL-17A in patients with severe asthma is inhibited by 1α,25-dihydroxyvitamin D3 in a glucocorticoid-independent fashion. The Journal of allergy and clinical immunology. 2013;132(2):297-304.e3.
283. Pavord ID, Brightling CE, Woltmann G, Wardlaw AJ. Non-eosinophilic corticosteroid unresponsive asthma. Lancet (London, England). 1999;353(9171):2213-4.
284. Cowan DC, Cowan JO, Palmay R, Williamson A, Taylor DR. Effects of steroid therapy on inflammatory cell subtypes in asthma. Thorax. 2010;65(5):384-90.
285. McKinley L, Alcorn JF, Peterson A, Dupont RB, Kapadia S, Logar A, et al. TH17 cells mediate steroid-resistant airway inflammation and airway hyperresponsiveness in mice. Journal of immunology (Baltimore, Md : 1950). 2008;181(6):4089-97.
286. Zhao J, Lloyd CM, Noble A. Th17 responses in chronic allergic airway inflammation abrogate regulatory T-cell-mediated tolerance and contribute to airway remodeling. Mucosal immunology. 2013;6(2):335-46.
287. Zijlstra GJ, Ten Hacken NH, Hoffmann RF, van Oosterhout AJ, Heijink IH. Interleukin-17A induces glucocorticoid insensitivity in human bronchial epithelial cells. The European respiratory journal. 2012;39(2):439-45.
288. Chang Y, Al-Alwan L, Alshakfa S, Audusseau S, Mogas AK, Chouiali F, et al. Upregulation of IL-17A/F from human lung tissue explants with cigarette smoke exposure: implications for COPD. Respiratory research. 2014;15(1):145.
289. Rich HE, Alcorn JF. IL-17 Strikes a Chord in Chronic Obstructive Pulmonary Disease Exacerbation. American journal of respiratory cell and molecular biology. 2018;58(6):669-70.
290. Östling J, van Geest M, Schofield JPR, Jevnikar Z, Wilson S, Ward J, et al. IL-17-high asthma with features of a psoriasis immunophenotype. The Journal of allergy and clinical immunology. 2019;144(5):1198-213.
291. Roos AB, Mori M, Gura HK, Lorentz A, Bjermer L, Hoffmann HJ, et al. Increased IL-17RA and IL-17RC in End-Stage COPD and the Contribution to Mast Cell Secretion of FGF-2 and VEGF. Respiratory research. 2017;18(1):48.
292. Asthma, by sex, provinces and territories (Diseases and Health Conditions) [Internet]. Government of Canada. 2015.

293. Zarcone MC, Duistermaat E, van Schadewijk A, Jedynska A, Hiemstra PS, Kooter IM. Cellular response of mucociliary differentiated primary bronchial epithelial cells to diesel exhaust. American journal of physiology Lung cellular and molecular physiology. 2016;311(1):L111-23.
294. Piyadasa H, Altieri A, Basu S, Schwartz J, Halayko AJ, Mookherjee N. Biosignature for airway inflammation in a house dust mite-challenged murine model of allergic asthma. Biology open. 2016;5(2):112-21.
295. Piyadasa H, Hemshekhar M, Osawa N, Lloyd D, Altieri A, Basu S, et al. Disrupting Tryptophan in the Central Hydrophobic Region Selectively Mitigates Immunomodulatory Activities of the Innate Defence Regulator Peptide IDR-1002. J Med Chem. 2021;64(10):6696-705.
296. Kilkenny C, Browne W, Cuthill IC, Emerson M, Altman DG. Animal research: reporting in vivo experiments: the ARRIVE guidelines. British journal of pharmacology. 2010;160(7):1577-9.
297. Altieri A, Piyadasa H, Recksiedler B, Spicer V, Mookherjee N. Cytokines IL-17, TNF and IFN-γ Alter the Expression of Antimicrobial Peptides and Proteins Disparately: A Targeted Proteomics Analysis using SOMAscan Technology. Vaccines. 2018;6(3).
298. Coombs KM, Simon PF, McLeish NJ, Zahedi-Amiri A, Kobasa D. Aptamer Profiling of A549 Cells Infected with Low-Pathogenicity and High-Pathogenicity Influenza Viruses. Viruses. 2019;11(11).
299. Glover KKM, Gao A, Zahedi-Amiri A, Coombs KM. Vero Cell Proteomic Changes Induced by Zika Virus Infection. Proteomics. 2019;19(4):e1800309.
300. Sher AA, Gao A, Coombs KM. Autophagy Modulators Profoundly Alter the Astrocyte Cellular Proteome. Cells. 2020;9(4).
301. Zahedi-Amiri A, Sequiera GL, Dhingra S, Coombs KM. Influenza a virus-triggered autophagy decreases the pluripotency of human-induced pluripotent stem cells. Cell Death Dis. 2019;10(5):337.
302. Schmittgen TD, Livak KJ. Analyzing real-time PCR data by the comparative C(T) method. Nature protocols. 2008;3(6):1101-8.
303. Battersby AJ, Khara J, Wright VJ, Levy O, Kampmann B. Antimicrobial Proteins and Peptides in Early Life: Ontogeny and Translational Opportunities. Frontiers in immunology. 2016;7:309.
304. Fjell CD, Hiss JA, Hancock RE, Schneider G. Designing antimicrobial peptides: form follows function. Nature reviews Drug discovery. 2011;11(1):37-51.
305. Levy O. Antimicrobial proteins and peptides: anti-infective molecules of mammalian leukocytes. Journal of leukocyte biology. 2004;76(5):909-25.
306. Huttner KM, Bevins CL. Antimicrobial peptides as mediators of epithelial host defense. Pediatr Res. 1999;45(6):785-94.
307. Schaller-Bals S, Schulze A, Bals R. Increased levels of antimicrobial peptides in tracheal aspirates of newborn infants during infection. American journal of respiratory and critical care medicine. 2002;165(7):992-5.
308. Rogan MP, Geraghty P, Greene CM, O'Neill SJ, Taggart CC, McElvaney NG. Antimicrobial proteins and polypeptides in pulmonary innate defence. Respiratory research. 2006;7(1):29.
309. Beisswenger C, Kandler K, Hess C, Garn H, Felgentreff K, Wegmann M, et al. Allergic airway inflammation inhibits pulmonary antibacterial host defense. Journal of immunology (Baltimore, Md : 1950). 2006;177(3):1833-7.
310. Andresen E, Gunther G, Bullwinkel J, Lange C, Heine H. Increased expression of beta-defensin 1 (DEFB1) in chronic obstructive pulmonary disease. PloS one. 2011;6(7):e21898.
311. Anderson RL, Hiemstra PS, Ward C, Forrest IA, Murphy D, Proud D, et al. Antimicrobial peptides in lung transplant recipients with bronchiolitis obliterans syndrome. The European respiratory journal. 2008;32(3):670-7.
312. Mookherjee N, Piyadasa H, Ryu MH, Rider CF, Ezzati P, Spicer V, et al. Inhaled diesel exhaust alters the allergen-induced bronchial secretome in humans. The European respiratory journal. 2018;51(1).
313. Piyadasa H, Hemshekhar M, Carlsten C, Mookherjee N. Inhaled Diesel Exhaust Decreases Antimicrobial Peptides Alpha-defensin and S100A7 in Human Bronchial Secretion. American journal of respiratory and critical care medicine. 2017.
314. Wu W, Jin Y, Carlsten C. Inflammatory health effects of indoor and outdoor particulate matter. The Journal of allergy and clinical immunology. 2018;141(3):833-44.

315. van Wetering S, van der Linden AC, van Sterkenburg MA, de Boer WI, Kuijpers AL, Schalkwijk J, et al. Regulation of SLPI and elafin release from bronchial epithelial cells by neutrophil defensins. American journal of physiology Lung cellular and molecular physiology. 2000;278(1):L51-8.
316. Chambers ES, Nanzer AM, Pfeffer PE, Richards DF, Timms PM, Martineau AR, et al. Distinct endotypes of steroid-resistant asthma characterized by IL-17A(high) and IFN-gamma(high) immunophenotypes: Potential benefits of calcitriol. The Journal of allergy and clinical immunology. 2015;136(3):628-37.e4.
317. Berry M, Brightling C, Pavord I, Wardlaw A. TNF-alpha in asthma. Current opinion in pharmacology. 2007;7(3):279-82.
318. Berry MA, Hargadon B, Shelley M, Parker D, Shaw DE, Green RH, et al. Evidence of a role of tumor necrosis factor alpha in refractory asthma. The New England journal of medicine. 2006;354(7):697-708.
319. Barnes PJ. Immunology of asthma and chronic obstructive pulmonary disease. Nature reviews Immunology. 2008;8(3):183-92.
320. Wenzel SE. Asthma phenotypes: the evolution from clinical to molecular approaches. Nature medicine. 2012;18(5):716-25.
321. Thomas PS, Yates DH, Barnes PJ. Tumor necrosis factor-alpha increases airway responsiveness and sputum neutrophilia in normal human subjects. American journal of respiratory and critical care medicine. 1995;152(1):76-80.
322. Borish L, Steinke JW. Interleukin-33 in asthma: how big of a role does it play? Current allergy and asthma reports. 2011;11(1):7-11.
323. McAllister F, Henry A, Kreindler JL, Dubin PJ, Ulrich L, Steele C, et al. Role of IL-17A, IL-17F, and the IL-17 receptor in regulating growth-related oncogene-alpha and granulocyte colony-stimulating factor in bronchial epithelium: implications for airway inflammation in cystic fibrosis. Journal of immunology (Baltimore, Md : 1950). 2005;175(1):404-12.
324. Agache I, Ciobanu C, Agache C, Anghel M. Increased serum IL-17 is an independent risk factor for severe asthma. Respiratory medicine. 2010;104(8):1131-7.
325. Molet S, Hamid Q, Davoine F, Nutku E, Taha R, Page N, et al. IL-17 is increased in asthmatic airways and induces human bronchial fibroblasts to produce cytokines. The Journal of allergy and clinical immunology. 2001;108(3):430-8.
326. Manni ML, Trudeau JB, Scheller EV, Mandalapu S, Elloso MM, Kolls JK, et al. The complex relationship between inflammation and lung function in severe asthma. Mucosal immunology. 2014;7(5):1186-98.
327. Fujimoto K, Imaizumi T, Yoshida H, Takanashi S, Okumura K, Satoh K. Interferon-gamma stimulates fractalkine expression in human bronchial epithelial cells and regulates mononuclear cell adherence. American journal of respiratory cell and molecular biology. 2001;25(2):233-8.
328. Shen F, Ruddy MJ, Plamondon P, Gaffen SL. Cytokines link osteoblasts and inflammation: microarray analysis of interleukin-17- and TNF-alpha-induced genes in bone cells. Journal of leukocyte biology. 2005;77(3):388-99.
329. Wu H, Zhang G, Minton JE, Ross CR, Blecha F. Regulation of cathelicidin gene expression: induction by lipopolysaccharide, interleukin-6, retinoic acid, and Salmonella enterica serovar typhimurium infection. Infection and immunity. 2000;68(10):5552-8.
330. Bando M, Zou X, Hiroshima Y, Kataoka M, Ross KF, Shinohara Y, et al. Mechanism of interleukin-1α transcriptional regulation of S100A9 in a human epidermal keratinocyte cell line. Biochimica et biophysica acta. 2013;1829(9):954-62.
331. Härkönen E, Virtanen I, Linnala A, Laitinen LL, Kinnula VL. Modulation of fibronectin and tenascin production in human bronchial epithelial cells by inflammatory cytokines in vitro. American journal of respiratory cell and molecular biology. 1995;13(1):109-15.
332. van der Velden JL, Ye Y, Nolin JD, Hoffman SM, Chapman DG, Lahue KG, et al. JNK inhibition reduces lung remodeling and pulmonary fibrotic systemic markers. Clin Transl Med. 2016;5(1):36.
333. Kato H, Endres J, Fox DA. The roles of IFN-γ versus IL-17 in pathogenic effects of human Th17 cells on synovial fibroblasts. Mod Rheumatol. 2013;23(6):1140-50.
334. Dittrich AM, Meyer HA, Hamelmann E. The role of lipocalins in airway disease. Clinical and experimental allergy : journal of the British Society for Allergy and Clinical Immunology. 2013;43(5):503-11.

335. Onishi RM, Gaffen SL. Interleukin-17 and its target genes: mechanisms of interleukin-17 function in disease. Immunology. 2010;129(3):311-21.
336. Scott A, Weldon S, Taggart CC. SLPI and elafin: multifunctional antiproteases of the WFDC family. Biochem Soc Trans. 2011;39(5):1437-40.
337. Tsai YS, Tseng YT, Chen PS, Lin MC, Wu CC, Huang MS, et al. Protective effects of elafin against adult asthma. Allergy and asthma proceedings. 2016;37(2):15-24.
338. Storm van's Gravesande K, Layne MD, Ye Q, Le L, Baron RM, Perrella MA, et al. IFN regulatory factor-1 regulates IFN-gamma-dependent cathepsin S expression. Journal of immunology (Baltimore, Md : 1950). 2002;168(9):4488-94.
339. Zheng T, Kang MJ, Crothers K, Zhu Z, Liu W, Lee CG, et al. Role of cathepsin S-dependent epithelial cell apoptosis in IFN-gamma-induced alveolar remodeling and pulmonary emphysema. Journal of immunology (Baltimore, Md : 1950). 2005;174(12):8106-15.
340. Sukhova GK, Shi GP, Simon DI, Chapman HA, Libby P. Expression of the elastolytic cathepsins S and K in human atheroma and regulation of their production in smooth muscle cells. The Journal of clinical investigation. 1998;102(3):576-83.
341. Yasuda Y, Li Z, Greenbaum D, Bogyo M, Weber E, Brömme D. Cathepsin V, a novel and potent elastolytic activity expressed in activated macrophages. The Journal of biological chemistry. 2004;279(35):36761-70.
342. Zhang Z, Biagini Myers JM, Brandt EB, Ryan PH, Lindsey M, Mintz-Cole RA, et al. β-Glucan exacerbates allergic asthma independent of fungal sensitization and promotes steroid-resistant T(H)2/T(H)17 responses. The Journal of allergy and clinical immunology. 2017;139(1):54-65.e8.
343. Chien JW, Lin CY, Yang KD, Lin CH, Kao JK, Tsai YG. Increased IL-17A secreting CD4+ T cells, serum IL-17 levels and exhaled nitric oxide are correlated with childhood asthma severity. Clinical and experimental allergy : journal of the British Society for Allergy and Clinical Immunology. 2013;43(9):1018-26.
344. Lang DM. Severe asthma: epidemiology, burden of illness, and heterogeneity. Allergy and asthma proceedings. 2015;36(6):418-24.
345. Verbeke H, Geboes K, Van Damme J, Struyf S. The role of CXC chemokines in the transition of chronic inflammation to esophageal and gastric cancer. Biochimica et biophysica acta. 2012;1825(1):117-29.
346. Simpson AJ, Maxwell AI, Govan JR, Haslett C, Sallenave JM. Elafin (elastase-specific inhibitor) has anti-microbial activity against gram-positive and gram-negative respiratory pathogens. FEBS letters. 1999;452(3):309-13.
347. Jones CE, Chan K. Interleukin-17 stimulates the expression of interleukin-8, growth-related oncogene-alpha, and granulocyte-colony-stimulating factor by human airway epithelial cells. American journal of respiratory cell and molecular biology. 2002;26(6):748-53.
348. Katz Y, Nadiv O, Beer Y. Interleukin-17 enhances tumor necrosis factor alpha-induced synthesis of interleukins 1,6, and 8 in skin and synovial fibroblasts: a possible role as a "fine-tuning cytokine" in inflammation processes. Arthritis Rheum. 2001;44(9):2176-84.
349. Noack M, Beringer A, Miossec P. Additive or Synergistic Interactions Between IL-17A or IL-17F and TNF or IL-1β Depend on the Cell Type. Frontiers in immunology. 2019;10:1726.
350. Fahy JV. Type 2 inflammation in asthma--present in most, absent in many. Nature reviews Immunology. 2015;15(1):57-65.
351. Lambrecht BN, Hammad H, Fahy JV. The Cytokines of Asthma. Immunity. 2019;50(4):975-91.
352. Pelletier M, Maggi L, Micheletti A, Lazzeri E, Tamassia N, Costantini C, et al. Evidence for a cross-talk between human neutrophils and Th17 cells. Blood. 2010;115(2):335-43.
353. Busse WW, Holgate S, Kerwin E, Chon Y, Feng J, Lin J, et al. Randomized, double-blind, placebo-controlled study of brodalumab, a human anti-IL-17 receptor monoclonal antibody, in moderate to severe asthma. American journal of respiratory and critical care medicine. 2013;188(11):1294-302.
354. Wenzel SE, Barnes PJ, Bleecker ER, Bousquet J, Busse W, Dahlén SE, et al. A randomized, double-blind, placebo-controlled study of tumor necrosis factor-alpha blockade in severe persistent asthma. American journal of respiratory and critical care medicine. 2009;179(7):549-58.

355. Morjaria JB, Chauhan AJ, Babu KS, Polosa R, Davies DE, Holgate ST. The role of a soluble TNFalpha receptor fusion protein (etanercept) in corticosteroid refractory asthma: a double blind, randomised, placebo controlled trial. Thorax. 2008;63(7):584-91.
356. Gaffen SL. Recent advances in the IL-17 cytokine family. Current opinion in immunology. 2011;23(5):613-9.
357. Wang X, Yang L, Huang F, Zhang Q, Liu S, Ma L, et al. Inflammatory cytokines IL-17 and TNF-α up-regulate PD-L1 expression in human prostate and colon cancer cells. Immunol Lett. 2017;184:7-14.
358. Sparna T, Rétey J, Schmich K, Albrecht U, Naumann K, Gretz N, et al. Genome-wide comparison between IL-17 and combined TNF-alpha/IL-17 induced genes in primary murine hepatocytes. BMC Genomics. 2010;11:226.
359. Zrioual S, Ecochard R, Tournadre A, Lenief V, Cazalis MA, Miossec P. Genome-wide comparison between IL-17A- and IL-17F-induced effects in human rheumatoid arthritis synoviocytes. Journal of immunology (Baltimore, Md : 1950). 2009;182(5):3112-20.
360. Hartupee J, Liu C, Novotny M, Li X, Hamilton T. IL-17 enhances chemokine gene expression through mRNA stabilization. Journal of immunology (Baltimore, Md : 1950). 2007;179(6):4135-41.
361. Schroll A, Eller K, Feistritzer C, Nairz M, Sonnweber T, Moser PA, et al. Lipocalin-2 ameliorates granulocyte functionality. European journal of immunology. 2012;42(12):3346-57.
362. Sallenave JM. The role of secretory leukocyte proteinase inhibitor and elafin (elastase-specific inhibitor/skin-derived antileukoprotease) as alarm antiproteinases in inflammatory lung disease. Respiratory research. 2000;1(2):87-92.
363. Ahuja SK, Murphy PM. The CXC chemokines growth-regulated oncogene (GRO) alpha, GRObeta, GROgamma, neutrophil-activating peptide-2, and epithelial cell-derived neutrophil-activating peptide-78 are potent agonists for the type B, but not the type A, human interleukin-8 receptor. The Journal of biological chemistry. 1996;271(34):20545-50.
364. Guardado S, Ojeda-Juárez D, Kaul M, Nordgren TM. Comprehensive review of lipocalin 2-mediated effects in lung inflammation. American journal of physiology Lung cellular and molecular physiology. 2021;321(4):L726-l33.
365. Sallenave JM, Shulmann J, Crossley J, Jordana M, Gauldie J. Regulation of secretory leukocyte proteinase inhibitor (SLPI) and elastase-specific inhibitor (ESI/elafin) in human airway epithelial cells by cytokines and neutrophilic enzymes. American journal of respiratory cell and molecular biology. 1994;11(6):733-41.
366. Elias JA. Airway remodeling in asthma. Unanswered questions. American journal of respiratory and critical care medicine. 2000;161(3 Pt 2):S168-71.
367. Millet P, Vachharajani V, McPhail L, Yoza B, McCall CE. GAPDH Binding to TNF-alpha mRNA Contributes to Posttranscriptional Repression in Monocytes: A Novel Mechanism of Communication between Inflammation and Metabolism. Journal of immunology (Baltimore, Md : 1950). 2016;196(6):2541-51.
368. Hiemstra PS, Amatngalim GD, van der Does AM, Taube C. Antimicrobial Peptides and Innate Lung Defenses: Role in Infectious and Noninfectious Lung Diseases and Therapeutic Applications. Chest. 2016;149(2):545-51.
369. Schatz M, Clark S, Camargo CA, Jr. Sex differences in the presentation and course of asthma hospitalizations. Chest. 2006;129(1):50-5.
370. Yung JA, Fuseini H, Newcomb DC. Hormones, sex, and asthma. Annals of allergy, asthma & immunology : official publication of the American College of Allergy, Asthma, & Immunology. 2018;120(5):488-94.
371. Hans M, Madaan Hans V. Epithelial antimicrobial peptides: guardian of the oral cavity. Int J Pept. 2014;2014:370297.
372. van Wetering S, Tjabringa GS, Hiemstra PS. Interactions between neutrophil-derived antimicrobial peptides and airway epithelial cells. Journal of leukocyte biology. 2005;77(4):444-50.
373. McCrudden MTC, O'Donnell K, Irwin CR, Lundy FT. Effects of LL-37 on Gingival Fibroblasts: A Role in Periodontal Tissue Remodeling? Vaccines. 2018;6(3).
374. Howarth PH, Babu KS, Arshad HS, Lau L, Buckley M, McConnell W, et al. Tumour necrosis factor (TNFalpha) as a novel therapeutic target in symptomatic corticosteroid dependent asthma. Thorax. 2005;60(12):1012-8.

375. Atkinson JJ, Senior RM. Matrix metalloproteinase-9 in lung remodeling. American journal of respiratory cell and molecular biology. 2003;28(1):12-24.
376. Manning BD, Toker A. AKT/PKB Signaling: Navigating the Network. Cell. 2017;169(3):381-405.
377. Altieri A, Piyadasa H, Recksiedler B, Spicer V, Mookherjee N. Cytokines IL-17, TNF and IFN-gamma Alter the Expression of Antimicrobial Peptides and Proteins Disparately: A Targeted Proteomics Analysis using SOMAscan Technology. Vaccines. 2018;6(3).
378. Warner RL, Beltran L, Younkin EM, Lewis CS, Weiss SJ, Varani J, et al. Role of stromelysin 1 and gelatinase B in experimental acute lung injury. American journal of respiratory cell and molecular biology. 2001;24(5):537-44.
379. Cabrera S, Maciel M, Hernández-Barrientos D, Calyeca J, Gaxiola M, Selman M, et al. Delayed resolution of bleomycin-induced pulmonary fibrosis in absence of MMP13 (collagenase 3). American journal of physiology Lung cellular and molecular physiology. 2019;316(5):L961-l76.
380. Lee IT, Lin CC, Wu YC, Yang CM. TNF-alpha induces matrix metalloproteinase-9 expression in A549 cells: role of TNFR1/TRAF2/PKCalpha-dependent signaling pathways. Journal of cellular physiology. 2010;224(2):454-64.
381. Lei J, Ingbar DH. Src kinase integrates PI3K/Akt and MAPK/ERK1/2 pathways in T3-induced Na-K-ATPase activity in adult rat alveolar cells. American journal of physiology Lung cellular and molecular physiology. 2011;301(5):L765-71.
382. Bousquet J, Jeffery PK, Busse WW, Johnson M, Vignola AM. Asthma. From bronchoconstriction to airways inflammation and remodeling. American journal of respiratory and critical care medicine. 2000;161(5):1720-45.
383. Busse W, Elias J, Sheppard D, Banks-Schlegel S. Airway remodeling and repair. American journal of respiratory and critical care medicine. 1999;160(3):1035-42.
384. Hough KP, Curtiss ML, Blain TJ, Liu RM, Trevor J, Deshane JS, et al. Airway Remodeling in Asthma. Front Med (Lausanne). 2020;7:191.
385. Petecchia L, Sabatini F, Usai C, Caci E, Varesio L, Rossi GA. Cytokines induce tight junction disassembly in airway cells via an EGFR-dependent MAPK/ERK1/2-pathway. Lab Invest. 2012;92(8):1140-8.
386. Hardyman MA, Wilkinson E, Martin E, Jayasekera NP, Blume C, Swindle EJ, et al. TNF-α-mediated bronchial barrier disruption and regulation by src-family kinase activation. The Journal of allergy and clinical immunology. 2013;132(3):665-75.e8.
387. Câmara J, Jarai G. Epithelial-mesenchymal transition in primary human bronchial epithelial cells is Smad-dependent and enhanced by fibronectin and TNF-alpha. Fibrogenesis Tissue Repair. 2010;3(1):2.
388. Baluk P, Yao LC, Feng J, Romano T, Jung SS, Schreiter JL, et al. TNF-alpha drives remodeling of blood vessels and lymphatics in sustained airway inflammation in mice. The Journal of clinical investigation. 2009;119(10):2954-64.
389. Demedts IK, Brusselle GG, Bracke KR, Vermaelen KY, Pauwels RA. Matrix metalloproteinases in asthma and COPD. Current opinion in pharmacology. 2005;5(3):257-63.
390. Hinks TSC, Brown T, Lau LCK, Rupani H, Barber C, Elliott S, et al. Multidimensional endotyping in patients with severe asthma reveals inflammatory heterogeneity in matrix metalloproteinases and chitinase 3-like protein 1. The Journal of allergy and clinical immunology. 2016;138(1):61-75.
391. Mattos W, Lim S, Russell R, Jatakanon A, Chung KF, Barnes PJ. Matrix metalloproteinase-9 expression in asthma: effect of asthma severity, allergen challenge, and inhaled corticosteroids. Chest. 2002;122(5):1543-52.
392. Vignola AM, Riccobono L, Mirabella A, Profita M, Chanez P, Bellia V, et al. Sputum metalloproteinase-9/tissue inhibitor of metalloproteinase-1 ratio correlates with airflow obstruction in asthma and chronic bronchitis. American journal of respiratory and critical care medicine. 1998;158(6):1945-50.
393. Matsumoto H, Niimi A, Takemura M, Ueda T, Minakuchi M, Tabuena R, et al. Relationship of airway wall thickening to an imbalance between matrix metalloproteinase-9 and its inhibitor in asthma. Thorax. 2005;60(4):277-81.

394. Vignola AM, Paganin F, Capieu L, Scichilone N, Bellia M, Maakel L, et al. Airway remodelling assessed by sputum and high-resolution computed tomography in asthma and COPD. The European respiratory journal. 2004;24(6):910-7.
395. Burrage PS, Mix KS, Brinckerhoff CE. Matrix metalloproteinases: role in arthritis. Frontiers in bioscience : a journal and virtual library. 2006;11:529-43.
396. Krymskaya VP, Penn RB, Orsini MJ, Scott PH, Plevin RJ, Walker TR, et al. Phosphatidylinositol 3-kinase mediates mitogen-induced human airway smooth muscle cell proliferation. Am J Physiol. 1999;277(1):L65-78.
397. Scott PH, Belham CM, al-Hafidh J, Chilvers ER, Peacock AJ, Gould GW, et al. A regulatory role for cAMP in phosphatidylinositol 3-kinase/p70 ribosomal S6 kinase-mediated DNA synthesis in platelet-derived-growth-factor-stimulated bovine airway smooth-muscle cells. The Biochemical journal. 1996;318 (Pt 3)(Pt 3):965-71.
398. Zhai J, Insel M, Addison KJ, Stern DA, Pederson W, Dy A, et al. Club Cell Secretory Protein Deficiency Leads to Altered Lung Function. American journal of respiratory and critical care medicine. 2019;199(3):302-12.
399. Brightling CE, Nair P, Cousins DJ, Louis R, Singh D. Risankizumab in Severe Asthma - A Phase 2a, Placebo-Controlled Trial. The New England journal of medicine. 2021;385(18):1669-79.
400. Castro M, Corren J, Pavord ID, Maspero J, Wenzel S, Rabe KF, et al. Dupilumab Efficacy and Safety in Moderate-to-Severe Uncontrolled Asthma. The New England journal of medicine. 2018;378(26):2486-96.
401. Rabe KF, Nair P, Brusselle G, Maspero JF, Castro M, Sher L, et al. Efficacy and Safety of Dupilumab in Glucocorticoid-Dependent Severe Asthma. The New England journal of medicine. 2018;378(26):2475-85.
402. Wenzel S, Castro M, Corren J, Maspero J, Wang L, Zhang B, et al. Dupilumab efficacy and safety in adults with uncontrolled persistent asthma despite use of medium-to-high-dose inhaled corticosteroids plus a long-acting β2 agonist: a randomised double-blind placebo-controlled pivotal phase 2b dose-ranging trial. Lancet (London, England). 2016;388(10039):31-44.
403. Raundhal M, Morse C, Khare A, Oriss TB, Milosevic J, Trudeau J, et al. High IFN-gamma and low SLPI mark severe asthma in mice and humans. The Journal of clinical investigation. 2015;125(8):3037-50.